

2000

Theoretical effective length factors for cross-braced solid round diagonals.

Zonghua. Chen
University of Windsor

Follow this and additional works at: <http://scholar.uwindsor.ca/etd>

Recommended Citation

Chen, Zonghua., "Theoretical effective length factors for cross-braced solid round diagonals." (2000). *Electronic Theses and Dissertations*. Paper 4367.

This online database contains the full-text of PhD dissertations and Masters' theses of University of Windsor students from 1954 forward. These documents are made available for personal study and research purposes only, in accordance with the Canadian Copyright Act and the Creative Commons license—CC BY-NC-ND (Attribution, Non-Commercial, No Derivative Works). Under this license, works must always be attributed to the copyright holder (original author), cannot be used for any commercial purposes, and may not be altered. Any other use would require the permission of the copyright holder. Students may inquire about withdrawing their dissertation and/or thesis from this database. For additional inquiries, please contact the repository administrator via email (scholarship@uwindsor.ca) or by telephone at 519-253-3000ext. 3208.

INFORMATION TO USERS

This manuscript has been reproduced from the microfilm master. UMI films the text directly from the original or copy submitted. Thus, some thesis and dissertation copies are in typewriter face, while others may be from any type of computer printer.

The quality of this reproduction is dependent upon the quality of the copy submitted. Broken or indistinct print, colored or poor quality illustrations and photographs, print bleedthrough, substandard margins, and improper alignment can adversely affect reproduction.

In the unlikely event that the author did not send UMI a complete manuscript and there are missing pages, these will be noted. Also, if unauthorized copyright material had to be removed, a note will indicate the deletion.

Oversize materials (e.g., maps, drawings, charts) are reproduced by sectioning the original, beginning at the upper left-hand corner and continuing from left to right in equal sections with small overlaps.

Photographs included in the original manuscript have been reproduced xerographically in this copy. Higher quality 6" x 9" black and white photographic prints are available for any photographs or illustrations appearing in this copy for an additional charge. Contact UMI directly to order.

Bell & Howell Information and Learning
300 North Zeeb Road, Ann Arbor, MI 48106-1346 USA
800-521-0600

UMI[®]

Theoretical Effective Length Factors for Cross-Braced Solid Round Diagonals

By

ZONGHUA CHEN

**A Thesis Submitted to
The College of Graduate Studies and Research
Through the Faculty of Engineering
(Civil Engineering Program)
In Partial Fulfillment of the Requirements for
The Degree of Master of Applied Science at the
University of Windsor**

**Windsor, Ontario, Canada
2000**



National Library
of Canada

Acquisitions and
Bibliographic Services

395 Wellington Street
Ottawa ON K1A 0N4
Canada

Bibliothèque nationale
du Canada

Acquisitions et
services bibliographiques

395, rue Wellington
Ottawa ON K1A 0N4
Canada

Your file *Votre référence*

Our file *Notre référence*

The author has granted a non-exclusive licence allowing the National Library of Canada to reproduce, loan, distribute or sell copies of this thesis in microform, paper or electronic formats.

The author retains ownership of the copyright in this thesis. Neither the thesis nor substantial extracts from it may be printed or otherwise reproduced without the author's permission.

L'auteur a accordé une licence non exclusive permettant à la Bibliothèque nationale du Canada de reproduire, prêter, distribuer ou vendre des copies de cette thèse sous la forme de microfiche/film, de reproduction sur papier ou sur format électronique.

L'auteur conserve la propriété du droit d'auteur qui protège cette thèse. Ni la thèse ni des extraits substantiels de celle-ci ne doivent être imprimés ou autrement reproduits sans son autorisation.

0-612-52526-0

Canada

912328

© Zonghua Chen 2000
All Rights Reserved

I hereby declare that I am the sole author of this document.

I authorize the UNIVERSITY OF WINDSOR to lend this document to other individuals for the purpose of scholarly research.

Zonghua Chen

I further authorize the UNIVERSITY OF WINDSOR to reproduce the document by photocopying or by other means, in total or in part, at the request of other institutions or individuals for the purpose of scholarly research.

Zonghua Chen

The UNIVERSITY OF WINDSOR requires the signature of all persons using this document.

Please sign below and give address and date.

ABSTRACT

The objective of the investigation is to determine theoretically the effective length factors of cross-braced solid round diagonals in all-welded steel communication towers. Three beam-column models with different boundary conditions (pinned, elastically restrained, and fixed) were investigated and it was shown that a beam-column with elastic restraints at ends and at cross-brace location is the most accurate. However, for design purposes, when the ratio of the diameter of the leg to the diameter of the diagonal exceeds three, beam-column model with fixed ends and elastic restraint at cross-brace location is satisfactory. The theoretical results were compared with results of tests on 26 specimens.

Based on small deflections and elastic behavior, theoretical equations were developed for symmetric and anti-symmetric deflection modes. It was shown that during initial stages of loading, symmetric deflection mode will dominate while anti-symmetric deflection mode will dominate at failure and ultimately, the failure is in anti-symmetric mode. The theoretical results were again compared with tests carried out on 26 specimens.

Finally, finite element analysis was carried out on one tower for the following six cases: (a) elastic stage with symmetric initial deflection, (b) elastic stage with anti-symmetric initial deflection, (c) elastic stage with superposition of symmetric and anti-symmetric initial deflection, (d) elastic-plastic stage with symmetric initial deflection, (e) elastic-plastic stage with anti-symmetric initial deflection, and (f) elastic-plastic stage with superposition of symmetric and anti-symmetric initial deflection. The effect of the magnitude of anti-symmetric deflection was studied for three towers. The finite-element analysis also confirmed that failure would be in the anti-symmetric mode.

ACKNOWLEDGEMENTS

The author wishes to express his sincere gratitude to his advisor Dr. Murty K. S. Madugula, Professor of Civil Engineering, for his patience, informative guidance and encouragement during the development of this research.

The author wishes to thank Dr. S. Bhattacharjee for his inspiration and continuous encouragement which he so enthusiastically provided throughout the research.

Special thanks are due to the technicians, Messrs. Richard Clark and Robert Tattersall for their help in the experimental setup and to the author's friends and colleagues, Yongcong Ding and Yean Sun for their help during testing.

The author extends special thanks to his family members for their encouragement during his graduate studies.

The author also wishes to acknowledge the financial support provided by University of Windsor and the Natural Sciences and Engineering Research Council of Canada in the form of Graduate Assistantship and Research Assistantship, respectively.

To My Brother

CONTENTS

ABSTRACT	vi
ACKNOWLEDGEMENTS.....	vii
LIST OF TABLES.....	xii
LIST OF FIGURES.....	xiii
NOTATION	xvi
CHAPTER 1: INTRODUCTION	1
1.1 GENERAL.....	1
1.2 NEED FOR RESEARCH.....	2
1.3 OBJECTIVES OF RESEARCH.....	6
1.4 ORGANIZATION OF THE THESIS.....	6
CHAPTER 2: EFFECTIVE LENGTH FACTORS FOR CROSS- BRACED DIAGONALS.....	8
2.1 GENERAL.....	8
2.2 MODEL 1: BEAM-COLUMN WITH PINNED ENDS.....	8
2.2.1 No rotational restraint at cross-brace location.....	8
2.2.2 Elastic rotational restraint at cross-brace location	10
2.2.3 Elastic vertical support at cross-brace location.....	13
2.3 MODEL 2: BEAM-COLUMN WITH FIXED ENDS.....	17
2.3.1 No rotational restraint at cross-brace location.....	17
2.3.2 Elastic rotational restraint at cross-brace location.....	19
2.4 MODEL 3: BEAM-COLUMN WITH ELASTIC ROTATIONAL RESTRAINTS AT ENDS AND AT CROSS-BRACE LOCATION	21
2.5 SUMMARY.....	25

CHAPTER 3: LOAD-DEFLECTION BEHAVIOR (ELASTIC STAGE).....	26
3.1 GENERAL.....	26
3.2 SYMMETRIC DEFLECTION.....	27
3.3 ANTI-SYMMETRIC DEFLECTION.....	31
3.3.1 General deflection equation.....	32
3.3.2 Load-deflection equation.....	34
3.4 SUMMARY.....	35
CHAPTER 4: EXPERIMENTAL INVESTIGATION.....	36
4.1 GENERAL.....	36
4.2 EXPERIMENTAL SET-UP.....	36
4.2.1 Overview of set-up.....	36
4.2.2 Strain measurements.....	37
4.2.3 Deflection measurements.....	39
4.3 TEST PROCEDURE.....	41
4.4 DESCRIPTION OF SPECIMENS AND TEST RECORD.....	42
CHAPTER 5: ANALYSIS OF TEST RESULTS.....	44
5.1 GENERAL.....	44
5.2 EFFECTIVE LENGTH FACTOR.....	44
5.2.1 Experimental versus theoretical values.....	44
5.2.2 Effect of leg size	46
5.2.3 Effect of tension diagonal.....	47
5.3 DEFLECTION OF DIAGONALS.....	48
5.3.1 Experimental Load-Deflection Behavior of Diagonals	48
5.3.2 Theoretical Load-Deflection Behavior of Diagonals....	51

CHAPTER 6: FINITE ELEMENT ANALYSIS.....	55
6.1 GENERAL.....	55
6.2 DESCRIPTION OF FINITE ELEMENT MODEL	55
6.3 RESULTS OF FINITE ELEMENT ANALYSIS.....	56
6.4 EFFECT OF MAGNITUDE OF ANTI-SYMMETRIC INITIAL DEFLECTION.....	65
6.5 SUMMARY.....	68
 CHAPTER 7: CONCLUSIONS.....	 69
 REFERENCES.....	 71
 APPENDIX A: TABLES OF TEST DATA.....	 73
 APPENDIX B: TABLES OF DEFLECTION RECORDS AND FIGURES OF DEFLECTED SHAPES	 109
 APPENDIX C: LOAD-DEFLECTION CURVES.....	 158
 VITA AUCTORIS.....	 183

LIST OF TABLES

Table 2-1	Relationship between K_{s2} and Effective Length Factor.....	12
Table 2-2	Relationship between K_{s3} and Effective Length Factor.....	16
Table 2-3	Relationship between K_{s2} and Effective Length Factor.....	20
Table 2-4	Relationship between K_{s1} and Effective Length Factor.....	25
Table 5-1	Effective Length Factors of Test Specimens.....	45
Table 6-1	Properties of Specimens.....	65
Table 6-2	Experimental Buckling Load.....	67

LIST OF FIGURES

Fig. 1.1	Cross-section of tower.....	1
Fig. 1.2	Cross-braced diagonals of tower.....	2
Fig. 2.1	Beam-column with pinned ends and no rotational restraint at cross-brace location.....	9
Fig. 2.2	Model of beam-column with pinned ends and elastic rotational restraint at cross-brace location.....	11
Fig. 2.3	Model of beam-column with pinned ends and elastic vertical support at cross-brace location.....	14
Fig. 2.4	Model of beam-column with fixed ends and no rotational restraint at cross-brace location.....	17
Fig. 2.5	Beam-column model with fixed ends and elastic rotational restraint at cross-brace location.....	20
Fig. 2.6	Beam-column model with elastic rotational restraints at ends and at cross-brace location.....	22
Fig. 2.7	Two panels of steel tower model.....	24
Fig. 3.1	Symmetric initial deflection of the beam-column model with fixed ends and elastic rotational restraint at cross-brace location.....	27
Fig. 3.2	Anti-symmetric initial deflection of the beam-column model with fixed ends and elastic rotational restraint at cross-brace location.....	31
Fig. 4.1	Test set-up overview.....	39
Fig. 4.2	Location of strain gauges.....	40
Fig. 4.3	Location of dial gauges.....	41
Fig. 4.4	Detail of connection between diagonals and legs.....	43
Fig. 5.1	Effective length factor vs. ratio of diameters.....	46
Fig. 5.2	Different stages of buckling of diagonal.....	49
Fig. 5.3	Deflected shape of diagonal of Specimen P5A.....	51

Fig. 5.4	Theoretical deflection of diagonal of Specimen P6A.....	53
Fig. 5.5	Comparison of theoretical and experimental deflections for Specimen P6A	54
Fig. 6.1	Initial deflection of diagonal of Specimen P6A.....	57
Fig. 6.2	Deflected shape of diagonal of Specimen P6A (Case 1)	57
Fig. 6.3	Load-deflection curve at cross-brace of diagonal of Specimen P6A...	58
Fig. 6.4	Deflected shape of diagonal of Specimen P6A (Case 2).....	58
Fig. 6.5	Load-deflection curve at maximum value of diagonal of Specimen P6A	59
Fig. 6.6a	Deflected shape of diagonal of Specimen P6A before failure (P = 55.13 kN) (Case 3).....	59
Fig. 6.6b	Deflected shape of diagonal of Specimen P6A at failure load (P=83.9 kN) (Case 3).....	60
Fig. 6.6c	Deflected shape of diagonal of Specimen P6A at post-failure state (P = 44.42 kN)(Case 3).....	60
Fig. 6.7	Load-deflection curves of diagonal of Specimen P6A for three critical points (Case 3).....	61
Fig. 6.8	Deflected shape of diagonal of Specimen P6A (Case 4)	61
Fig. 6.9	Load-deflection curve of diagonal of Specimen P6A(Case 4).....	62
Fig. 6.10	Deflected shape of diagonal of Specimen P6A (Case 5).....	62
Fig. 6.11	Load-deflection curve of diagonal of Specimen P6A (Case 5).....	63
Fig. 6.12	Deflected shape of diagonal of Specimen P6A (Case 6).....	63
Fig. 6.13	Load-deflection curve of diagonal of Specimen P6A at cross-brace location and at two critical points (Case 6).....	64
Fig. 6.14	Load-deflection curve of diagonal of Specimen P6A at cross-brace location (Case 6).....	64
Fig. 6.15a	Buckling load vs initial anti-symmetric deflection of diagonal of Specimen P6A	67
Fig. 6.15b	Buckling load vs initial anti-symmetric deflection of diagonal of Specimen P8B	67
Fig. 6.15c	Buckling load vs initial anti-symmetric deflection of diagonal of Specimen S6B	67

Fig. A.1 Location of dial gauges on compression diagonal	73
Fig. A.2 Test set-up	74

NOTATION

A	= area of cross-section = constant (deflection equation)
A_{amp}	= amplification factor of deflection
B	= constant in deflection equation
C	= constant in deflection equation
C_{cr}	= critical load of diagonal
C_e	= Euler Load
C_T	= tangent modulus load
D	= diameter of leg = constant (deflection equation)
E	= modulus of elasticity = constant (deflection equation)
E_r	= reduced modulus
E_T	= tangent modulus
F	= constant in deflection equation
G	= shear modulus = constant (deflection equation)
H	= height of tower section = constant (deflection equation)
I	= moment inertia of diagonal
J	= the torsion constant of leg
K	= effective length factor of compression diagonal
K_{s1}	= spring constants of rotation restraint at ends of diagonal
K_{s2}	= spring constants of rotation restraint at cross-point location of diagonal
K_{s3}	= spring constants of out-of-plane restrain at cross braced location
L_0	= total length of diagonal(from center to center of legs)
L	= half length of diagonal, $L_0 = 2 * L$
M	= bending moment

N	= axial force of tension diagonal
P	= compression force of compression diagonal
T	= torque
Δ	= deflection at cross-braced position
b	= width of tower
d	= diameter of diagonal
k	= $\sqrt{P / EI}$
l	= panel length of tower
m	= D/d
n_1	= $K_{s2}/(EI/L)$
n_2	= $K_{s3}/(EI/L^3)$
r	= radius of gyration
v	= deflection of diagonal
v_0	= initial deflection of diagonal
x	= coordinate position of cross-section in diagonal
α	= angle between diagonal and leg
δ	= maximum initial deflection
θ	= angle of rotation of diagonal section
φ_1	= rotational angle of leg at connection point
φ_2	= out-of- plane bending angle of diagonals

CHAPTER 1

INTRODUCTION

1.1 GENERAL

In the information industry, satellites, antenna towers and cables are used to transmit the signal of communication. Among them, antenna towers are the best choice because they are relatively economical and effective for remote transmission, especially in Canada where land area is large and distances among the cities and towns are great. Antenna tower transmission of signals is the best medium, which is widely used not only in Canada, but also in USA and Europe.

These kinds of steel towers have their own characteristics. They are very tall and very slender. They stand there with several points of support by guy cables. The cross-section of the tower itself may vary, but triangular cross section as shown in Fig. 1.1, is the most popular. Legs, diagonals and horizontals are welded together as shown in Fig 1.2. A real tower specimen section is shown in Fig. A.2.

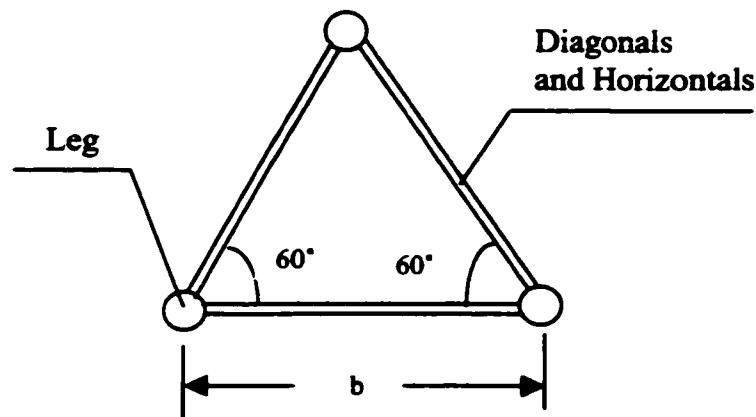


Fig. 1.1 Cross-section of tower

During the fabrication, tower diagonals can be arranged as follows:

- Compression diagonals inside, and tension diagonals outside.
- Compression diagonals outside and tension diagonals inside.

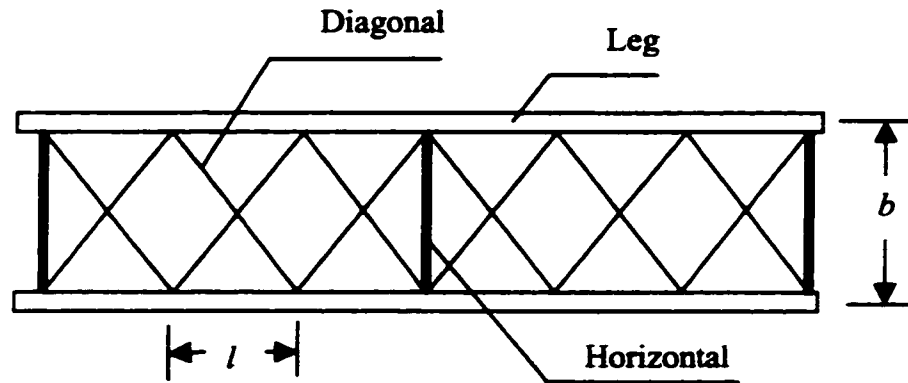


Fig. 1.2 Cross-braced diagonals of tower

Erecting tower is subjected to many kinds of loads, such as self-weight, snow, and wind. Tower structures are also subjected to earthquake loads in seismic areas. These loads can be classified as two catalogues: vertical loads and transverse loads. Leg members bear vertical loads and bending moments caused by transverse loads. But most of the shear force is borne by cross-brace diagonals, one in compression and the other in tension. The behavior of diagonals of cross-braced steel guyed communication towers is very complicated.

1.2 NEED FOR RESEARCH

In designing communication towers, not only the strength and stiffness but also the stability problems should be considered. Different countries use different values for the effective length factors used in designing the diagonals; e.g., in Canada, $K=0.75$ of total length of diagonal and in China, $K=0.4$. In the United States, different companies use different effective length factors. The problem here is that the behavior of diagonals is not very clear, though many theoretical and experimental studies have been done.

The first experiments on lattice girders treated as cantilevers were made in 1857 by H. Lohse [Todhunter 1960]. Single, double, triple, and fourfold types of bracings were used.

The bars were riveted to each other. The loads at which the bracing buckled were noted. It is noteworthy that in several cases the bracing bars bent elastically into an approximate S-form, a result which the researchers at the time did not take into account in their theoretical analysis. From these experiments, a great increase of strength due to multiple bracing and to the riveting together of the bracing bars, was noticed. Wöhler in 1855 [Todhunter 1960] deduced the stresses in the bracing bars of a girder from purely statical consideration. De Clercq in 1857 and Winkler in 1859 theoretically analyzed lattice girders and the stresses in the bracing bars [Todhunter 1960].

For cross-bracings or tension-compression diagonals, Jasinsky was the first to investigate the stability of the compressed diagonals and to evaluate the strengthening afforded by the diagonals in tension in lattice trusses [Timoshenko 1953].

DeWolf and Pelliccione [1979] reported that the design practice for cross-bracing members adopted at that time, which entirely neglected the contribution of the compression member and relied solely on the tension member, was conservative and resulted in overdesign. The stiffness, α , furnished by the tension member acting on compression member in the out-of-plane direction was given as follows;

$$\alpha = \frac{48EI}{L^3} \left[\frac{u^3}{3(u - \tanh u)} \right] \quad (1-1)$$

where, L represents the total length of the diagonal, and

$$u = \frac{L}{2} \sqrt{\frac{T}{EI}} ,$$

in which T is the force in tension member.

A theoretical investigation was made by Vickers [1982] into the behavior and design of cross-bracing. His discussion emphasized the use of cruciform (star shaped) double angle struts for bracing members. The extent of lateral support provided to the compression diagonal by the tension diagonal at their point of intersection was analyzed. From his study, it was concluded that the design concept of shared load between tension

and compression members, with the compression member designed using an effective length factor equal to half the total length of the diagonals, is more realistic than “ tension only” bracing design.

El-Tayem and Goel [1986] studied experimentally and theoretically full-scale cross-bracing specimens. Five single angles and one double angle cross-bracing specimens, made of ASTM A36 steel, were included in the study. Quasi-static cyclic loading was used in the tests and strain gauges were attached to measure the loads. It was noticed that the interconnection provided an elastic restraint against both lateral and rotational deformations of the compression diagonal at the point of intersection. It was concluded that for cross-bracing systems made from single equal-leg angles, an effective length of 0.85 times of the half diagonal length is reasonable.

Picard and Beaulieu [1987] performed a theoretical study aimed at the determination of the transverse stiffness offered by the tension diagonal in cross-bracing systems and at the evaluation of this stiffness on the out-of-plane buckling resistance of the compression diagonal. When the diagonals are continuous and attached at the intersection, it was concluded that the effective length of the compression diagonal is 0.5 times the total diagonal length. A simpler form of equation was given by the writers for the stiffness, α , provided by the tension diagonal, assuming the two diagonals to be equal in length and to have the same cross-sectional area:

$$\alpha = \frac{6EI}{L^3} + 4.36 \frac{T}{2L} \quad (1-2)$$

where, L is the half length of the diagonal, and T is the force in tension diagonal. They also suggested that the effective length factor, K , for calculating the buckling load of the compression diagonal to be as follows:

$$K = \sqrt{0.523 - \frac{0.428}{C/T}} \geq 0.5 \quad (1.3)$$

where C and T are the forces, just before buckling, in the compression and the tension diagonals, respectively.

The theoretical analysis carried out in 1987 by the same authors was generalized in 1989 [Picard and Beaulieu, 1989a and 1989b], which gave the following effective length factor for cross-bracings:

$$K = \sqrt{\frac{1 - 0.818/(C/T)}{1 + 0.911(I_t/I_c)}} \quad (1-4)$$

where, C/T is the ratio of the force in compression member just before buckling to the force in tension diagonal, and I_t/I_c is the ratio of moment of inertia of the tension diagonal to the moment of inertia of the compression diagonal. This theoretical study was also verified by fifteen buckling tests carried out in 1988 [Picard and Beaulieu 1988].

Kemp and Behncke [1998] described a series of tests on cross-bracing systems with slenderness ratios in the range of 102 to 160. Other variables included the inclination of the main legs and bracing, the number of bolts in each end connection, and the size of the main leg relative to the bracing. The measured behavior was compared with the results of a flexibility-based analysis and the formulas from the American and European Transmission Tower Design manuals. The results confirmed the complexity of the behavior of cross-bracing in latticed towers. Strain measurements showed that yielding of the extreme fiber of the strut in the central region of the largest subspan is the primary cause of failure. The effect of the end eccentricity was partially alleviated by the restraint provided by the main legs to the ends of the compression diagonal. Consequently the ultimate strength in the tests was increased by up to 17% by changing the number of bolts at the end connection from one to two. A smaller but nevertheless significant 10% benefit was obtained by increasing the size of the main leg relative to the bracing.

The experimental investigations carried out by Jaboo [1998] and Sun [1999] help in arriving at effective length factors for cross-braced diagonals based on the results of tests of full-scale communication towers. However, no theoretical basis was so far given for the determination of the effective length factors for cross-braced solid round diagonals of all-welded steel communication towers.

1.3 OBJECTIVES OF RESEARCH

The following are the objectives of the present research:

1. To determine the most accurate beam-column model for the estimation of effective length factors.
2. To compare these values with the experimental values available in the literature and to ensure that they are in good agreement with one another.
3. To determine the effect of the ratio of the diameter of leg to the diameter of diagonal on the effective length factor.
4. To determine the effect of the rotational restraint offered by the tension diagonal on the effective length factor and the buckling mode.
5. To investigate the effect of the magnitude of the tension force in the tension diagonal on the effective length factor.
6. To study the effect of symmetric and anti-symmetric initial deflections on the critical load of the compression diagonal.
7. To determine the mode of buckling, viz., in-plane or out-of-plane, of the compression diagonals.
8. To compare the results from theoretical studies with results from finite element analysis.

1.4 ORGANIZATION OF THE THESIS

This thesis is divided into seven chapters. In Chapter 1, the need for research and the objectives of the research are presented. In Chapter 2, several ideal models are established, and the corresponding critical load C_{cr} and effective length factor K are derived. The most reasonable model is recommended for practical use.

In the third chapter, the equations about load-deflection within the elastic range are derived in detail. Two kinds of initial deflection and their superposition are provided in

this chapter. In the fourth chapter, experimental set-up is described and the results are presented.

In the fifth chapter, the experimental and theoretical results are compared. The behavior of diagonals is described in detail. The results of finite element analysis are included in Chapter 6.

Finally, based on theoretical studies and experimental investigations, various conclusions arrived are presented in the seventh chapter. Tables of test data, deflection records, figures of deflected shapes of diagonals, and load-deflection curves are included in the Appendixes.

CHAPTER 2

EFFECTIVE LENGTH FACTORS FOR CROSS-BRACED DIAGONALS

2.1 GENERAL

Compression diagonals in steel tower as shown in Fig. 2.1 can be considered as two-span continuous beam-columns. In order to derive the critical axial compressive force, the following assumptions regarding the geometry, kinematics, and material of the column are necessary:

1. Beam-column is perfectly straight.
2. The material is linear, without considering material yielding.
3. Deflection of diagonal is small.
4. Shear force deformation is ignored.
5. Axial force is applied along the central axis of the beam-column.

In order to find out the most reasonable model, several kinds of models are considered in this chapter. Each model is different in boundary conditions and the restraint provided by the cross-brace. These models include beam-column with pinned ends, beam-column with fixed ends, and beam-column with elastic restraints at ends. Elastic rotational restraint at cross-brace location is discussed for each model respectively. Critical load and effective length factor are found for each case.

2.2 MODEL 1: BEAM-COLUMN WITH PINNED ENDS

2.2.1 No rotational restraint at cross-brace location

Fig. 2.1 shows a two-span continuous beam with one hinged support and two roller supports loaded by an axial force P applied along its central axis.

The fourth-order differential equation for segment 1 is

$$v_1^{IV} + k^2 v_1'' = 0 \quad (2.1)$$

where,

$$k^2 = P / EI \quad (2.2)$$

The general solution is assumed to be

$$v_1 = A \sin kx_1 + B \cos kx_1 + Cx_1 + D \quad (2.3)$$

Similarly, the fourth-order differential equation for segment 2 is

$$v_2^{IV} + k^2 v_2'' = 0 \quad (2.4)$$

and the corresponding general solution is assumed to be

$$v_2 = E \sin kx_2 + F \cos kx_2 + Gx_2 + H \quad (2.5)$$

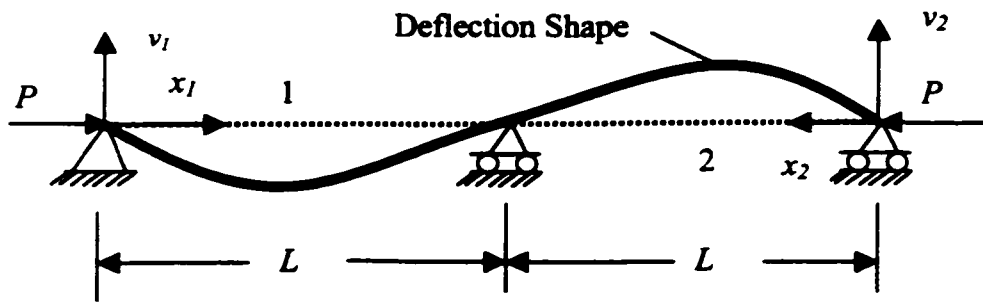


Fig. 2.1 Beam-column with pinned ends and no rotational restraint at cross-brace location

By using the boundary conditions

$$v_1(0) = 0, \quad v_1''(0) = 0 \quad v_1(L) = 0 \quad (2.6)$$

$$v_2(0) = 0, \quad v_2''(0) = 0 \quad v_2(L) = 0 \quad (2.6a)$$

and the continuity conditions

$$v_1'(L) = -v_2'(L) \quad (2.6b)$$

$$v_1''(L) = v_2''(L) \quad (2.6c)$$

it is shown that

$$B = D = F = H = 0 \quad (2.7)$$

$$\begin{bmatrix} \sin kL & 0 & 0 & 0 \\ \sin kL & L & 0 & 0 \\ 0 & 0 & \sin kL & L \\ 0 & 0 & k \cos kL & 1 \end{bmatrix} \begin{Bmatrix} A - E \\ C - G \\ A + E \\ C + G \end{Bmatrix} = \begin{Bmatrix} 0 \\ 0 \\ 0 \\ 0 \end{Bmatrix} \quad (2.8)$$

and the characteristic equation is obtained

$$\sin kL(\sin kL - kL \cos kL) = 0 \quad (2.9)$$

Critical load can be expressed as follows:

$$C_\sigma = \frac{\pi^2 EI}{L^2} \quad (2.10)$$

Thus, the effective length factor of this model is equal to 0.5 of $2L$, which is very conservative.

2.2.2 Elastic rotational restraint at cross-brace location

This model is different from previous one in that elastic rotational restraint is imposed at cross-brace location as indicated in Fig. 2.2.

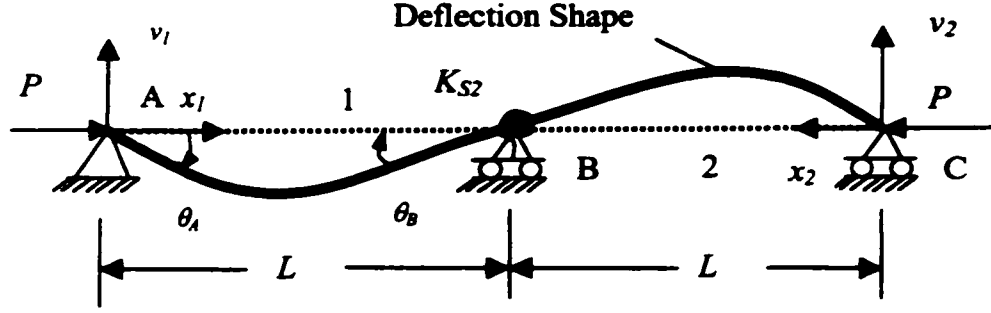


Fig. 2.2 Model of beam-column with pinned ends and elastic rotational restraint at cross-brace location

Let us consider the equilibrium of point B. First, suppose that there is a rotation θ_B at B, and θ_A at points A and C. Using the theory of beam-columns, the bending moment at the end of beam can be expressed as follows:

$$M_{CB} = M_{AB} = \frac{EI}{L}(s_{ii}\theta_A + s_{ij}\theta_B) = 0 \quad (2.11)$$

$$M_{BA} = M_{BC} = \frac{EI}{L}(s_{ij}\theta_A + s_{ji}\theta_B) \quad (2.12)$$

where,

$$s_{ii} = s_{jj} = \frac{kL \sin kL - (kL)^2 \cos kL}{2 - 2 \cos kL - kL \sin kL} \quad (2.13)$$

$$s_{ij} = s_{ji} = \frac{(kL)^2 - kL \sin kL}{2 - 2 \cos kL - kL \sin kL} \quad (2.14)$$

From (2-11), θ_A can be expressed as

$$\theta_A = -\frac{s_{ij}}{s_{ii}}\theta_B \quad (2.15)$$

Equation of equilibrium at point B is as follows:

$$2\frac{EI}{L}(s_{ii} - \frac{s_{ij}^2}{s_{ii}})\theta_B + K_{s2}\theta_B = 0 \quad (2.16)$$

θ_B should not be equal to zero. Thus, the characteristic equation of this model is:

$$2\frac{EI}{L}(s_{ii} - \frac{s_{ij}^2}{s_{ii}}) + K_{s2} = 0 \quad (2.17)$$

from which a general solution for critical load can be obtained in terms of K_{s2} . The effect of K_{s2} on the critical load is given in following Table 2-1.

Table 2-1: Relationship between K_{s2} and Effective Length Factor

$n_1 = K_{s2}/(EI/L)$	0	1	2	4	8	16
kL	3.142	3.286	3.406	3.591	3.829	4.066
Effective Length factor K	0.50	0.478	0.461	0.438	0.347	0.350

It is expensive to increase the buckling load by enlarging rotational restraint. The buckling mode is anti-symmetric, which is similar to a sine curve.

For the special case of solid round diagonals of all-welded steel towers, if $G=1/2.6E$, spring constants of rotational restraint at mid-span are

$$K_{s2} = \frac{4EI}{2.6L} \quad (2.18)$$

Then, the characteristic equation (2.17) is simplified as follows:

$$(s_{ii} - \frac{s_{ij}^2}{s_{ii}}) = -0.7692 \quad (2.19)$$

By trial and error, the smallest value of k that satisfies the characteristic equation is

$$kL = 3.328 \quad (2.20)$$

Using $k^2 = P/EI$, the critical load is derived

$$C_{\sigma} = \frac{\pi^2 EI}{(0.944L)^2} \quad (2.21)$$

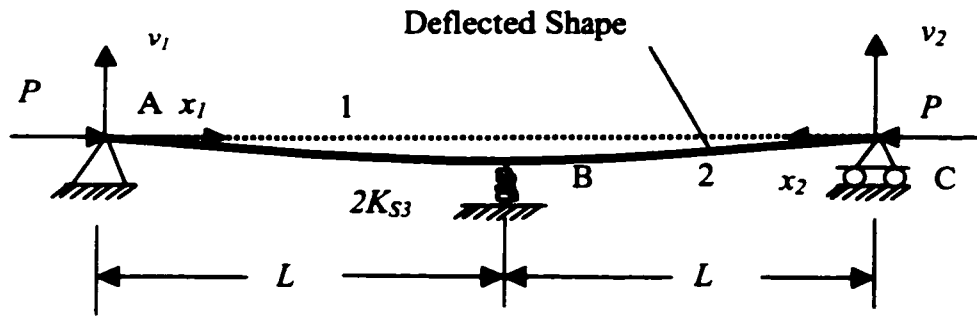
Thus, the effective length factor of this model K is equal to 0.472 of $2L$.

2.2.3 Elastic vertical support at cross-brace location

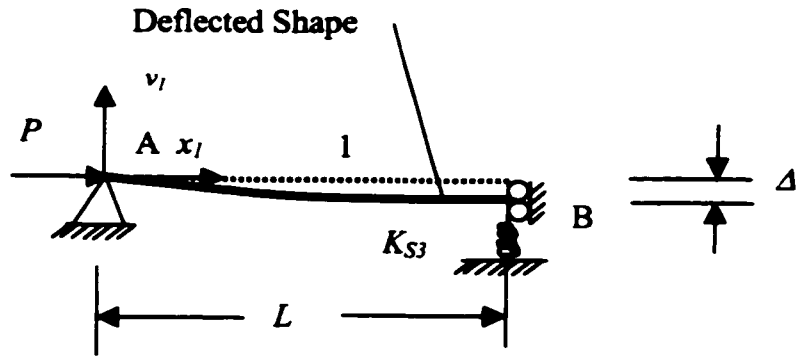
The diagonals in steel tower are welded at the intersection points. After the load is applied, the compression diagonal will deflect like a beam with two ends pinned. But the tension diagonal will restrain this deflection as if a spring is applied on the diagonal as demonstrated in the Fig. 2.3a.

The model can be simplified to one span model because of its symmetry with respect to both load and geometry as in Fig. 2.3a. In this simplified model there is no rotation at B. But the vertical movement is elastically restrained by a spring. The spring coefficient is K_{s3} . The solution of this model is as follows:

Suppose the general solution is



(a)



(b) Simplified Model

Fig. 2.3 Model of beam-column with pinned ends and elastic vertical support at cross-brace location

$$v_1 = A \sin kx_1 + B \cos kx_1 + Cx_1 + D \quad (2.22)$$

And the boundary conditions are

$$v_1(0) = 0, \quad v_1'(0) = 0, \quad (2.23)$$

$$v_1(L) = \Delta \quad v_1'(L) = 0 \quad (2.23a)$$

Then,

$$B = D = 0 \quad (2.24)$$

and

$$Ak \cos kL + C = 0 \quad (2.25a)$$

$$A \sin kL + CL - \Delta = 0 \quad (2.25b)$$

At point B, shear force can be expressed as

$$Q = -EI(v'' + k^2 v') = K_{s3} \Delta \quad (2.25c)$$

$$CEIk^2 + K_{s3} \Delta = 0 \quad (2.25d)$$

These boundary equations can be expressed in the form of matrix (2.25), and the characteristic equation is derived in (2.26).

$$\begin{bmatrix} k \cos kL & 1 & 0 \\ \sin kL & L & -1 \\ 0 & EIk^2 & K_{s3} \end{bmatrix} \begin{Bmatrix} A \\ C \\ \Delta \end{Bmatrix} = \begin{Bmatrix} 0 \\ 0 \\ 0 \end{Bmatrix} \quad (2.25)$$

$$\det \begin{bmatrix} k \cos kL & 1 & 0 \\ \sin kL & L & -1 \\ 0 & EIk^2 & K_{s3} \end{bmatrix} = 0 \quad (2.26)$$

(2.26) can be simplified as follows:

$$(kL + \frac{EIk^3}{K_{s3}}) \cos kL - \sin kL = 0 \quad (2.27)$$

For the special case of diagonals for the towers tested, K_{s3} is as follows

$$K_{s3} = \frac{12EI}{L^3} \quad (2.28)$$

The simplified characteristic equation is

$$(kL + \frac{(kL)^3}{12}) \cos kL - \sin kL = 0 \quad (2.29)$$

By the trial and error method, the critical load and effective length factor are derived. The results are as follows:

$$kL = 4.635 \quad (2.30)$$

and

$$C_\sigma = \frac{\pi^2 EI}{(0.678L)^2} \quad (2.31)$$

The effective length factor K is equal to 0.339 of $2L$.

The effect of K_{s3} on the effective length factor is shown in Table 2-2.

Table 2-2: Relationship between K_{s3} and Effective Length Factor

$n_2 = K_{s3}/(EI/L^3)$	0	1	10	100	1000	∞
kL	1.571	4.711	4.702	4.644	4.531	4.488
Effective Length factor K	1	0.333	0.334	0.337	0.347	0.350

From Table 2-1, for $n_1 = 0$ (i.e., no rotational restraint at cross-brace location), $K = 0.5$ and the mode of buckling is anti-symmetric. The mode of buckling does not change with increase in the value of n_1 . From Table 2-2, for $n_2 = 0$ (i.e., no vertical restraint at cross-brace location), the effective length factor is 1 and the mode of buckling is symmetric. However, the mode of buckling suddenly changes to anti-symmetric even for a slight increase in the value of n_2 , lowering the value of " K ".

2.3 MODEL 2: BEAM-COLUMN WITH FIXED ENDS

2.3.1 No rotational restraint at cross-brace location

Fig. 2.4 shows the model of beam-column of two continuous spans with fixed ends and a vertical fixed restraint at mid-point (no rotational restraint). The fourth-order differential equation for segment 1 is

$$v_1'''' + k^2 v_1'' = 0 \quad (2.32)$$

where,

$$k^2 = P / EI \quad (2.32a)$$

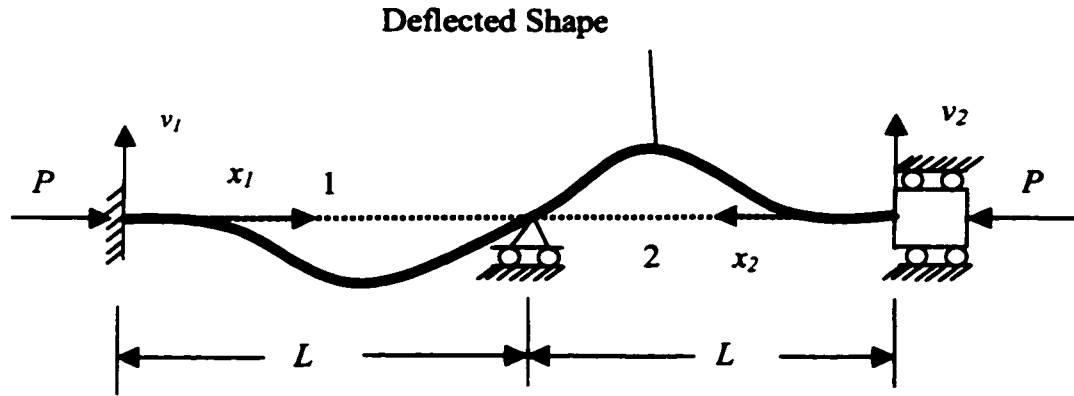


Fig. 2.4 Model of beam-column with fixed ends and no rotational restraint at cross-brace location

The general solution is

$$v_1 = A \sin kx_1 + B \cos kx_1 + Cx_1 + D \quad (2.33)$$

Similarly, the fourth-order differential equation for segment 2 is

$$v_2'''' + k^2 v_2'' = 0 \quad (2.34)$$

and the general solution is

$$v_2 = E \sin kx_2 + F \cos kx_2 + Gx_2 + H \quad (2.35)$$

By using the boundary conditions

$$v_1(0) = 0, \quad v_2(0) = 0 \quad (2.36)$$

$$v_1'(0) = 0, \quad v_2(L) = 0 \quad (2.36a)$$

$$v_1(L) = 0, \quad v_2'(0) = 0 \quad (2.36b)$$

and the continuity conditions

$$v_1'(L) = -v_2'(L), \quad v_1(L) = v_2(L) \quad (2.36c)$$

the following equations are available:

$$\begin{bmatrix} \sin kL - kL & \cos kL - 1 & 0 & 0 \\ 0 & 0 & \sin kL - kL & \cos kL - 1 \\ \cos kL - 1 & -\sin kL & \cos kL - 1 & \sin kL \\ \sin kL & \cos kL & -\sin kL & -\cos kL \end{bmatrix} \begin{Bmatrix} A_1 \\ B_1 \\ A_2 \\ B_2 \end{Bmatrix} = \begin{Bmatrix} 0 \\ 0 \\ 0 \\ 0 \end{Bmatrix} \quad (2.38)$$

The characteristic equation is:

$$\det \begin{bmatrix} \sin kL - kL & \cos kL - 1 & 0 & 0 \\ 0 & 0 & \sin kL - kL & \cos kL - 1 \\ \cos kL - 1 & -\sin kL & \cos kL - 1 & \sin kL \\ \sin kL & \cos kL & -\sin kL & -\cos kL \end{bmatrix} = 0 \quad (2.37)$$

which can be simplified as follows

$$(\sin kL - kL \cos kL)(2 - 2 \cos kL - kL \sin kL) = 0 \quad (2.39)$$

The lowest critical load is obtained by solving the second factor of the equation. The solution is $kL=4.4934$, from which the critical load is obtained:

$$C_{\sigma} = \frac{\pi^2 EI}{(0.699L)^2} \quad (2.40)$$

For this buckling load, the mode of buckling is anti-symmetric, as shown in Fig. 2.5.

If the first factor is equated to zero, the solution is $kL=2\pi$, from which the critical load is

$$C_{\sigma} = \frac{\pi^2 EI}{(0.5L)^2} \quad (2.41)$$

The shape of this buckling is symmetrical. Since this critical load is larger than the former one, it is impossible to happen.

So, the effective length factor K is equal to 0.350 of $2L$ for this model.

2.3.2 Elastic rotational restraint at cross-brace location

In this model, compared with the model in section 2.3.1 a constant rotational restraint spring K_{s2} is imposed at cross-brace location B, as shown in Fig. 2.5. Both the rotation and vertical displacement at point A and C are zero. Let us consider the moment equilibrium at point B. The equilibrium equations are as follows

$$(M_{BA} + M_{BC} + K_{s2}\theta_B) = 0 \quad (2.42)$$

$$M_{BA} = M_{BC} = \frac{EI}{L}(s_{ij}\theta_A + s_{ji}\theta_B) \quad (2.43)$$

where, the values of s_{ii} and s_{ij} can be calculate by equation (2.13) and (2.14).

From the boundary conditions at point A and C, rotation at A and C is zero

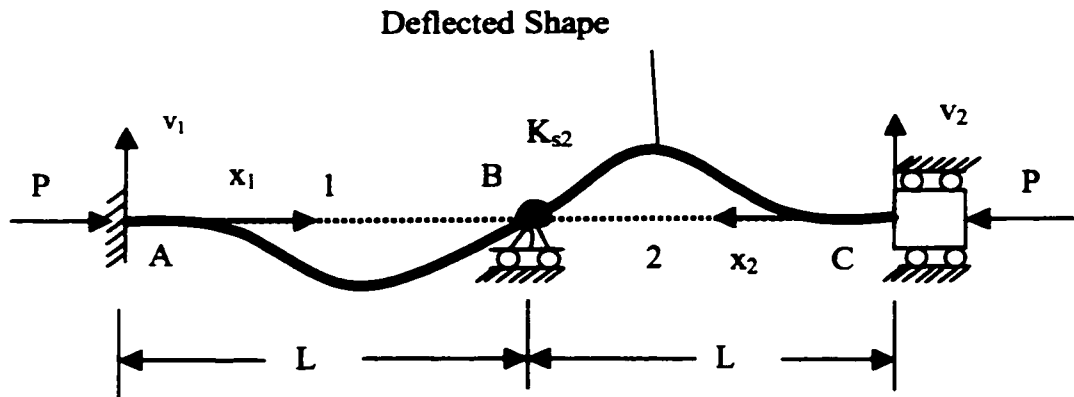


Fig. 2.5 Beam-column model with fixed ends and elastic rotational restraint at cross-brace location

$$\theta_A = \theta_C = 0 \quad (2.44)$$

Based on (2.42), (2.43) and (2.44), the characteristic equation is derive

$$s_{ii} + \frac{LK_{s2}}{2EI} = 0 \quad (2.45)$$

For several values of K_{s2} , the solutions are given in Table 2-3.

Table 2-3: Relationship between K_{s2} and Effective Length Factor

$n_1 = K_{s2}/(EI/L)$	0	1	2	4	8	16	32	∞
kL	4.493	4.653	4.792	5.018	5.328	5.662	5.928	6.283
Effective Length factor K	0.350	0.338	0.328	0.313	0.295	0.278	0.265	0.25

For the special case of diagonals in the steel towers tested, where $K_{s2}=4EI/(2.6L)$

$$kL = 4.702 \quad (2.46)$$

and the critical load is

$$C_{\sigma} = \frac{\pi^2 EI}{(0.668L)^2} \quad (2.47)$$

and the effective length factor is 0.334 of 2L.

2.4 MODEL 3: BEAM-COLUMN WITH ELASTIC ROTATIONAL RESTRAINTS AT ENDS AND AT CROSS-BRACE LOCATION

In this section, let us consider that a diagonal is modeled as a two-span continuous beam-column with elastic restraints at end points, and at cross-brace location.

Fig. 2.6 demonstrates this model, the spring constant of both ends is K_{s1} , and the spring coefficient at cross-brace location is K_{s2} . At three supports, vertical displacement is zero. At point A, horizontal movement is not allowed, but at points B and C, their horizontal movement is possible by providing roller supports.

Since the model is symmetric, under the load, the rotation at A and C is equal. Let us suppose that there is rotation θ_A at A and C and θ_B at point B. The equilibrium equation at point A and B are as follows respectively

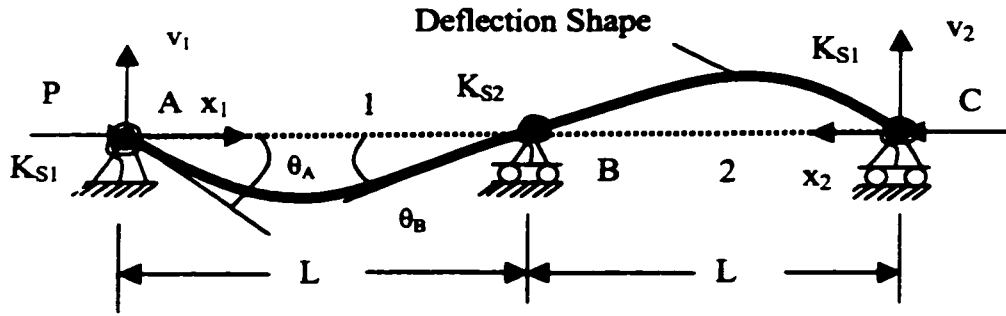


Fig. 2.6 Beam-column model with elastic rotational restraints at ends and at cross-brace location

$$M_A = \frac{EI}{L}(s_{ii}\theta_A + s_{ij}\theta_B) + K_{s1}\theta_A = 0 \quad (2.48)$$

$$M_B = 2\frac{EI}{L}(s_{ij}\theta_A + s_{ii}\theta_B) + K_{s2}\theta_B = 0 \quad (2.49)$$

where the values of s_{ii} and s_{ij} are expressed in Eqs. (2.13) and (2.14) respectively. Let

$$K_{s1} = n_1 \frac{EI}{L} \quad K_{s2} = n_2 \frac{EI}{L} \quad (2.50)$$

The characteristic equation of this model is

$$(s_{ii} + n_1)(2s_{ii} + n_2) - 2s_{ij}^2 = 0 \quad (2.51)$$

For every pair of n_1 and n_2 , its critical load can be solved by trial and error method.

Now let us consider the case of tower diagonals. In Fig. 2.7, two panels of steel tower are shown, where the rotation of legs at end nodes is fixed. The diameter of legs is D , and the diameter of diagonal is d . The length of leg of one panel is l , and the whole length of

diagonal is $2L$, the angle between diagonal and leg is α . Based on this model, the spring constant of diagonal at end point K_{s1} is derived approximately as follows:

$$T = 2M \sin \alpha \quad (2.52a)$$

$$\varphi_1 = \frac{T}{GJ} \quad (2.52b)$$

$$J = \frac{1}{32} \pi D^4 = 2I \left(\frac{D}{d} \right)^4 \quad (2.52c)$$

$$\varphi_2 = \varphi_1 \sin \alpha \quad (2.52d)$$

where, T is the torque of the leg;

M is the out of plane bending moment of diagonal at end point;

J is the torsion constant of leg;

I is the moment inertia of diagonals;

φ_1 is the rotational angle of leg at connection point;

φ_2 is the out-of- plane bending angle of diagonals.

From Eq. (2.52a) to (2.52d), the moment M is expressed as follows:

$$M = \frac{EI}{L} \left(\frac{(\frac{D}{d})^4 L}{3l \sin^2 \alpha} \right) \varphi_2 \quad (2.52e)$$

It is obvious that K_{s2} is as follows:

$$K_{s1} = \frac{EI}{L} \left(\frac{(\frac{D}{d})^4 L}{3l \sin^2 \alpha} \right) \quad (2.52)$$

Let

$$m = D/d$$

The coefficient n_1 in equation (2.51) is

$$n_1 = \frac{m^4 L}{3l \sin^2 \alpha} \quad (2.53)$$

As has been known, the coefficient n_2 is equal to $4/2.6$. In order to discuss the effect of

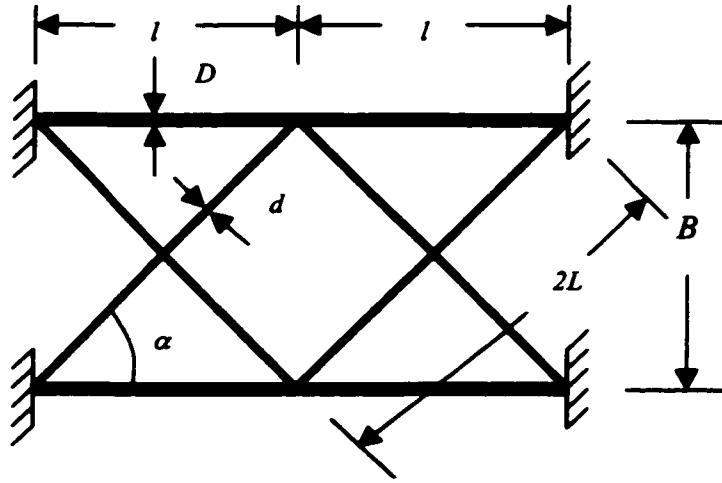


Fig. 2.7 Two panels of steel tower model

leg restraint on the diagonal, equation (2-51) is rewritten

$$(s_{ii} + n_1)(2s_{ii} + \frac{4}{2.6}) - 2s_{ij}^2 = 0 \quad (2.54)$$

Let

$\alpha=50^\circ$, $B=914$ mm , $l=762$ mm, then

$$n_1 = 0.4435m^4 \quad (2.55)$$

From Table 2-4, if the diameter ratio of leg to diagonal is larger than 3, diagonals can be regarded as fixed supports at the end nodes when diagonals connect with legs. By comparing the critical loads of different leg sizes of towers, it is found that error is less than 5% in calculation of critical load of the diagonals.

In this model, almost all restraint factors on diagonals are considered. Thus it is the most accurate model in theoretical analysis of cross-braced diagonals in steel communication towers, but it is very inconvenient to use because direct critical load formulas are

impossible to be given and because there are two spring constants waiting to be determined. Fortunately, diameter of the legs is usually larger than three times that of diagonals. Thus, the diagonals can be regarded as fixed at the nodes connected with legs.

Table 2-4 Relationship between K_{s1} and Effective Length Factor

Spring Coefficient $n_1 = K_{s1}/(EI/L)$	0	1	2	4	8	16	32	∞
kL	3.328	3.594	3.782	4.025	4.268	4.454	4.569	4.698
Effective Length factor K	0.472	0.437	0.416	0.391	0.368	0.353	0.344	0.345

2.5 SUMMARY

The general theories about stability problem of two-span beam-columns are derived in detail in this chapter. For several kinds of boundary conditions, their effective length factors are computed. Although deflected shapes vary from case to case, anti-symmetric full sine-wave deflected shapes have the lowest buckling loads. The actual effective length factor depends on the connection, and the ratio of stiffness between members.

For the special case of steel towers tested, fixed end support model, as described in section 2.3.2, is regarded to be accurate enough in the determination of effective length factor. The following chapter is based on this model to study the load-deflection behavior of diagonals in steel towers.

CHAPTER 3

LOAD-DEFLECTION BEHAVIOR (ELASTIC STAGE)

3.1 GENERAL

The critical axial forces and the effective length factors of several models of cross-braced diagonals in steel communication towers were fully investigated in Chapter 2, where it was assumed that the beam-column was perfectly straight. In fact, this perfect beam-column does not exist. There is a slightly initial deflection in every beam-column, even though it looks very straight. This initial imperfection will affect the behavior of beam-column. The buckling load will be smaller than that of the ideal one, and the deflections will increase gradually. This is different from the behavior of ideal beam-column in which deflection happens suddenly. In order to further investigate the behavior of cross-braced diagonals, initial deflections should be considered.

In this chapter, the material is still assumed to be elastic, and the deflections are small. That means only second order nonlinear problem is considered. Initial deflection can be expressed as the Fourier series:

$$v_0(x) = a_0 + \sum_{i=1}^{\infty} (a_i + jb_i)e^{-j(i\pi x)} \quad (3-1)$$

The initial deflection should satisfy the boundary conditions and continuity conditions. Another fact that should be known is that initial deflection can be decomposed into two parts: symmetric initial deflection and anti-symmetric initial deflection, as shown in Eqs. (3-2), and their effects can be superimposed.

$$v_0 = v_{10} + v_{20} \quad (3-2)$$

where, v_0 is the total initial deflection of beam-column, v_{10} and v_{20} are symmetric initial deflection and anti-symmetric initial deflection respectively.

Usually, two or three items of equation (3-1) are accurate enough for practical purposes. Based on this theory, two series of initial deflections (one symmetric and the other anti-symmetric) are considered in the analysis of the load-deflection behavior of cross-braced diagonals. From Chapter 2, it is found that the beam-column model with fixed ends and elastic rotational restraint at cross-brace location (Fig 2-5) is accurate enough, and therefore will be used for analysis in this chapter.

3.2 SYMMETRIC DEFLECTION

Diagonals in tower are members of cross-braced structure. They are welded together at the intersection point. The equation of initial deflection is as (3-3) for section 1 (Fig. 3.1), since the model is symmetric and it is sufficient to consider one-half of the diagonal.

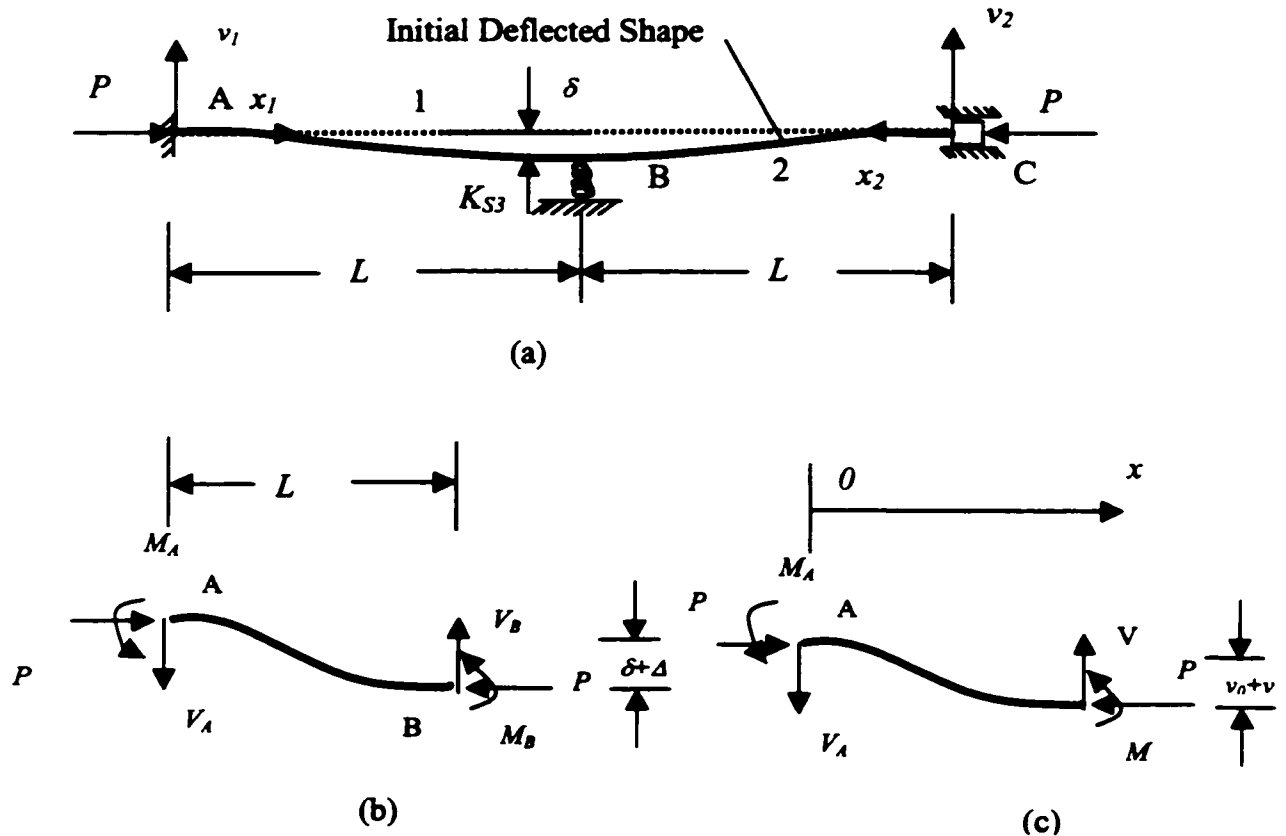


Fig. 3.1 Symmetric initial deflection of the beam-column model with fixed ends and elastic rotational restraint at cross-brace location

Assume that the initial deflection of diagonal is

$$v_0 = \frac{\delta}{2} (1 - \cos(\pi \frac{x}{L})) \quad (3-3)$$

Referring to Fig. 3.1b, the equilibrium equation is expressed as

$$M_A = -V_A L - M_B + P(\delta + \Delta) \quad (3-4)$$

where,

$$V_B = V_A = \frac{1}{2} K_{s3} \Delta \quad (3-5)$$

Δ = deflection at B

V_A, V_B = shear force at A and B respectively

M_A, M_B = bending moment at A and B respectively

K_{s3} = vertical spring constant at B

At an arbitrary point of segment 1 (see Fig. 3-1c), the equation of equilibrium can be written as

$$M_A + M + V_A x - P(v_0 + v) = 0 \quad (3-6)$$

which can be rewritten as equation (3-7) or (3-7a), if the initial deflection equation is substituted into equation (3-6):

$$-EIv'' - P(v_0 + v) + M_A + \frac{1}{2} K_{s3} \Delta x = 0 \quad (3-7)$$

$$EIv'' + Pv - \frac{1}{2} P\delta \cos \frac{\pi x}{L} - \frac{1}{2} K_{s3} \Delta x - M_A + \frac{1}{2} P\delta = 0 \quad (3-7a)$$

Assume that the general solution of differential equation (3-7a) is

$$v = A \sin(kx) + B \cos(kx) + C \cos(\frac{\pi x}{L}) + Dx + E \quad (3-8)$$

By substituting Eq. (3-8) into Eq. (3-7a), the following expressions are derived.

$$C = \frac{P\delta}{2P - 2EI\left(\frac{\pi}{L}\right)^2} \quad (3-9)$$

$$D = \frac{K_{s3}\Delta}{2P} \quad (3-10)$$

$$E = \frac{M_A}{P} - \frac{\delta}{2} \quad (3-11)$$

Now, let us consider the boundary conditions of segment 1: the rotation and movement at A are fixed. Since the structure will deflect in a symmetric way, the rotation at B is equal to zero. Thus the following boundary conditions should be considered:

$$v_I(0)=0, \quad v_I'(0)=0, \quad v_I(L)=\Delta, \quad v_I'(L)=0 \quad (3-12)$$

Substituting these into Eq. (3-8),

$$B + C + \frac{M_A}{P} - \frac{\delta}{2} = 0 \quad (3-13)$$

$$Ak \cos kL - Bk \sin kL - C + \frac{K_{s3}\Delta}{2P} = 0 \quad (3-14)$$

$$Ak + \frac{K_{s3}\Delta}{2P} = 0 \quad (3-15)$$

$$A \sin kL + B \cos kL - C + \frac{K_{s3}\Delta}{2P} L + \left(\frac{M_A}{P} - \frac{\delta}{2}\right) - \Delta = 0 \quad (3-16)$$

By solving Eq. (3-9) to (3-11) and (3-13) to (3-16), unknowns A, B, C, D, E, Δ , and M_A , are expressed in terms of the axial force P:

$$C = \frac{P\delta}{2P - 2EI\left(\frac{\pi}{L}\right)^2} \quad (3-17)$$

$$\Delta = \frac{2C \sin kL}{\frac{K_{s3}}{2kP}(2 \cos kL + kL \sin kL - 2) - \sin kL} \quad (3-18)$$

$$A = -\frac{K_{s3}}{2kP} \Delta \quad (3-19)$$

$$B = \frac{K_{s3}}{2kP} \left(\frac{1}{\sin kL} - c \tan kL \right) \Delta \quad (3-20)$$

$$D = \frac{K_{s3}}{2P} \Delta \quad (3-21)$$

$$E = \frac{M_A}{P} - \frac{\delta}{2} \quad (3-22)$$

where,

$$M_A = \left(\frac{\delta}{2} - B - C \right) P \quad (3-23)$$

It should be noted that these solutions are based on the assumption that the material behaves elastically and the deflections are small. That means these solutions can only be used when M_A and M_B are less than the value of yield moment, M_y , of diagonals.

$$M_B = -\frac{1}{2} K_{s3} \Delta L - M_A + P(\delta + \Delta) \quad (3-24)$$

It should also be pointed out that K_{s3} is assumed to be constant in Eqs. (3-16) to (3-24). In fact, K_{s3} will increase as tension force in tension diagonal increases. If tension force is taken into account, K_{s3} can be expressed as follows [Picard and Beaulieu, 1987]

$$K_{s3} = \frac{6EI}{L^3} + 2.18 \frac{T}{L} \quad (3-25)$$

where, T is the axial tension force in tension diagonal. Thus K_{s3} is increased as the force in the tension diagonal increases.

3.3 ANTI-SYMMETRIC DEFLECTION

Another initial deflection that is different from the previous one is the anti-symmetric initial deflection.. Usually the maximum value of deflection is taken as 0.1% of the span, that is $\delta = L/1000$. Since the initial deflection curve is anti-symmetric, the deflection of diagonal will also be anti-symmetric. Thus the model of Fig. 3.2 can be used.

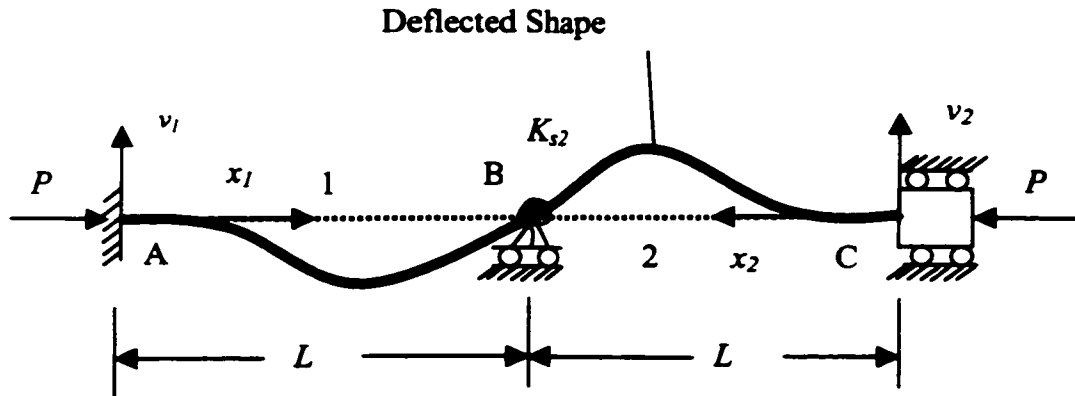


Fig. 3.2 Anti-symmetric initial deflection of the beam-column model with fixed ends and elastic rotational restraint at cross-brace location

3.3.1 General deflection equation

The general deflection equation of beam-column is [Chen and Liu 1987]

$$v_1 = -\frac{1}{Elk^2} \left(\frac{\cos kL}{\sin kL} \sin kx_1 - \cos kx_1 - \frac{x_1}{L} + 1 \right) M_A - \frac{1}{Elk^2} \left(\frac{\sin kx_1}{\sin kL} - \frac{x_1}{L} \right) M_B \quad (3-26)$$

from which

$$v_1' = -\frac{1}{Elk} \left(\frac{\cos kL}{\sin kL} \cos kx_1 + \sin kx_1 - \frac{1}{kL} \right) M_A - \frac{1}{Elk} \left(\frac{\cos kx_1}{\sin kL} - \frac{1}{kL} \right) M_B \quad (3-26a)$$

The rotation at A and B can be expressed as follows:

$$\theta_A = \frac{L}{EI} \left(\frac{\sin kL - kL \cos kL}{(kL)^2 \sin kL} \right) M_A + \frac{L}{EI} \left(\frac{\sin kL - kL}{(kL)^2 \sin kL} \right) M_B \quad (3-27)$$

$$\theta_B = \frac{L}{EI} \left(\frac{\sin kL - kL}{(kL)^2 \sin kL} \right) M_A + \frac{L}{EI} \left(\frac{\sin kL - kL \cos kL}{(kL)^2 \sin kL} \right) M_B \quad (3-28)$$

From Eq. (3-27) and (3-28), bending moment of M_A and M_B can be expressed as the function of θ_A and θ_B as follows:

$$M_A = \frac{EI}{L} (s_{ii} \theta_A + s_{ij} \theta_B) \quad (3-29)$$

$$M_B = \frac{EI}{L}(s_{ij}\theta_A + s_{ii}\theta_B) \quad (3-30)$$

where

$$s_{ii} = \frac{kL \sin kL - (kL)^2 \cos kL}{2 - 2 \cos kL - kL \sin kL} \quad (3-31)$$

$$s_{ij} = \frac{(kL)^2 - kL \sin kL}{2 - 2 \cos kL - kL \sin kL} \quad (3-32)$$

Let us investigate the boundary condition at point A. The end is fixed, that is

$$\theta_A = 0 \quad (3-33)$$

On the other hand, the equilibrium equation at B can be written as

$$2M_B + K_{s2}\theta_B = 0 \quad (3-34)$$

From Chapter 2,

$$K_{s2} = \frac{4}{2.6} \frac{EI}{L} \quad (3-35)$$

After simplification, Eq. (3-26) becomes

$$v_1 = -\frac{M_A}{EI k^2} (1 - \cos kx_1 + 0.1771 \sin kx_1 - 0.8328 \frac{x_1}{L}) \quad (3-36)$$

where

M_A is the bending moment at point A,

I is the moment of inertia of the diagonal, and

$$k=4.702/L$$

from which,

$$v_1' = -\frac{M_A}{EI k} (\sin kx_1 + 0.1771 \cos kx_1 - 0.8328 \frac{1}{kL}) \quad (3-37)$$

The maximum deflection is at the point where v' is equal to zero. That is

$$x_1 = 0.593L \quad (3-38)$$

and the maximum deflection is

$$v_{\max} = -\frac{3M_A}{2EI k^2} \quad (3-39)$$

3.3.2 Load-deflection equation

When an ideal column is compressed, deflections do not exist before buckling. But every beam-column has initial deflection (imperfection). After the axial compression force is applied, the deflection will become larger and larger. In the section 3.2, the symmetric initial deflection was discussed. At the beginning, the symmetric deflection is restrained by tension diagonal to some degree. As this symmetric deflection becomes larger, the restraint of tensional diagonal becomes larger. In the end, this kind of deflection is fully restrained, and it doesn't increase any more. At this time, anti-symmetric mode develops very fast. In order to investigate this behavior, the following anti-symmetric initial deflection is considered:

$$v_0 = \delta(1 - \cos kx_1 + 0.1771 \sin kx_1 - 0.8328 \frac{x_1}{L}) \quad (3-40)$$

and the assumed general solution is

$$v_1 = \Delta(1 - \cos kx_1 + A \sin kx_1 - B \frac{x_1}{L}) \quad (3-41)$$

By substituting this initial deflection equation (3-40), and general solution equation (3-41) to differential equilibrium equation (3-42) of segment 1 in diagonal (See Fig.3.2),

$$EI v_1'' + P(v_0 + v_1) + (1 - \frac{x}{L})M_A - \frac{x_1}{L}M_B = 0 \quad (3-42)$$

the following results can be derived

$$\Delta = \frac{\delta P}{C_{\sigma} - P} \quad (3-43)$$

$$A = 0.1771 \quad (3-43a)$$

$$B = 0.8328 \quad (3-43b)$$

where, C_{σ} is the critical load of diagonal. It is rewritten in (3-43c)

$$C_{\sigma} = \frac{\pi^2 EI}{(0.668L)^2} \quad (3-43c)$$

It is interesting to find that the shape of deflection is the same as the initial one. The amplification factor of deflection is

$$A_{amp} = \frac{1}{1 - \frac{P}{C_{\sigma}}} \quad (3-44)$$

3.4 SUMMARY

Two kinds of initial deflections are investigated in this chapter, one symmetric curve, and the other anti-symmetric curve. Their general solutions are obtained by substituting assumed deflection equations into differential equilibrium equation. Since one is symmetric and the other is anti-symmetric, the two cases are independent. They can be superposed into a general solution for the diagonals of steel tower. The theories in this chapter are based on the assumption that the material is elastic. Elastic-plastic behavior is studied in Chapter 6.

CHAPTER 4

EXPERIMENTAL INVESTIGATION

4.1 GENERAL

Theoretical studies about elastic-plastic behavior of cross-braced diagonals are very difficult, if not impossible. Experimental investigation should be carried out for practical engineering. Many design standards heavily rely on the results of tests.

The purpose of the experimental investigation is:

1. To estimate the effective length factors of cross-braced diagonals.
2. To investigate load-deflection behavior of diagonals.
3. To determine factors affecting the stability of diagonals
4. To observe the buckling mode.

Twenty six specimens of prototype communicational tower sections, with different sizes of diagonals and legs, were tested. Diagonals of all of the specimens were solid round sections connected to legs with welds. All the specimens were loaded with a vertical concentrated vertical load until failure. For all specimens, strain gauges were attached at critical locations to determine the load at failure of the diagonal. Out-of-plane deflections of the diagonals were measured by means of five dial gauges located along the length of the compression diagonal. Tension tests of diagonals were carried out to determine the yield stress of diagonals.

4.2 EXPERIMENTAL SET-UP

4.2.1 Overview of set-up

The specimens were placed in a horizontal position, with simple supports at the ends. A central concentrated load on the top leg was applied as shown in Fig. 4.1. One photo picture of test set-up is also enclosed in Appendix-A (Fig. A-2). It is known that

specimens without horizontals most likely will fail first in panel C (for 6-panel specimens) or panel D (for 8-panel specimens). Specimens with horizontals most likely will fail first in the panel adjacent to the support. In order to study the behavior of diagonals, it is important to instrument the diagonal which is most likely to fail first. If there are no horizontals at middle of specimen, panel adjacent to the centre was chosen for test; otherwise, panel near the support was chosen. In order to make sure that the instrumented compression diagonal failed first, all other compression diagonals were reinforced with angles and U-clamps. It proved to be effective.

4.2.2 Strain measurements

Electric resistance strain gauges, type N11-FA-5-120-11, with a gauge length of 5 mm, 120.3 Ω , were used to measure strains of the compression and tension diagonals. The location of strain gauges is shown in Fig. 4.2. At every section, one pair of strain gauges was attached, one outside and one inside (both out-of-plane) as shown in Fig. 4.2b and Fig.4.2c. Before strain gauges were attached, the surface was polished by grinding and cleaning. Immediately after the gauge attachment points well prepared and dry, strain gauges with special adhesive were pressed on the diagonal. To keep the strain gauge axes parallel to the longitudinal axis of the diagonal is also very important. Usually eight pairs of strain gauges were attached, half for front panel, and half for rear panel. But for some specimens, additional strain gauges were necessary for checking of equilibrium. It took about twelve hours for glue to be dry enough to transfer the strain. The strain gauge was soldered with a wire and connected to the Datascan data acquisition system, which was used to record the data of both loads and strains. Datascan can be used in many kinds of measurement. For the measurement of axial strain, the electric circuit should be connected as half bridge. The amplifier should be set to fit with the gauge factor.

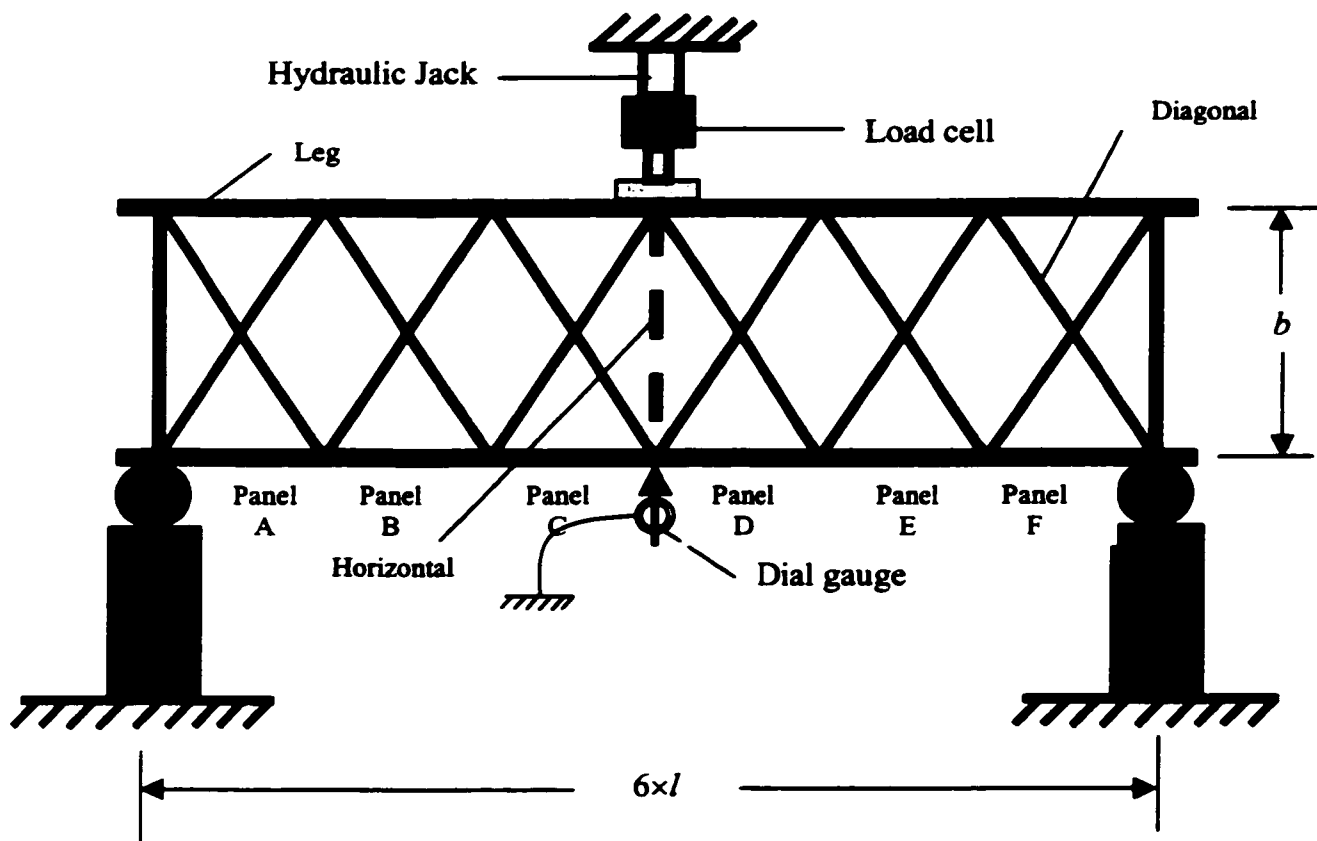


Fig. 4.1a Front view of specimen with six panels in test position

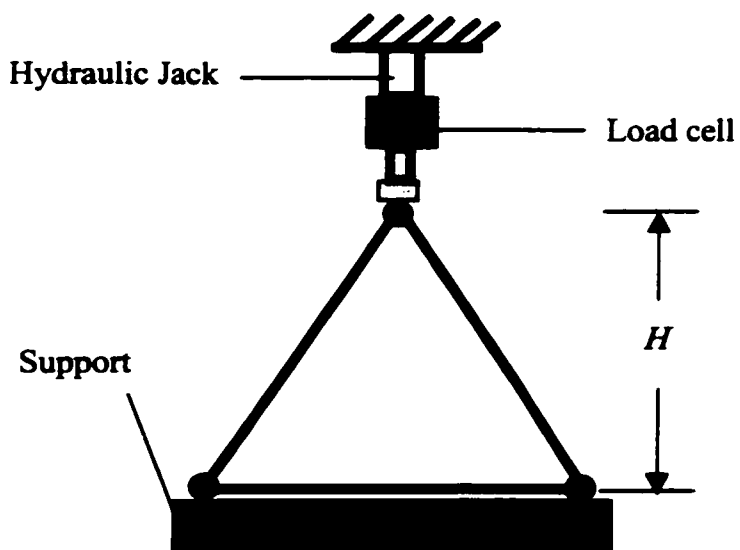


Fig. 4.1b Cross-section of specimen

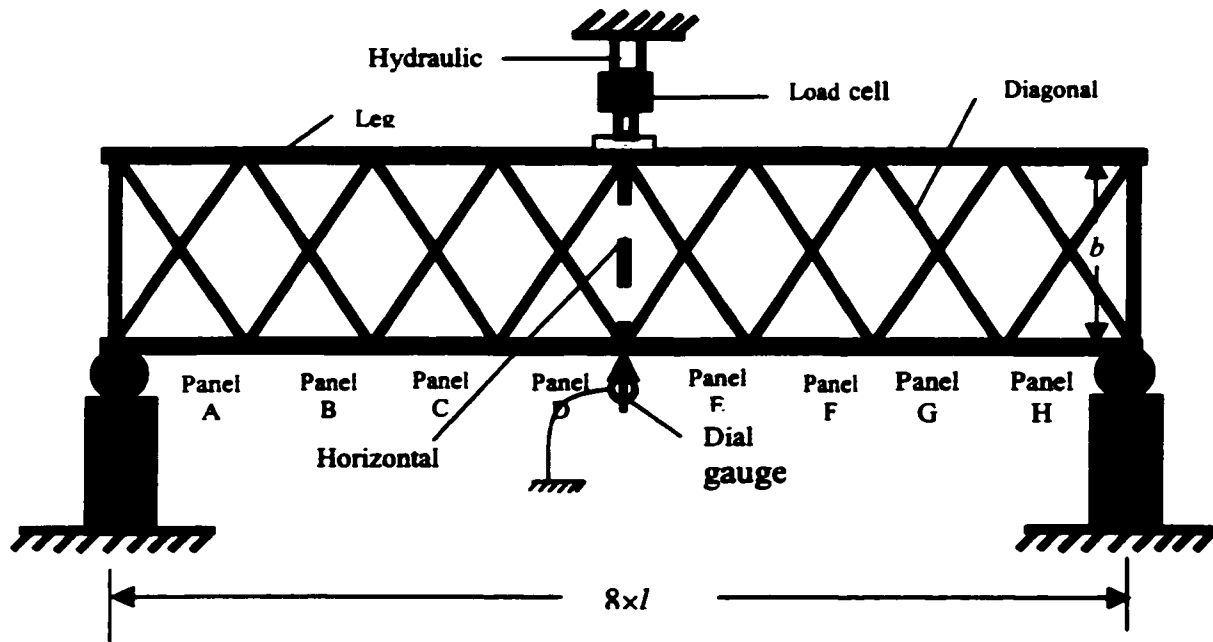


Fig. 4.1c Front view of specimen with eight panels in test position

Fig. 4.1 Test set-up overview

4.2.3 Deflection measurements

Dial gauges were used for deflection measurement. In order to find out the deflected shape of the diagonal, five dial gauges were attached to the front face of the compression diagonal. The locations of dial gauges are shown in Fig. 4.3. (The values of x_1 , x_2 , x_3 , x_4 , and x_5 are given in Appendix B for all specimens). All dial gauges were attached to measure the out-of-plane deflection.

Shims were attached to the compression diagonal at each gauge location point, to facilitate reading of deflections. It was ensured that dial gauges were perpendicular to the

shims. It was observed that if the compression diagonal was inside the tension diagonal, then that diagonal would deflect initially towards inside of the tower; if the compression

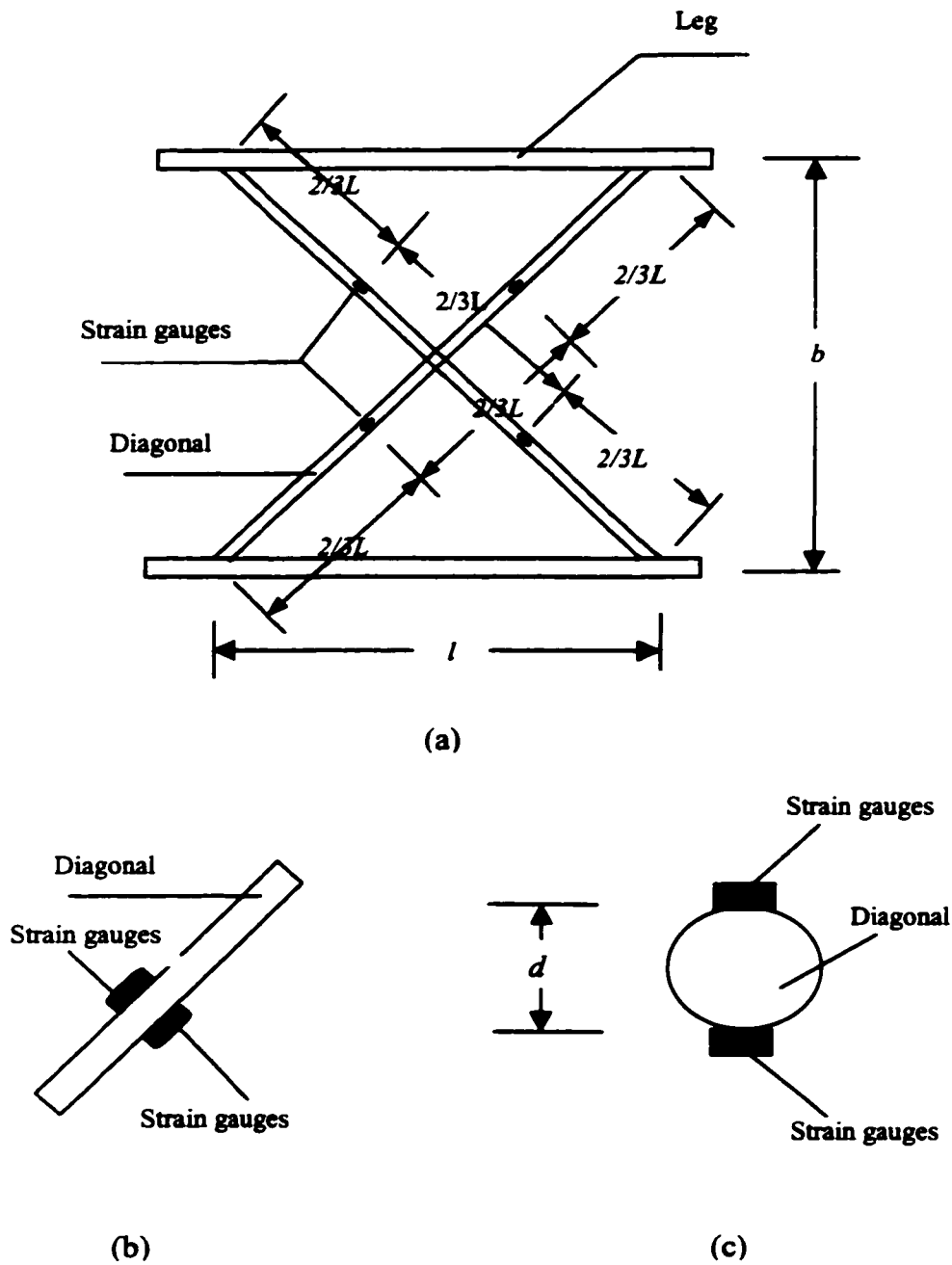


Fig. 4.2 Location of strain gauges

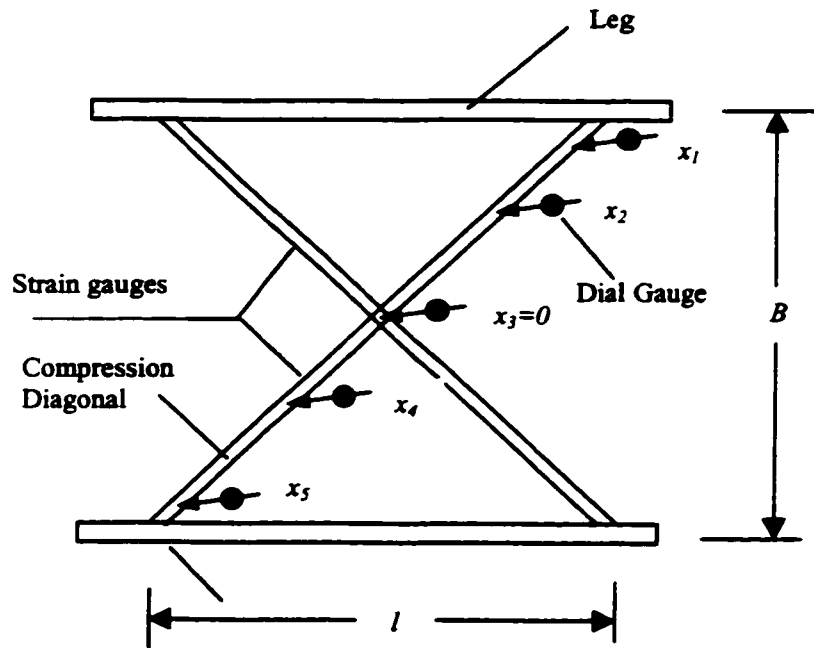


Fig. 4.3 Location of dial gauges

diagonal was outside the tension diagonal, it would initially deflect outside of the tower. Vertical deflections at midspan were also recorded for completeness, though not utilized in this thesis.

4.3 TEST PROCEDURE

First, test number and identification of the specimen were noted down. Geometry of specimen, including diameters of leg, diagonal and horizontal were measured and test diagonals were located.

Second, the ultimate failure load of the test specimen (tower structure) was estimated, and the test frame was checked to ensure that it can carry this load safely. The capacity of the load cell and hydraulic jack were also checked.

Third, the specimen was placed in test position and sections to be strain gauged were polished and well prepared. Strain gauges were attached. Other compression diagonals were reinforced.

Fourth, after twelve hours, strain gauges were soldered with wires and connected to Datascan. Dial gauges were attached after that. The load cell was connected to the Datascan in full bridge circuit.

Fifth, one-tenth of estimated failure load was applied on specimen and released; this process was repeated three times. Every time, data were taken and checked to see if the test is normal.

Sixth, load was applied step by step. In the initial stages of loading, the load increments were approximately one-tenth of the estimated failure load and load, strain and deflection data were taken. Towards advanced stages of loading, load increments were kept small so that the failure load could be noted. Attention was paid to the deformation of specimen. Load was increased until the specimen failed. If possible, test was continued until both front and rear diagonals buckled. Location of failure, failure load and mode of buckling of compression diagonal were noted.

Seventh, two or three of sections of diagonal were cut and tensile tests were carried out to determine the yield stress of the material of the diagonal.

4.4 DESCRIPTION OF SPECIMENS AND TEST RECORD

Test specimens were provided by two different company of United States.

- Fourteen Specimens identified with ID # starting with "S" were provided by ERI, Inc., Chandler, Indiana, USA.
- Twelve Specimens identified with ID # starting with "P" were provided by PIROD Inc., Plymouth, Indiana, USA.

Diagonals are connected with legs by welding, but there are two types of connections as shown in Fig. 4.4.

Type A: Diagonals were cut, and welded to legs.

Type B: Diagonals were bent, and welded to legs.

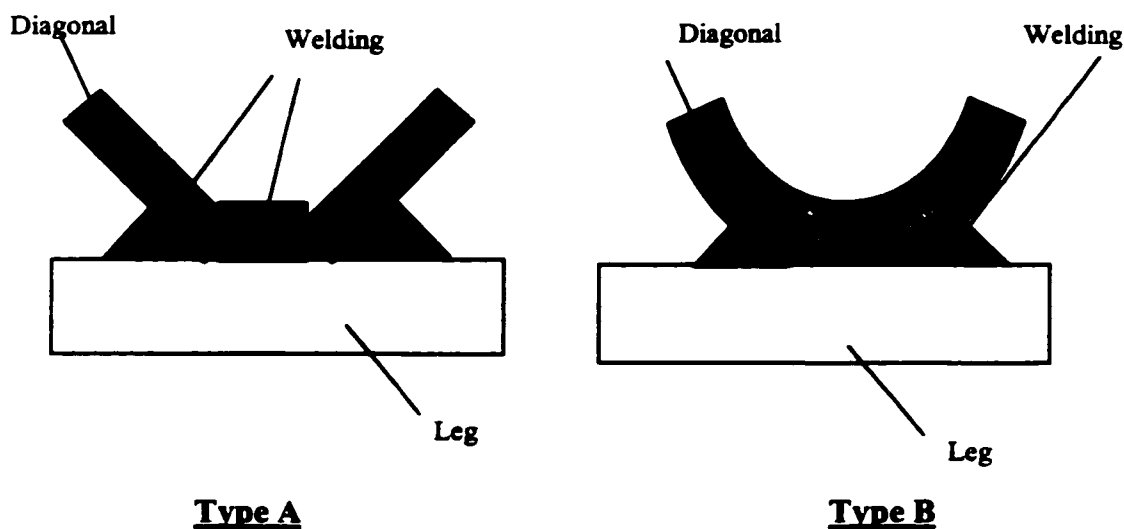


Fig. 4.4 Detail of connection between diagonals and legs

Diagonals were arranged with compressed diagonals inside and tensile diagonals outside, or vice versa. If, in one face in one panel, the compression diagonal is inside, then the compression diagonal must be outside on the same face in the adjacent panel. In addition, symmetry about span center must be maintained. Another rule of arrangement is that in the same panel, if the compression diagonal in the front face is inside, then the one on rear face must be outside, and vice versa (See Fig. A-2).

Details of specimens and test records are given in Tables A-1 to A-34.

CHAPTER 5

ANALYSIS OF TEST RESULTS

5.1 GENERAL

The test results, as expected, greatly support the theories developed in Chapters 2 and 3. Analyses of test data and comparison of the experimental results and theoretical analysis are described in this chapter in detail. The factors affecting effective length factor are investigated further. The behavior of diagonals in steel tower are explored. With these efforts, the behavior of diagonals in the elastic state was clearly understood.

5.2 EFFECTIVE LENGTH FACTOR

5.2.1 Experimental versus theoretical values

The problem of effective length factor was investigated experimentally by Sun (1999) already. The test results are listed in Appendix-A. But some problems still deserve to be discussed. The effective length factors of each test specimen by both AISC-LRFD and CSA S16.1-94 are listed in Table 5-1. The theoretical effective length factor is based on characteristic equation (2.54) which, in turn, depends on the ratio of the diameter of leg to the diameter of the diagonal.

Effective length factors computed from theory, CSA S16.1-94 and AISC-LRFD are compared in Fig. 5.1. An examination of Fig. 5.1 shows that the experimental values lie evenly about the theoretical curve, indicating good agreement between theory and tests. Thus theory and tests reinforce each other.

Table 5-1 Effective Length Factors of Test Specimens

Test No.	Specimen ID	Test Panel	Dial. of LEG D (mm)	Dial. Of Diag. D (mm)	m= D/d	K Value by AISC-LRFD K ₁	K Value by CSA S16.1-94 K ₂	Theoretical K Value K _T
1	S4A	A	50.8	14.3	3.55	0.353	0.343	0.339
2	S5A	C (Front)	69.9	15.9	4.40	0.420	0.416	0.336
		C(Rear)	69.9	15.9	4.40	0.427	0.424	0.336
3	S4B	A	50.8	14.3	3.55	0.317	0.296	0.339
4	S2A	A(Front)	38.1	12.7	3.00	0.325	0.318	0.343
		A(Rear)	38.1	12.7	3.00	0.330	0.325	0.343
5	S4C	A(Front)	50.8	14.3	3.55	0.342	0.327	0.339
		A(Rear)	50.8	14.3	3.55	0.332	0.313	0.339
6	S1A	C(Front)	38.1	12.7	3.00	0.333	0.325	0.343
		C(Rear)	38.1	12.7	3.00	0.355	0.352	0.343
7	S3A	C(Front)	50.8	14.3	3.55	0.343	0.331	0.339
		C(Rear)	50.8	14.3	3.55	0.360	0.351	0.339
8	S2B	A(Front)	38.1	12.7	3.00	0.337	0.333	0.343
		A(Rear)	38.1	12.7	3.00	0.337	0.333	0.343
10	S5B	C	69.9	15.9	4.40	0.336	0.312	0.336
11	S6A	A(Front)	69.9	15.9	4.40	0.374	0.358	0.336
		A(Rear)	69.9	15.9	4.40	0.361	0.342	0.336
12	S5C	C(Front)	69.9	15.9	4.40	0.362	0.343	0.336
		C(Rear)	69.9	15.9	4.40	0.355	0.334	0.336
13	S6B	A	69.9	15.9	4.40	0.375	0.387	0.336
15	P6B	D	57.2	22.2	2.58	0.359	0.323	0.349
19	P8B	D	38.1	22.2	1.72	0.394	0.355	0.391
20	P4B	D(Front)	50.8	19.1	2.66	0.399	0.369	0.350
		D(Rear)	50.8	19.1	2.66	0.405	0.376	0.350
21	P2A	D	50.8	19.1	2.66	0.368	0.345	0.350
23	S2C	A(Front)	38.1	12.7	3.00	0.337	0.319	0.343
		A(Rear)	38.1	12.7	3.00	0.328	0.315	0.343
25	S3B	C(Front)	50.8	14.3	3.55	0.351	0.342	0.339
		C(Rear)	50.8	14.3	3.55	0.353	0.345	0.339
27	P2B	D(Front)	38.1	15.9	2.40	0.414	0.403	0.354
		D(Rear)	38.1	15.9	2.40	0.364	0.341	0.354
28	P6A	D(Front)	57.2	22.2	2.58	0.393	0.356	0.349
		D(Rear)	57.2	22.2	2.58	0.424	0.388	0.349
29	P4A	D	50.8	19.1	2.66	0.385	0.412	0.350
30	P3A	A(Front)	50.8	19.1	2.66	0.382	0.351	0.350
		A(Rear)	50.8	19.1	2.66	0.396	0.366	0.350
31	P1A	A(Front)	38.1	15.9	2.40	0.391	0.375	0.354
		A(Rear)	38.1	15.9	2.40	0.372	0.351	0.354
32	P3B	A(Front)	50.8	19.1	2.66	0.360	0.327	0.350
		A(Rear)	50.8	19.1	2.66	0.419	0.393	0.350
33	P8A	D	38.1	22.2	1.72	0.425	0.383	0.391
34	P5B	A	57.2	22.2	2.58	0.404	0.367	0.349

5.2.2 Effect of leg size

Diagonals are connected to legs by welding. If the compression diagonal deflects, the end of diagonal will rotate. But this rotation is restrained by leg. The size of leg can affect effective length factor. It is also found from Fig. 5.1 that:

- 1 Effective length factor is related to the ratio of the diameter of the leg and the diameter of the diagonal $m=D/d$. The larger the ratio, the larger the rotational restraint provided by the leg to the diagonal., and the less the effective length factor of the diagonal.

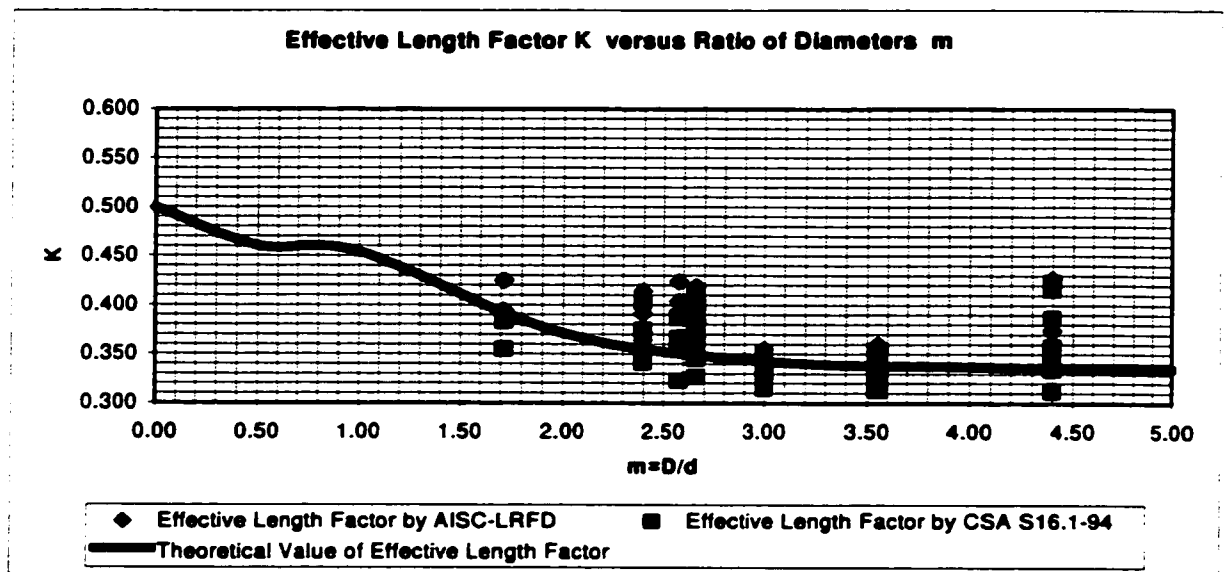


Fig. 5.1 Effective length factor vs. ratio of diameters

- 2 Usually the diameter of leg is larger than three times that of the diagonal. When the ratio is larger than 3, effective length factors change very little. Diagonals can be regarded as fixed at the connection between leg and diagonal. The effective length factor can take a value 0.334.
3. If diameter ratio is less than three, the effect of leg size should be taken into account..

5.2.3 Effect of tension diagonal

As investigated in Chapter 2 by theoretical approach, tension diagonal changes the mode of buckling of compression one. The rotational restraint of tension diagonal increases the buckling load of compression diagonal to some degree. But the value of out-of-plane restraint, mostly provided by bending stiffness of tension diagonal, does not affect the buckling load. In practical engineering, compression diagonal obviously has initial deflection as half sine curve, where the maximum initial value is at cross-brace location. After the load is applied, compression diagonal will bend out-of-plane in the shape of initial deflection, and the tension diagonal will restrain this deflection. If tension diagonal is too weak to resist such deflection, tension diagonal will fail first. Then this restraint is released. Compression diagonal will buckle not in anti-symmetric mode which is regarded as two span beam-column, but in symmetric mode which is regarded as one span beam column with two fixed ends. The tests firmly support this argument. Almost all compression diagonals buckled in anti-symmetric mode.

Tension diagonals play a very important role in cross-braced steel towers. In practice, the direction of transverse load is undetermined. Tension diagonal can become compression diagonal and vice versa. Thus, all cross-braced members should be designed as compression diagonals.

From the tests, it was found that tension force is very small in panel C or D (middle panel, see Fig. 4.1), but the value of tension force in panel A (Panel near support) is almost equal to the axial compression force in compression diagonal. This may be due to vertical deflection of top leg. If top leg is bent, the connection nodes will move down. The forces in tension diagonal will be released. In end panels, on the contrary, bending of legs is very little.

Although the tension force is different in two cases above, the effective length factor does not seem to have been affected (see Table 5.1). Tension force in tension diagonal will increase the restraint to compression diagonals in out-of-plane direction. This increase

does not contribute to reduce the effective length factor. But the load-deflection behavior of compression diagonal will be changed.

On the whole, effective length factor is determined by the geometry of steel tower. Other factors such as elastic modulus and yield stress of material don't relate to it at all.

5.3 DEFLECTION OF DIAGONALS

There are diagonal deflection records of 24 specimens. The deflection shapes and load-deflection curves are included in Appendix-B.

5.3.1 Experimental load-deflection behavior of diagonals

Compression diagonals have initial deflection as described in Chapter 3. During fabrication, tension diagonal and compression diagonal are welded together, and then connected to leg by welding too. The two cross-braced members are not in the same plane, one is bent around the other. On average, the initial deflection at crossing point is about fifty percent of diameter of diagonal. This initial deflection is shown in Fig. 5.2a.

The other kind of initial deflection is anti-symmetric one. This kind of initial deflection is too small to be observed. The maximum value of this deflection is difficult to measure. For design purposes, a value of 0.1 percent of the length of diagonal is assumed.

From the tests, the load-deflection behaviors of diagonals can be found. Buckling of diagonal can be divided into five steps, as shown in Fig. 5.2

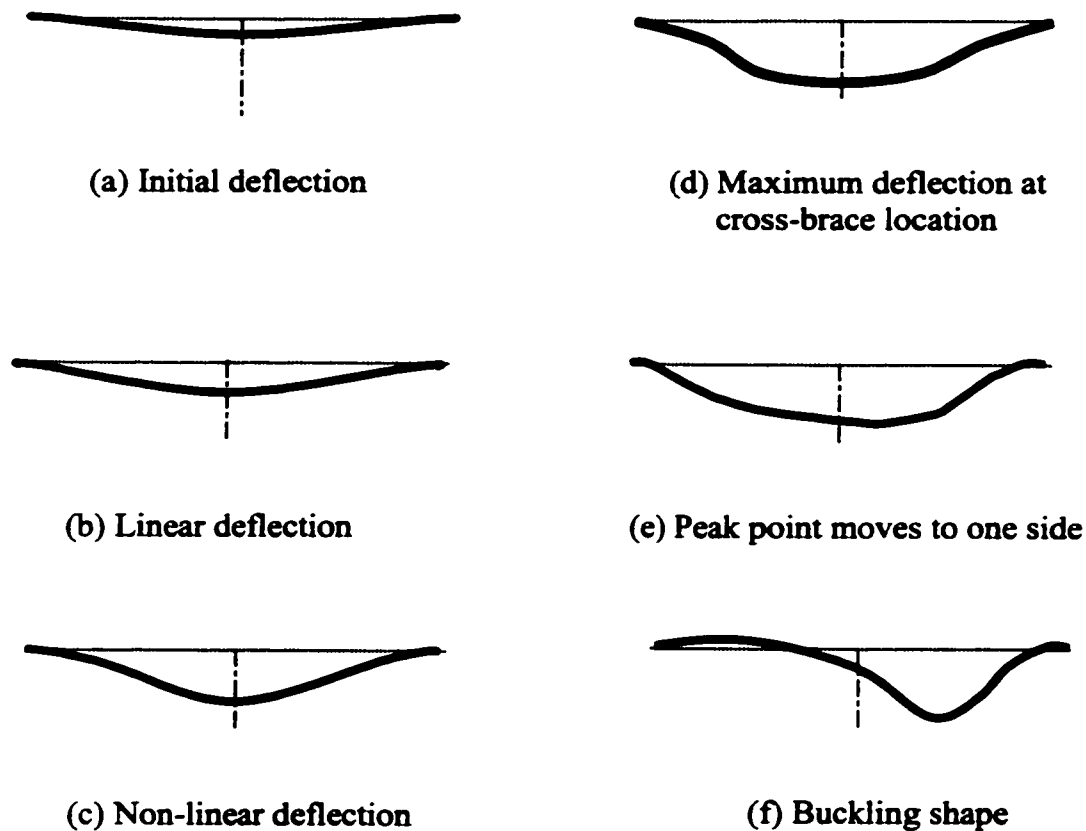


Fig. 5.2 Different stages of buckling of diagonal

1. When the steel tower is loaded with the transverse concentrated load, the diagonals bear the shear force of the tower. Diagonal is bent in the way of initial deflection. The shape of deflection is almost the same as half sine curve which is symmetric curve as shown in Fig. 5.2 b. At the cross-brace location, there is no rotation at all. At this stage, deflection is proportional to the axial compression force of diagonal. Tension force contributes very little to the restraint of deflection.
2. As the load is increasing, the deflection is increasing too. The deflection of diagonal is not proportional to axial compression force at this stage (Fig. 5.2c). The diagonal seems likely to buckle at the cross-brace location. The maximum deflection is still at cross-brace location..

3. The deflection at cross-brace location slows down due to the out-of plane restraint of tension diagonal (Fig. 5.2d). The restraint stiffness increases as tension force becomes large. But deflection at midpoint is still continuing to increase.
4. The deflection at cross-brace location stops (Fig. 5.2e). The location of maximum deflection moves to one side from the centre. Rotation at cross-brace location occurs at this time. Initial deflection of anti-symmetric one becomes dominant. Compression force and tension force remain unchanged. The restraint of tension diagonal stops increasing.
5. The peak of deflection shape transfers to the point at one third of the whole diagonal length (Fig.5.2.f). The peak value increases rapidly. But the deflection at cross-brace location decreases. The axial compression force unloads until the diagonal completely buckles. Buckling load is determined by anti-symmetric initial deflection and buckling mode is anti-symmetric curve.

Deflection shape of diagonal a typical test (Test No. 26-Specimen ID: P5A) is given in Fig. 5-3. Deflection shapes of diagonals of all specimen are given in Appendix-B. Diagonals always buckled out-of-plane. Direction of buckling is determined by the position of compression diagonal. If it is inside of tension diagonal, it will buckle with out-of-plane inside. Otherwise, it will buckle out-of-plane outside. During the tests, deflection in steps 4 and 5 is very difficult to be gauged, since it happens rapidly. The curve is drawn based on observations.

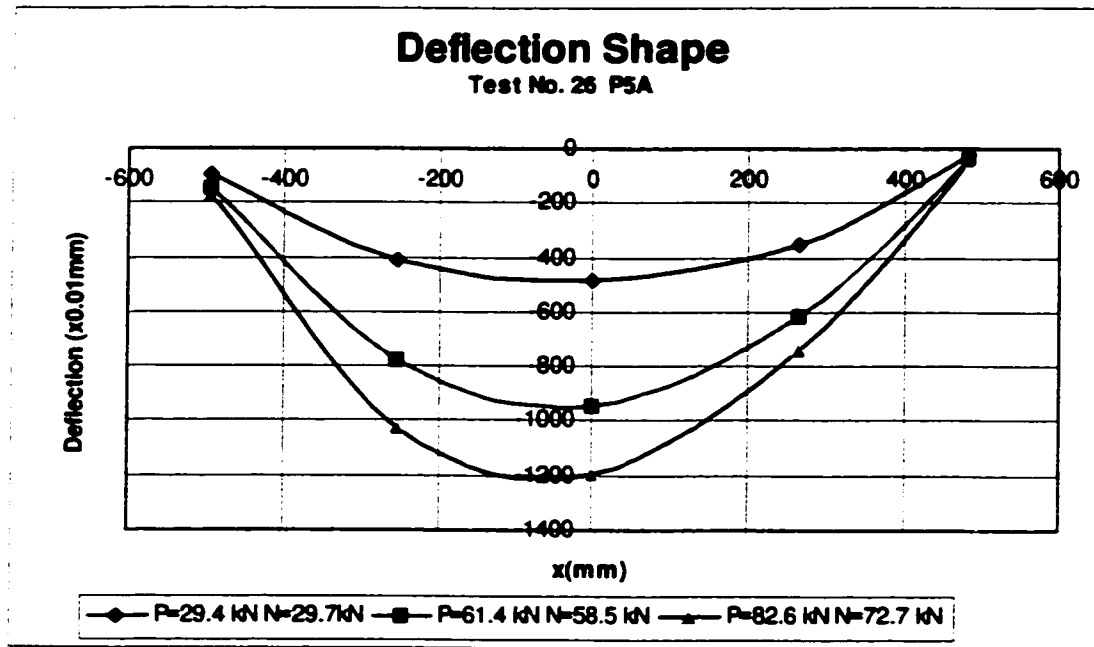


Fig. 5.3 Deflection shape of test No. 26

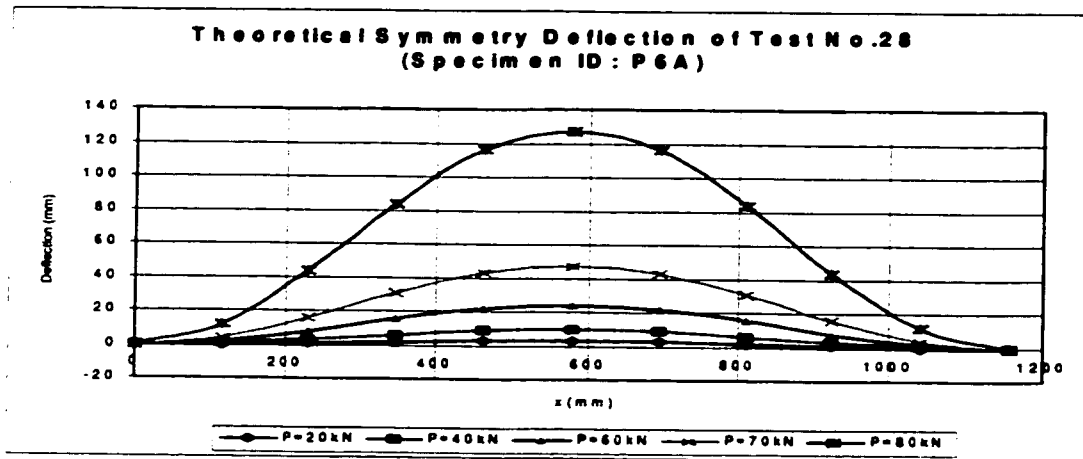
5.3.2 Theoretical load-deflection behavior of diagonals

The processes of deflection are described in the last section. Twenty-four experimental load-deflection curves are shown in Appendix-C. As can be seen, the deflection is almost proportional to the axial compressive force at the beginning. But when the axial force becomes larger, it increases fast, and behaves non-linearly.

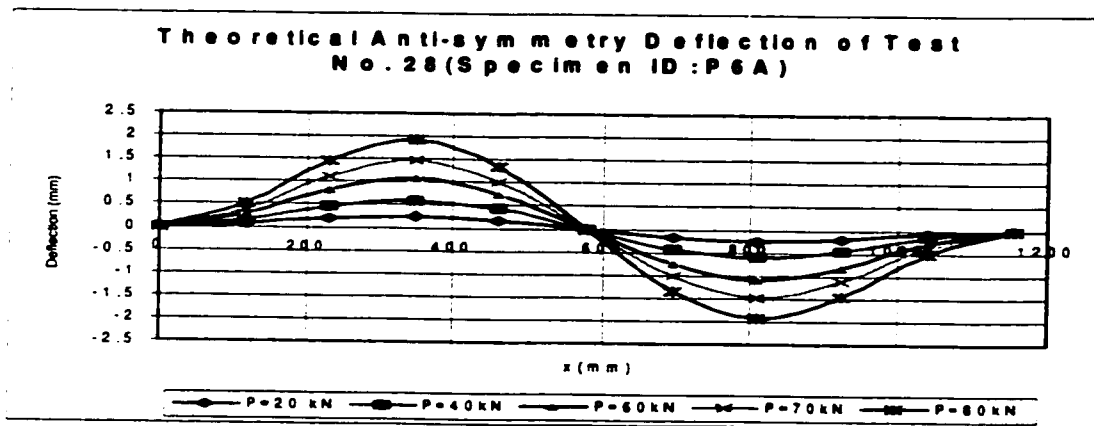
The theories of load-deflection behaviors are developed in Chapter 3. The deflection of compression diagonal can be calculated by Eq. (3-8). Here the theoretical result for Test No. 28 (Specimen ID P6B) is given as an example. The diameter of diagonal is 22.2 mm. The length of diagonal is 1158 mm and the elastic modulus is 200 GPa. The maximum symmetric initial deflection is assumed to be 11 mm, and the maximum deflection of anti-symmetry is 1 mm. Deflection development due to two different initial deflections is

solved independantly, as shown in Fig. 5.4a and Fig.5.4b. Their values can be superposed, as in Fig. 5.4c. This result agrees quite well with the result of experimental investigation when deflection is small. From Fig. 5.4, it is found that before the diagonal buckles, the deflection of symetric mode prevails and anti-symetric deflection can be neglected. It is also found that deflection developed very fast as loads close to the Euler critical load of diagonal as if tension diagonal restraint did not exist. The shape of deflection before buckling is almost the same as experimental one. It seems that in the elastic state, the theories developed in Chapter 3 can explain the behavior of cross-braced diagonals of steel tower. But as can be found, the value of deflection is quite different from experimental one when the deflection becomes larger (see Fig. 5.5). This is due to three reasons.

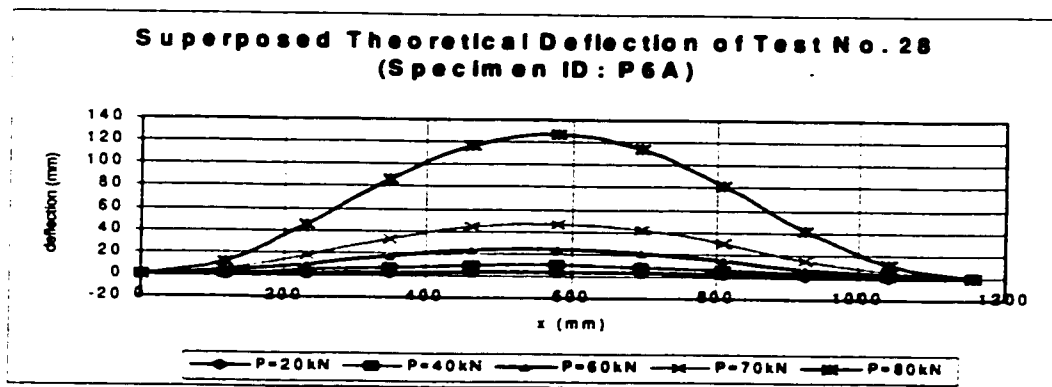
First, in the theoretical analysis, the tension diagonal is assumed to provide vertical restraint irrespective of the magnitude of the tension force in the tension diagonal. As a result, deflection at cross-brace location increases without end. In fact, when deflection develops to some degree, the restraint provided by tension diagonal will prevent the deflection at cross-brace location from increasing as compression force increases. Second, the initial deflection value is very difficult to evaluate. Third, due to yielding both at ends and cross-brace location, theoretical equations are no longer valid.



(a)



(b)



(c)

Fig. 5.4 Theoretical deflection of specimen P6A

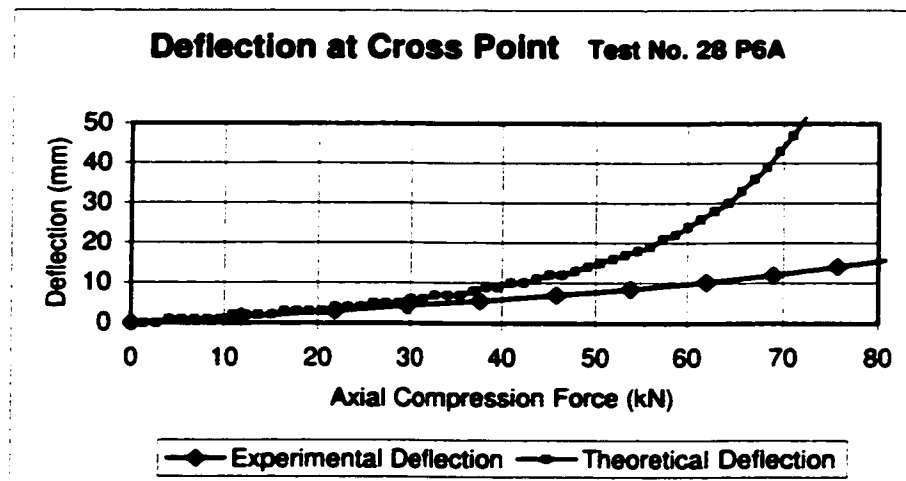


Fig. 5.5 Comparison of theoretical and experimental deflections for Specimen P6A

CHAPTER 6

FINITE ELEMENT ANALYSIS

6.1 GENERAL

The principal objective of this chapter is to find the buckling behavior of cross-braced diagonals under compression force applied to the compression diagonal. Three kinds of initial deflection are considered, viz., symmetric initial deflection, anti-symmetric initial deflection, and their superposition. Both elastic and elastic-plastic materials are analyzed. Thus, six cases are considered in this chapter.

6.2 DESCRIPTION OF FINITE ELEMENT MODEL

Test No. 28 (Specimen ID P6A) was modeled in this section. The dimensions of the model are as follows:

Diameter of leg: 57.2 mm

Diameter of diagonal: 22.2 mm

Length of diagonal: 1158 mm

The ends of diagonals are assumed to be fixed, but they are free to move in the direction along length. Tension diagonal is connected to compression diagonal by welding. In the finite element model, one rigid element was used to connect tension diagonal with compression diagonal. Both compression diagonal and tension diagonal were meshed into 10 Beam elements, and type B31 elements provided by ABAQUS were used in both tension diagonal and compression diagonal.

The properties of material are as follows:

Elastic Modulus: 200 GPa

Yield Stress: 442 Mpa

Poisson's ratio: 0.3

- Equation of symmetric initial deflection

$$v_{10} = \frac{\delta_1}{2} (1 - \cos(\pi \frac{x}{L})) \quad (6-1)$$

where, δ_1 is assumed to be 11 mm.

- Equation of anti-symmetric deflection

$$v_{20} = \delta_2 (1 - \cos(kx) + 0.1771 \sin(kx) - 0.8328 \frac{x}{L}) \quad (6-2)$$

where, δ_2 is assumed to be 1 mm;

$$k = 4.7023/L;$$

L is half the length of diagonal.

- Equation of superposition

$$v_0 = v_{10} + v_{20} \quad (6-3)$$

These initial deflections are shown in the chart of Figure 6.1.

6.3 RESULT OF FINITE ELEMENT ANALYSIS

The finite element analysis was done by ABAQUS [Hibbitt, Karlsson and Sorensen, Inc. 1997] program. Since the post-buckling was considered, the approach of modified Riks algorithm is chosen to control the calculation procedure. Both the elastic state and elastic-plastic state were included in the section, therefor, there are six cases that were analyzed:

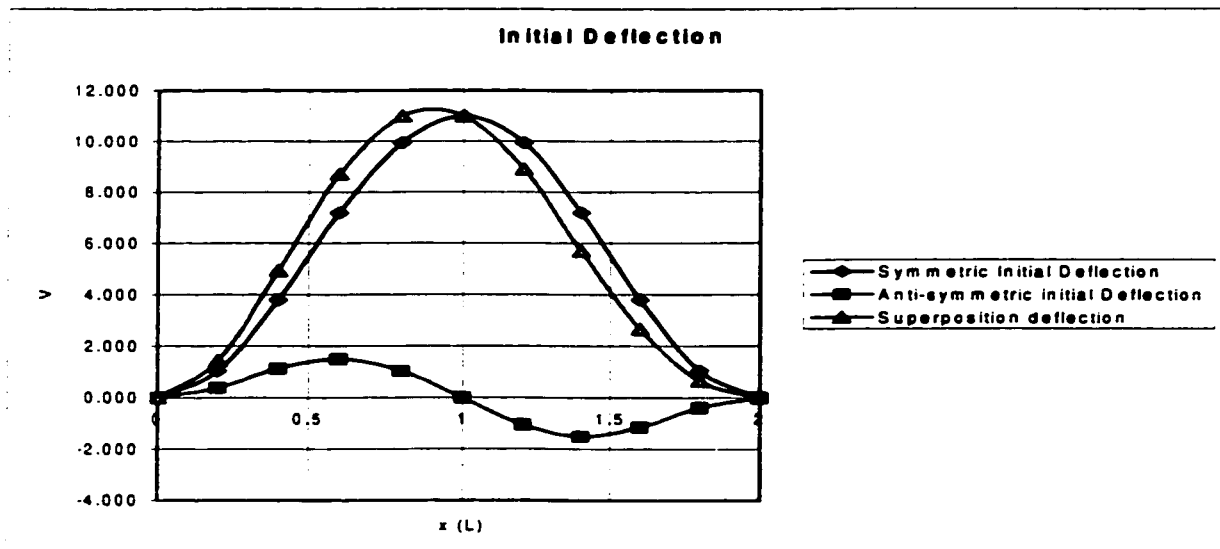


Fig. 6.1 Initial deflection of diagonal of Specimen P6A

- **Case 1: Elastic-plastic behavior with symmetric initial deflection**
 - Deflected Shape

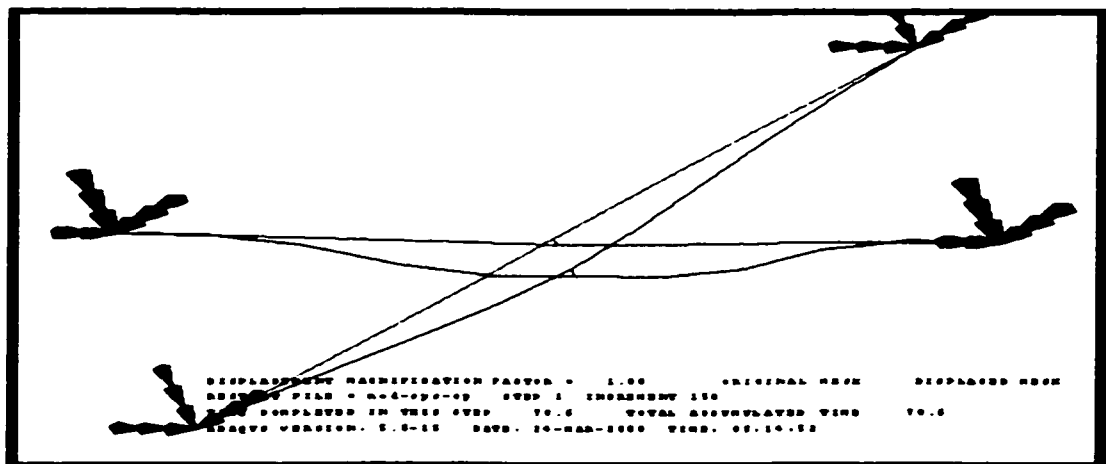


Fig. 6.2 Deflected shape of diagonal of Specimen P6A

- Load deflection curve

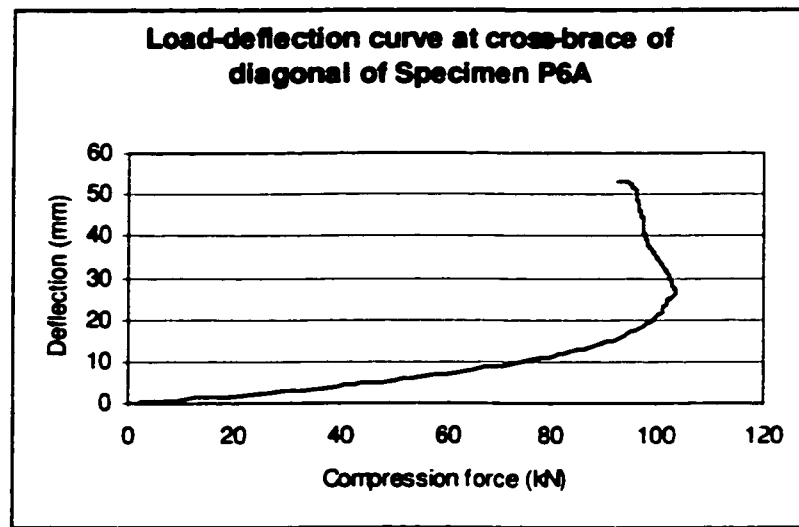


Fig. 6.3 Load-deflection curve at cross-brace of diagonal of Specimen P6A

- Failure load: 103.7 kN.
- Case 2: Elastic-plastic behavior with anti-symmetric initial deflection
- Deflected shape

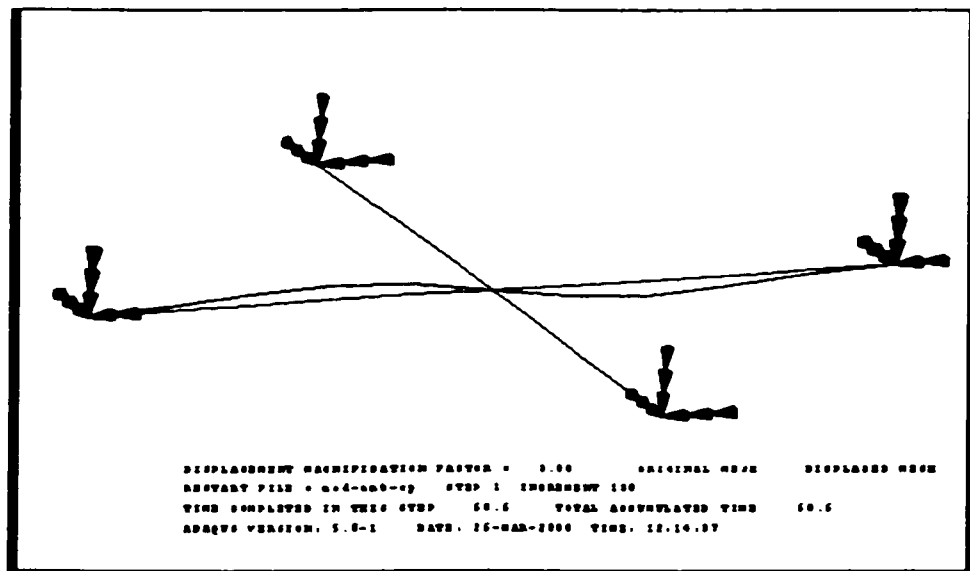


Fig. 6.4 Deflected shape of diagonal of Specimen P6A (Case 2)

- Load-deflection curve

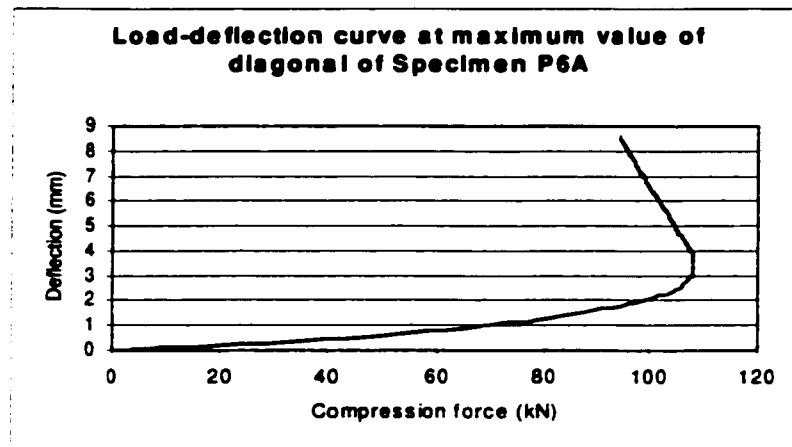


Fig. 6.5 Load-deflection curve at maximum value of diagonal of Specimen P6A

- Failure load: 108.1 kN
- Case 3: Elastic-plastic behavior with initial deflection of superposition
- Deflected Shape

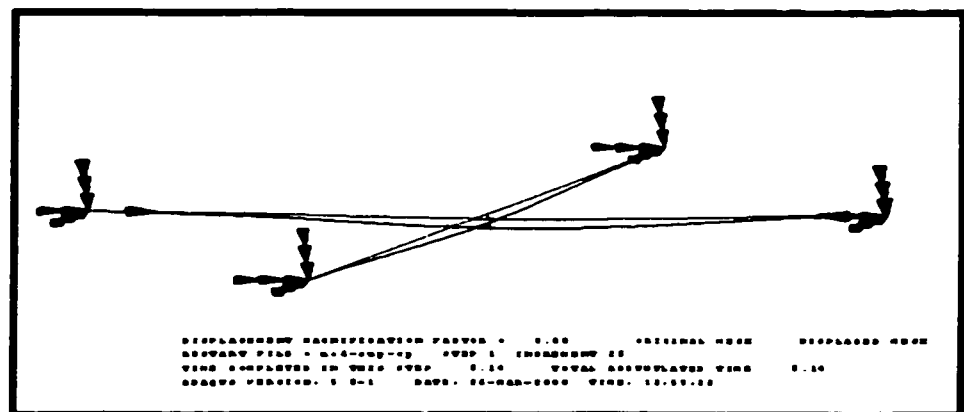


Fig. 6.6a Deflected shape of diagonal of Specimen P6A before failure ($P = 55.13$ kN)

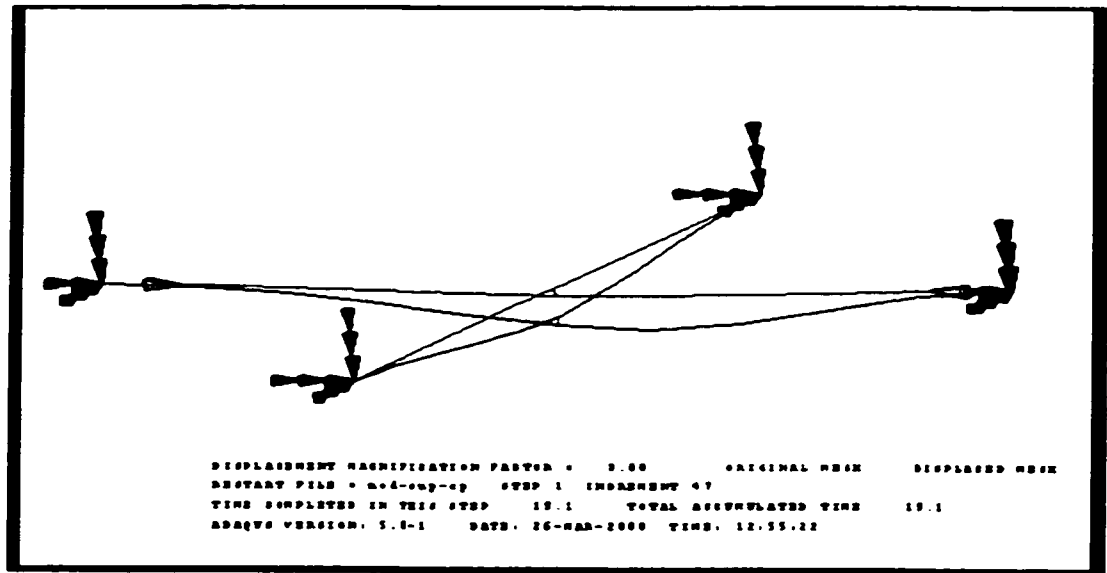


Fig. 6.6b Deflected shape of diagonal of Specimen P6A at failure load ($P=83.9$ kN) (Case 3)

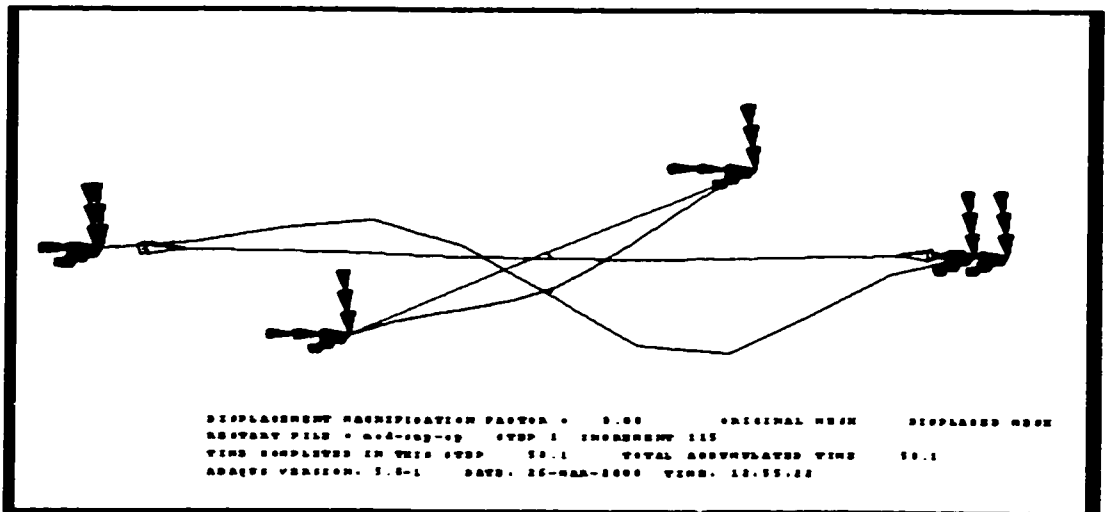


Fig. 6.6c Deflected shape of diagonal of Specimen P6A at post-failure state ($P = 44.42$ kN)(Case 3)

- Failure load: 83.90 kN

- Load-deflection Curve

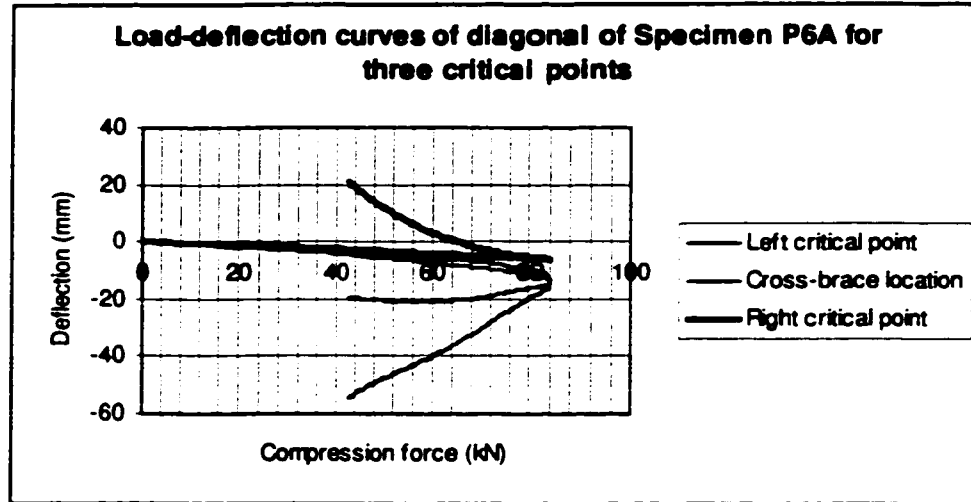


Fig. 6.7 Load-deflection curves of diagonal of Specimen P6A for three critical points(Case 3)

- Case 4: Elastic behavior with symmetric initial deflection

- Deflected shape

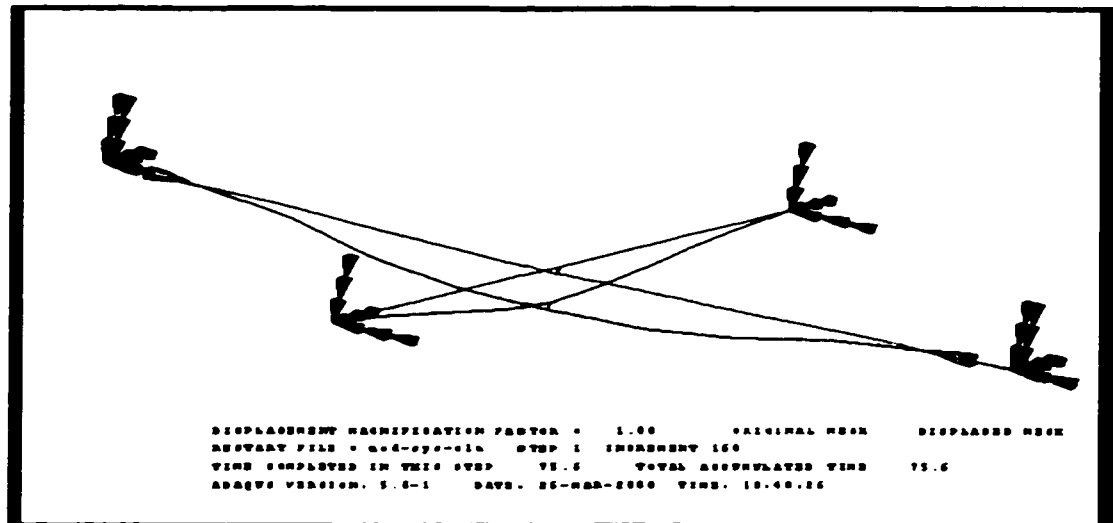


Fig. 6.8 Deflected shape of diagonal of Specimen P6A(Case 4)

- Failure Load: Not available for this case.
- Load-deflection curve

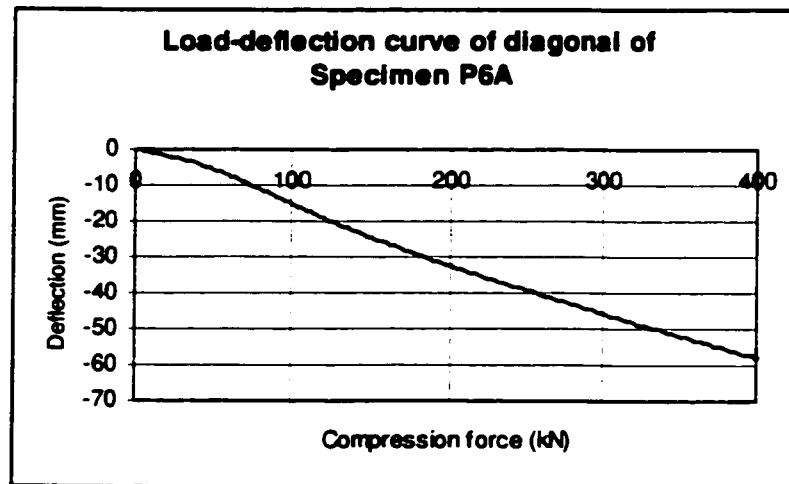


Fig. 6.9 Load-deflection curve of diagonal of Specimen P6A (Case 4)

- Case 5: Elastic behavior with anti-symmetric deflection
- Deflected shape

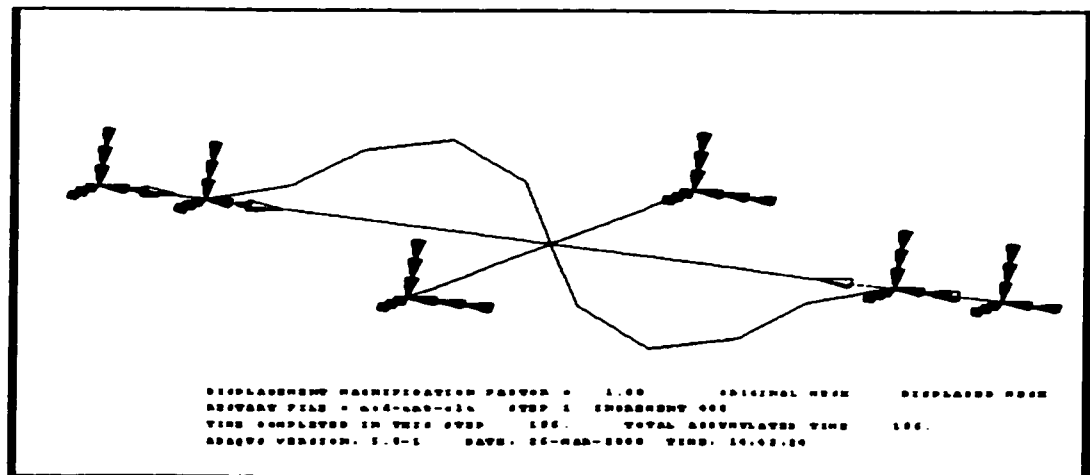


Fig. 6.10 Deflected shape of diagonal of Specimen P6A (Case 5)

- Failure Load: 206.4 kN
- Load deflection curve

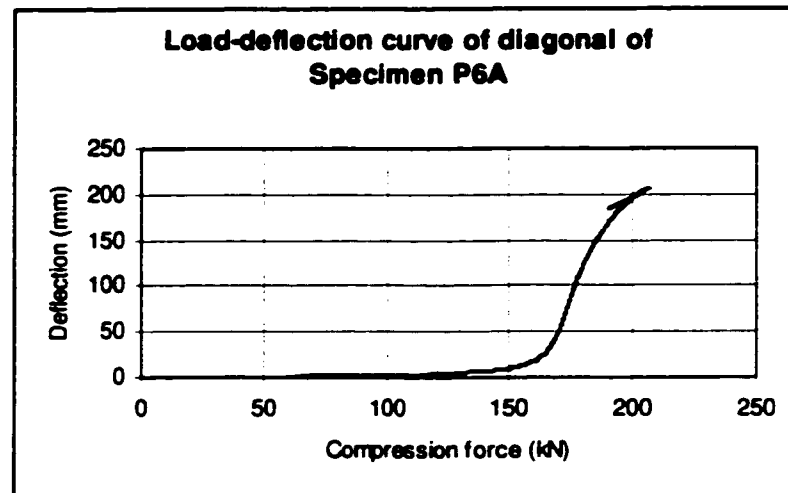


Fig. 6.11 Load-deflection curve of diagonal of Specimen P6A (Case 5)

- **Case 6: Elastic behavior with initial deflection of superposition**
- Deflected Shape

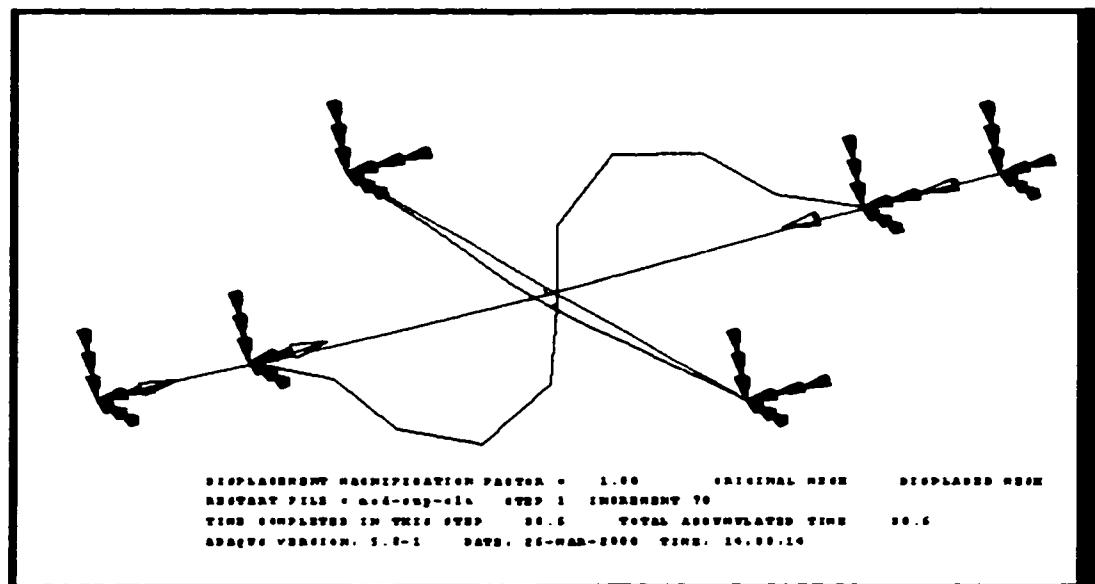


Fig. 6.12 Deflected shape of diagonal of Specimen P6A Case 6)

- Failure load: 206.0 kN
- Load-deflection curve

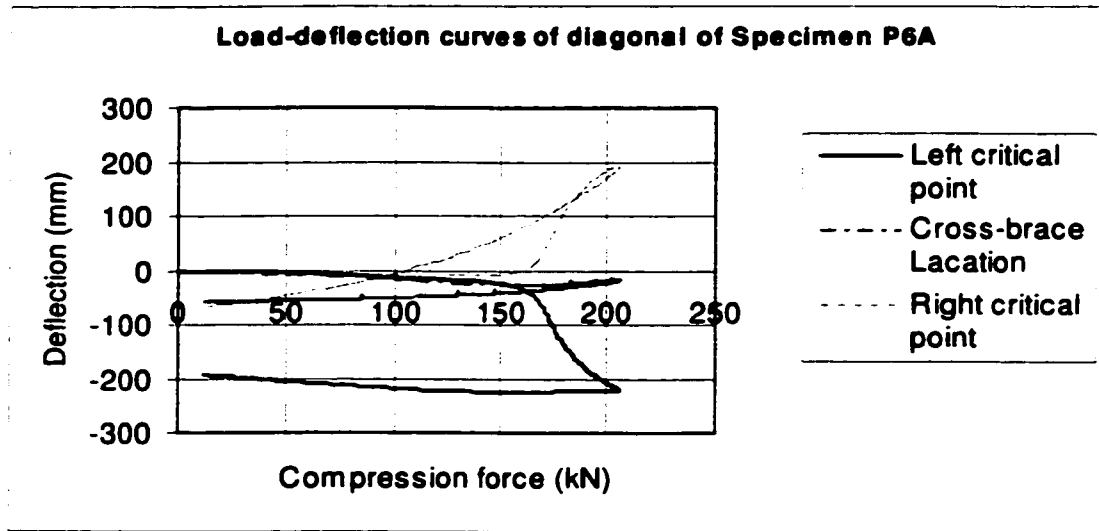


Fig. 6.13 Load-deflection curve of diagonal of Specimen P6A at cross-brace location and at two critical points (Case 6)

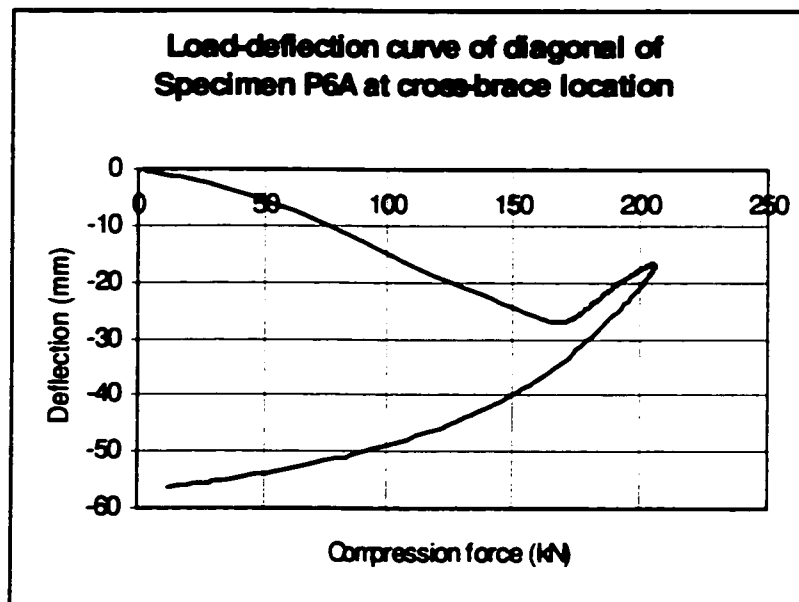


Fig. 6.14 Load-deflection curve of diagonal of Specimen P6A at cross-brace location (Case 6)

6.4 EFFECT OF MAGNITUDE OF ANTI-SYMETRIC INITIAL DEFLECTION

Three specimens (P6A, P8B, and S6B) were analyzed to investigate the effect of magnitude of anti-symmetric initial deflection. Material is assumed to be elastic-plastic. The maximum symmetric initial deflection was given as half of the diameter of diagonal. But the initial deflection of anti-symmetric case is different. Properties of specimens are shown in Table 6-1. Relationship between buckling load and anti-symmetric deflection is shown in Fig. 6.15 (a), (b), and (c), for the three specimens. Table 6-2 gives the experimental buckling loads of the diagonals of the three specimens.

Table 6-1 Properties of Specimens

Properties of Specimens	Test No.13	Test No. 19	Test No. 28
Length of Diagonal (mm)	1190	1158	1158
Diameter of Leg (mm)	69.9	38.1	57.2
Diameter of Diagonal (mm)	15.9	22.2	22.2
Elastic Modulus(GPa)	200	200	200
Maximum symmetric Initial Deflection (mm)	7.95	11	11
Yield Stress (MPa)	382	349	442

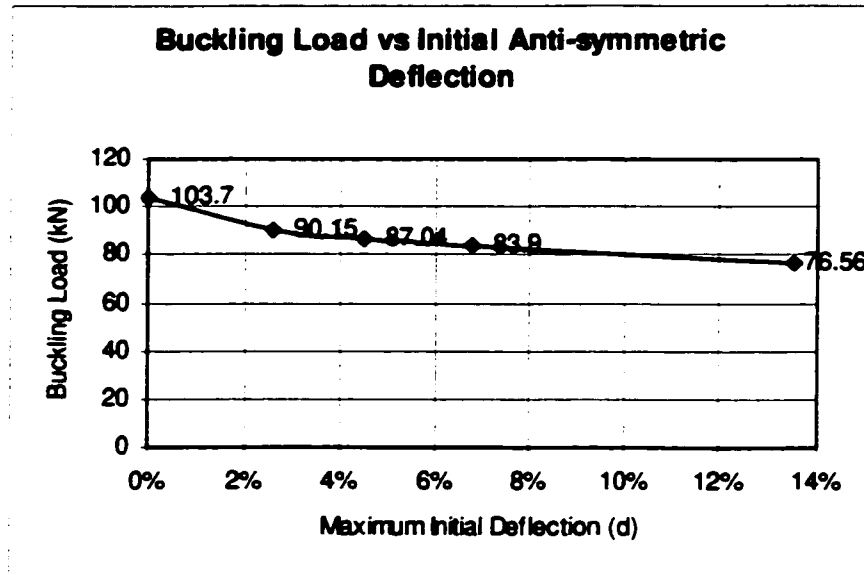


Fig. 6.15a Buckling load vs initial anti-symmetric deflection of diagonal of Specimen P6A

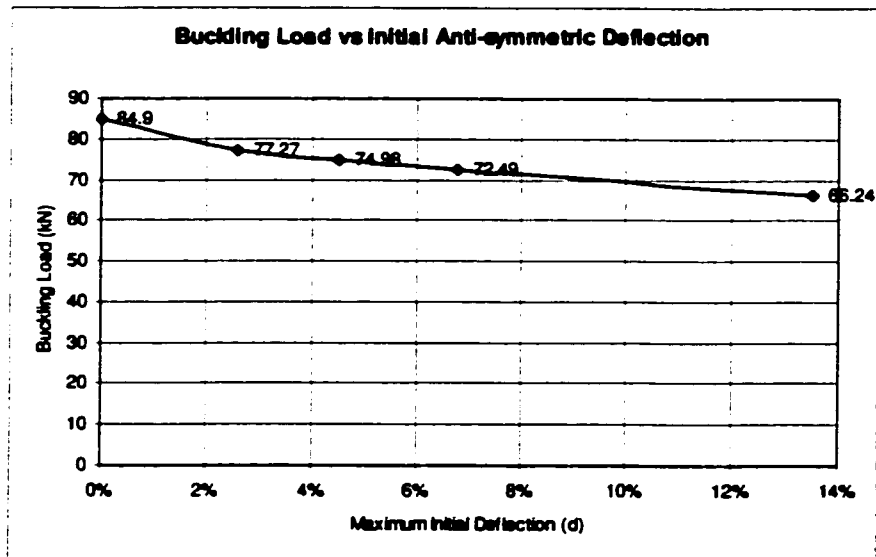


Fig. 6.15b Buckling load vs initial anti-symmetric deflection of diagonal of Specimen P8B

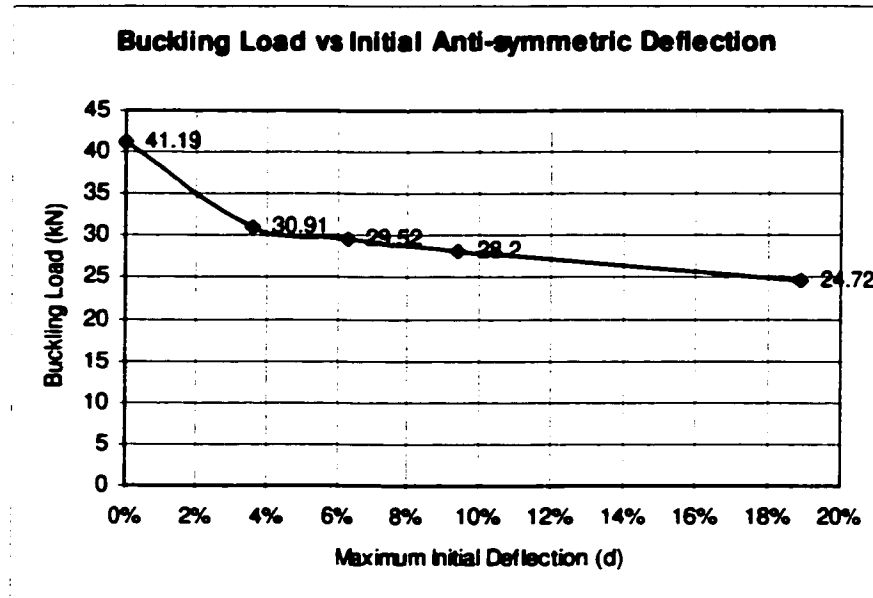


Fig. 6.15c Buckling load vs initial anti-symmetric deflection of diagonal of Specimen S6B

Table 6-2 Experimental Buckling Loads

Specimen	Test No. 13 (ID: S6B)	Test No. 19 (ID:P8B)	Test No. 28 (ID:P6A)
Buckling Load of Front Diagonal (kN)	25.4	82	91.3
Buckling Load of Rear Diagonal (kN)	-	-	82.5

6.5 SUMMARY

From finite element analysis, it is found that

- In the case of initial deflection with superposition of both symmetric deflection and anti-symmetric one, the results of elastic-plastic finite element analysis fit the experimental results very well.
- When material is elastic-plastic, both symmetric initial deflection and anti-symmetric deflection affect buckling load of diagonal. The buckling load of superposition is the least one.
- When material is assumed to be elastic, symmetric initial deflection does not seem to have any effect on buckling load of diagonal.

CHAPTER 7

CONCLUSIONS

Theories of several stability models for diagonals in steel communication towers are developed. The most reasonable model is recommended for cross-braced steel tower. Theoretical effective length factor and load-deflection equations are also derived. Furthermore, experimental investigation was also done on 26 tower specimens, with solid round welded cross-braced diagonals. Based on theoretical studies and experimental investigation, the following conclusions can be drawn:

1. Beam-column model with elastic end restraints and elastic rotational restraint at cross-brace location, where the effect of leg size is taken into account, is regarded to be the best model to calculate the effective length factor. However, it is very complicated to study the stability behavior of diagonal. Beam-column model with fixed ends and elastic rotational restraint at cross-brace location can be used with no loss of accuracy to investigate the behavior of diagonals of cross-braced steel towers.
2. The results of theoretical studies are in agreement with the results from experimental investigation, especially in the determination of effective length factor.
3. If the ratio of diameter of leg to diameter of diagonal is more than 3, diagonals can be regarded as fixed at ends connected with legs. Theoretical effective length factor is 0.334 for this condition. If the diameter ratio of leg to diagonal is less than 3, the effect of leg size should be taken into account in evaluating effective length factor. The chart in Fig. 5.1 can be used as a guide to estimate the effective length factor.

4. Elastic out-of-plane restraint of tension diagonal at cross-brace location changes the buckling mode of compression diagonal from symmetric to anti-symmetric mode. But the magnitude of elastic restraint does not affect the effective length factor. On the other hand, elastic rotational restraint furnished by tension diagonal reduces only slightly the value of effective length factor .
5. There is no relationship between effective length factor and tension force. Effective length factor is dependent only on the geometry and boundary conditions. But tension force in tension diagonal does affect the deflection of diagonals.
6. Symmetric initial deflection does not affect the critical load of diagonal. On the other hand, anti-symmetric initial deflection does, though it is much less than symmetric initial deflection. Before buckling, symmetric deflection is much larger than anti-symmetric deflection. But when the applied load nearly reach its critical one, anti-symmetric deflection will prevail.
7. All the compression diagonals in steel communication tower buckle out-of-plane.
8. Results of finite element analysis support the conclusions from the theoretical development.

There are still many problems waiting for future research. Elastic-plastic behavior of diagonals is still unknown. Even in elastic state, theoretical studies are also not completely solved if tension force is considered. Thus behavior of diagonals in cross-braced steel towers deserves to be further investigated theoretically.

REFERENCES

- Chen, W.F., Liu, E.M., 1987, “ **Structural Stability**”, Elsevier Science Publishing Co. Inc., New York, USA.
- CSA, 1994, “**Antenna, Towers, and Antenna Supporting Structures**,” CSA S37-94, Canadian Standards Association, Etobicoke, Ontario.
- DeWolf, J.T. and Pelliccione, J.F., 1979, “**Cross-Bracing Design**,” Journal of the Structural Division, ASCE, ST7, July, pp. 1379-1391.
- El-Tayem, A.A. and Goel, S.C., 1986, “**Effective Length Factor for The Design of X-Bracing Systems**,” AISC, Engineering Journal, First Quarter, 1986, Chicago, Ill., pp. 41-45.
- HIBBITT, KARLSSON & SORENSEN, INC., 1997, “**ABAQUS, THEORY MANUAL**”, V5.7, Pawtucket, RI, USA.
- Jaboo, K. S., 1998, “ **Effective length factors for solid round diagonal bracing members in lattice towers**”, M. A. Sc. Thesis, University of Windsor, Windsor, Ontario, Canada.
- Kemp, A.R. and Behncke, R.H., 1998, “**Behavior of Cross-Bracing in Latticed Towers**,” Journal of Structural Engineering, ASCE, April, pp. 360-367.
- Picard, A. and Beaulieu, D., 1987, “**Design of Diagonal Cross-Bracings; Part 1: Theoretical Study**,” Engineering Journal, American Institute of Steel Construction, Third Quarter, pp. 122-126.

Picard, A. and Beaulieu, D., 1988, "**Design of Diagonal Cross-Bracings; Part 2: Experimental Study,**" Engineering Journal, American Institute of Steel Construction, Fourth Quarter, pp.156-160.

Picard, A. and Beaulieu, D., 1989a, "**Theoretical Study of The Buckling Strength of Compression Members Connected to Coplanar Tension Members,**" Canadian Journal of Civil Engineers, Vol. 16, pp. 239-248.

Picard, A. and Beaulieu, D., 1989b, "**Experimental Study of The Buckling Strength of Compression Members Connected to Coplanar Tension Members,**" Canadian Journal of Civil Engineers, Vol. 16, pp. 249-257.

Sun, Y., 1999, "**The Effective Length Factor of Diagonals for Communication Tower**", M. A. Sc. Thesis, University of Windsor, Windsor, Ontario, Canada.

Timoshenko, S.P., 1953, "**History of Strength of Materials,**" McGraw-Hill Book Co., Inc., New York, NY.

Timoshenko, S.P. and Gere, J.M., 1961, "**Theory of Elastic Stability,**" Second Ed., McGraw-Hill Book Co., Inc., New York, NY.

Todhunter, I., 1960, "**A History of the Elasticity and Strength of Materials,**" Dover Publications, (originally published by Cambridge University Press, 1893).

Vickers, D.G., 1982, "**Tension-Compression Cross-Bracing Using Star Angles,**" Master of Engineering Project Report, Dept. Of Civil Engineering, McGill University, Montreal, Quebec.

Wood, A.B., 1975, "**Buckling Tests on Crossed Diagonals in Latticed Towers,**" CIGRE Report, Electra, No. 38, pp. 88-99.

APPENDIX-A

Tables of Test Records

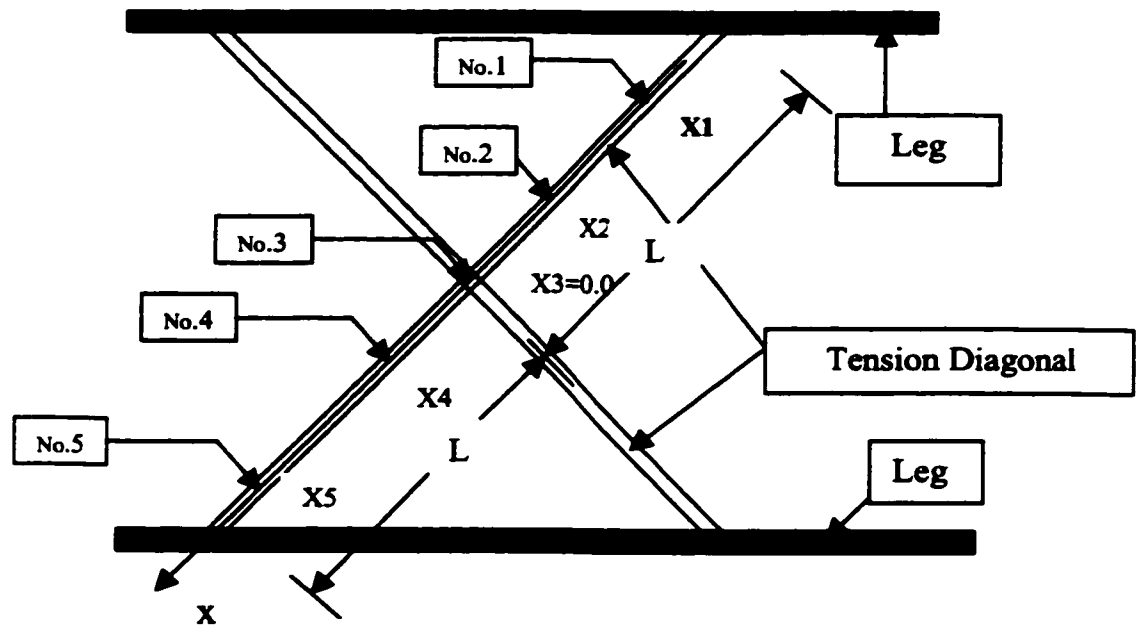


Fig. A.1 Location of dial gauges on compression diagonal

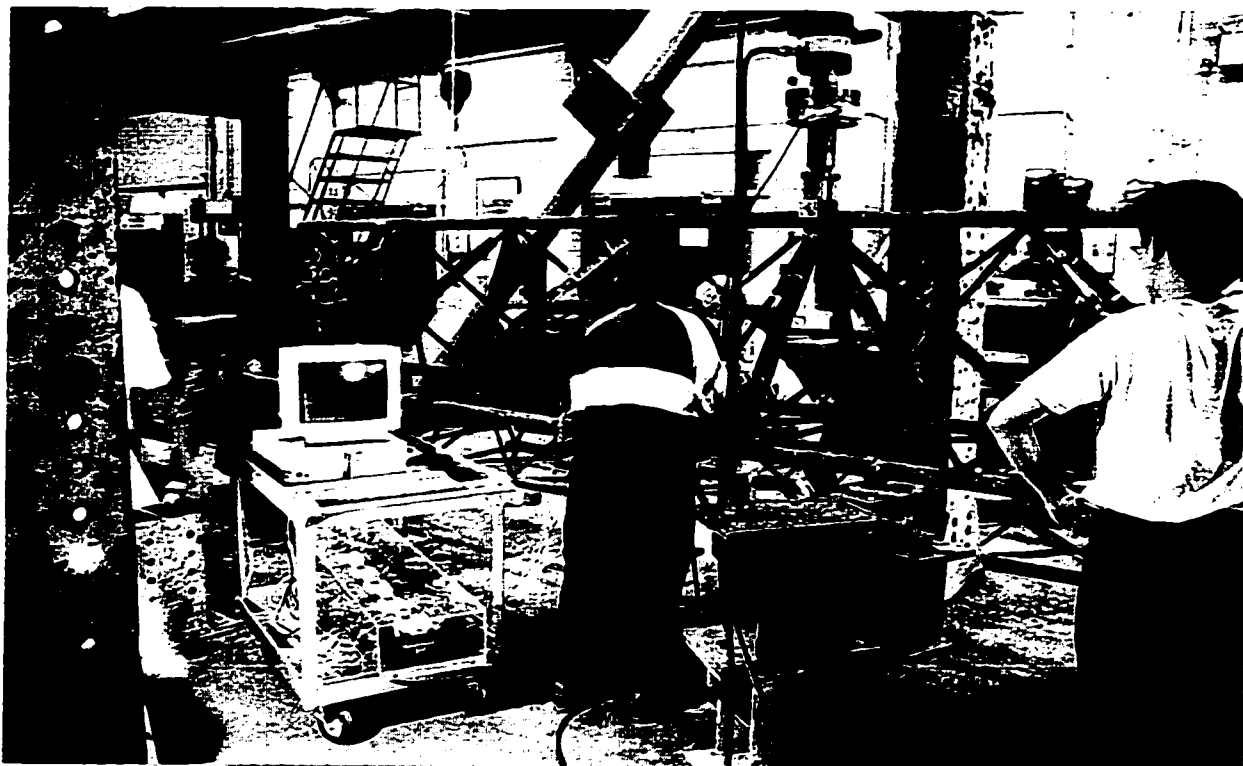


Fig. A.2 Test set-up

Table A-1 Record of Test No.1

Specimen ID:S4A

Description of Specimen	Horizontal (YES/NO)	YES	Diameter of Leg (mm)	50.8
	Diameter of Diagonal (mm)	14.3	Diameter of Horizontal (mm)	-
	Length of Diagonal (mm)	1190	Width of Face (mm)	914
	Length of Panel (mm)	762	Number of Panel	6
	Which Panel Tested?	A	Position of Front Face	
	Connection Type between Legs and Diagonal (A/B) (Refer to Fig. 4.4)	A	Compression Diagonal In Test Panel (INSIDE/ OUTSIDE)	-
	Elastic Modulus (GPa)	200	Yield Stress of Diagonal (MPa)	378
Result of Test	Failure Load of Tower (kN)	110		
	Buckling Load of Front Diagonal (kN)	20.1	Buckling Load of Rear Diagonal (kN)	-
	Effective Length Factor of Front Diagonal by AISC-LRFD	0.353	Effective Length Factor of Rear Diagonal by AISC-LRFD	-
	Effective Length Factor of Front Diagonal by CSA S16.1-94	0.343	Effective Length Factor of Rear Diagonal by CSA S16.1-94	-
Description of Test	Panel A: Top half of front diagonal buckled inside and bottom outside. Panel B: Bottom half of front diagonal buckled outside and top inside Panel C: Top half of front diagonal buckled inside and top half of rear diagonal buckled inside			

Table A-2 Record of Test No.2

Specimen ID: S5A

Description of Specimen	Horizontal (YES/NO)	NO	Diameter of Leg (mm)	69.9
	Diameter of Diagonal (mm)	15.9	Diameter of Horizontal (mm)	-
Description of Specimen	Length of Diagonal (mm)	1190	Width of Face (mm)	914
	Length of Panel (mm)	762	Number of Panel	6
	Which Panel Tested?	C	Position of Front Face	
	Connection Type between Legs and Diagonal (A/B) (Refer to Fig. 4.4)	A	Compression Diagonal In Test Panel (INSIDE/ OUTSIDE)	-
	Elastic Modulus (GPa)	200	Yield Stress of Diagonal (MPa)	385
	Failure Load of Tower (kN)	71.6		
Result of Test	Buckling Load of Front Diagonal (kN)	21.6	Buckling Load of Rear Diagonal (kN)	20.9
	Effective Length Factor of Front Diagonal by AISC-LRFD	0.420	Effective Length Factor of Rear Diagonal by AISC-LRFD	0.427
	Effective Length Factor of Front Diagonal by CSA S16.1-94	0.416	Effective Length Factor of Rear Diagonal by CSA S16.1-94	0.424
	Panel C: Top half of front diagonal buckled outside totally and rear diagonal buckled inside Panel D: Front compression diagonal buckled outside totally and rear diagonal inside			

Table A-3 Record of Test No.3

Specimen ID:S4B

Description of Specimen	Horizontal (YES/NO)		YES	Diameter of Leg (mm)		50.8	
	Diameter of Diagonal (mm)		14.3	Diameter of Horizontal (mm)		19.1	
	Length of Diagonal (mm)		1190	Width of Face (mm)		914	
	Length of Panel (mm)		762	Number of Panel		6	
	Which Panel Tested?		A	Position of Front Face		-	
	Connection Type between Legs and Diagonal (A/B) (Refer to Fig. 4.4)		A	Compression Diagonal In Test Panel (INSIDE/ OUTSIDE)			
	Elastic Modulus (GPa)		200	Yield Stress of Diagonal (MPa)			378
	Result of Test	Failure Load of Tower (kN)		145			
		Buckling Load of Front Diagonal (kN)		24.9	Buckling Load of Rear Diagonal (kN)		-
		Effective Length Factor of Front Diagonal by AISC-LRFD		0.317	Effective Length Factor of Rear Diagonal by AISC-LRFD		-
Effective Length Factor of Front Diagonal by CSA S16.1-94		0.296	Effective Length Factor of Rear Diagonal by CSA S16.1-94		-		
Description of Test	Panel A: Top half of front diagonal buckled inside and bottom half outside Rear diagonal buckled with top half outside and bottom inside						

Table A-4 Record of Test No.4

Specimen ID: S2A

Description of Specimen	Horizontal (YES/NO)	YES	Diameter of Leg (mm)	38.1	
	Diameter of Diagonal (mm)	12.7	Diameter of Horizontal (mm)	19.1	
	Length of Diagonal (mm)	1190	Width of Face (mm)	914	
	Length of Panel (mm)	762	Number of Panel	6	
	Which Panel Tested?	A	Position of Front Face	-	
	Connection Type between Legs and Diagonal (A/B) (Refer to Fig. 4.4)	A	Compression Diagonal In Test Panel (INSIDE/ OUTSIDE)		
	Elastic Modulus (GPa)	200	Yield Stress of Diagonal (MPa)		378
	Result of Test	Failure Load of Tower (kN)	95		
		Buckling Load of Front Diagonal (kN)	14.8	Buckling Load of Rear Diagonal (kN)	14.3
		Effective Length Factor of Front Diagonal by AISC-LRFD	0.325	Effective Length Factor of Rear Diagonal by AISC-LRFD	0.330
Effective Length Factor of Front Diagonal by CSA S16.1-94		0.318	Effective Length Factor of Rear Diagonal by CSA S16.1-94	0.325	
Description of Test	Panel A: Front diagonal buckled with bottom half outside and top half inside Rear diagonal (first)buckled with top half outside and bottom inside				

Table A-5 Record of Test No.5

Specimen ID:S4C

Description of Specimen	Horizontal (YES/NO)	YES	Diameter of Leg (mm)	50.8
	Diameter of Diagonal (mm)	14.3	Diameter of Horizontal (mm)	19.1
Description of Specimen	Length of Diagonal (mm)	1190	Width of Face (mm)	914
	Length of Panel (mm)	762	Number of Panel	6
	Which Panel Tested?	A	Position of Front Face	-
	Connection Type between Legs and Diagonal (A/B) (Refer to Fig. 4.4)	A	Compression Diagonal In Test Panel (INSIDE/ OUTSIDE)	
	Elastic Modulus (GPa)	200	Yield Stress of Diagonal (MPa)	367
	Failure Load of Tower (kN)	145		
Result of Test	Buckling Load of Front Diagonal (kN)	21.4	Buckling Load of Rear Diagonal (kN)	22.8
	Effective Length Factor of Front Diagonal by AISC-LRFD	0.342	Effective Length Factor of Rear Diagonal by AISC-LRFD	0.332
	Effective Length Factor of Front Diagonal by CSA S16.1-94	0.327	Effective Length Factor of Rear Diagonal by CSA S16.1-94	0.313
	Panel A: Front diagonal buckled with top half inside			
Description of Test				

Table A-6 Record of Test No.6

Specimen ID:S1A

Description of Specimen	Horizontal (YES/NO)	NO	Diameter of Leg (mm)	38.1
	Diameter of Diagonal (mm)	12.7	Diameter of Horizontal (mm)	-
	Length of Diagonal (mm)	1190	Width of Face (mm)	914
	Length of Panel (mm)	762	Number of Panel	6
	Which Panel Tested?	C	Position of Front Face	
	Connection Type between Legs and Diagonal (A/B) (Refer to Fig. 4.4)	A	Compression Diagonal In Test Panel (INSIDE/ OUTSIDE)	-
	Elastic Modulus (GPa)	200	Yield Stress of Diagonal (MPa)	357
Result of Test	Failure Load of Tower (kN)	50		
	Buckling Load of Front Diagonal (kN)	14.1	Buckling Load of Rear Diagonal (kN)	12.4
	Effective Length Factor of Front Diagonal by AISC-LRFD	0.333	Effective Length Factor of Rear Diagonal by AISC-LRFD	0.355
	Effective Length Factor of Front Diagonal by CSA S16.1-94	0.325	Effective Length Factor of Rear Diagonal by CSA S16.1-94	0.352
Description of Test	Panel C: Front diagonal buckled with top half inside			

Table A-7 Record of Test No.7

Specimen ID:S3A

Description of Specimen	Horizontal (YES/NO)	NO	Diameter of Leg (mm)	50.8
	Diameter of Diagonal (mm)	14.3	Diameter of Horizontal (mm)	-
Description of Specimen	Length of Diagonal (mm)	1190	Width of Face (mm)	914
	Length of Panel (mm)	762	Number of Panel	6
	Which Panel Tested?	C	Position of Front Face	
	Connection Type between Legs and Diagonal (A/B) (Refer to Fig. 4.4)	A	Compression Diagonal In Test Panel (INSIDE/ OUTSIDE)	-
	Elastic Modulus (GPa)	200	Yield Stress of Diagonal (MPa)	385
	Failure Load of Tower (kN)	72.5		
Result of Test	Buckling Load of Front Diagonal (kN)	21.3	Buckling Load of Rear Diagonal (kN)	19.4
	Effective Length Factor of Front Diagonal by AISC-LRFD	0.343	Effective Length Factor of Rear Diagonal by AISC-LRFD	0.360
	Effective Length Factor of Front Diagonal by CSA S16.1-94	0.331	Effective Length Factor of Rear Diagonal by CSA S16.1-94	0.351
	Panel C: Front diagonal buckled first with bottom half outside Rear diagonal buckled second with top half inside			

Table A-8 Record of Test No.8

Specimen ID:S2B

Description of Specimen	Horizontal (YES/NO)	YES	Diameter of Leg (mm)	38.1
	Diameter of Diagonal (mm)	12.7	Diameter of Horizontal (mm)	19.1
	Length of Diagonal (mm)	1190	Width of Face (mm)	914
	Length of Panel (mm)	762	Number of Panel	6
	Which Panel Tested?	A	Position of Front Face	
	Connection Type between Legs and Diagonal (A/B) (Refer to Fig. 4.4)	A	Compression Diagonal In Test Panel (INSIDE/ OUTSIDE)	-
	Elastic Modulus (GPa)	200	Yield Stress of Diagonal (MPa)	369
	Failure Load of Tower (kN)	97.5		
	Buckling Load of Front Diagonal (kN)	13.7	Buckling Load of Rear Diagonal (kN)	13.7
	Effective Length Factor of Front Diagonal by AISC-LRFD	0.337	Effective Length Factor of Rear Diagonal by AISC-LRFD	0.337
Result of Test	Effective Length Factor of Front Diagonal by CSA S16.1-94	0.333	Effective Length Factor of Rear Diagonal by CSA S16.1-94	0.333
	Panel A: Rear diagonal buckled first with top half inside			
Description of Test				

Table A-9 Record of Test No.9

Specimen ID:

Description of Specimen	Horizontal (YES/NO)			Diameter of Leg (mm)	
	Diameter of Diagonal (mm)			Diameter of Horizontal (mm)	
	Length of Diagonal (mm)			Width of Face (mm)	
	Length of Panel (mm)			Number of Panel	
	Which Panel Tested?			Position of Front Face	
	Connection Type between Legs and Diagonal (A/B) (Refer to Fig. 4.4)			Compression Diagonal In Test Panel (INSIDE/ OUTSIDE)	
	Elastic Modulus (GPa)			Yield Stress of Diagonal (MPa)	
Result of Test	Failure Load of Tower (kN)				
	Buckling Load of Front Diagonal (kN)			Buckling Load of Rear Diagonal (kN)	
	Effective Length Factor of Front Diagonal by AISC-LRFD			Effective Length Factor of Rear Diagonal by AISC-LRFD	
	Effective Length Factor of Front Diagonal by CSA S16.1-94			Effective Length Factor of Rear Diagonal by CSA S16.1-94	
Description of Test	Test failed. No result available.				

Table A-10 Record of Test No.10

Specimen ID:S5B

Description of Specimen	Horizontal (YES/NO)	NO	Diameter of Leg (mm)	69.9
	Diameter of Diagonal (mm)	15.9	Diameter of Horizontal (mm)	-
	Length of Diagonal (mm)	1190	Width of Face (mm)	914
	Length of Panel (mm)	762	Number of Panel	6
	Which Panel Tested?	A	Position of Front Face Compression Diagonal In Test Panel (INSIDE/ OUTSIDE)	-
Result of Test	Connection Type between Legs and Diagonal (A/B) (Refer to Fig. 4.4)	A		
	Elastic Modulus (GPa)	200	Yield Stress of Diagonal (MPa)	385
	Failure Load of Tower (kN)	100		
	Buckling Load of Front Diagonal (kN)	33.2	Buckling Load of Rear Diagonal (kN)	-
	Effective Length Factor of Front Diagonal by AISC-LRFD	0.336	Effective Length Factor of Rear Diagonal by AISC-LRFD	-
Description of Test	Effective Length Factor of Front Diagonal by CSA S16.1-94	0.312	Effective Length Factor of Rear Diagonal by CSA S16.1-94	-
	Panel A: Front diagonal buckled with top half inside			

Table A-11 Record of Test No.11

Specimen ID: S6A

Description of Specimen	Horizontal (YES/NO)		Diameter of Leg (mm)	
	Diameter of Diagonal (mm)	YES	Diameter of Horizontal (mm)	69.9
	Length of Diagonal (mm)	15.9		19.1
	Length of Panel (mm)	1190	Width of Face (mm)	914
	Which Panel Tested?	762	Number of Panel	6
	Connection Type between Legs and Diagonal (A/B) (Refer to Fig. 4.4)	A	Position of Front Face Compression Diagonal In Test Panel (INSIDE/ OUTSIDE)	-
	Elastic Modulus (GPa)	A	Yield Stress of Diagonal (MPa)	385
	Failure Load of Tower (kN)	200		
	Buckling Load of Front Diagonal (kN)	144	Buckling Load of Rear Diagonal (kN)	29.2
	Effective Length Factor of Front Diagonal by AISC-LRFD	27.3	Effective Length Factor of Rear Diagonal by AISC-LRFD	0.361
Result of Test	Effective Length Factor of Front Diagonal by CSA S16.1-94	0.374	Effective Length Factor of Rear Diagonal by CSA S16.1-94	0.342
Description of Test	Panel A: Front diagonal first buckled with top half inside Rear diagonal buckled with top half outside			

Table A-12 Record of Test No.12

Specimen ID:S5C

Description of Specimen	Horizontal (YES/NO)	NO	Diameter of Leg (mm)	69.9	
	Diameter of Diagonal (mm)	15.9	Diameter of Horizontal (mm)	-	
	Length of Diagonal (mm)	1190	Width of Face (mm)	914	
	Length of Panel (mm)	762	Number of Panel	6	
	Which Panel Tested?	C	Position of Front Face	-	
	Connection Type between Legs and Diagonal (A/B) (Refer to Fig. 4.4)	A	Compression Diagonal In Test Panel (INSIDE/ OUTSIDE)		
	Elastic Modulus (GPa)	200	Yield Stress of Diagonal (MPa)		385
	Result of Test	Failure Load of Tower (kN)	81.7		
		Buckling Load of Front Diagonal (kN)	29.0	Buckling Load of Rear Diagonal (kN)	30.2
Effective Length Factor of Front Diagonal by AISC-LRFD		0.362	Effective Length Factor of Rear Diagonal by AISC-LRFD	0.355	
Effective Length Factor of Front Diagonal by CSA S16.1-94		0.343	Effective Length Factor of Rear Diagonal by CSA S16.1-94	0.334	
Description of Test	Panel A: Front diagonal first buckled with bottom half inside Rear diagonal buckled with bottom half outside				

Table A-13 Record of Test No.13

Specimen ID:S6B

Description of Specimen	Horizontal (YES/NO)	YES	Diameter of Leg (mm)	69.9
	Diameter of Diagonal (mm)	15.9	Diameter of Horizontal (mm)	19.1
	Length of Diagonal (mm)	1190	Width of Face (mm)	914
	Length of Panel (mm)	762	Number of Panel	6
	Which Panel Tested?	A	Position of Front Face	
	Connection Type between Legs and Diagonal (A/B) (Refer to Fig. 4.4)	A	Compression Diagonal In Test Panel (INSIDE/ OUTSIDE)	-
	Elastic Modulus (GPa)	200	Yield Stress of Diagonal (MPa)	382
Result of Test	Failure Load of Tower (kN)	154.4		
	Buckling Load of Front Diagonal (kN)	25.4	Buckling Load of Rear Diagonal (kN)	-
	Effective Length Factor of Front Diagonal by AISC-LRFD	0.375	Effective Length Factor of Rear Diagonal by AISC-LRFD	-
	Effective Length Factor of Front Diagonal by CSA S16.1-94	0.387	Effective Length Factor of Rear Diagonal by CSA S16.1-94	-
Description of Test	Panel A: Front diagonal first buckled with top half outside			

Table A-14 Record of Test No.14

Specimen ID:31SRB

Description of Specimen	Horizontal (YES/NO)	YES	Diameter of Leg (mm)	33.3
	Diameter of Diagonal (mm)	22.2	Diameter of Horizontal (mm)	-
	Length of Diagonal (mm)	938	Width of Face (mm)	787
	Length of Panel (mm)	1016	Number of Panel	6
	Which Panel Tested?	ALL	Position of Front Face	
	Connection Type between Legs and Diagonal (A/B) (Refer to Fig. 4.4)	A	Compression Diagonal In Test Panel (INSIDE/ OUTSIDE)	-
	Elastic Modulus (GPa)	200	Yield Stress of Diagonal (MPa)	382
Result of Test	Failure Load of Tower (kN)	143.6		
	Buckling Load of Front Diagonal (kN)	-	Buckling Load of Rear Diagonal (kN)	-
	Effective Length Factor of Front Diagonal by AISC-LRFD	-	Effective Length Factor of Rear Diagonal by AISC-LRFD	-
	Effective Length Factor of Front Diagonal by CSA S16.1-94	-	Effective Length Factor of Rear Diagonal by CSA S16.1-94	-
Description of Test	Top leg buckled first. No diagonal buckled			

Table A-15 Record of Test No.15

Specimen ID:P6B

Description of Specimen	Horizontal (YES/NO)	NO	Diameter of Leg (mm)	57.2
	Diameter of Diagonal (mm)	22.2	Diameter of Horizontal (mm)	-
	Length of Diagonal (mm)	1158	Width of Face (mm)	914
	Length of Panel (mm)	711	Number of Panel	8
	Which Panel Tested?	D	Position of Front Face	OUTSIDE
	Connection Type between Legs and Diagonal (A/B) (Refer to Fig. 4.4)	B	Compression Diagonal In Test Panel (INSIDE/ OUTSIDE)	
Result of Test	Elastic Modulus (GPa)	200	Yield Stress of Diagonal (MPa)	442
	Failure Load of Tower (kN)	287		
	Buckling Load of Front Diagonal (kN)	-	Buckling Load of Rear Diagonal (kN)	101.5
	Effective Length Factor of Front Diagonal by AISC-LRFD	-	Effective Length Factor of Rear Diagonal by AISC-LRFD	0.359
	Effective Length Factor of Front Diagonal by CSA S16.1-94	-	Effective Length Factor of Rear Diagonal by CSA S16.1-94	0.323
	Description of Test	Panel D: Rear diagonal buckled with top half inside		

Table A-16 Record of Test No.16

Specimen ID:33SRC

Description of Specimen	Horizontal (YES/NO)	YES	Diameter of Leg (mm)	58.0
	Diameter of Diagonal (mm)	28.6	Diameter of Horizontal (mm)	-
	Length of Diagonal (mm)	980	Width of Face (mm)	838
	Length of Panel (mm)	1016	Number of Panel	6
	Which Panel Tested?	ALL	Position of Front Face	
	Connection Type between Legs and Diagonal (A/B) (Refer to Fig. 4.4)	A	Compression Diagonal In Test Panel (INSIDE/ OUTSIDE)	-
	Elastic Modulus (GPa)	200	Yield Stress of Diagonal (MPa)	364
	Failure Load of Tower (kN)	460		
	Buckling Load of Front Diagonal (kN)	148.6	Buckling Load of Rear Diagonal (kN)	150.5
Result of Test	Effective Length Factor of Front Diagonal by AISC-LRFD	0.559	Effective Length Factor of Rear Diagonal by AISC-LRFD	0.551
	Effective Length Factor of Front Diagonal by CSA S16.1-94	0.502	Effective Length Factor of Rear Diagonal by CSA S16.1-94	0.495
	Description of Test Panel B: Rear diagonal buckled inside Panel C: Front diagonal buckled outside			

Table A-17 Record of Test No.17

Specimen ID:P7B

Description of Specimen	Horizontal (YES/NO)		YES	Diameter of Leg (mm)	38.1
	Diameter of Diagonal (mm)				
	Length of Diagonal (mm)		22.2	Diameter of Horizontal (mm)	22.2
	Length of Panel (mm)		1158	Width of Face (mm)	914
	Which Panel Tested?		711	Number of Panel	8
	Connection Type between Legs and Diagonal (A/B) (Refer to Fig. 4.4)		A	Position of Front Face Compression Diagonal In Test Panel (INSIDE/ OUTSIDE)	OUTSIDE
	Elastic Modulus (GPa)		B	Yield Stress of Diagonal (MPa)	378
	Failure Load of Tower (kN)		200		
	Buckling Load of Front Diagonal (kN)		223	Buckling Load of Rear Diagonal (kN)	-
	Effective Length Factor of Front Diagonal by AISC-LRFD		-	Effective Length Factor of Rear Diagonal by AISC-LRFD	-
	Effective Length Factor of Front Diagonal by CSA S16.1-94		-	Effective Length Factor of Rear Diagonal by CSA S16.1-94	-
Description of Test	Top leg buckled inplane. No diagonal buckled.				

Table A-18 Record of Test No.18

Specimen ID:P7A

Description of Specimen	Horizontal (YES/NO)	YES	Diameter of Leg (mm)	38.1
	Diameter of Diagonal (mm)	22.2	Diameter of Horizontal (mm)	22.2
	Length of Diagonal (mm)	1158	Width of Face (mm)	914
	Length of Panel (mm)	711	Number of Panel	8
	Which Panel Tested?	A	Position of Front Face	OUTSIDE
	Connection Type between Legs and Diagonal (A/B) (Refer to Fig. 4.4)	B	Compression Diagonal in Test Panel (INSIDE/ OUTSIDE)	
Result of Test	Elastic Modulus (GPa)	200	Yield Stress of Diagonal (MPa)	378
	Failure Load of Tower (kN)	236		
	Buckling Load of Front Diagonal (kN)	-	Buckling Load of Rear Diagonal (kN)	-
	Effective Length Factor of Front Diagonal by AISC-LRFD	-	Effective Length Factor of Rear Diagonal by AISC-LRFD	-
	Effective Length Factor of Front Diagonal by CSA S16.1-94	-	Effective Length Factor of Rear Diagonal by CSA S16.1-94	-
	Description of Test	Top leg buckled outplane. No diagonal buckled.		

Table A-19 Record of Test No.19

Specimen ID:P8B

Description of Specimen	Horizontal (YES/NO)	NO	Diameter of Leg (mm)	38.1
	Diameter of Diagonal (mm)	22.2	Diameter of Horizontal (mm)	-
Description of Specimen	Length of Diagonal (mm)	1158	Width of Face (mm)	914
	Length of Panel (mm)	711	Number of Panel	8
	Which Panel Tested?	D	Position of Front Face	INSIDE
	Connection Type between Legs and Diagonal (A/B) (Refer to Fig. 4.4)	B	Compression Diagonal In Test Panel (INSIDE/ OUTSIDE)	
	Elastic Modulus (GPa)	200	Yield Stress of Diagonal (MPa)	349
Result of Test	Failure Load of Tower (kN)	193		
	Buckling Load of Front Diagonal (kN)	82.0	Buckling Load of Rear Diagonal (kN)	-
	Effective Length Factor of Front Diagonal by AISC-LRFD	0.394	Effective Length Factor of Rear Diagonal by AISC-LRFD	-
	Effective Length Factor of Front Diagonal by CSA S16.1-94	0.355	Effective Length Factor of Rear Diagonal by CSA S16.1-94	-
Description of Test	Panel D: Front diagonal buckled with top half inside			

Table A-20 Record of Test No.20

Specimen ID:P4B

Description of Specimen	Horizontal (YES/NO)	NO	Diameter of Leg (mm)	50.8
	Diameter of Diagonal (mm)	19.1	Diameter of Horizontal (mm)	-
	Length of Diagonal (mm)	1158	Width of Face (mm)	914
	Length of Panel (mm)	711	Number of Panel	8
	Which Panel Tested?	D	Position of Front Face	INSIDE
	Connection Type between Legs and Diagonal (A/B) (Refer to Fig. 4.4)	B	Compression Diagonal in Test Panel (INSIDE/ OUTSIDE)	
	Elastic Modulus (GPa)	200	Yield Stress of Diagonal (MPa)	409
Result of Test	Failure Load of Tower (kN)	166		
	Buckling Load of Front Diagonal (kN)	51.5	Buckling Load of Rear Diagonal (kN)	50.2
	Effective Length Factor of Front Diagonal by AISC-LRFD	0.399	Effective Length Factor of Rear Diagonal by AISC-LRFD	0.405
	Effective Length Factor of Front Diagonal by CSA S16.1-94	0.369	Effective Length Factor of Rear Diagonal by CSA S16.1-94	0.376
Description of Test	Panel D: Front diagonal buckled with top half inside Rear diagonal buckled with top half outside			

Table A-21 Record of Test No.21

Specimen ID:P2A

Description of Specimen	Horizontal (YES/NO)		NO	Diameter of Leg (mm)		50.8	
	Diameter of Diagonal (mm)		19.1	Diameter of Horizontal (mm)		-	
	Length of Diagonal (mm)		1158	Width of Face (mm)		914	
	Length of Panel (mm)		711	Number of Panel		8	
	Which Panel Tested?		D	Position of Front Face		INSIDE	
	Connection Type between Legs and Diagonal (A/B) (Refer to Fig. 4.4)		B	Compression Diagonal In Test Panel (INSIDE/ OUTSIDE)			
	Elastic Modulus (GPa)		200	Yield Stress of Diagonal (MPa)			409
	Result of Test	Failure Load of Tower (kN)		86.4			
		Buckling Load of Front Diagonal (kN)		-	Buckling Load of Rear Diagonal (kN)		29.7
		Effective Length Factor of Front Diagonal by AISC-LRFD		-	Effective Length Factor of Rear Diagonal by AISC-LRFD		0.368
Effective Length Factor of Front Diagonal by CSA S16.1-94		-	Effective Length Factor of Rear Diagonal by CSA S16.1-94		0.345		
Description of Test	Panel D: Front diagonal not buckled. Rear diagonal buckled with top half outside						

Table A-22 Record of Test No.22

Specimen ID:P1A

Description of Specimen	Horizontal (YES/NO)	YES	Diameter of Leg (mm)	38.1
	Diameter of Diagonal (mm)	15.9	Diameter of Horizontal (mm)	22.4
	Length of Diagonal (mm)	1158	Width of Face (mm)	914
	Length of Panel (mm)	711	Number of Panel	8
	Which Panel Tested?	A	Position of Front Face Compression Diagonal In Test Panel (INSIDE/ OUTSIDE)	OUTSIDE
	Connection Type between Legs and Diagonal (A/B) (Refer to Fig. 4.4)	B		
	Elastic Modulus (GPa)	200		
	Failure Load of Tower (kN)	146	Yield Stress of Diagonal (MPa)	-
	Buckling Load of Front Diagonal (kN)	-	Buckling Load of Rear Diagonal (kN)	-
	Effective Length Factor of Front Diagonal by AISC-LRFD	-	Effective Length Factor of Rear Diagonal by AISC-LRFD	-
Result of Test	Effective Length Factor of Front Diagonal by CSA S16.1-94	-	Effective Length Factor of Rear Diagonal by CSA S16.1-94	-
	Panel D: No diagonal buckled			
Description of Test				

Table A-23 Record of Test No.23

Specimen ID:S2C

Description of Specimen	Horizontal (YES/NO)		YES	Diameter of Leg (mm)		38.1
	Diameter of Diagonal (mm)		12.7	Diameter of Horizontal (mm)		19.1
	Length of Diagonal (mm)		1190	Width of Face (mm)		914
	Length of Panel (mm)		762	Number of Panel		6
	Which Panel Tested?		A	Position of Front Face		OUTSIDE
	Connection Type between Legs and Diagonal (A/B) (Refer to Fig. 4.4)		A	Compression Diagonal In Test Panel (INSIDE/ OUTSIDE)		
	Elastic Modulus (GPa)		200	Yield Stress of Diagonal (MPa)		353
Result of Test	Failure Load of Tower (kN)		94			
	Buckling Load of Front Diagonal (kN)		14.5	Buckling Load of Rear Diagonal (kN)		14.8
	Effective Length Factor of Front Diagonal by AISC-LRFD		0.337	Effective Length Factor of Rear Diagonal by AISC-LRFD		0.328
	Effective Length Factor of Front Diagonal by CSA S16.1-94		0.319	Effective Length Factor of Rear Diagonal by CSA S16.1-94		0.315
Description of Test	Panel A: Front diagonal buckled with bottom half outside Rear diagonal buckled with top half inside and bottom half outside					

Table A-24 Record of Test No.24

Specimen ID:S6C

Description of Specimen	Horizontal (YES/NO)	YES	Diameter of Leg (mm)	69.9
	Diameter of Diagonal (mm)	15.9	Diameter of Horizontal (mm)	19.1
	Length of Diagonal (mm)	1190	Width of Face (mm)	914
	Length of Panel (mm)	762	Number of Panel	6
	Which Panel Tested?	A	Position of Front Face	INSIDE
	Connection Type between Legs and Diagonal (A/B) (Refer to Fig. 4.4)	A	Compression Diagonal In Test Panel (INSIDE/ OUTSIDE)	
Result of Test	Elastic Modulus (GPa)	200	Yield Stress of Diagonal (MPa)	-
	Failure Load of Tower (kN)	175		
	Buckling Load of Front Diagonal (kN)	-	Buckling Load of Rear Diagonal (kN)	-
	Effective Length Factor of Front Diagonal by AISC-LRFD	-	Effective Length Factor of Rear Diagonal by AISC-LRFD	-
	Effective Length Factor of Front Diagonal by CSA S16.1-94	-	Effective Length Factor of Rear Diagonal by CSA S16.1-94	-
Description of Test	Panel A: Diagonal not buckled. Horizontal buckled first, and panel C&D buckled			

Table A-25 Record of Test No.25

Specimen ID:S3B

Description of Specimen	Horizontal (YES/NO)		NO	Diameter of Leg (mm)	50.8
	Diameter of Diagonal (mm)		14.3	Diameter of Horizontal (mm)	-
	Length of Diagonal (mm)		1190	Width of Face (mm)	914
	Length of Panel (mm)		762	Number of Panel	6
	Which Panel Tested?		C	Position of Front Face	OUTSIDE
Connection Type between Legs and Diagonal (A/B) (Refer to Fig. 4.4)		A	Compression Diagonal In Test Panel (INSIDE/ OUTSIDE)		
Elastic Modulus (GPa)		200	Yield Stress of Diagonal (MPa)		
Result of Test	Failure Load of Tower (kN)		71.9		
	Buckling Load of Front Diagonal (kN)		20.4	Buckling Load of Rear Diagonal (kN)	20.1
	Effective Length Factor of Front Diagonal by AISC-LRFD		0.351	Effective Length Factor of Rear Diagonal by AISC-LRFD	0.353
	Effective Length Factor of Front Diagonal by CSA S16.1-94		0.342	Effective Length Factor of Rear Diagonal by CSA S16.1-94	0.345
Description of Test	Panel C: Front Diagonal buckled with top half outside Rear diagonal buckled with top half inside				

Table A-26 Record of Test No.26

Specimen ID:P5A

Description of Specimen	Horizontal (YES/NO)	YES	Diameter of Leg (mm)	57.2
	Diameter of Diagonal (mm)	22.2	Diameter of Horizontal (mm)	22.2
	Length of Diagonal (mm)	1158	Width of Face (mm)	914
	Length of Panel (mm)	711	Number of Panel	8
	Which Panel Tested?	A	Position of Front Face Compression Diagonal In Test Panel (INSIDE/ OUTSIDE)	INSIDE
	Connection Type between Legs and Diagonal (A/B) (Refer to Fig. 4.4)	B		
	Elastic Modulus (GPa)	200	Yield Stress of Diagonal (MPa)	-
	Failure Load of Tower (kN)	413		
	Buckling Load of Front Diagonal (kN)	-	Buckling Load of Rear Diagonal (kN)	-
	Effective Length Factor of Front Diagonal by AISC-LRFD	-	Effective Length Factor of Rear Diagonal by AISC-LRFD	-
Result of Test	Effective Length Factor of Front Diagonal by CSA S16.1-94	-	Effective Length Factor of Rear Diagonal by CSA S16.1-94	-
Description of Test	Front horizontal buckled first. Panel D&E diagonal buckled outside			

Table A-27 Record of Test No.27

Specimen ID:P2B

Description of Specimen	Horizontal (YES/NO)	NO	Diameter of Leg (mm)	38.1
	Diameter of Diagonal (mm)	15.9	Diameter of Horizontal (mm)	-
	Length of Diagonal (mm)	1158	Width of Face (mm)	914
	Length of Panel (mm)	711	Number of Panel	8
	Which Panel Tested?	D	Position of Front Face	INSIDE
Connection Type between Legs and Diagonal (A/B) (Refer to Fig. 4.4)	B	Compression Diagonal In Test Panel (INSIDE/ OUTSIDE)		
Result of Test	Elastic Modulus (GPa)	200	Yield Stress of Diagonal (MPa)	373
	Failure Load of Tower (kN)	83.9		
	Buckling Load of Front Diagonal (kN)	23.5	Buckling Load of Rear Diagonal (kN)	30.2
	Effective Length Factor of Front Diagonal by AISC-LRFD	0.414	Effective Length Factor of Rear Diagonal by AISC-LRFD	0.364
	Effective Length Factor of Front Diagonal by CSA S16.1-94	0.403	Effective Length Factor of Rear Diagonal by CSA S16.1-94	0.341
Description of Test	Panel D: Front daigonal buckled with top half outside Rear diagonal buckled with bottom half inside			

Table A-28 Record of Test No.28

Specimen ID:P6A

Description of Specimen	Horizontal (YES/NO)		NO	Diameter of Leg (mm)		57.2
	Diameter of Diagonal (mm)		22.2	Diameter of Horizontal (mm)		-
	Length of Diagonal (mm)		1158	Width of Face (mm)		914
	Length of Panel (mm)		711	Number of Panel		8
	Which Panel Tested?		D	Position of Front Face		INSIDE
	Connection Type between Legs and Diagonal (A/B) (Refer to Fig. 4.4)		B	Compression Diagonal In Test Panel (INSIDE/ OUTSIDE)		
	Elastic Modulus (GPa)		200	Yield Stress of Diagonal (MPa)		
Result of Test	Failure Load of Tower (kN)		267			
	Buckling Load of Front Diagonal (kN)		91.3	Buckling Load of Rear Diagonal (kN)		82.5
	Effective Length Factor of Front Diagonal by AISC-LRFD		0.393	Effective Length Factor of Rear Diagonal by AISC-LRFD		0.424
	Effective Length Factor of Front Diagonal by CSA S16.1-94		0.356	Effective Length Factor of Rear Diagonal by CSA S16.1-94		0.388
Description of Test	Panel D: Front daigonal buckled with top half inside Rear diagonal buckled with bottom half inside					

Table A-29 Record of Test No.29

Specimen ID:P4A

Description of Specimen	Horizontal (YES/NO)	NO	Diameter of Leg (mm)	50.8
	Diameter of Diagonal (mm)	19.1	Diameter of Horizontal (mm)	-
	Length of Diagonal (mm)	1158	Width of Face (mm)	914
	Length of Panel (mm)	711	Number of Panel	8
	Which Panel Tested?	D	Position of Front Face	OUTSIDE
	Connection Type between Legs and Diagonal (A/B) (Refer to Fig. 4.4)	B	Compression Diagonal in Test Panel (INSIDE/ OUTSIDE)	
	Elastic Modulus (GPa)	200	Yield Stress of Diagonal (MPa)	
Result of Test	Failure Load of Tower (kN)	164		
	Buckling Load of Front Diagonal (kN)	-	Buckling Load of Rear Diagonal (kN)	48.7
	Effective Length Factor of Front Diagonal by AISC-LRFD	-	Effective Length Factor of Rear Diagonal by AISC-LRFD	0.385
	Effective Length Factor of Front Diagonal by CSA S16.1-94	-	Effective Length Factor of Rear Diagonal by CSA S16.1-94	0.412
Description of Test	Panel E: Buckled first.			
	Panel D: Front daigonal not buckled Rear diagonal buckled with top half inside			

Table A-30 Record of Test No.30

Specimen ID:P3A

Description of Specimen	Horizontal (YES/NO)	YES	Diameter of Leg (mm)	50.8
	Diameter of Diagonal (mm)	19.1	Diameter of Horizontal (mm)	22.2
	Length of Diagonal (mm)	1158	Width of Face (mm)	914
	Length of Panel (mm)	711	Number of Panel	8
	Which Panel Tested?	A	Position of Front Face Compression Diagonal In Test Panel (INSIDE/ OUTSIDE)	INSIDE
Result of Test	Connection Type between Legs and Diagonal (A/B) (Refer to Fig. 4.4)	B	Yield Stress of Diagonal (MPa)	408
	Elastic Modulus (GPa)	200		
	Failure Load of Tower (kN)	259		
	Buckling Load of Front Diagonal (kN)	55.0	Buckling Load of Rear Diagonal (kN)	52.0
	Effective Length Factor of Front Diagonal by AISC-LRFD	0.382	Effective Length Factor of Rear Diagonal by AISC-LRFD	0.396
Description of Test	Effective Length Factor of Front Diagonal by CSA S16.1-94	0.351	Effective Length Factor of Rear Diagonal by CSA S16.1-94	0.366
	Panel D: Front daigonal buckled with top half inside and bottom a little inside (First) Rear diagonal buckled with bottom half outside and top half a little inside			

Table A-31 Record of Test No.31

Specimen ID:P1B

Description of Specimen	Horizontal (YES/NO)	YES	Diameter of Leg (mm)	38.1
	Diameter of Diagonal (mm)	15.9	Diameter of Horizontal (mm)	22.2
	Length of Diagonal (mm)	1158	Width of Face (mm)	914
	Length of Panel (mm)	711	Number of Panel	8
	Which Panel Tested?	A	Position of Front Face	OUTSIDE
	Connection Type between Legs and Diagonal (A/B) (Refer to Fig. 4.4)	B	Compression Diagonal In Test Panel (INSIDE/ OUTSIDE)	
	Elastic Modulus (GPa)	200	Yield Stress of Diagonal (MPa)	375
Result of Test	Failure Load of Tower (kN)	155		
	Buckling Load of Front Diagonal (kN)	26.3	Buckling Load of Rear Diagonal (kN)	29.0
	Effective Length Factor of Front Diagonal by AISC-LRFD	0.391	Effective Length Factor of Rear Diagonal by AISC-LRFD	0.372
	Effective Length Factor of Front Diagonal by CSA S16.1-94	0.375	Effective Length Factor of Rear Diagonal by CSA S16.1-94	0.351
Description of Test	Panel D: Front daigonal buckled with bottom half outside Rear daigonal buckled with top half inside			

Table A-32 Record of Test No.32

Specimen ID:P3B

Description of Specimen	Horizontal (YES/NO)	YES	Diameter of Leg (mm)	50.8
	Diameter of Diagonal (mm)	19.1	Diameter of Horizontal (mm)	22.2
	Length of Diagonal (mm)	1158	Width of Face (mm)	914
	Length of Panel (mm)	711	Number of Panel	8
	Which Panel Tested?	A	Position of Front Face	INSIDE
	Connection Type between Legs and Diagonal (A/B) (Refer to Fig. 4.4)	B	Compression Diagonal In Test Panel (INSIDE/ OUTSIDE)	
	Elastic Modulus (GPa)	200	Yield Stress of Diagonal (MPa)	409
Result of Test	Failure Load of Tower (kN)	268		
	Buckling Load of Front Diagonal (kN)	60.0	Buckling Load of Rear Diagonal (kN)	47.3
	Effective Length Factor of Front Diagonal by AISC-LRFD	0.360	Effective Length Factor of Rear Diagonal by AISC-LRFD	0.419
	Effective Length Factor of Front Diagonal by CSA S16.1-94	0.327	Effective Length Factor of Rear Diagonal by CSA S16.1-94	0.393
	Panel A: Front daigonal buckled with top half inside Rear diagonal buckled with bottom half outside			
Description of Test				

Table A-33 Record of Test No.33

Specimen ID:P8A

Description of Specimen	Horizontal (YES/NO)	NO	Diameter of Leg (mm)	38.1
	Diameter of Diagonal (mm)	22.2	Diameter of Horizontal (mm)	-
	Length of Diagonal (mm)	1158	Width of Face (mm)	914
	Length of Panel (mm)	711	Number of Panel	8
	Which Panel Tested?	D	Position of Front Face	OUTSIDE
	Connection Type between Legs and Diagonal (A/B) (Refer to Fig. 4.4)	B	Compression Diagonal In Test Panel (INSIDE/ OUTSIDE)	
	Elastic Modulus (GPa)	200	Yield Stress of Diagonal (MPa)	
	Failure Load of Tower (kN)	192		
	Buckling Load of Front Diagonal (kN)	75.4	Buckling Load of Rear Diagonal (kN)	-
Result of Test	Effective Length Factor of Front Diagonal by AISC-LRFD	0.425	Effective Length Factor of Rear Diagonal by AISC-LRFD	-
	Effective Length Factor of Front Diagonal by CSA S16.1-94	0.383	Effective Length Factor of Rear Diagonal by CSA S16.1-94	-
	Panel A: Front daigonal buckled with top half outside			
Description of Test				

Table A-34 Record of Test No.34

Specimen ID:P5B

Description of Specimen	Horizontal (YES/NO)	YES	Diameter of Leg (mm)	57.2
	Diameter of Diagonal (mm)	22.2	Diameter of Horizontal (mm)	22.2
Description of Specimen	Length of Diagonal (mm)	1158	Width of Face (mm)	914
	Length of Panel (mm)	711	Number of Panel	8
	Which Panel Tested?	A	Position of Front Face	OUTSIDE
	Connection Type between Legs and Diagonal (A/B) (Refer to Fig. 4.4)	B	Compression Diagonal In Test Panel (INSIDE/ OUTSIDE)	
	Elastic Modulus (GPa)	200	Yield Stress of Diagonal (MPa)	
	Failure Load of Tower (kN)	464		442
Result of Test	Buckling Load of Front Diagonal (kN)	-	Buckling Load of Rear Diagonal (kN)	88.2
	Effective Length Factor of Front Diagonal by AISC-LRFD	-	Effective Length Factor of Rear Diagonal by AISC-LRFD	0.404
	Effective Length Factor of Front Diagonal by CSA S16.1-94	-	Effective Length Factor of Rear Diagonal by CSA S16.1-94	0.367
	Panel A: Rear daigonal buckled with top half inside			
Description of Test				

APPENDIX-B

Tables of Load-deflection Records and Deflection-shape

LOAD DEFLECTION DATA - SPECIMEN S-4B

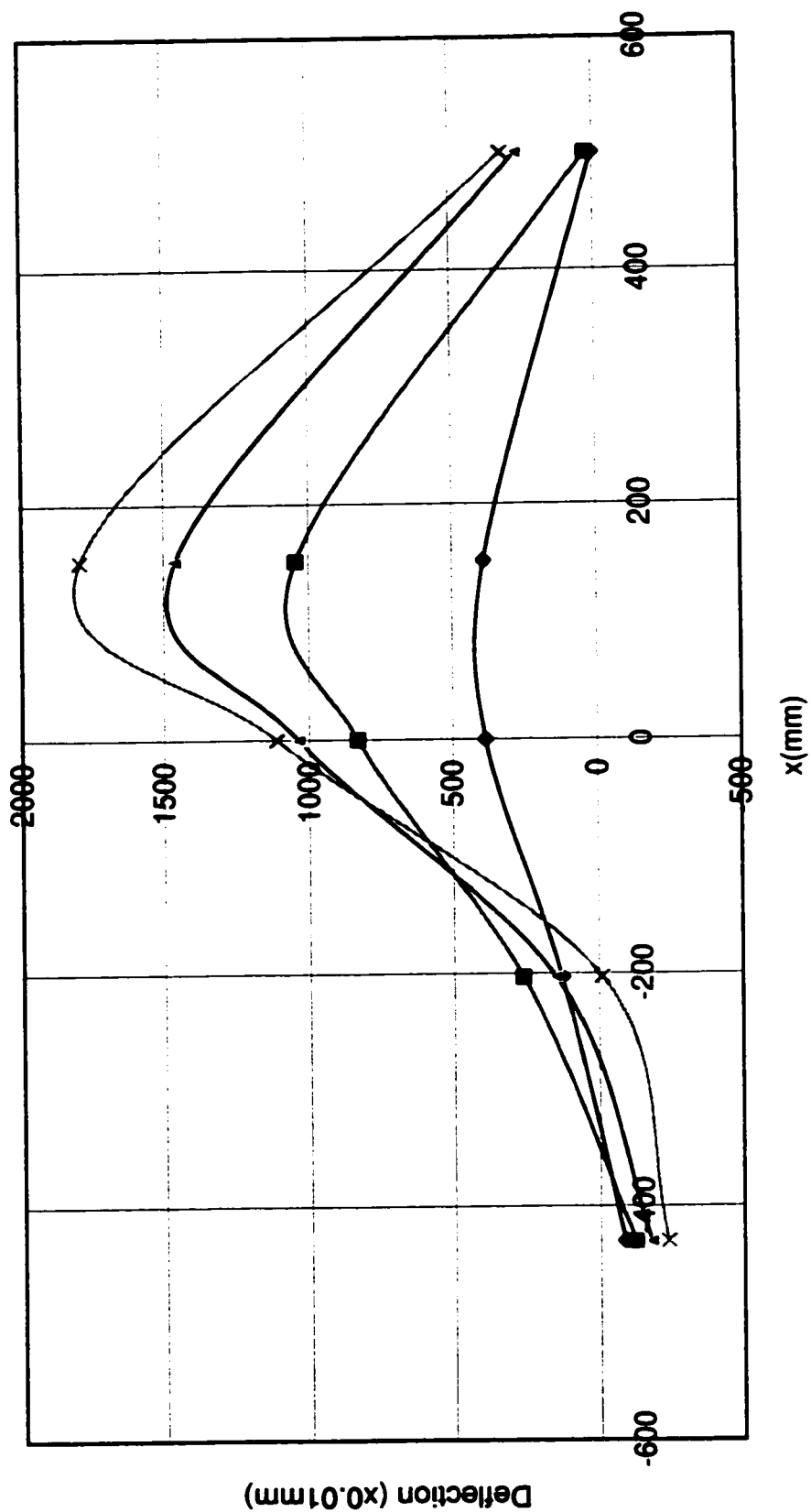
Test No. 3

Test No. 3							
No.	Load Applied on Specimen	Axcial Force in Comp. Diagonal	Out-of-plane of Diagonal				
			Dial Gauge No.1	Dial Gauge No.2	Dial Gauge No.3	Dial Gauge No.4	Dial Gauge No.5
Location (mm)			-430	-203	0	152	500
	kN	kN	x0.01 mm	x0.01 mm	x0.01 mm	x0.01 mm	x0.01 mm
1	10.0	2.1	-28	19	77	77	-16
2	20.0	3.9	-55	40	152	154	-15
3	30.0	5.7	-72	70	237	240	-6
4	35.0	6.7	-75	90	286	289	-4
5	40.0	7.5	-79	110	338	345	-4
6	45.0	8.3	-86	127	385	389	5
7	47.5	8.8	-86	137	416	726	8
8	50.0	9.2	-86	145	435	550	12
9	52.5	9.6	-103	155	459	579	18
10	55.0	10.0	-103	162	482	595	23
11	60.0	10.8	-103	180	529	660	34
12	65.0	11.6	-107	196	574	704	45
13	70.0	12.3	-109	210	620	766	57
14	75.0	13.1	-110	213	663	812	70
15	80.0	13.9	-113	235	708	877	84
16	85.0	14.7	-116	244	750	935	98
17	90.0	15.4	-120	253	793	985	112
18	92.5	15.8	-121	256	815	1011	120
19	95.0	16.1	-123	259	830	1046	27
20	97.5	16.5	-127	260	854	1076	34
21	100.0	17.0	-130	261	876	1099	138
22	102.5	17.3	-132	262	894	1127	150
23	105.0	17.9	-135	264	913	1160	158
24	107.5	17.3	-137	264	930	1190	168
25	110.0	17.6	-140	262	950	1224	176
26	112.5	18.7	-142	259	968	1258	186
27	115.0	19.9	-146	253	985	1285	196
28	117.5	21.6	-149	245	998	1317	202
29	120.0	22.4	-144	235	1011	1350	212
30	122.5	23.1	-160	222	1018	1368	225
31	125.0	23.9	-165	205	1025	1385	336
32	127.5	24.9	-172	185	1029	1395	253
33	130.0	25.5	-179	148	1039	1460	268
34	132.5	23.8	-195	100	1093	1490	291
35	135.0	17.0	-239	-11	1114	1795	318
36	137.5	14.8	-276	-81	1114	1910	345
37	140.0	14.1	-287	-114	1129	1990	363
38	142.5	13.3	-306	-155	1133	2091	386

* Refer to Figure-A-1 for Location of Dial Gauges

Deflection Shape

Test No. 3 S4B



—◆— $P=8.3\text{kN}$ —■— $P=16.1\text{kN}$ —+— $P=25.5\text{kN}$ —x— $P=17.0\text{kN}(\text{Unload})$

LOAD DEFLECTION DATA - SPECIMEN S-2A

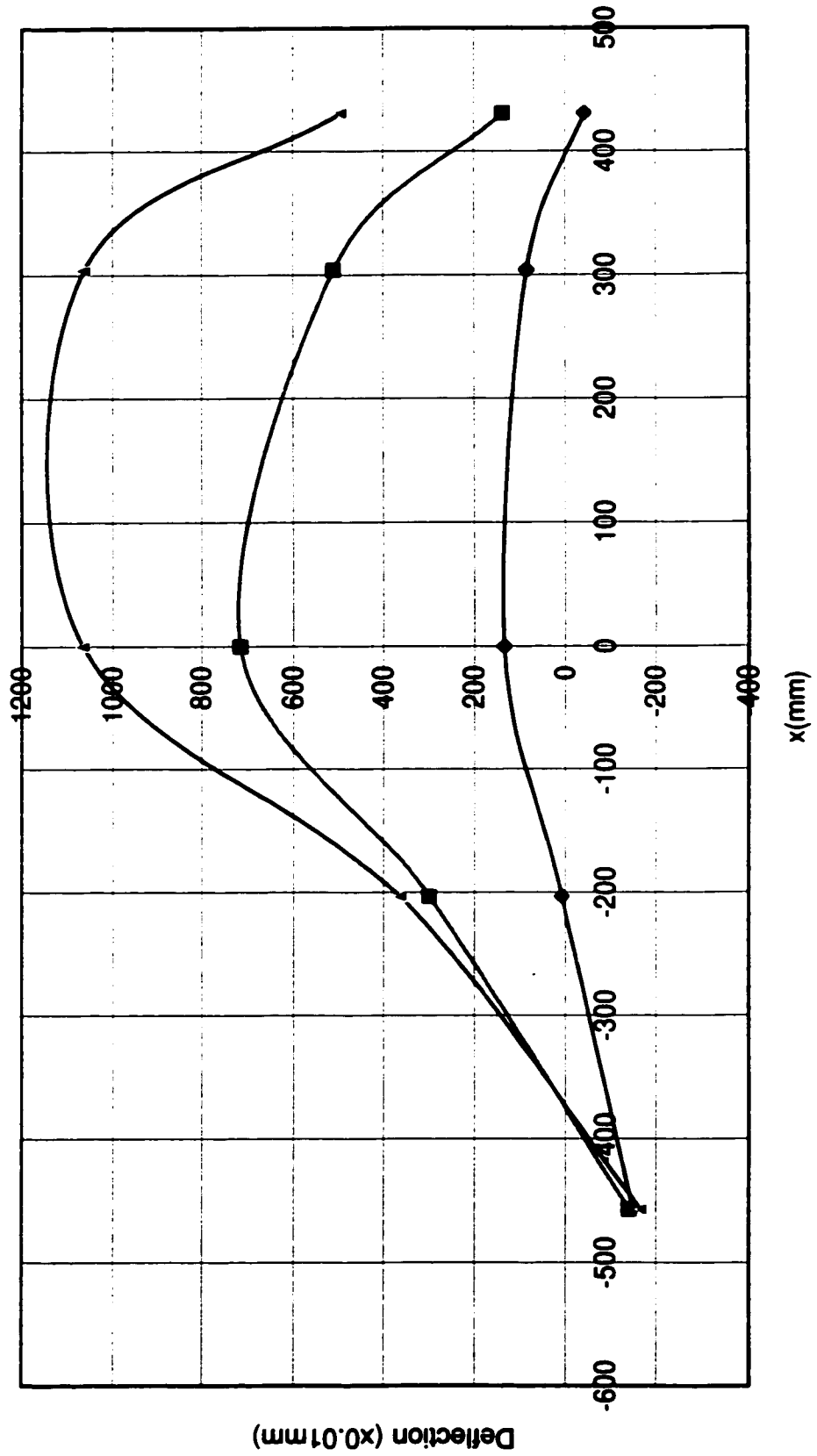
Test No. 4

No.	Load Applied on Specimen	Axial Force In Comp. Diagonal	Out-of-plane of Diagonal						Midspan Deflection (Vertical)		
			Dial Gauge No.1	Dial Gauge No.2	Dial Gauge No.3	Dial Gauge No.4	Dial Gauge No.5	Dial Gauge No.6	Dial Gauge No.7		
	Location (mm)		-457	-203	0	304	431	Front	Rear		
	kN	kN	x0.01 mm	x0.01 mm	x0.01 mm	x0.01 mm	x0.01 mm	x0.01 mm	x0.01 mm		
	0	0	0	0	0	0	0				
1	10	2.3	-87	-39	0	11	-57				
2	20	4.2	-137	-30	57	37	-60				
3	30	6	-147	8	134	85	-43				
4	40	7.9	-147	79	264	167	-10				
5	50	9.7	-147	152	406	263	33				
6	60	11.4	-143	219	546	367	73				
7	70	13.2	-139	299	716	509	137				
8	75	13.8	-138	323	784	575	165				
9	77.5	14.1	-138	333	814	607	179				
10	80	13.5	-138	347	864	673	208				
11	82.5	14.9	-137	351	892	805	225				
12	85	15.4	-137	354	943	779	257				
13	87.5	15.8	-140	352	979	833	315				
14	90	16.2	-148	337	1023	912	375				
15	92.5	16.9	-165	365	1065	1062	492				
16	95	15.9	-204	73	1052	1333	-				

* Refer to Figure-A-1 for Location of Dial Gauges

Deflection Shape

Test No. 4 S2A



—◆— P=6.0 kN N=3.45 kN —■— P=13.2kN N=9.42 kN —▲— P=16.9kN N=13.96 kN

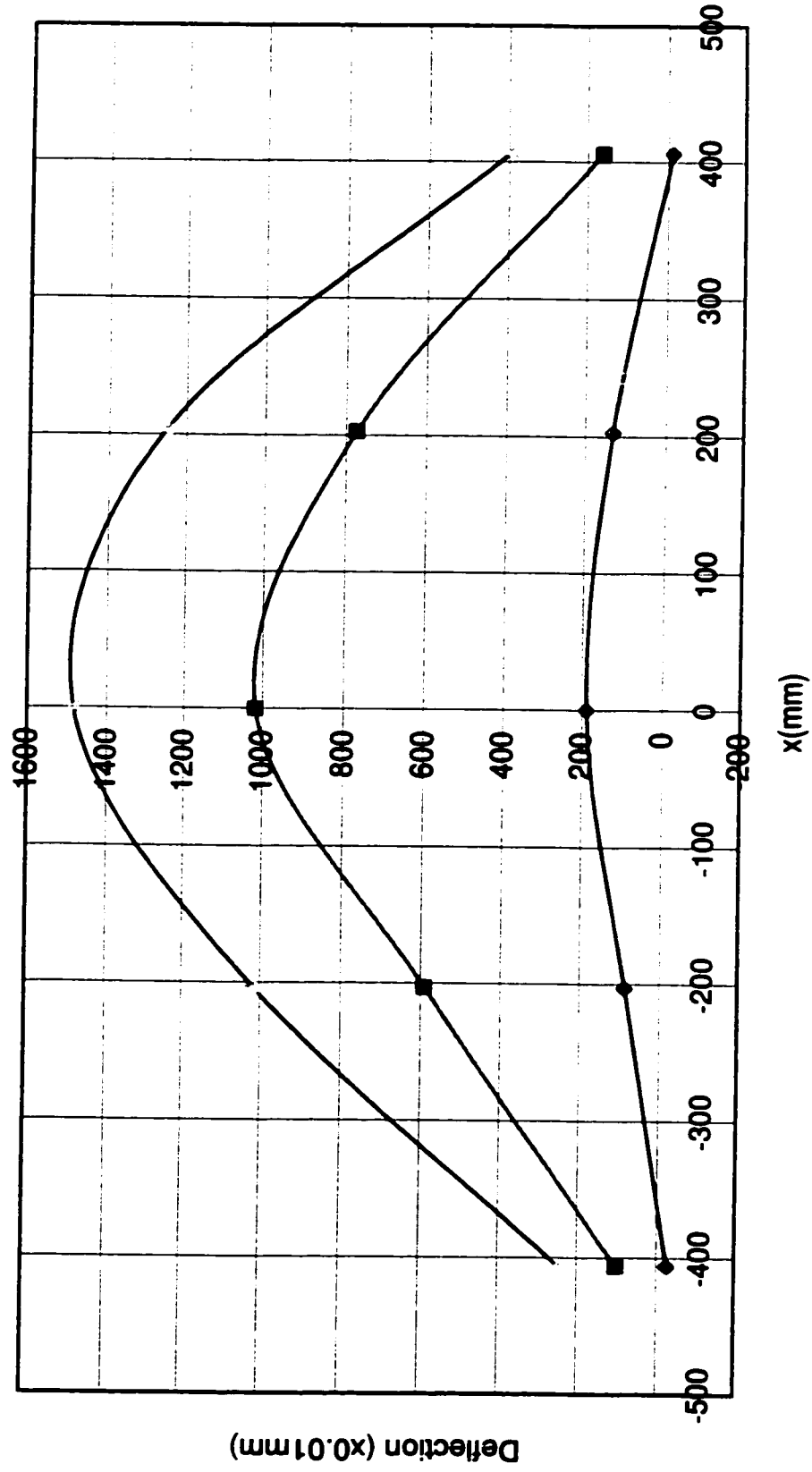
LOAD DEFLECTION DATA - SPECIMEN S-3A **Test No. 7**

No.	Load Applied on Specimen	Axial Force In Comp. Diagonal	Out-of-plane Deflection of Diagonal						Midspan Deflection (Vertical)	
			Dial Gauge No.1	Dial Gauge No.2	Dial Gauge No.3	Dial Gauge No.4	Dial Gauge No.5	Dial Gauge No.6	Dial Gauge No.7	
		Location (mm)	-406	-203	0	203	406	Front	Rear	
		kN	x0.01 mm	x0.01 mm	x0.01 mm	x0.01 mm	x0.01 mm	x0.01 mm	x0.01 mm	
		0	0	0	0	0	0			
1	10.0	3.2	-14	10	28	14	2			
2	20.0	6.5	-34	23	79	47	-24			
3	30.0	10.1	-25	86	188	130	-12			
4	40.0	13.5	-10	181	350	256	16			
5	50.0	16.9	34	343	618	466	74			
6	55.0	18.6	64	461	813	612	113			
7	57.5	19.4	80	526	913	694	138			
8	60.0	20.4	100	590	1018	774	160			
9	62.5	21.4	120	663	1132	866	186			
10	65.0	22.2	142	735	1240	952	212			
11	67.5	23.6	168	821	1372	1054	238			
12	70.0	24.1	192	881	1386	1126	362			
13	72.5	26.4	248	1019	1486	1252	396			

* Refer to Figure A-1 for Location of Dial Gauges

Deflection Shape

Test No. 7 S3A



—◆— $P=10.1 \text{ kN}$ $N=1.44 \text{ kN}$ —■— $P=20.4 \text{ kN}$ $N=3.62 \text{ kN}$ —●— $P=26.4 \text{ kN}$ $N=4.59 \text{ kN}$

LOAD DEFLECTION DATA - SPECIMEN S-5B

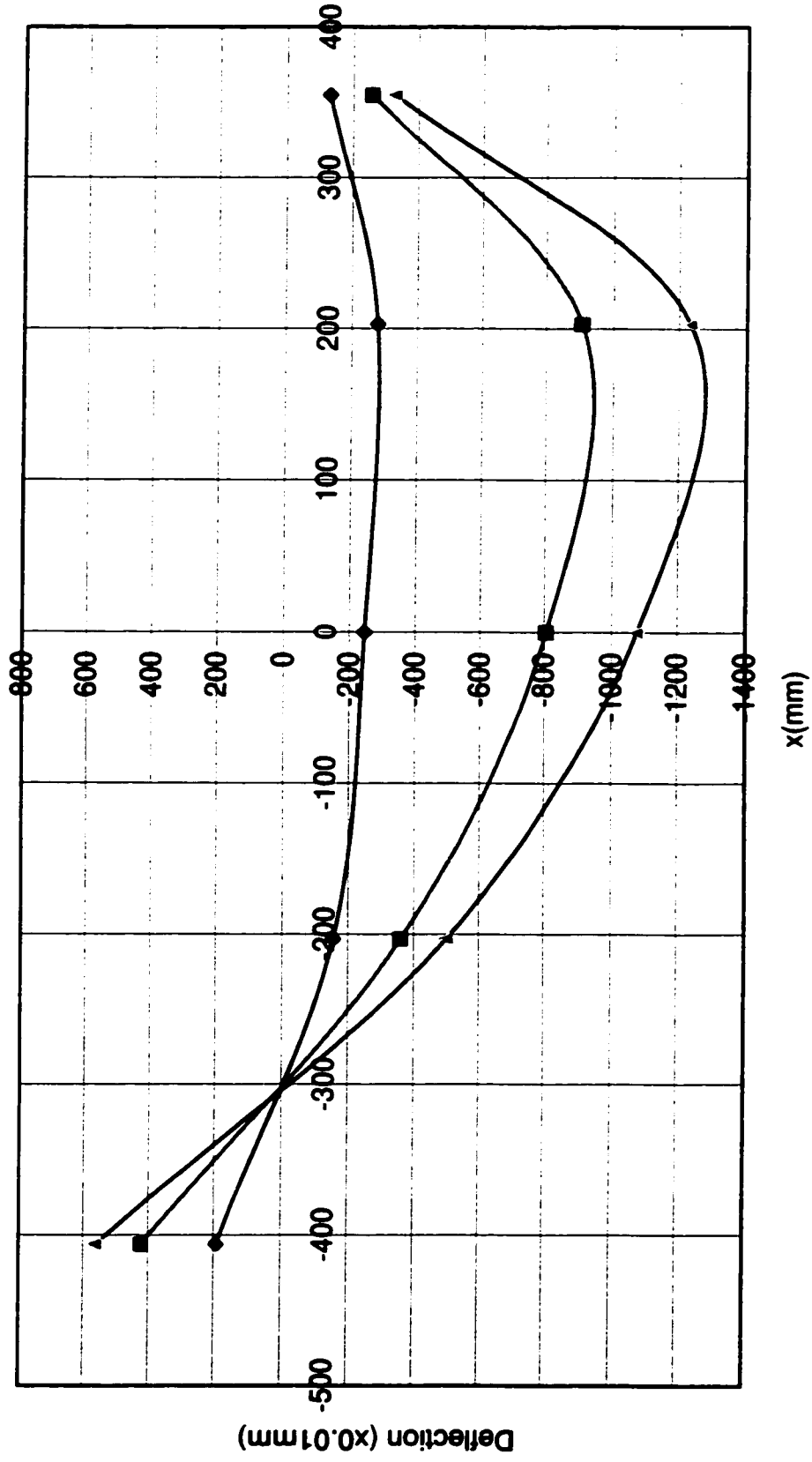
Test No. 10

No.	Load Applied on Specimen	Axial Force In Comp. Diagonal	Out-of-plane Deflection of Diagonal						Midspan Deflection (Vertical)	
			Dial Gauge No.1	Dial Gauge No.2	Dial Gauge No.3	Dial Gauge No.4	Dial Gauge No.5	Dial Gauge No.6	Dial Gauge No.7	
	Location (mm)		-406	-203	0	203	355	Front	Rear	
	kN		x0.01 mm	x0.01 mm	x0.01 mm	x0.01 mm	x0.01 mm	x0.01 mm	x0.01 mm	
	0	0	0	0	0	0	0			
1	10	3.6	53	-44	-100	-100	-44			
2	20	7	82	-68	-155	-141	-65			
3	30	11.3	192	-154	-245	-280	-129			
4	40	12.4	240	-190	-387	-366	-156			
5	50	16.6	307	-249	-555	-586	-197			
6	60	19.9	370	-310	-715	-736	-230			
7	70	22.3	422	-360	-805	-906	-258			
8	75	23.7	452	-386	-845	-1046	-271			
9	80	24.3	477	-415	-881	-1066	-284			
10	85	26.1	512	-450	-990	-1165	-309			
11	90	27.7	562	-500	-1077	-1236	-329			

* Refer to Figure A-1 for Location of Dial Gauges

Deflection Shape

Test No. 10 S5B



—◆— N=11.3 kN T=3.41 kN —■— N=22.3 kN T=7.25 kN —▲— N=27.7 kN T=9.74 kN

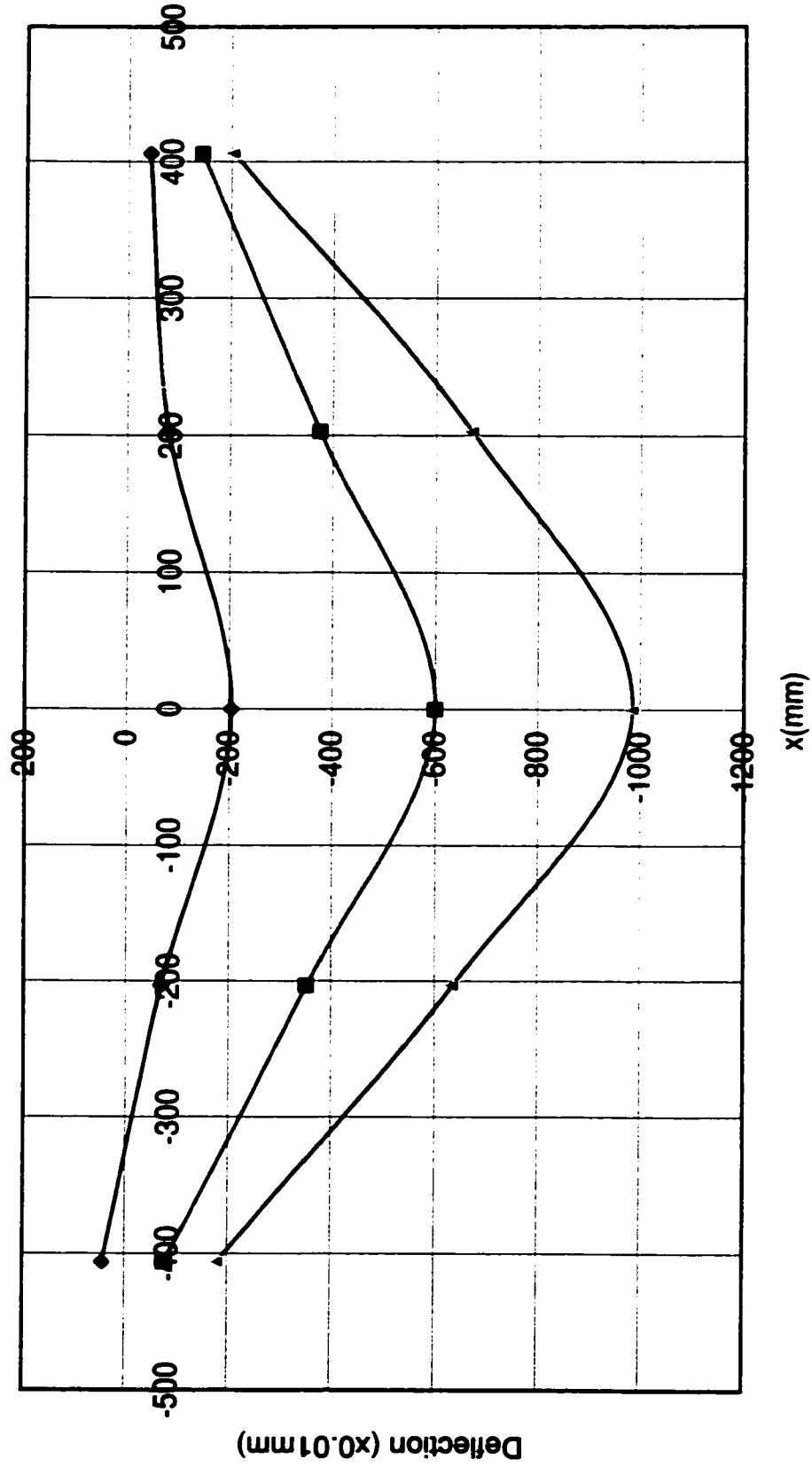
LOAD DEFLECTION DATA - SPECIMEN S-5C **Test No. 12**

No.	Load Applied on Specimen	Axial Force In Comp. Diagonal	Out-of-plane Deflection of Diagonal						Midspan Deflection (Vertical)	
			Dial Gauge No.1	Dial Gauge No.2	Dial Gauge No.3	Dial Gauge No.4	Dial Gauge No.5	Dial Gauge No.6	Dial Gauge No.7	
	Location (mm)		-406	-203	0	203	406	Front	Rear	
	kN	kN	x0.01 mm	x0.01 mm	x0.01 mm	x0.01 mm	x0.01 mm	x0.01 mm	x0.01 mm	
	0	0	0	0	0	0	0	0	0	
1	10.5	3.6	44	-70	-205	-80	-43	72	63	
2	20.0	7.1	62	-133	-305	-145	-73	118	104	
3	31.1	11.7	54	-260	-460	-274	-113	181	163	
4	40.0	15.2	-77	-354	-600	-376	-143	225	206	
5	50.0	19.2	-130	-491	-690	-520	-173	280	260	
6	60.0	26.8	-180	-635	-985	-670	-205	323	304	
7	65.0	27.6	-255	-735	-	-652	-303	385	373	
8	71.1	29.1	-295	-	-	-566	-283	410	403	

* Refer to Figure A-1 for Location of Dial Gauges

Deflection Shape

Test No. 12 S5C



—◆— $P=3.6 \text{ kN}$ $N=0.55 \text{ kN}$ —■— $P=15.2 \text{ kN}$ $N=2.46 \text{ kN}$ —▲— $P=26.8 \text{ kN}$ $N=4.97 \text{ kN}$

LOAD DEFLECTION DATA - SPECIMEN S-6B

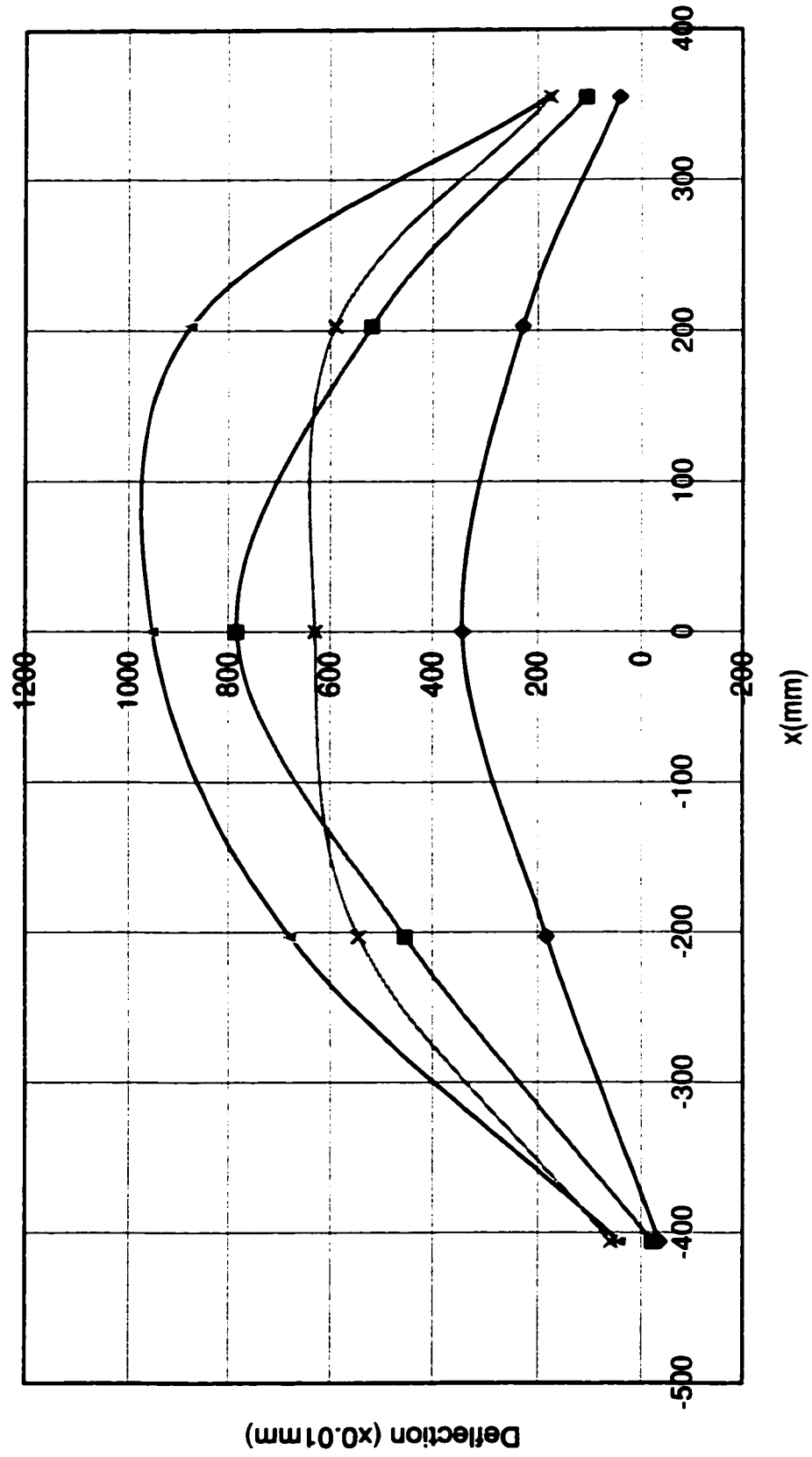
Test No. 13

No.	Load Applied on Specimen	Axial Force in Comp. Diagonal	Out-of-plane Deflection of Diagonal						Midspan Deflection (Vertical)	
			Dial Gauge No.1	Dial Gauge No.2	Dial Gauge No.3	Dial Gauge No.4	Dial Gauge No.5	Dial Gauge No.6	Dial Gauge No.7	
	Location (mm)		-406	-203	0	203	355	Front	Rear	
	kN	kN	x0.01 mm	x0.01 mm	x0.01 mm	x0.01 mm	x0.01 mm	x0.01 mm	x0.01 mm	
	0	0	0	0	0	0	0	0	0	
1	23.7	3.3	-26	49	119	89	15	118	141	
2	40.8	5.7	-30	114	227	157	26	198	199	
3	58.8	8.3	-35	182	344	229	41	273	266	
4	77.4	10.7	-36	256	461	307	56	351	331	
5	96.1	13.2	-30	334	594	386	75	430	394	
6	105.5	14.4	-26	373	654	430	84	470	431	
7	114.5	15.5	-22	414	724	472	95	509	467	
8	124.1	16.7	-21	453	784	519	105	549	503	
9	133.4	17.8	-20	493	851	567	117	589	540	
10	142.4	18.9	-16	535	922	617	131	628	575	
11	151.7	20.1	-9	581	944	674	145	674	610	
12	153.8	21.2	42	679	951	874	179	755	638	
13	122.1	13.2	59	544	630	590	174	597	644	

* Refer to Figure A-1 for Location of Dial Gauges

Deflection Shape

Test No.13 P6B



—◆— P=8.3kN N=8.54 kN —■— P=16.7kN N=18.8 kN —▲— P=21.2kN N=24.5 kN —x— P=23.4kN N=23.4 kN(Unload)

LOAD DEFLECTION DATA - SPECIMEN P7B

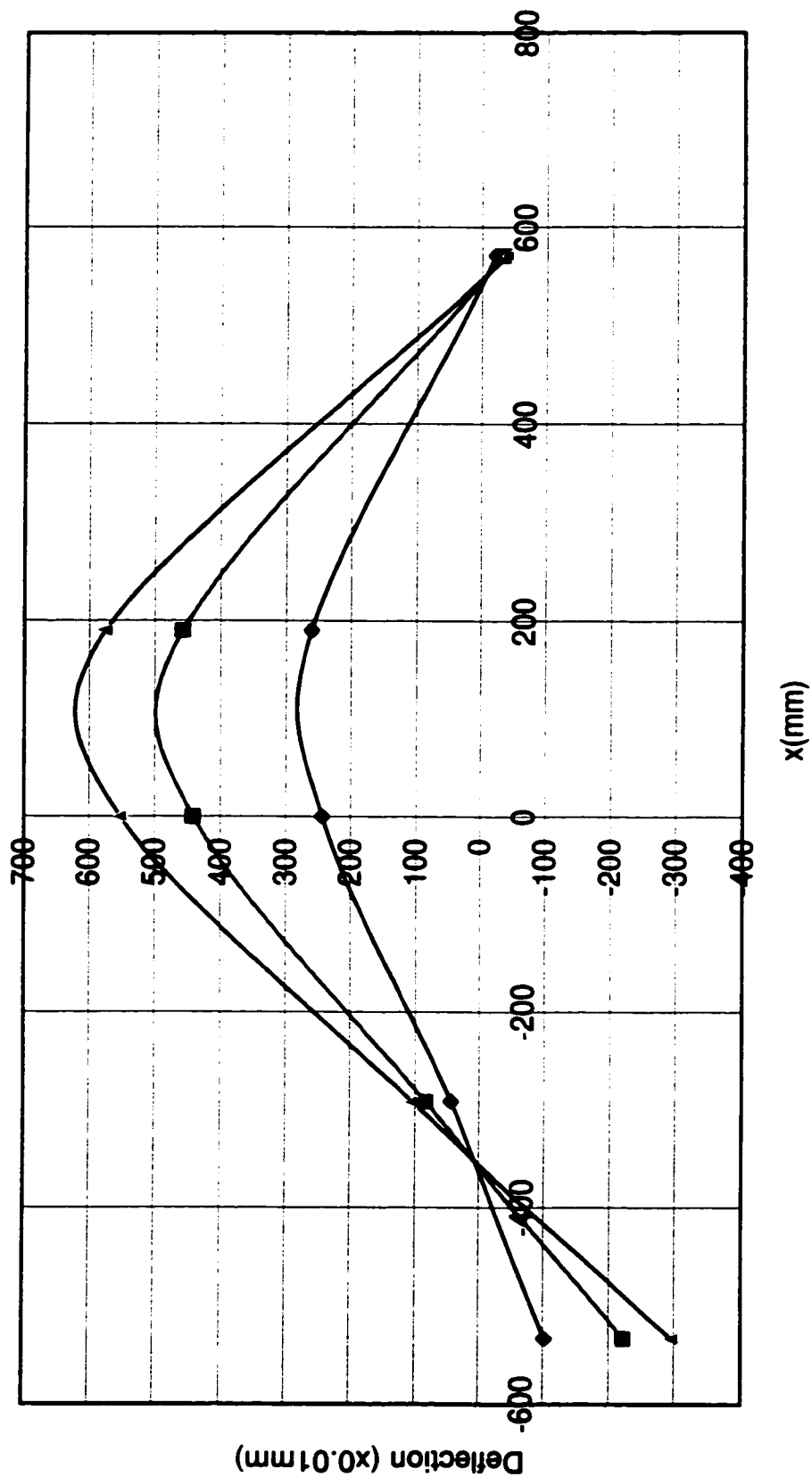
Test No. 17

No.	Load Applied on Specimen	Axial Force in Comp. Diagonal	Out-of-plane Deflection of Diagonal						Midspan Deflection (Vertical)	
			Dial Gauge						Dial Gauge No.6	Dial Gauge No.7
			No.1	No.2	No.3	No.4	No.5	No.6	No.7	
Location (mm)			-533	-292	0	190	571	Front	Rear	
		kN	x0.01 mm	x0.01 mm	x0.01 mm	x0.01 mm	x0.01 mm	x0.01 mm	x0.01 mm	
	0	0	0	0	0	0	0	0	0	
1	-30.7	5.7	-6	26	103	108	-7	257	244	
2	-40.5	7.6	-22	31	133	141	-10	337	318	
3	-50.5	9.4	-40	36	162	172	-13	414	392	
4	-61.0	11.4	-59	40	190	205	-16	494	468	
5	-67.7	12.6	-73	42	207	225	-18	545	518	
6	-78.5	14.6	-90	44	229	246	-19	623	594	
7	-85.7	15.8	-102	45	244	261	-22	675	645	
8	-95.9	17.8	-116	49	265	281	-24	748	717	
9	-110.9	20.5	-139	55	298	314	-24	856	823	
10	-121.7	22.4	-154	60	323	339	-26	934	900	
11	-132.7	24.4	-167	65	349	365	-28	1014	977	
12	-144.0	26.2	-183	70	374	390	-31	1094	1056	
13	-158.5	28.7	-204	77	406	423	-32	1198	1160	
14	-173.7	31.2	-223	84	442	458	-34	1306	1369	
15	-185.0	33.1	-239	88	468	485	-35	1385	1449	
16	-199.3	35.3	-259	95	497	517	-37	1490	1553	
17	-211.4	37.2	-278	101	528	548	-38	1586	1650	
18	-223.1	39.1	-297	104	552	575	-39	1687	1750	

* Refer to Figure A-1 for Location of Dial Gauges

Deflection Shape

Test No. 17 P7B



◆ P=15.8kN N=15.8 kN —■— P=31.2kN N=31.9 kN —▲— P=39.1kN N=41.1 kN

LOAD DEFLECTION DATA - SPECIMEN P7A

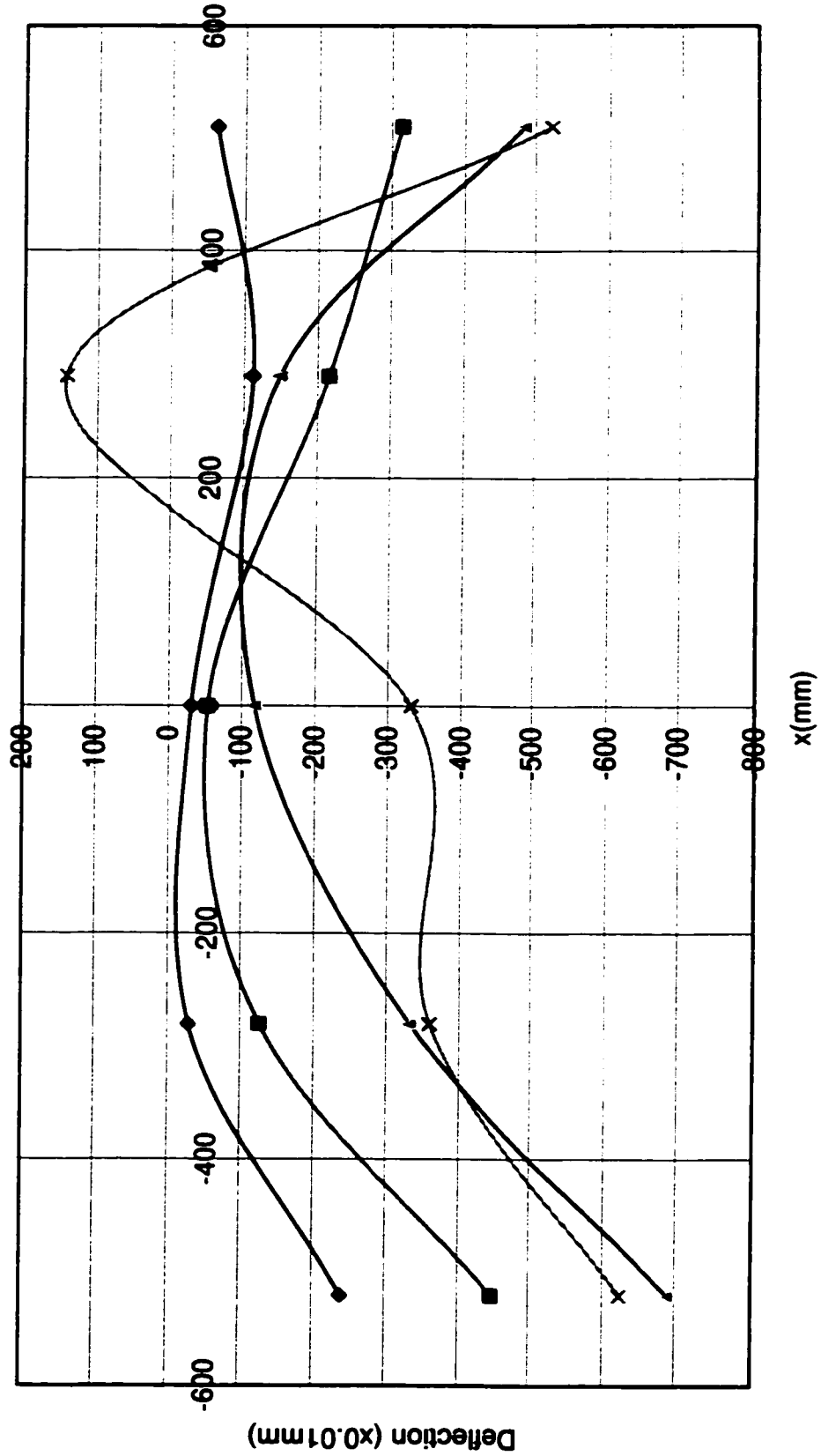
Test No. 18

No.	Load Applied on Specimen	Axial Force In Comp. Diagonal	Out-of-plane Deflection of Diagonal						Midspan Deflection (Vertical)	
			Dial Gauge No.1	Dial Gauge No.2	Dial Gauge No.3	Dial Gauge No.4	Dial Gauge No.5	Dial Gauge No.6	Dial Gauge No.7	
	Location (mm)									
	kN	kN	x0.01 mm	x0.01 mm	x0.01 mm	x0.01 mm	x0.01 mm	x0.01 mm	Front	Rear
	0	0	0	0	0	0	0	0	0	0
1	-39.9	7.2	-139	-17	-21	-65	-93	304	333	333
2	-53.7	9.7	-184	-23	-26	-86	-123	408	438	438
3	-71.8	13	-239	-30	-32	-112	-63	543	572	572
4	-90.2	16.3	-291	-38	-36	-138	-202	681	709	709
5	-109.1	19.6	-342	-46	-43	-164	-230	819	843	843
6	-128.4	22.8	-394	-85	-48	-189	-177	956	1080	1080
7	-148	26	-447	-126	-55	-216	-315	1093	1116	1116
8	-167.3	29	-501	-167	-63	-243	-340	1230	1252	1252
9	-186.9	32.2	-596	-212	-74	-271	-391	1368	1391	1391
10	-192.2	32.8	-590	-239	-81	-288	-415	1451	1475	1475
11	-213	36.2	-613	-259	-87	-300	-422	1492	1532	1532
12	-220.5	37.4	-635	-278	-93	-312	-432	1545	1589	1589
13	-224.2	37.9	-657	-299	-100	-325	-448	1601	1644	1644
14	-231.3	38.8	-690	-333	-117	-149	-485	1685	1733	1733
15	-183.8	35.2	-623	-360	-332	141	-522	1884	1928	1928

* Refer to Figure A-1 for Location of Dial Gauges

Deflection of Diagonal

Test No. 18 P7A



—◆— P=13kN N=15.2kN —■— P=26kN N=30.6kN —▲— P=38.8kN N=47.0kN —x— P=48.75kN (Unload)

LOAD DEFLECTION DATA - SPECIMEN P8B

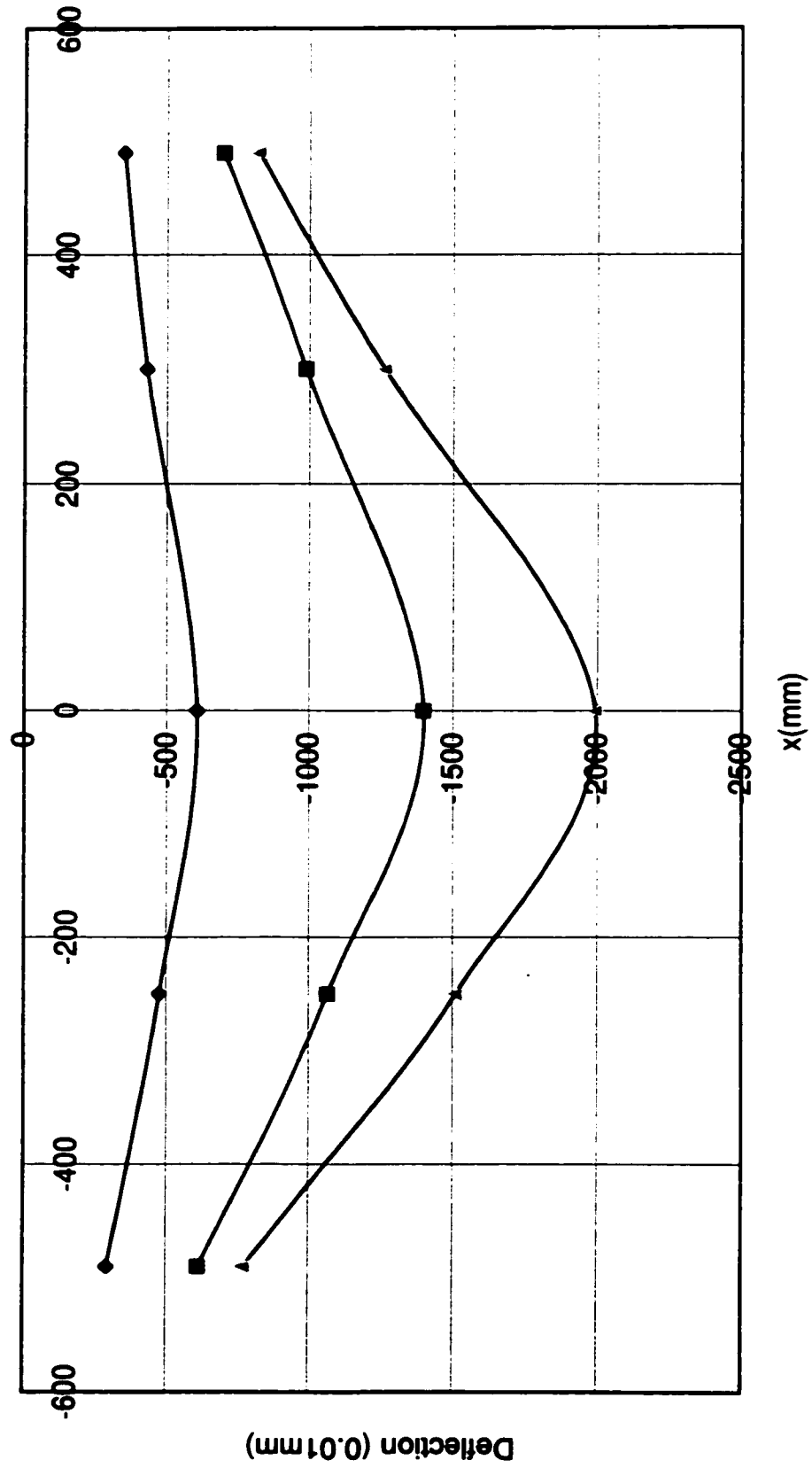
Test No. 19

No.	Load Applied on Specimen	Axial Force In Comp. Diagonal	Out-of-plane Deflection of Diagonal						Midspan Deflection (Vertical)	
			Dial Gauge No.1	Dial Gauge No.2	Dial Gauge No.3	Dial Gauge No.4	Dial Gauge No.5	Dial Gauge No.6	Dial Gauge No.7	
	Location (mm)		-490	-250	0	300	490	Front	Rear	
	kN	kN	x0.01 mm	x0.01 mm	x0.01 mm	x0.01 mm	x0.01 mm	x0.01 mm	x0.01 mm	
1	-34.8	13.4	-137	-219	-280	-171	-170	260	240	
2	-54.0	20.4	-214	-344	-438	-307	-210	383	360	
3	-74.1	27.6	-290	-474	-607	-429	-346	509	478	
4	-94.6	34.8	-366	-607	-781	-561	-432	634	595	
5	-115.3	41.9	-446	-750	-972	-680	-521	756	713	
6	-136.1	49.1	-528	-903	-1176	-830	-609	877	831	
7	-156.6	59.4	-613	-1068	-1397	-989	-696	994	947	
8	-169.6	72.7	-673	-1209	-1592	-1098	-750	1067	1022	
9	-175.4	76.7	-703	-1290	-1709	-1154	-758	1101	1058	
10	-181.2	78.1	-737	-1393	-1845	-1210	-798	1133	1095	
11	-186.1	80.2	-768	-1511	-1994	-1262	-817	1162	1126	

* Refer to Figure A-1 for Location of Dial Gauges

Deflection Shape

Test No. 19 P8B



—◆— $P=27.6 \text{ kN}$ $N=7.68 \text{ kN}$ —■— $P=59.4 \text{ kN}$ $N=14.9 \text{ kN}$ —▲— $P=80.2 \text{ kN}$ $N=19.5 \text{ kN}$

LOAD DEFLECTION DATA - SPECIMEN P4B

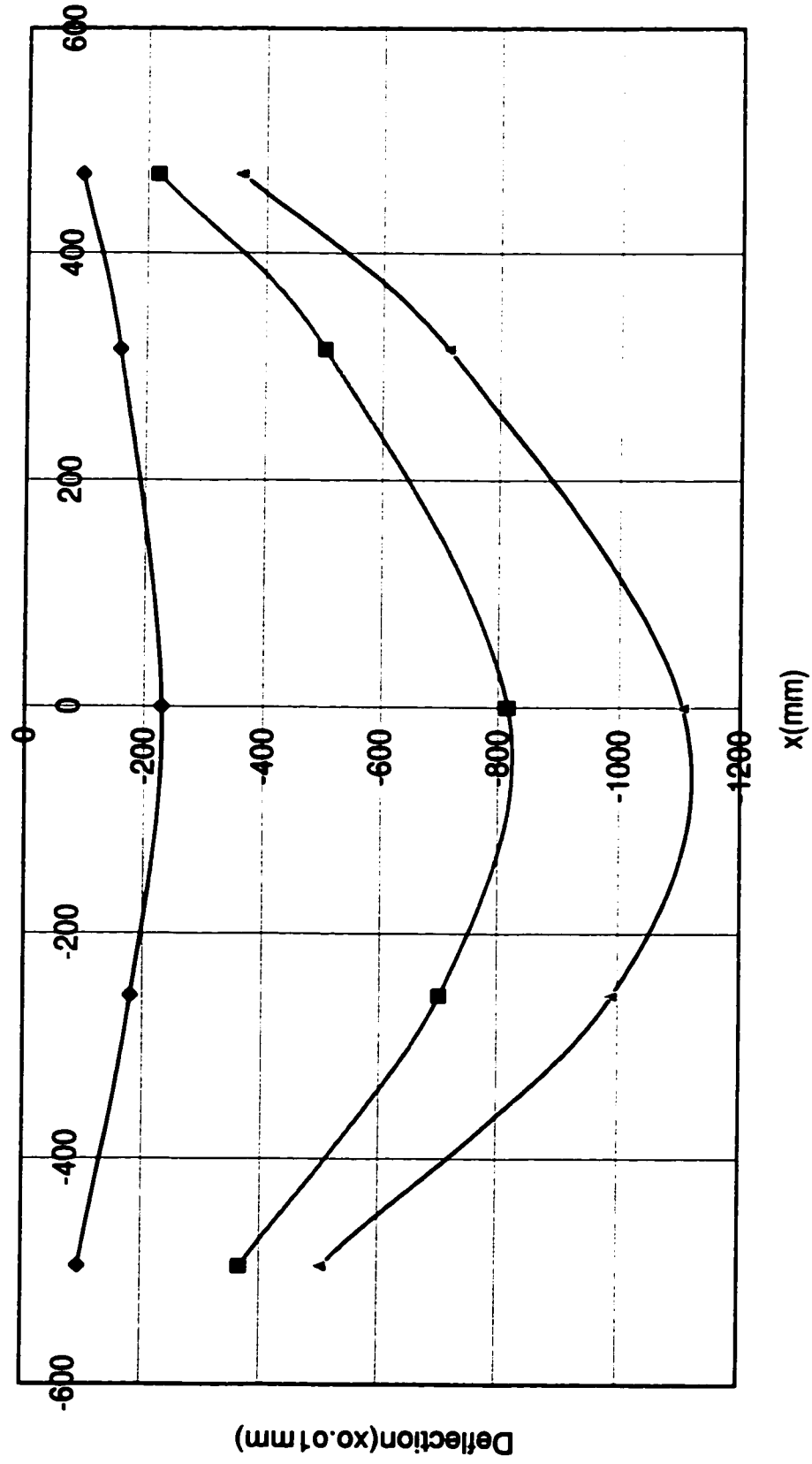
Test No. 20

No.	Load Applied on Specimen	Axial Force In Comp. Diagonal	Out-of-plane Deflection of Diagonal						Midspan Deflection (Vertical)	
			Dial Gauge No.1	Dial Gauge No.2	Dial Gauge No.3	Dial Gauge No.4	Dial Gauge No.5	Dial Gauge No.6	Dial Gauge No.7	
	Location (mm)		-495	-255	0	315	470	Front	Rear	
	kN	kN	x0.01 mm	x0.01 mm	x0.01 mm	x0.01 mm	x0.01 mm	x0.01 mm	x0.01 mm	
	0	0	0	0	0	0	0	0	0	
1	-24.0	9.0	-95	-181	-230	-157	-92	172	143	
2	-41.0	15.2	-182	-324	-407	-267	-150	268	243	
3	-59.0	21.6	-270	-408	-600	-380	-210	364	343	
4	-77.0	28.0	-367	-700	-816	-502	-218	460	445	
5	-92.0	33.0	-437	-841	-1000	-603	-223	538	520	
6	-108.0	37.8	-503	-990	-1105	-710	-359	615	595	
7	-119.0	41.3	-549	-1111	-	-792	-390	671	651	

* Refer to Figure A-1 for Location of Dial Gauges

Deflection Shape

Test No. 20 P4B



—◆— P=9.0kN N=2.37 kN —■— P=28.0kN N=6.24 kN —▲— P=37.7kN N=8.24 kN

LOAD DEFLECTION DATA - SPECIMEN P2A

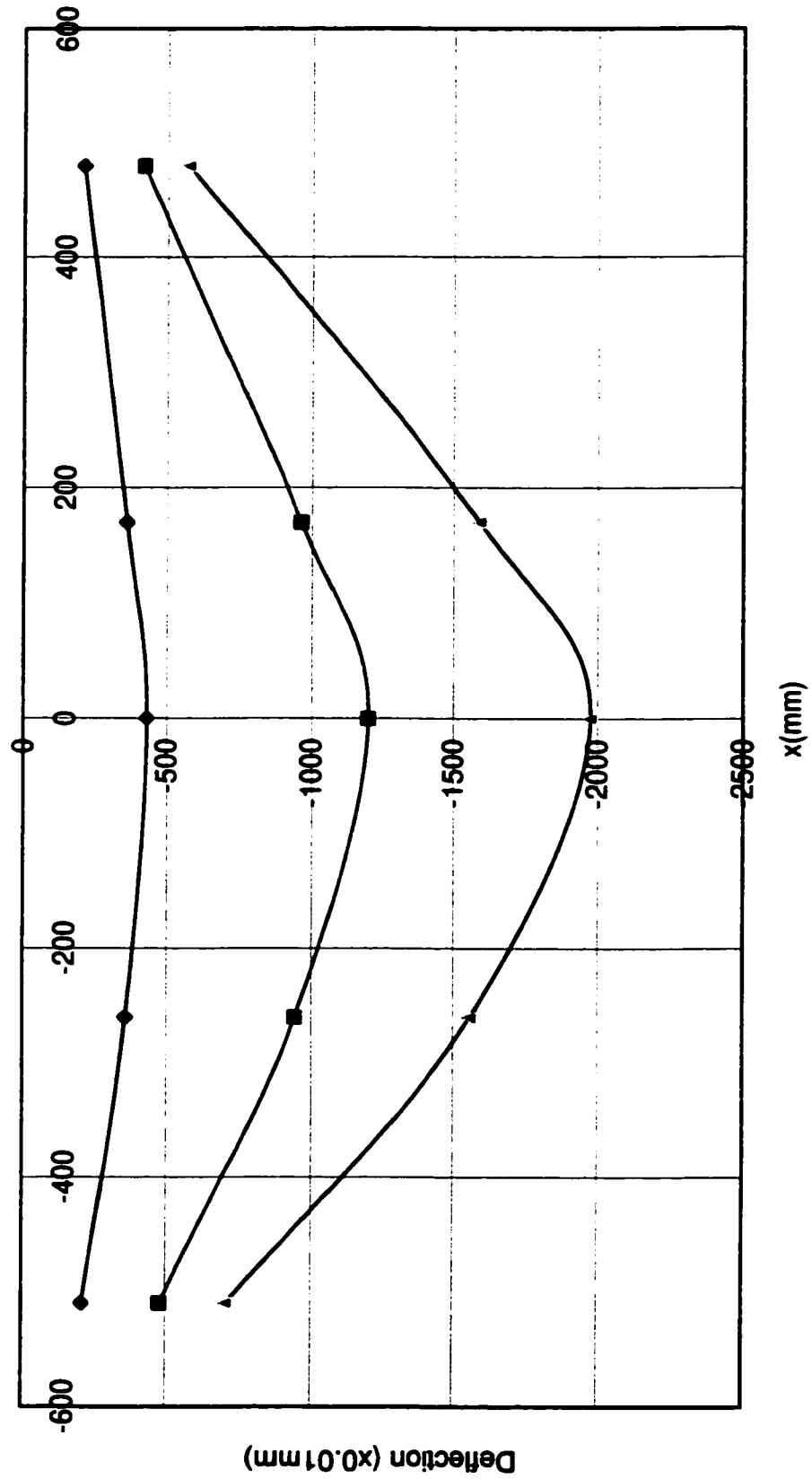
Test No. 21

No.	Load Applied on Specimen	Axial Force in Comp. Diagonal	Out-of-plane Deflection of Diagonal						Midspan Deflection (Vertical)	
			Dial Gauge No.1	Dial Gauge No.2	Dial Gauge No.3	Dial Gauge No.4	Dial Gauge No.5	Dial Gauge No.6	Dial Gauge No.7	
	Location (mm)		-510	-260	0	170	480	Front	Rear	
	kN	kN	x0.01 mm	x0.01 mm	x0.01 mm	x0.01 mm	x0.01 mm	x0.01 mm	x0.01 mm	
	0	0	0	0	0	0	0	0	0	
1	-27.5	9.4	-208	-355	-429	-357	-207	255	236	
2	-34.0	11.7	-264	-398	-562	-465	-249	309	293	
3	-41.0	14.1	-322	-578	-711	-583	-293	361	345	
4	-50.0	17.2	-401	-751	-940	-759	-355	430	415	
5	-59.0	20.2	-480	-942	-1196	-963	-416	496	475	
6	-70.0	23.8	-581	-1200	-1559	-1235	-491	574	547	
7	-74.0	25.1	-622	-1313	-1712	-1352	-520	602	575	
8	-81.6	27.5	-709	-1558	-1976	-1590	-572	654	622	

* Refer to Figure A-1 for Location of Dial Gauges

Deflection Shape

Test No. 21 P2A



—◆— P=9.4kN N=1.54 kN —■— P=20.2kN N=4.59 kN —▲— P=27.5kN N=8.24 kN

LOAD DEFLECTION DATA - SPECIMEN P1A

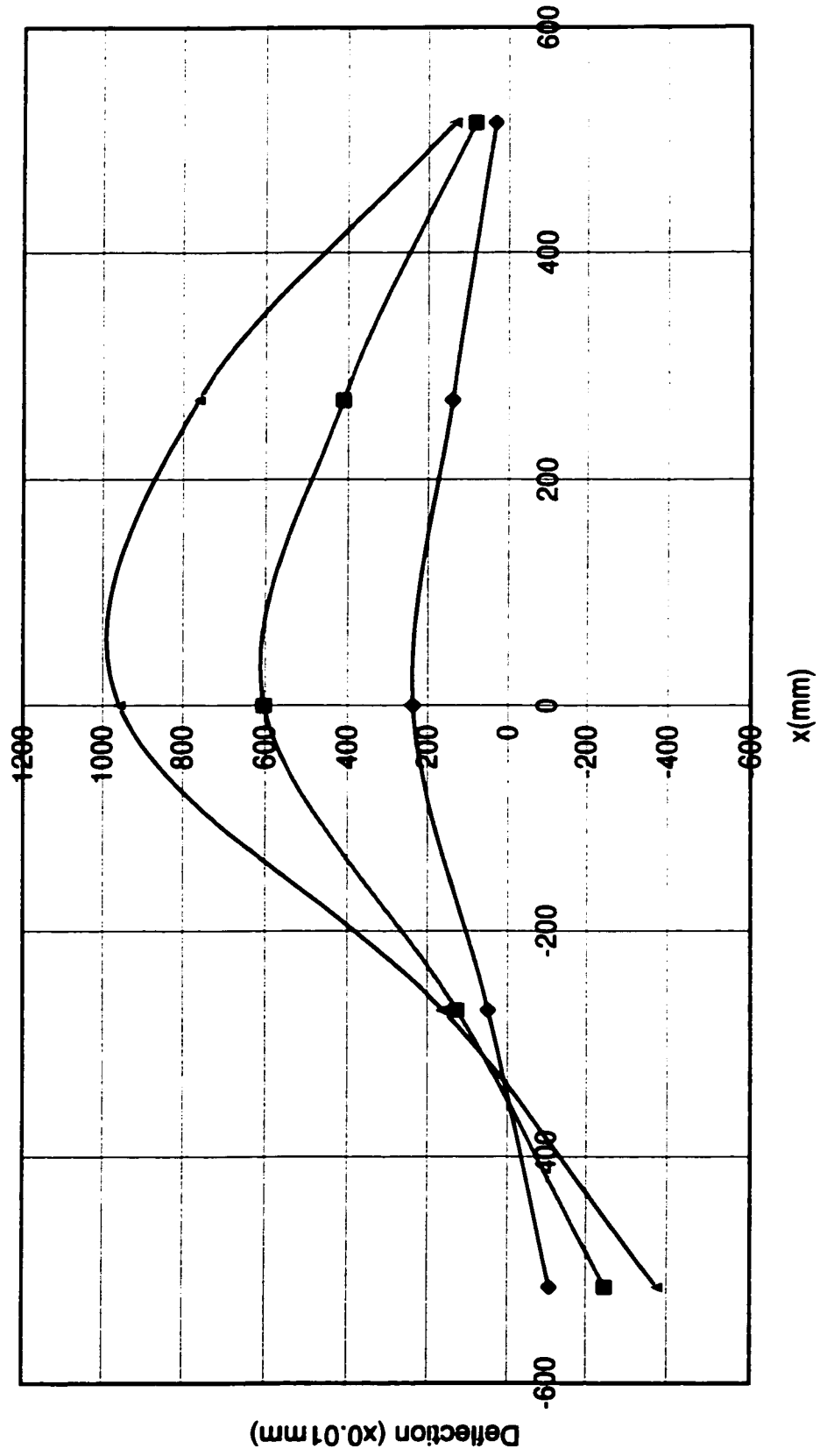
Test No. 22

No.	Load Applied on Specimen	Axial Force in Comp. Diagonal	Out-of-plane Deflection of Diagonal						Midspan Deflection (Vertical)	
			Dial Gauge No.1	Dial Gauge No.2	Dial Gauge No.3	Dial Gauge No.4	Dial Gauge No.5	Dial Gauge No.6	Dial Gauge No.7	
	Location (mm)		-515	-270	0	270	515	Front	Rear	
	kN	kN	x0.01 mm	x0.01 mm	x0.01 mm	x0.01 mm	x0.01 mm	x0.01 mm	x0.01 mm	
	0	0	0	0	0	0	0	0	0	
1	-28.5	5.8	-76	39	168	100	23	277	279	
2	-39.5	7.9	-109	50	238	141	33	384	390	
3	-56.5	11.4	-157	75	352	217	50	549	556	
4	-74.5	14.5	-202	99	471	305	66	712	718	
5	-92.5	17.8	-248	127	603	411	84	883	887	
6	-110.5	20.9	-294	148	739	537	103	1053	1057	
7	-128.5	24.1	-345	162	884	680	124	1226	1227	
8	-137.5	25.6	-375	162	959	762	135	1311	1314	

* Refer to Figure A-1 for Location of Dial Gauges

Deflection Shape

Test No. 22 P1A



—◆— $P=7.9 \text{ kN}$ $N=6.4 \text{ kN}$ —■— $P=17.8 \text{ kN}$ $N=15.1 \text{ kN}$ —▲— $P=25.6 \text{ kN}$ $N=22.4 \text{ kN}$

LOAD DEFLECTION DATA - SPECIMEN S2C

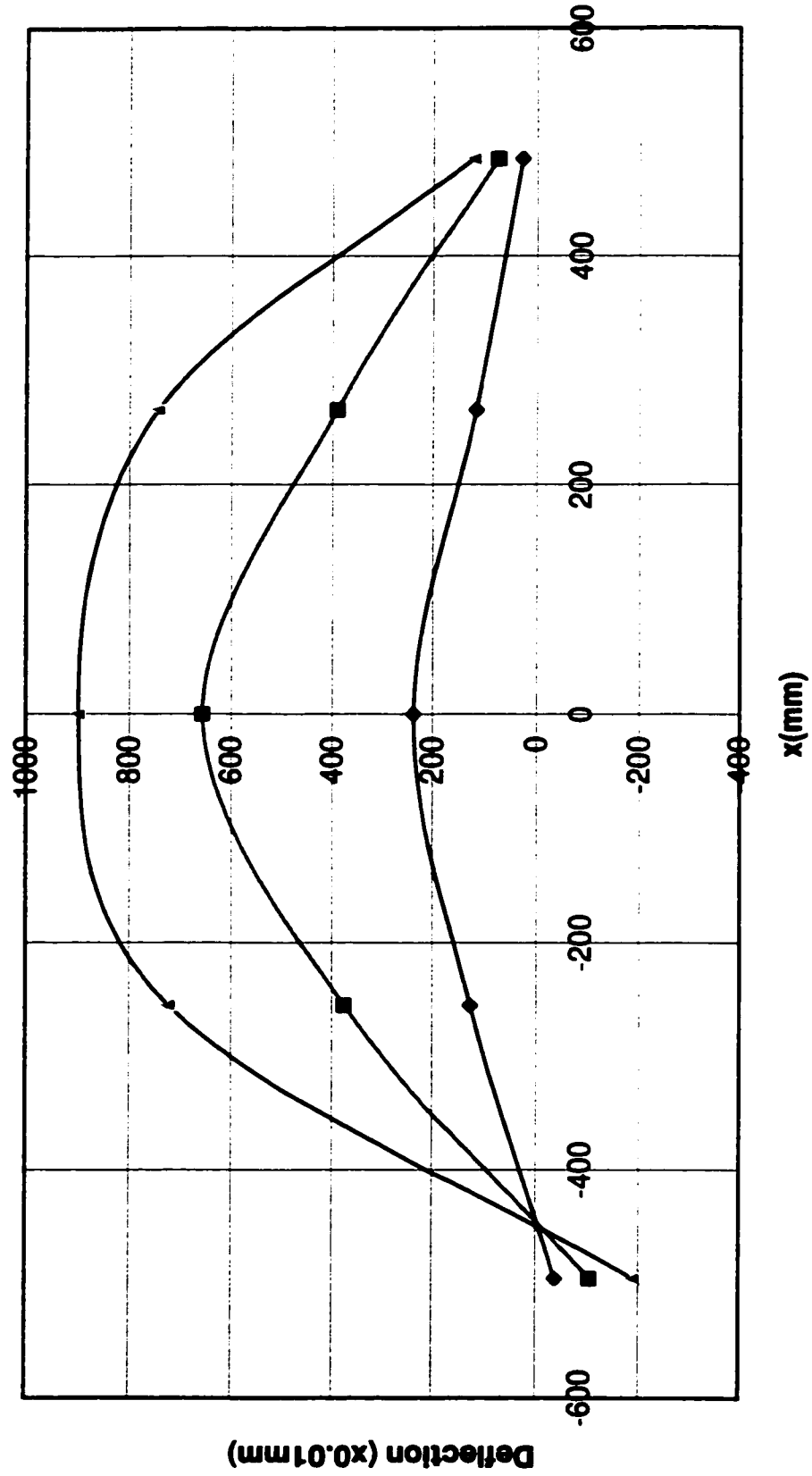
Test No. 23

No.	Load Applied on Specimen	Axial Force in Comp. Diagonal	Out-of-plane Deflection of Diagonal						Midspan Deflection (Vertical)	
			Dial Gauge No.1	Dial Gauge No.2	Dial Gauge No.3	Dial Gauge No.4	Dial Gauge No.5	Dial Gauge No.6	Dial Gauge No.7	
	Location (mm)		-495	-255	0	265	485			
	kN	kN	x0.01 mm	x0.01 mm	x0.01 mm	x0.01 mm	x0.01 mm	x0.01 mm	x0.01 mm	
		0	0	0	0	0	0	0	0	
1	-23.9	4.2	-38	128	237	118	28	178	160	
2	-30.6	5.4	-49	191	315	166	28	207	204	
3	-39.3	6.8	-58	195	390	212	44	277	262	
4	-45.3	7.6	-74	260	465	261	52	326	300	
5	-56.3	9.2	-103	328	581	338	66	402	375	
6	-62.3	10.2	-106	376	657	391	75	452	426	
7	-69.3	11.2	-120	423	731	444	85	502	473	
8	-72.3	11.7	-126	446	765	470	89	526	497	
9	-76.3	12.4	-132	470	803	499	94	552	522	
10	-82.3	13.1	-144	521	873	552	104	601	573	
11	-95.3	14.1	-160	575	940	605	113	652	622	
12	-94.3	13.9	-190	723	899	744	123	700	675	

* Refer to Figure A-1 for Location of Dial Gauges

Deflection Shape

Test No. 23 S2C



—◆— $P=4.2\text{ kN}$ $N=3.79\text{ kN}$ —■— $P=10.2\text{ kN}$ $N=10.2\text{ kN}$ —▲— $P=13.9\text{ kN}$ $N=15.2\text{ kN}$

LOAD DEFLECTION DATA - SPECIMEN S6C

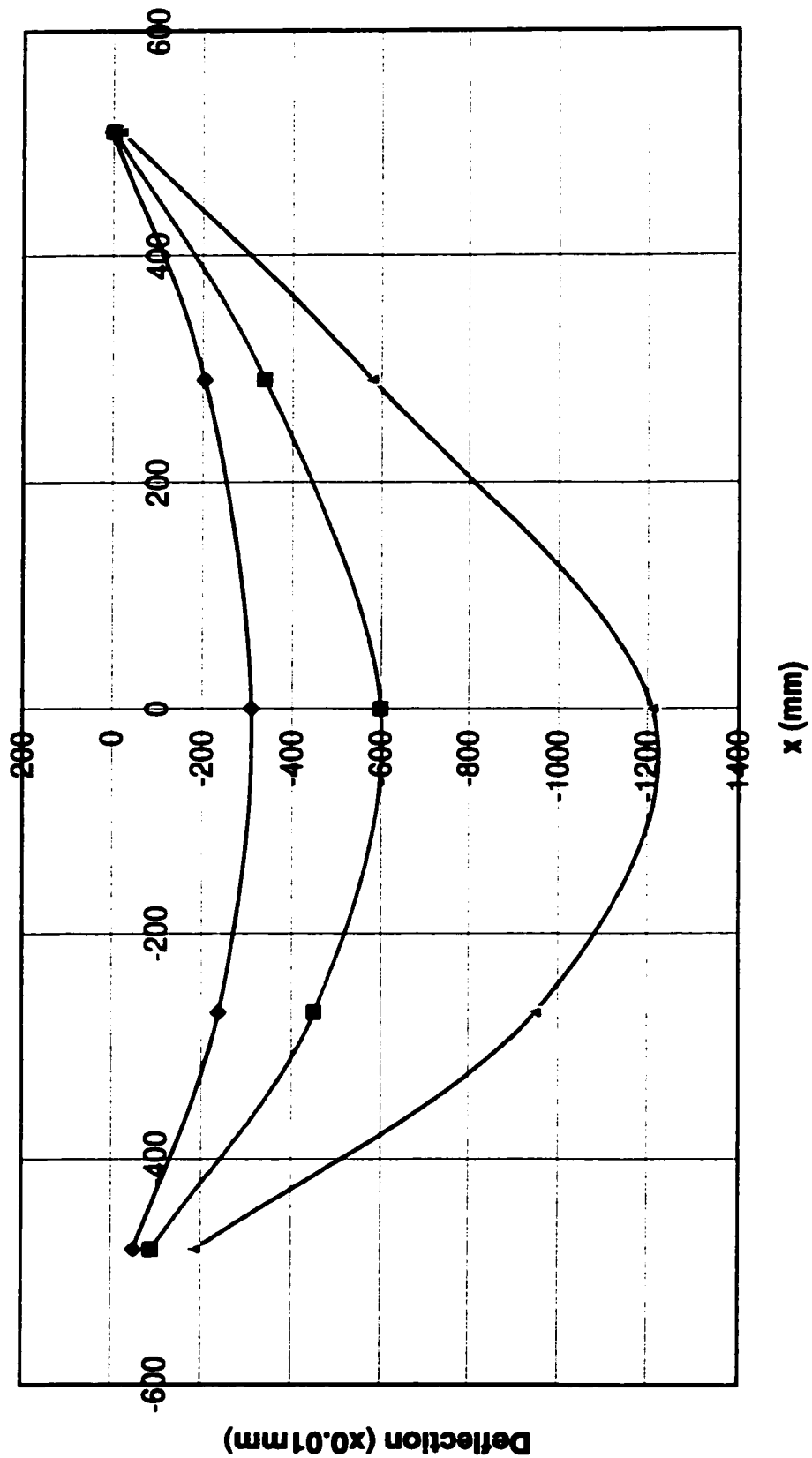
Test No. 24

No.	Load Applied on Specimen	Axial Force in Comp. Diagonal	Out-of-plane Deflection of Diagonal						Midspan Deflection (Vertical)	
			Dial Gauge No.1	Dial Gauge No.2	Dial Gauge No.3	Dial Gauge No.4	Dial Gauge No.5	Dial Gauge No.6	Dial Gauge No.7	
	Location (mm)		-480	-270	0	290	510	Front	Rear	
	kN	kN	x0.01 mm	x0.01 mm	x0.01 mm	x0.01 mm	x0.01 mm	x0.01 mm	x0.01 mm	
		0	0	0	0	0	0	0	0	
1	-35.0	6.6	-32	-150	-193	-148	3	155	160	
2	-55.7	10.5	-50	-237	-309	-204	3	235	246	
3	-72.1	13.6	-62	-304	-400	-248	1	296	311	
4	-89.0	16.7	-30	-374	-495	-292	0	358	275	
5	-106.8	19.8	-88	-451	-599	-338	-1	421	443	
6	-118.4	21.9	-99	-508	-673	-371	-1	462	488	
7	-136.7	25.0	-114	-599	-790	-419	-3	525	537	
8	-154.2	27.9	-131	-695	-912	-468	-5	587	625	
9	-172.4	30.7	-147	-800	-1039	-518	-8	649	697	
10	-183.0	32.4	-160	-874	-1130	-553	-9	690	740	
11	-187.6	32.9	-187	-949	-1210	-579	-17	720	763	

* Refer to Figure A-1 for Location of Dial Gauges

Deflection Shape

Test 24 S6C



—◆— $P=10.5 \text{ kN}$ $N=7.70 \text{ kN}$ —■— $P=19.8 \text{ kN}$ $N=14.9 \text{ kN}$ —▲— $P=32.9 \text{ kN}$ $N=26.9 \text{ kN}$

LOAD DEFLECTION DATA - SPECIMEN EA3

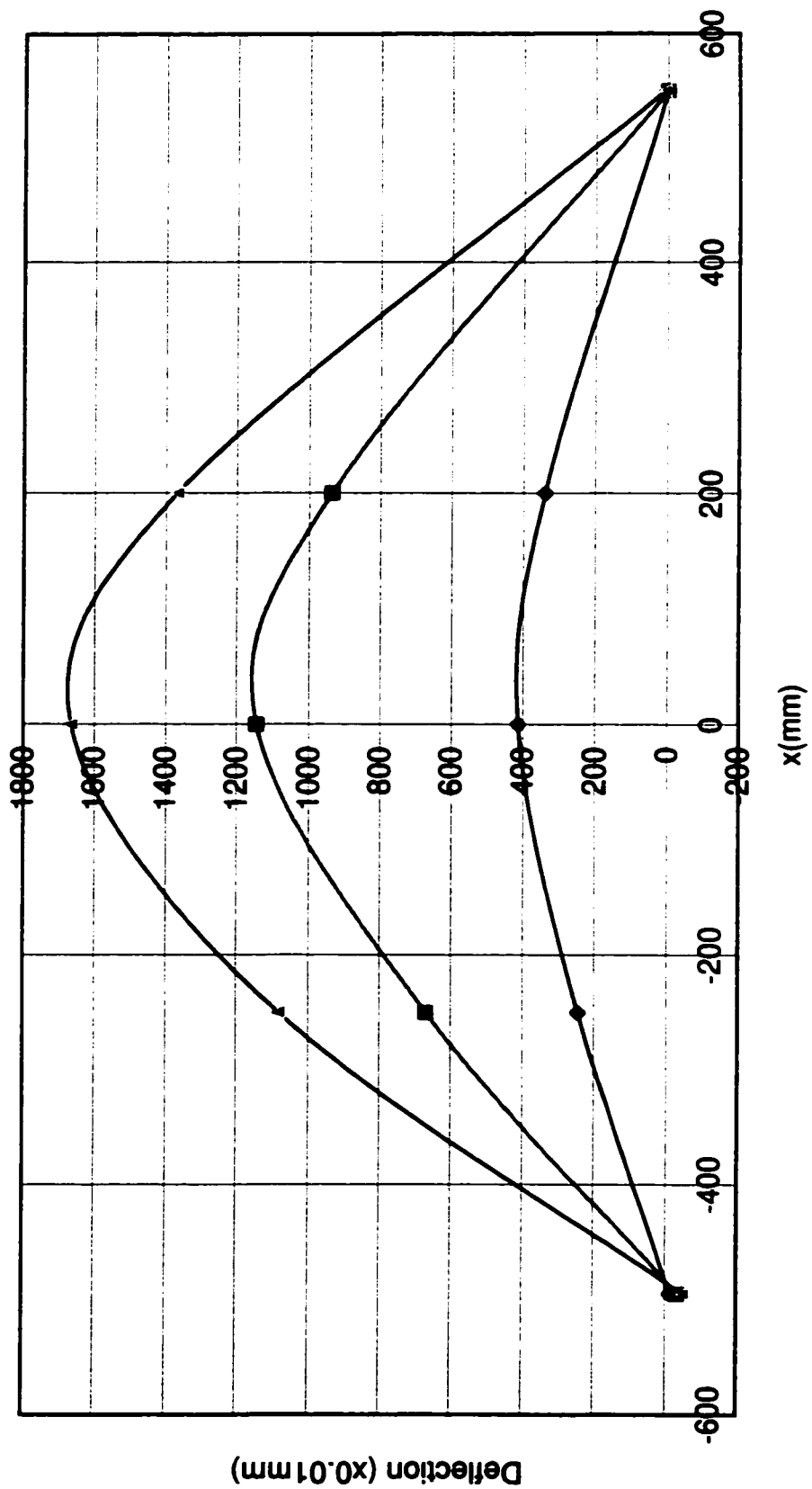
Test No. 25

No.	Load Applied on Specimen	Axial Force in Comp. Diagonal	Out-of-plane Deflection of Diagonal						Midspan Deflection (Vertical)	
			Dial Gauge No.1	Dial Gauge No.2	Dial Gauge No.3	Dial Gauge No.4	Dial Gauge No.5	Dial Gauge No.6	Dial Gauge No.7	
	Location (mm)		-495	-250	0	200	550	Front	Rear	
	kN	kN	x0.01 mm	x0.01 mm	x0.01 mm	x0.01 mm	x0.01 mm	x0.01 mm	x0.01 mm	
	0	0	0	0	0	0	0	0	0	
1	-24.8	7.8	-13	244	413	339	0	125	119	
2	-34.1	10.3	-20	368	631	516	-6	167	165	
3	-43.1	12.6	-27	512	879	717	-4	204	210	
4	-52.2	14.6	-35	669	1145	937	0	236	253	
5	-58.0	15.9	-40	777	1322	1084	3	254	280	
6	-63.5	16.9	-44	894	1500	1233	6	272	303	
7	-69.0	20.5	-49	1083	1665	1367	9	291	327	
8	Failure	-	-2	1380	1417	524	-3	307	325	

* Refer to Figure A-1 for Location of Dial Gauges

Deflection Shape

Test No. 25 S3B



—◆— $P=7.8 \text{ kN}$ $N=1.86 \text{ kN}$ —■— $P=14.6 \text{ kN}$ $N=5.18 \text{ kN}$ —▲— $P=20.5 \text{ kN}$ $N=8.10 \text{ kN}$

LOAD DEFLECTION DATA - SPECIMEN P5A

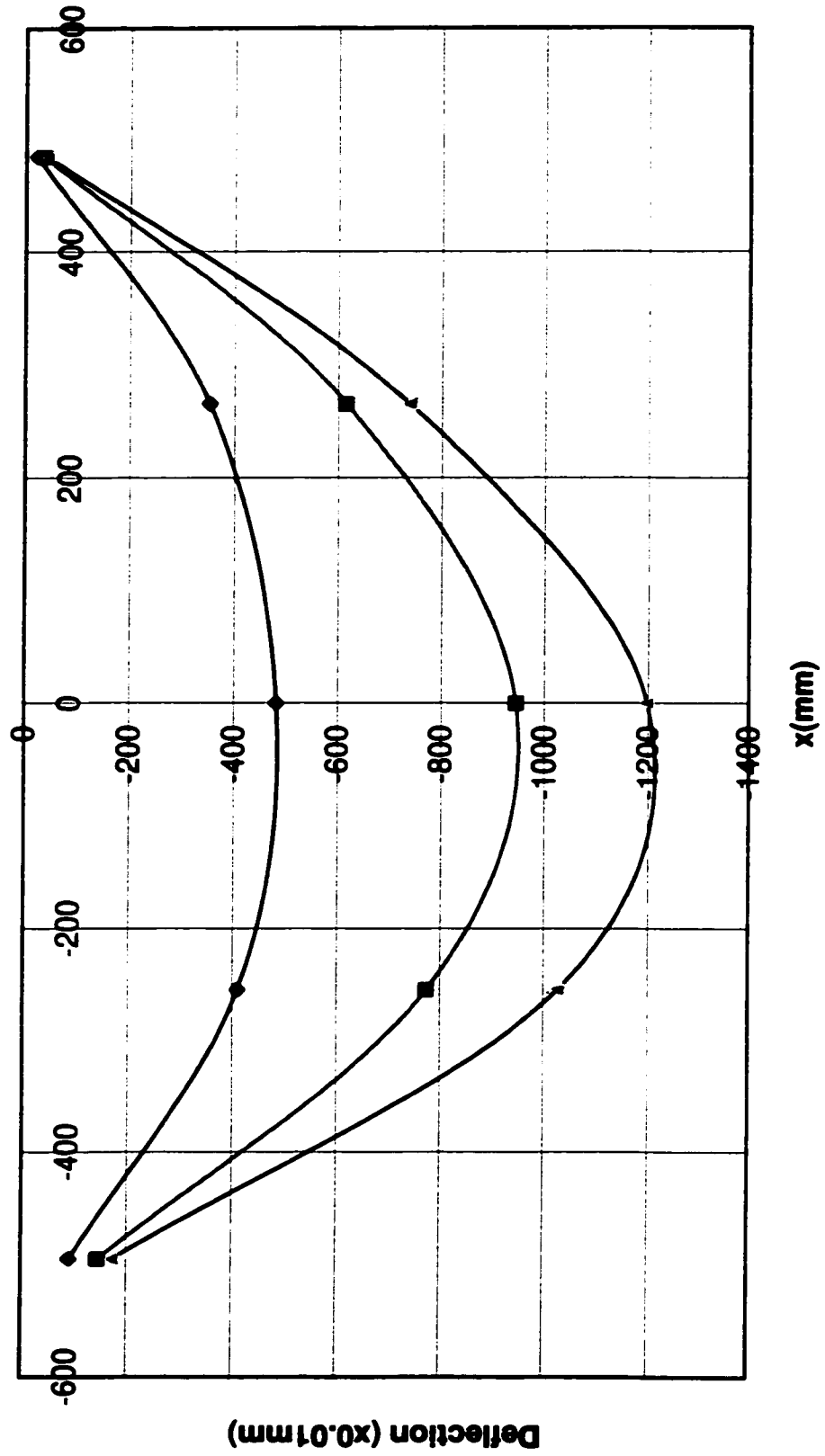
Test No. 26

No.	Load Applied on the Specimen	Axial Force In Comp. Diagonal	Out-of-plane Deflection of Diagonal						Midspan Deflection (Vertical)	
			Dial Gauge No.1	Dial Gauge No.2	Dial Gauge No.3	Dial Gauge No.4	Dial Gauge No.5	Dial Gauge No.6	Dial Gauge No.7	
	Location (mm)		-495	-255	0	265	485			
	kN	kN	x0.01 mm	x0.01 mm	x0.01 mm	x0.01 mm	x0.01 mm	x0.01 mm	x0.01 mm	x0.01 mm
		0	0	0	0	0	0	0	0	0
1	-35.4	6.9	-26	-105	-119	-94	-6	165		177
2	-64.5	11.9	-26	-186	-212	-164	-11	299		323
3	-95.6	17.6	-63	-264	-304	-258	-15	339		353
4	-127.6	23.4	-78	-337	-392	-289	-18	582		605
5	-161.5	29.4	-92	-410	-482	-352	-22	732		750
6	-196.5	35.6	-105	-504	-573	-449	-25	883		896
7	-231.2	41.8	-116	-597	-664	-465	-78	1034		1040
8	-265.5	48.4	-146	-633	-758	-522	-31	1188		1180
9	-299.9	55.7	-139	-716	-857	-578	-34	1342		1326
10	-322.2	61.4	-146	-774	-946	-616	-36	1445		1413
11	-344.0	67.4	-153	-839	-1000	-653	-37	1548		1512
12	-357.9	72.2	-159	-905	-1054	-679	-39	1620		1578
13	-364.5	74.3	-162	-911	-1081	-691	-39	1655		1609
14	-383.2	79.3	-168	-1008	-1151	-722	-40	1748		1692
15	-393.3	82.6	-172	-1026	-1197	-738	-41	1806		1723

* Refer to Figure A-1 for Location of Dial Gauges

Deflection Shape

Test No. 26 P5A



—◆— P=29.4 kN N=29.7kN —■— P=61.4 kN N=58.5 kN —▲— P=82.6 kN N=72.7 kN

LOAD DEFLECTION DATA - SPECIMEN P2B

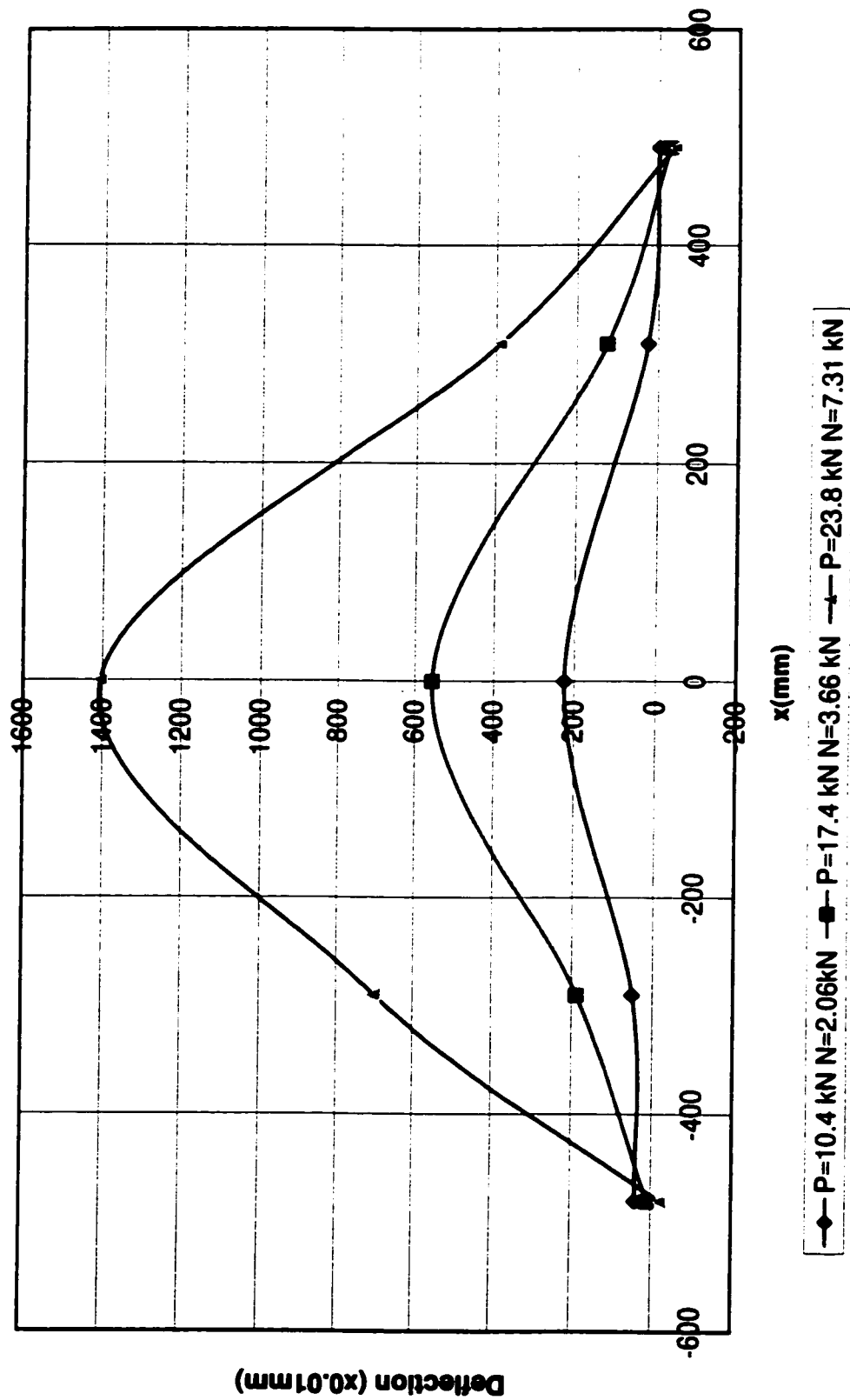
Test No. 27

No.	Load Applied on the Specimen	Axial Force in Comp. Diagonal	Out-of-plane Deflection of Diagonal						Midspan Deflection (Vertical)	
			Dial Gauge No.1	Dial Gauge No.2	Dial Gauge No.3	Dial Gauge No.4	Dial Gauge No.5	Dial Gauge No.6	Dial Gauge No.7	
	Location (mm)		-480	-290	0	310	490	Front	Rear	
	kN	kN	x0.01 mm	x0.01 mm	x0.01 mm	x0.01 mm	x0.01 mm	x0.01 mm	x0.01 mm	
		0	0	0	0	0	0	0	0	
1	-29.4	10.4	40	50	225	25	0	222	240	
2	-34.3	12.0	33	75	190	40	-8	260	277	
3	-41.6	14.4	23	160	408	45	-15	315	331	
4	-49.5	17.4	10	188	555	125	-28	337	389	
5	-50.7	17.8	0	275	744	190	-30	431	450	
6	-65.6	21.3	-10	384	960	265	-35	488	507	
7	-69.7	22.3	-15	450	1095	310	-36	515	537	
8	-77.1	23.8	-20	700	1405	390	-40	565	588	

* Refer to Figure A-1 for Location of Dial Gauges

Deflection Shape

Test No. 27 P2B



LOAD DEFLECTION DATA - SPECIMEN P6A

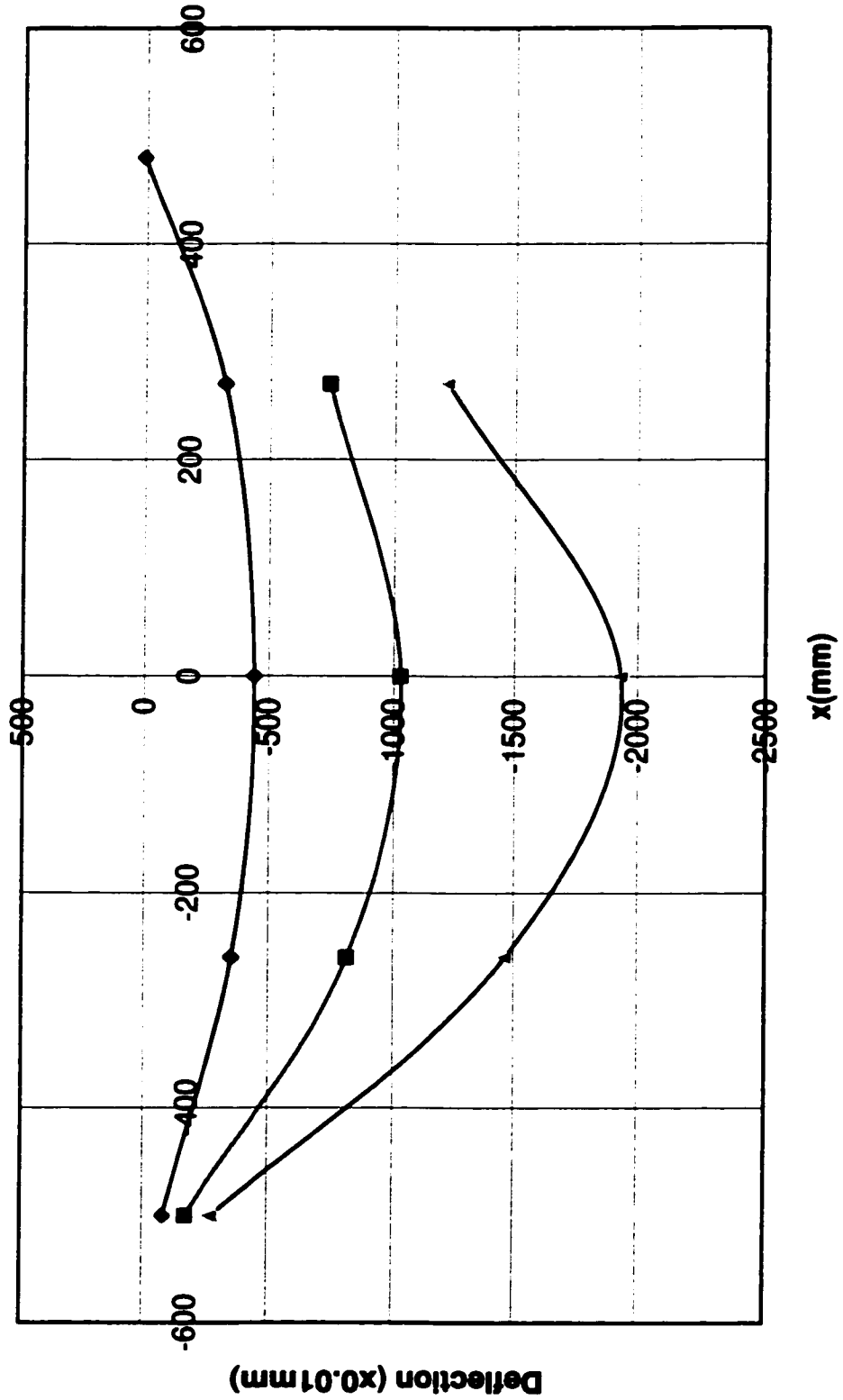
Test No. 28

No.	Load Applied on the Specimen	Axial Force In Comp. Diagonal	Out-of-plane Deflection of Diagonal						Midspan Deflection (Vertical)	
			Dial Gauge No.1	Dial Gauge No.2	Dial Gauge No.3	Dial Gauge No.4	Dial Gauge No.5	Dial Gauge No.6	Dial Gauge No.7	
	Location (mm)		-500	-260	0	270	480	Front	Rear	
	kN	kN	x0.01 mm	x0.01 mm	x0.01 mm	x0.01 mm	x0.01 mm	x0.01 mm	x0.01 mm	
	0	0	0	0	0	0	0			
1	-34.5	11.8	-33	-139	-156	-128	64	165	158	
2	-63.7	21.8	-62	-261	-305	-268	33	287	287	
3	-86.8	29.6	-84	-356	-443	-324	10	386	381	
4	-110.4	37.6	-126	-458	-553	-458	-13	487	471	
5	-134.6	45.8	-129	-566	-696	-516	-43	589	571	
6	-158.6	53.8	-151	-702	-847	-620	-	688	664	
7	-183.3	62.0	-179	-814	-1028	-738	-	784	758	
8	-202.6	68.9	-202	-940	-1200	-845	-	858	832	
9	-220.8	75.7	-227	-1086	-1407	-962	-	1030	902	
10	-238.4	82.8	-243	-1263	-1650	-1094	-	998	972	
11	-252.6	88.7	-281	-1464	-1933	-1224	-	1056	1025	
12										

* Refer to Figure A-1 for Location of Dial Gauges

Deflection Shape

Test No. 28 P6A



—◆— P=29.6 kN N=5.63kN —■— P=62.0 kN N=11.3kN —▲— P=88.7kN N=18.1kN

LOAD DEFLECTION DATA - SPECIMEN P4A

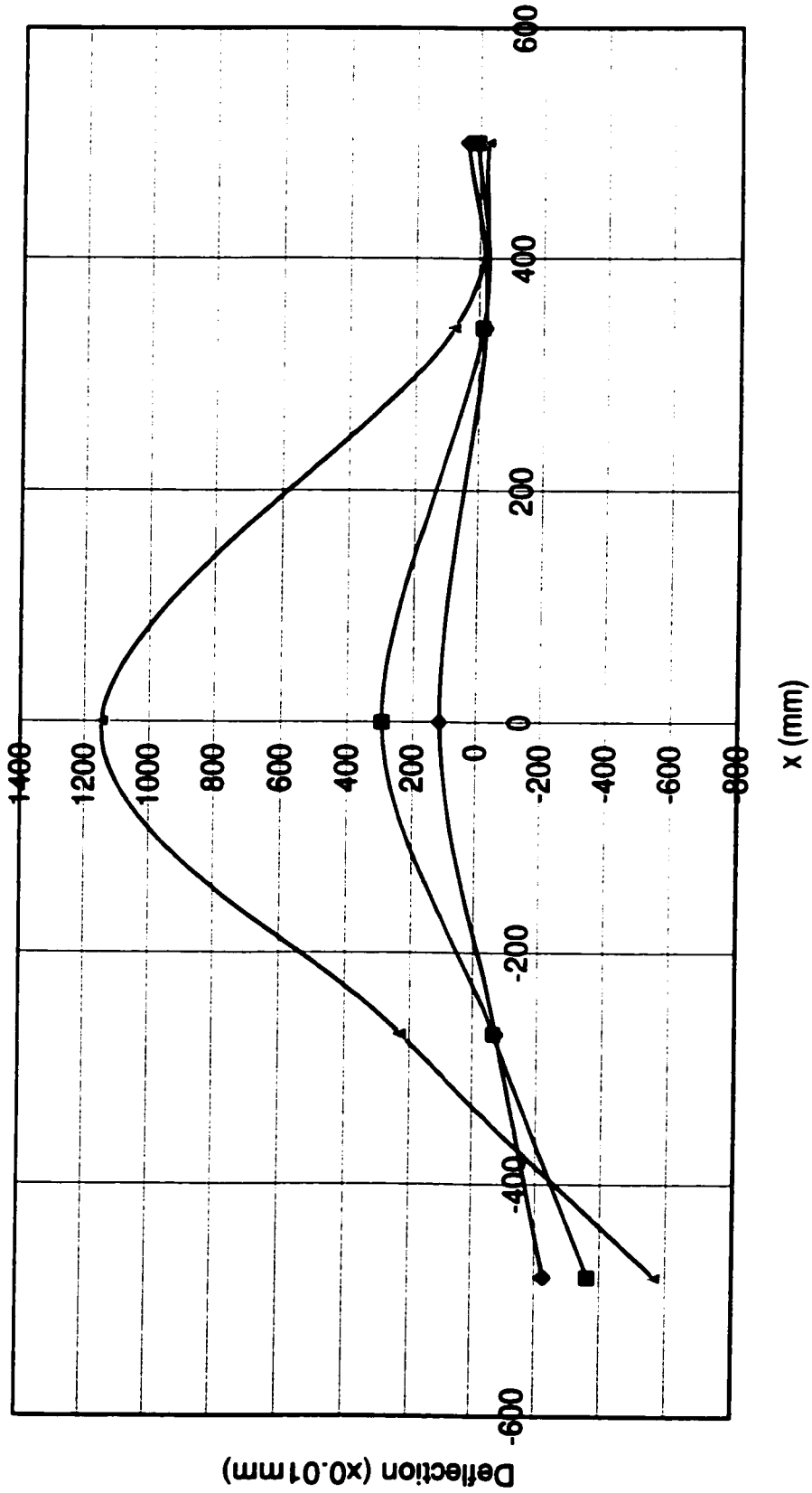
Test No. 29

No.	Load Applied on Specimen	Axial Force in Comp. Diagonal	Out-of-plane Deflection of Diagonal						Midspan Deflection (Vertical)	
			Dial Gauge No.1	Dial Gauge No.2	Dial Gauge No.3	Dial Gauge No.4	Dial Gauge No.5	Dial Gauge No.6	Dial Gauge No.7	
	Location (mm)		-480	-270	0	340	500	Front	Rear	
	kN	kN	x0.01 mm	x0.01 mm	x0.01 mm	x0.01 mm	x0.01 mm	x0.01 mm	x0.01 mm	
		0	0	0	0	0	0	0	0	
1	-29.3	11.4	-128	-47	49	-18	59	199	186	
2	-40.4	15.2	-179	-63	78	-21	48	253	253	
3	-51.6	19.0	-227	-73	116	-22	37	307	320	
4	-62.8	22.7	-273	-77	160	-22	26	360	382	
5	-65.0	23.5	-320	-76	223	-19	16	421	448	
6	-86.6	30.5	-363	-66	294	-15	6	478	508	
7	-98.7	34.2	-401	-46	383	-7	-3	539	568	
8	-111.9	38.3	-441	-12	504	5	-11	608	630	
9	-126.3	42.1	-482	35	658	22	-19	677	692	
10	-139.5	45.3	-513	103	851	44	-24	741	748	
11	-154.5	48.1	-567	229	1146	75	-29	818	810	

* Refer to Figure A-1 for Location of Dial Gauges

Deflection Shape

Test No. 29 P4A



◆ P=19.0kN N=5.27kN ■ P=30.5 kN N=8.18kN — P=48.1 kN N=15.9 kN

LOAD DEFLECTION DATA - SPECIMEN P3A

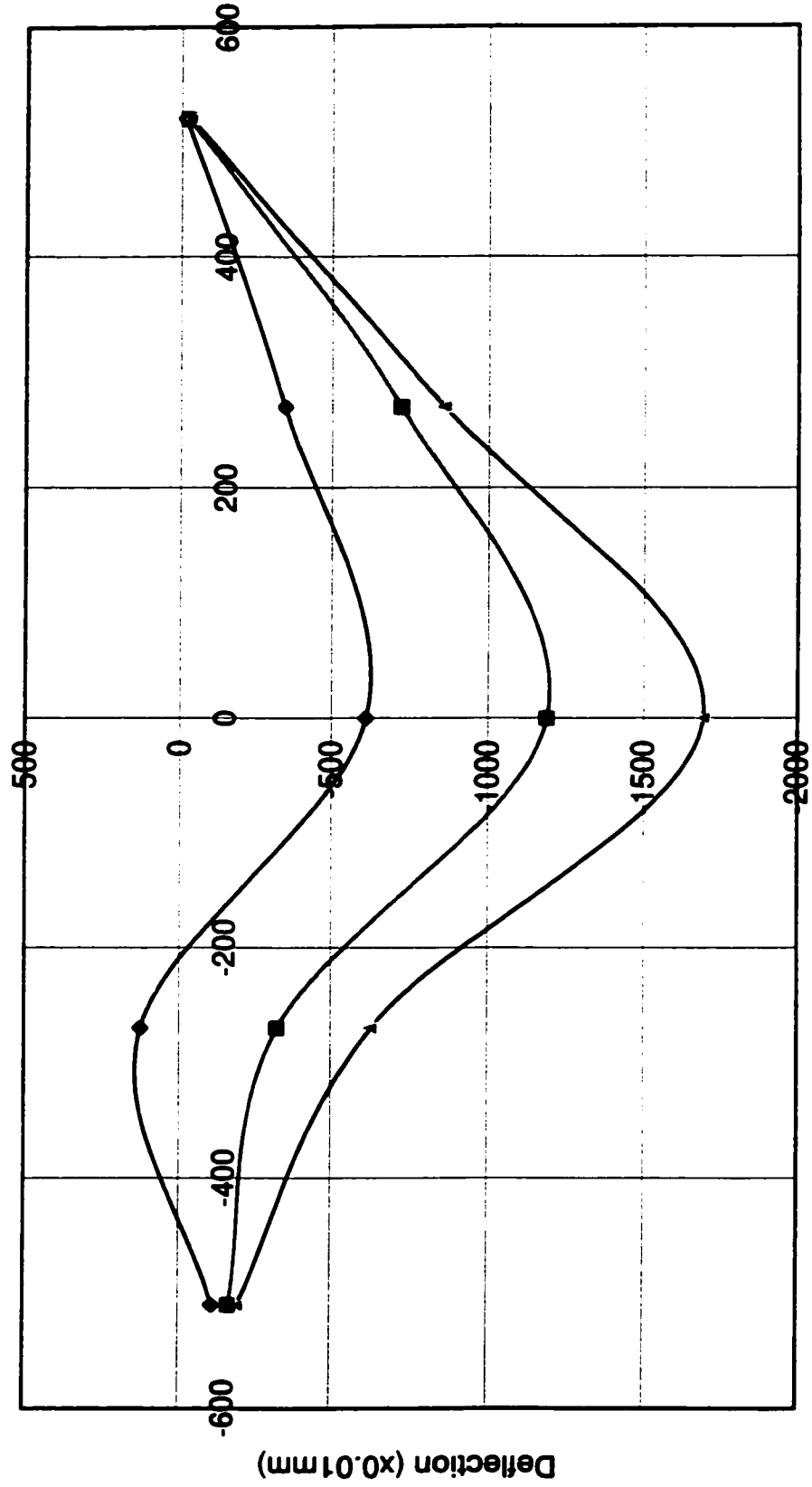
Test No. 30

No.	Load Applied on Specimen	Axial Force in Comp. Diagonal	Out-of-plane Deflection of Diagonal						Midspan Deflection (Vertical)	
			Dial Gauge No.1	Dial Gauge No.2	Dial Gauge No.3	Dial Gauge No.4	Dial Gauge No.5	Dial Gauge No.6	Dial Gauge No.7	
	Location (mm)									
	kN	kN	x0.01 mm	x0.01 mm	x0.01 mm	x0.01 mm	x0.01 mm	x0.01 mm	Front	Rear
		0	0	0	0	0	0	0	0	0
1	-33.6	8.1	-44	319	-228	-117	-6	233	231	
2	-55.9	12.9	-73	209	-364	-204	-9	359	351	
3	-83.5	18.3	-93	100	-511	-188	33	518	521	
4	-102.5	22.1	-107	126	-612	-347	-14	627	629	
5	-126.2	26.6	-124	-66	-734	-419	-17	759	753	
6	-148.3	30.8	-136	-149	-844	-511	-20	881	880	
7	-169.5	35.0	-152	-249	-982	-564	-22	1031	1032	
8	-196.0	39.9	-163	-326	-1192	-726	-24	1144	1148	
9	-208.6	42.5	-170	-380	-1304	-769	-25	1215	1221	
10	-223.4	45.2	-185	-432	-1357	-812	-26	1298	1300	
11	-235.9	47.3	-184	-508	-1445	-852	-27	1369	1370	
12	-252.0	51.4	-192	-631	-1696	-863	-27	1469	1462	

* Refer to Figure A-1 for Location of Dial Gauges

Deflection Shape

Test No. 30 P3A



\diamond — $P = 22.1 \text{ kN}$ $N = 20.3 \text{ kN}$
 \blacksquare — $P = 39.9 \text{ kN}$ $N = 36.7 \text{ kN}$
 \blacktriangle — $P = 51.4 \text{ kN}$ $N = 45.6 \text{ kN}$

LOAD DEFLECTION DATA - SPECIMEN P1B

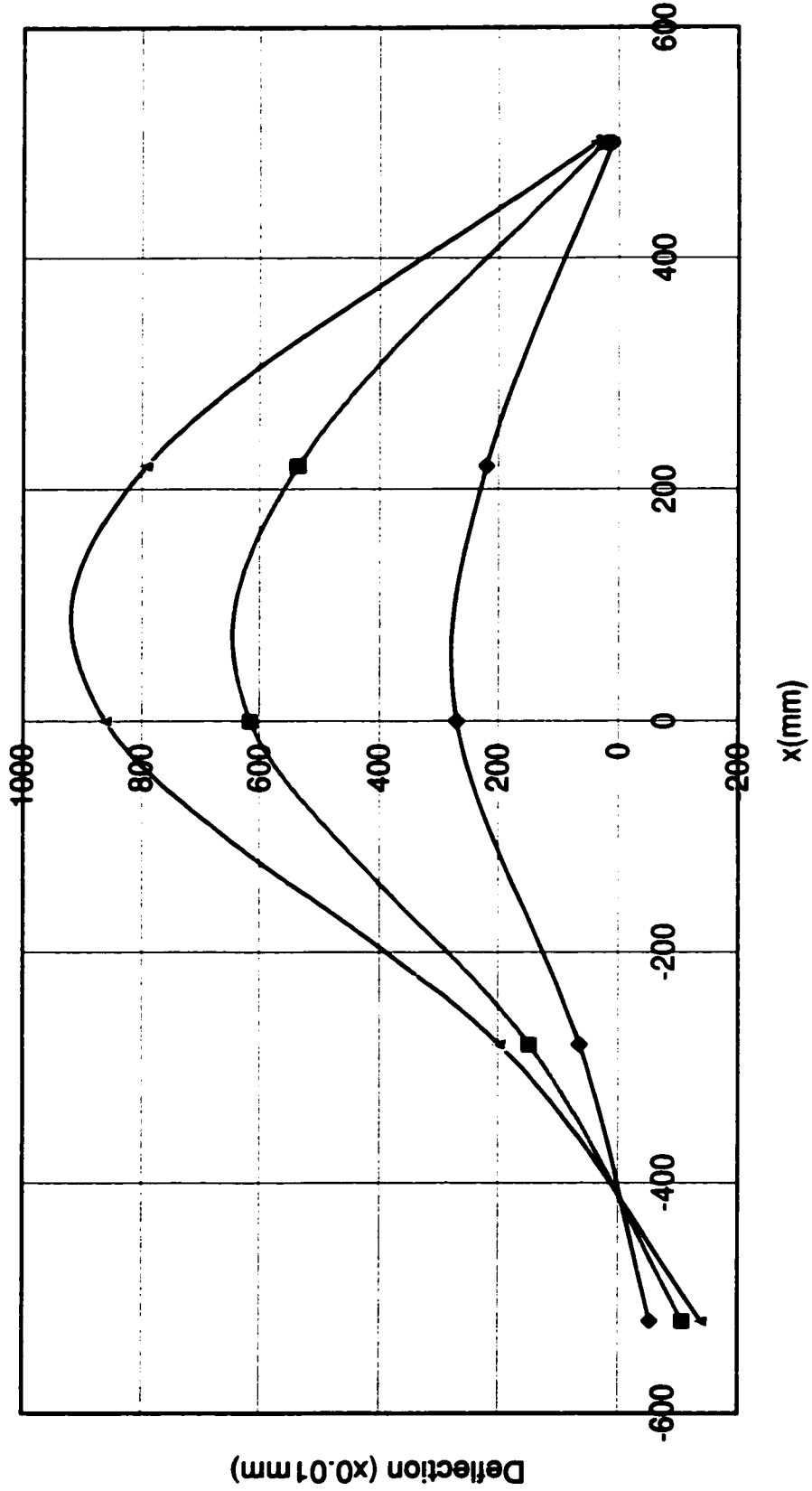
Test No. 31

No.	Load Applied on Specimen	Axial Force in Comp. Diagonal	Out-of-plane Deflection of Diagonal						Midspan Deflection (Vertical)		
			Dial Gauge No.1	Dial Gauge No.2	Dial Gauge No.3	Dial Gauge No.4	Dial Gauge No.5	Dial Gauge No.6	Dial Gauge No.7		
	Location (mm)		-520	-280	0	220	500	Front	Rear		
	kN	kN	x0.01 mm	x0.01 mm	x0.01 mm	x0.01 mm	x0.01 mm	x0.01 mm	x0.01 mm		
		0	0	0	0	0	0	0	0		
1	-27.0	4.9	-31	27	134	107	0	245	263		
2	-39.4	7.2	-43	46	203	260	8	352	373		
3	-51.9	9.7	-53	64	270	220	10	447	481		
4	-65.8	11.7	-65	85	349	286	13	577	602		
5	-76.8	13.6	-75	99	406	339	16	673	700		
6	-88.7	14.6	-85	115	569	398	18	774	804		
7	-102.2	17.8	-97	133	543	467	22	891	985		
8	-114.8	19.8	-107	148	616	537	25	999	1036		
9	-133.5	22.7	-122	174	728	648	30	1159	1201		
10	-151.8	25.8	-139	198	861	792	37	1322	1370		

* Refer to Figure A-1 for Location of Dial Gauges

Deflection Shape

Test No. 31 P1B



—◆— P=9.7 kN N=9.86 kN —■— P=19.8 kN N=21.0 kN —▲— P=25.8 kN N=27.3 kN

LOAD DEFLECTION DATA - SPECIMEN P3B

Test No. 32

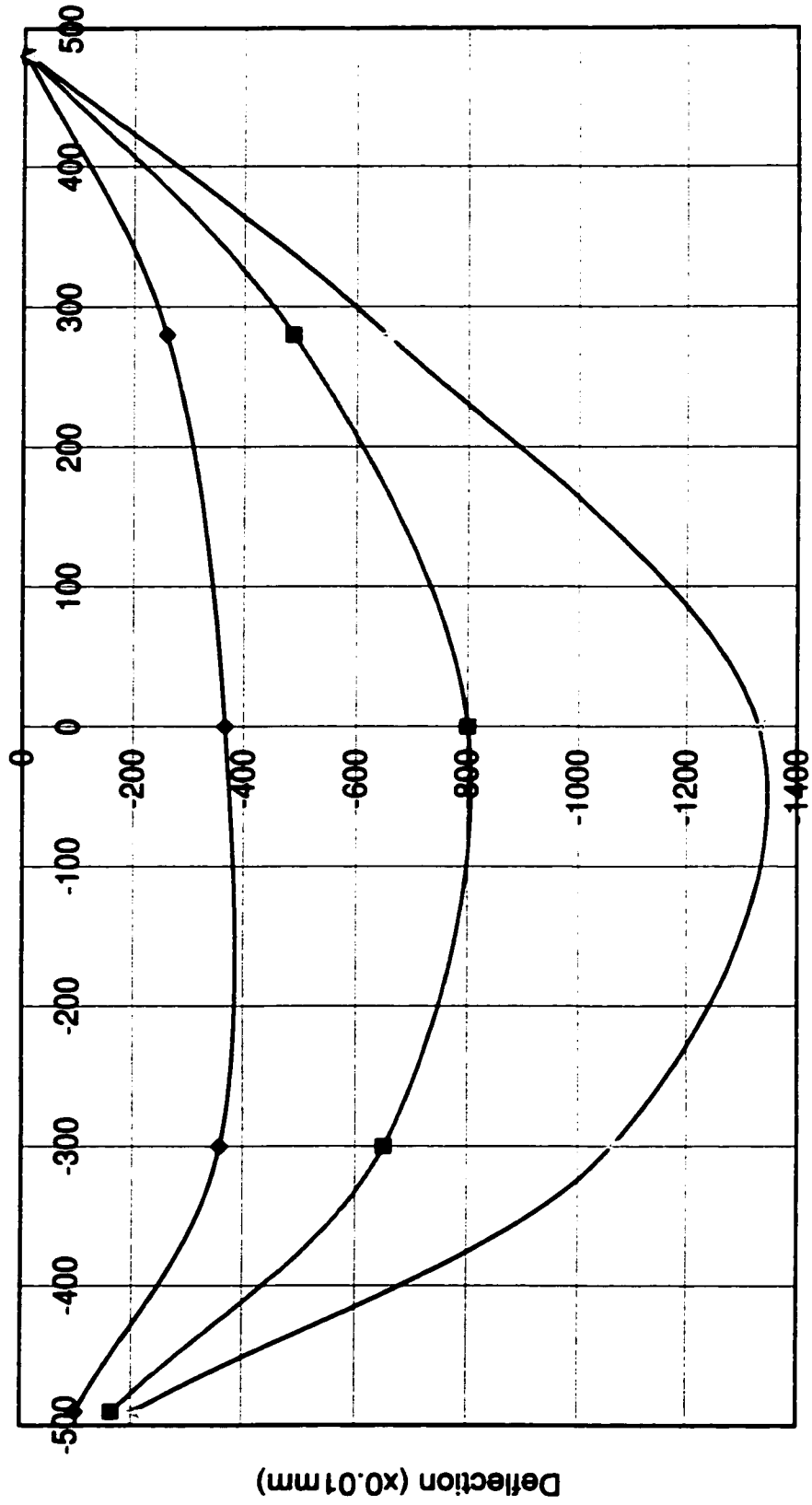
No.	Load Applied on Specimen	Axial Force In Comp. Diagonal	Out-of-plane Deflection of Diagonal						Midspan Deflection (Vertical)	
			Dial Gauge No.1	Dial Gauge No.2	Dial Gauge No.3	Dial Gauge No.4	Dial Gauge No.5	Dial Gauge No.6	Dial Gauge No.7	
	Location (mm)		-490	-300	0	280	480	Front	Rear	
	kN	kN	x0.01 mm	x0.01 mm	x0.01 mm	x0.01 mm	x0.01 mm	x0.01 mm	x0.01 mm	
	0	0	0	0	0	0	0	0	0	
1	-37.5	9.1	-44	-158	-100	-115	-2	271	246	
2	-67.7	15.6	-78	-278	-261	-204	-4	451	432	
3	-78.3	20.0	-99	-358	-366	-259	-6	575	556	
4	-119.3	26.5	-127	-466	-520	-340	-7	751	747	
5	-146.7	31.9	-166	-551	-647	-405	-9	909	895	
6	-180.1	41.0	-165	-651	-801	-486	-10	1099	1077	
7	-202.6	42.8	-176	-715	-906	-539	-10	1222	1199	
8	-222.7	46.9	-182	-771	-1003	-584	-10	1335	1284	
9	-234.3	49.9	-184	-817	-1085	-619	-10	-	-	
10	-252.4	53.8	-198	-904	-1193	-657	-12	-	-	
11	-268.2	60.0	-204	-1064	-1331	-654	-10	-	-	

* Refer to Figure A-1 for Location of Dial Gauges

Deflection Shape

Test No. 32 P3B

x (mm)



—◆— P= 20.0 kN N=18.8kN —■— P=41.0 kN N=38.9kN - - - P=60.0 kN N=53.2kN

LOAD DEFLECTION DATA - SPECIMEN P8A

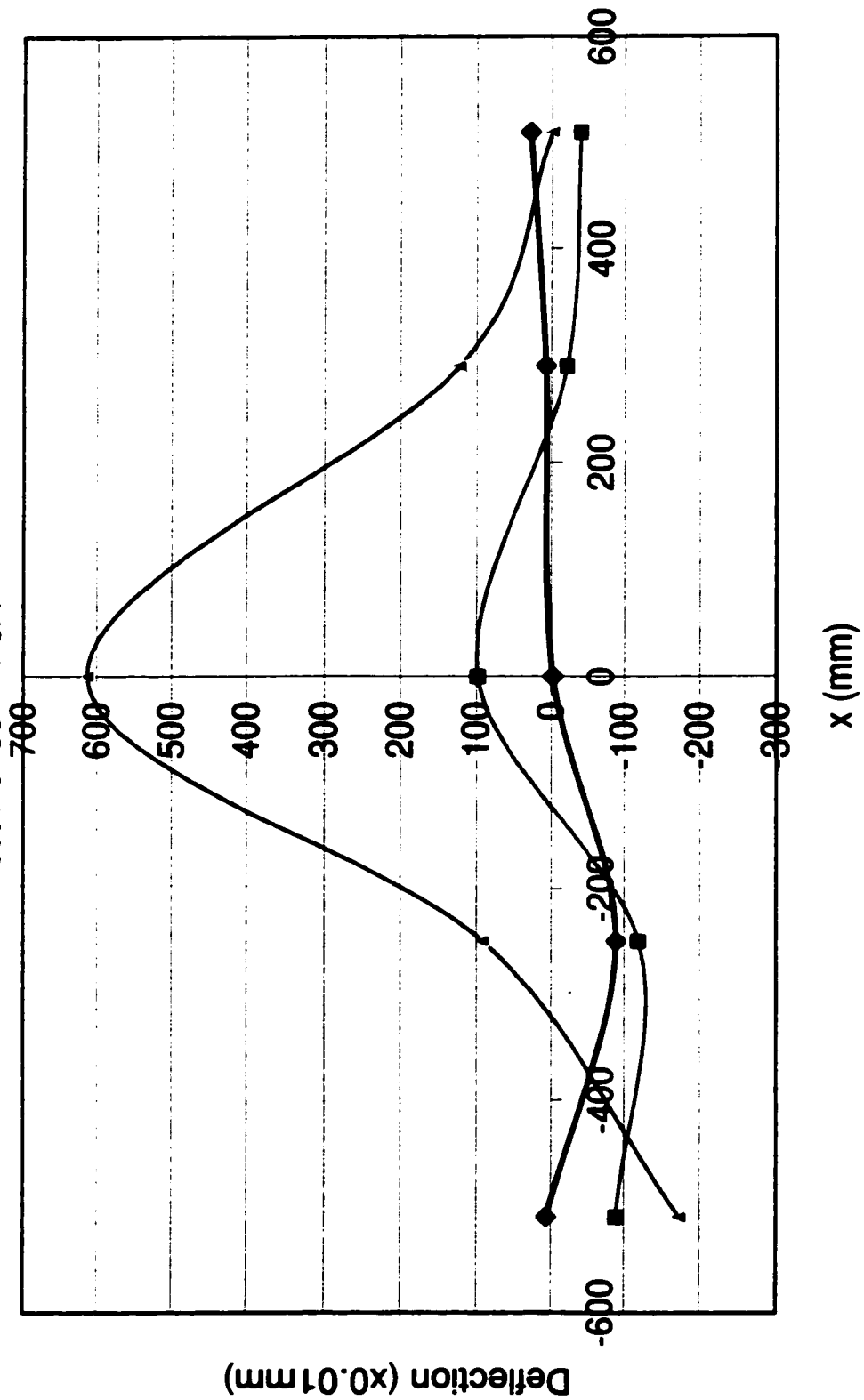
Test No. 33

No.	Load Applied on Specimen	Axial Force In Comp. Diagonal	Out-of-plane Deflection of Diagonal					Midspan Deflection (Vertical)		
			Dial Gauge No.1	Dial Gauge No.2	Dial Gauge No.3	Dial Gauge No.4	Dial Gauge No.5	Dial Gauge No.6	Dial Gauge No.7	
	Location (mm)		-510	-250	0	290	510	Front	Rear	
	kN	kN	x0.01 mm	x0.01 mm	x0.01 mm	x0.01 mm	x0.01 mm	x0.01 mm	x0.01 mm	
	0	0	0	0	0	0	0	0	0	
1	-33.5	14.3	-59	-59	-5	34	51	247		286
2	-51.6	21.5	7	-89	-2	8	29	365		416
3	-70.4	28.6	-123	-107	16	-10	6	489		541
4	-89.7	36.0	-54	-118	46	-21	-4	616		664
5	-111.9	44.4	-89	-119	98	-21	-40	761		806
6	-124.8	49.3	-108	-111	147	-15	-54	843		886
7	-140.6	55.0	-130	-84	233	5	-71	945		985
8	-152.6	59.2	-147	-48	329	34	-78	1001		1057
9	-163.1	63.2	-161	7	448	69	8	1089		1122
10	-166.9	65.1	-174	92	613	122	-1	1560		1184

* Refer to Figure A-1 for Location of Dial Gauges

Deflection Shape

Test No. 33 P8A



—◆— $P=21.5 \text{ kN}$ N=3.76kN —■— $P=44.4 \text{ kN}$ N=6.79kN —▲— $P=65.1 \text{ kN}$ N=12.5kN

LOAD DEFLECTION DATA - SPECIMEN P5B

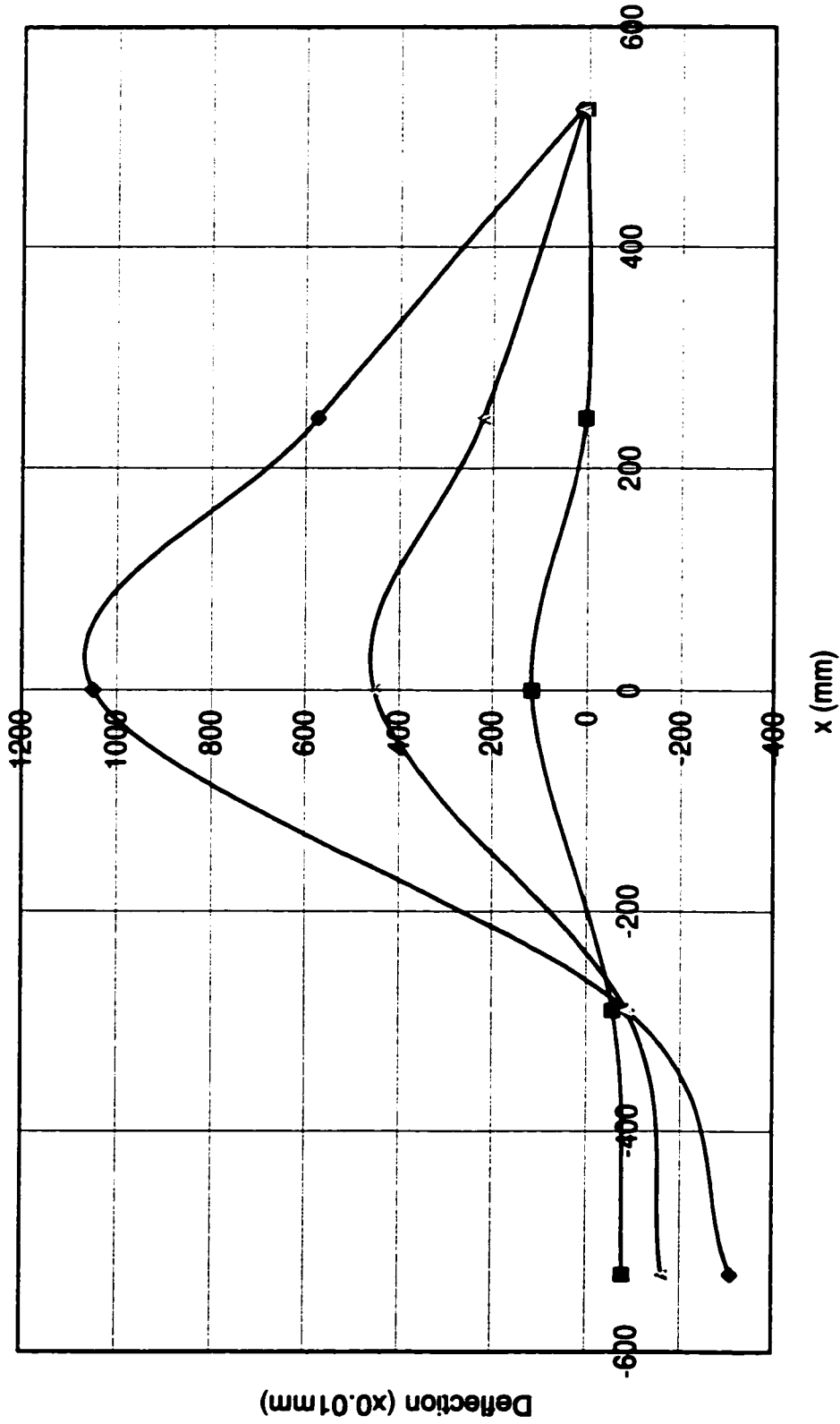
Test No. 34

No.	Load Applied on Specimen	Axial Force In Comp. Diagonal	Out-of-plane Deflection of Diagonal						Midspan Deflection (Vertical)	
			Dial Gauge No.1	Dial Gauge No.2	Dial Gauge No.3	Dial Gauge No.4	Dial Gauge No.5	Dial Gauge No.6	Dial Gauge No.7	
	Location (mm)		-530	-290	0	245	525	Front	Rear	
	kN	kN	x0.01 mm	x0.01 mm	x0.01 mm	x0.01 mm	x0.01 mm	x0.01 mm	x0.01 mm	
	0	0	0	0	0	0	0	0	0	
1	-40.3	9.3	-41	-44	35	-26	1	96	217	
2	-68.7	15.4	-59	-55	73	-17	2	330	350	
3	-98.7	21.5	-78	-56	118	4	4	468	490	
4	-133.4	28.3	-96	-64	165	29	6	621	695	
5	-175.8	36.5	-118	-59	247	62	8	798	833	
6	-226.8	45.0	-144	-88	387	187	10	1104	1056	
7	-260.8	50.9	-160	-84	453	220	11	1146	1201	
8	-292.7	56.4	-177	-79	520	255	13	1277	1342	
9	-323.7	61.7	-194	-77	586	291	15	1404	1480	
10	-353.7	67.1	-212	-71	703	328	16	1536	1619	
11	-382.0	73.6	-240	-68	739	348	18	1661	1756	
12	-387.9	74.9	-249	-64	820	412	10	1786	1892	
13	-429.0	80.6	-268	-65	898	447	21	1893	2015	
14	-438.6	83.1	-287	-70	971	507	13	1988	2129	
15	-460.0	86.4	-312	-86	1050	573	15	2076	2243	

* Refer to Figure A-1 for Location of Dial Gauges

Deflection Shape

Test No. 34 P5B



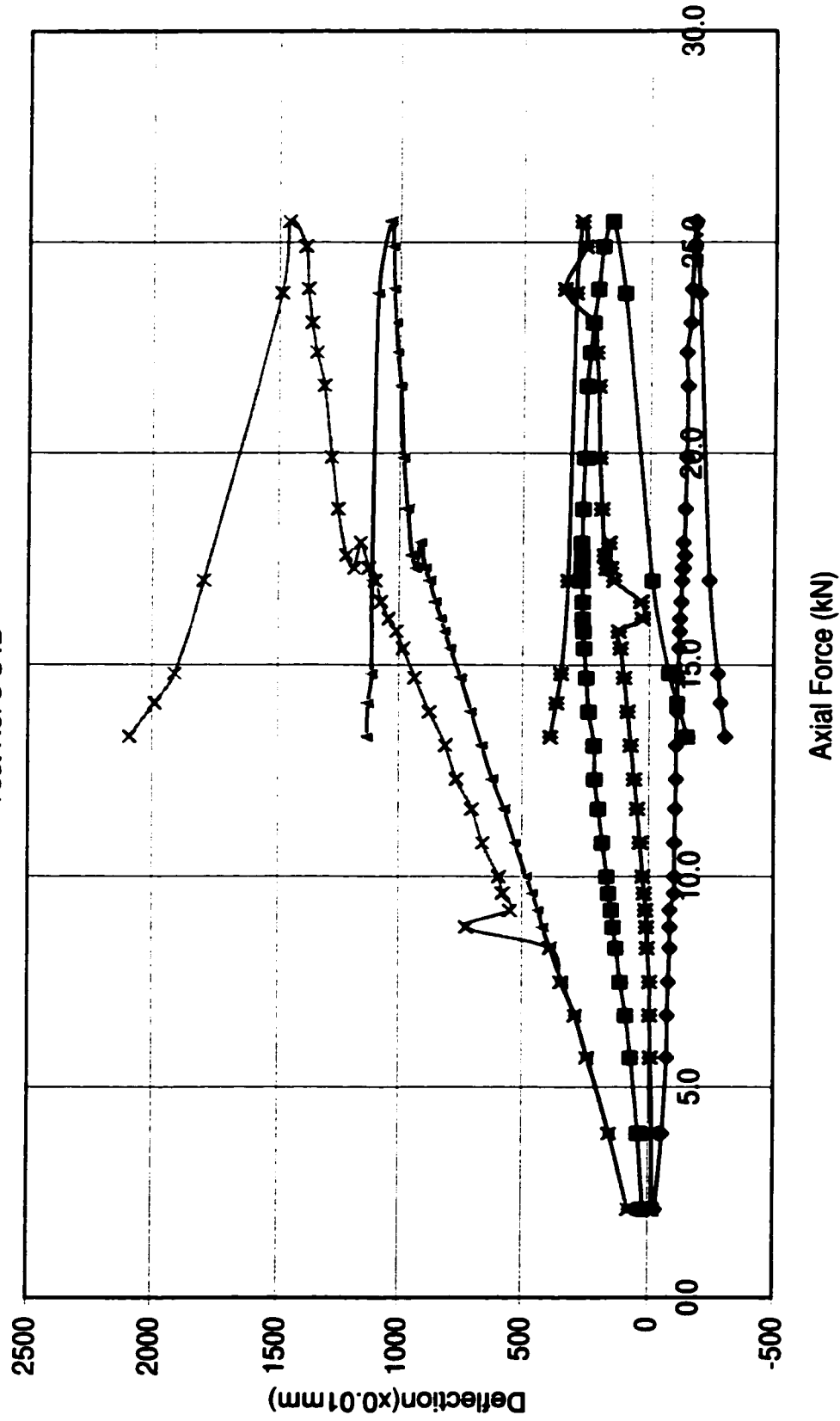
—◆— P=86.4 kN N=72.9 kN —■— P=21.5 kN N=16.4 kN —▲— P=50.9 kN N=40.87 kN

APPENDIX-C

Load-deflection Curves

Deflection of Diagonal

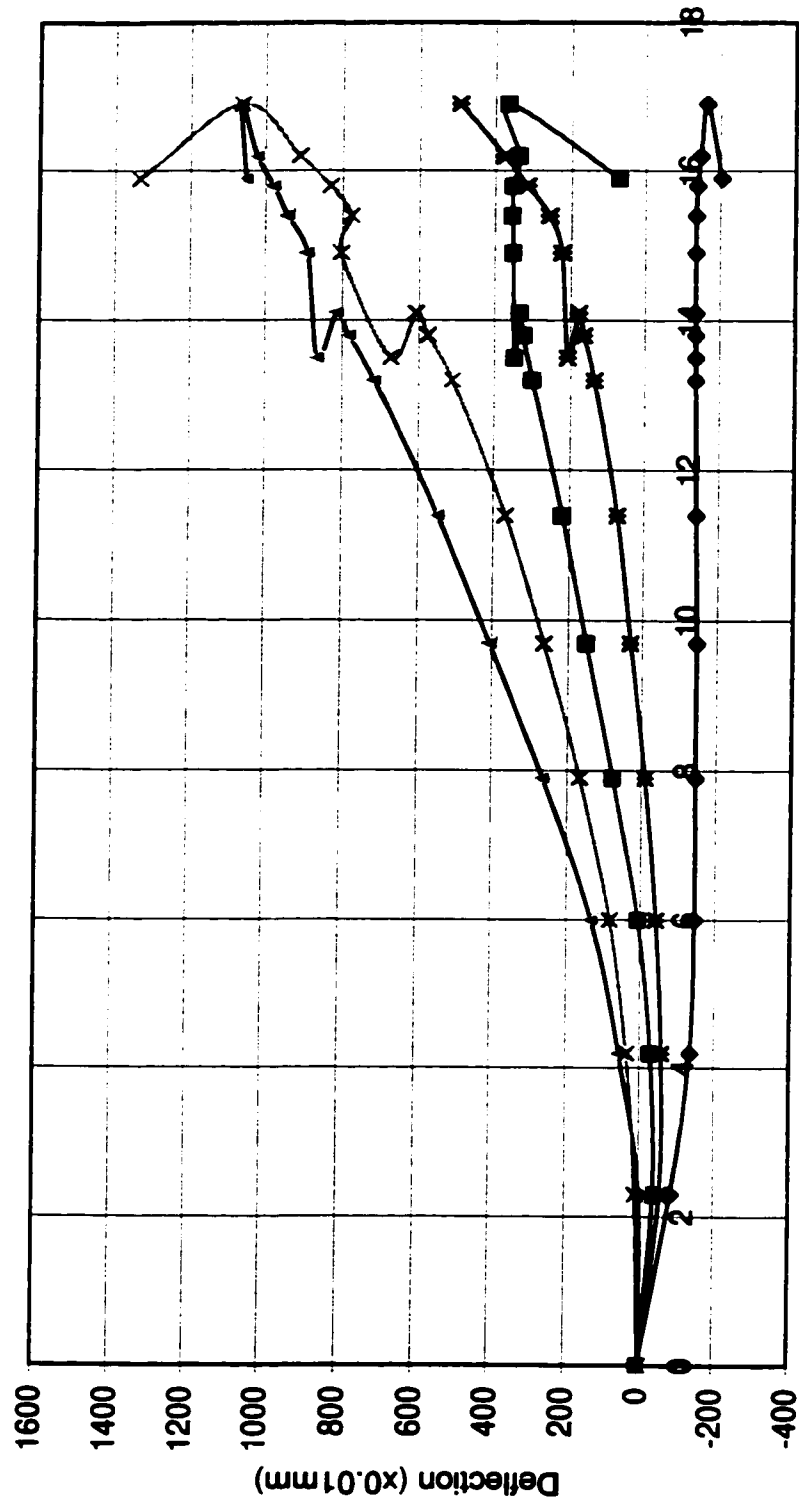
Test No. 3 S4B



—◆— No. 1 —■— No. 2 —▲— No. 3 —×— No. 4 —*— No. 5

Deflection of Diagonal

Test No. 4 S2A

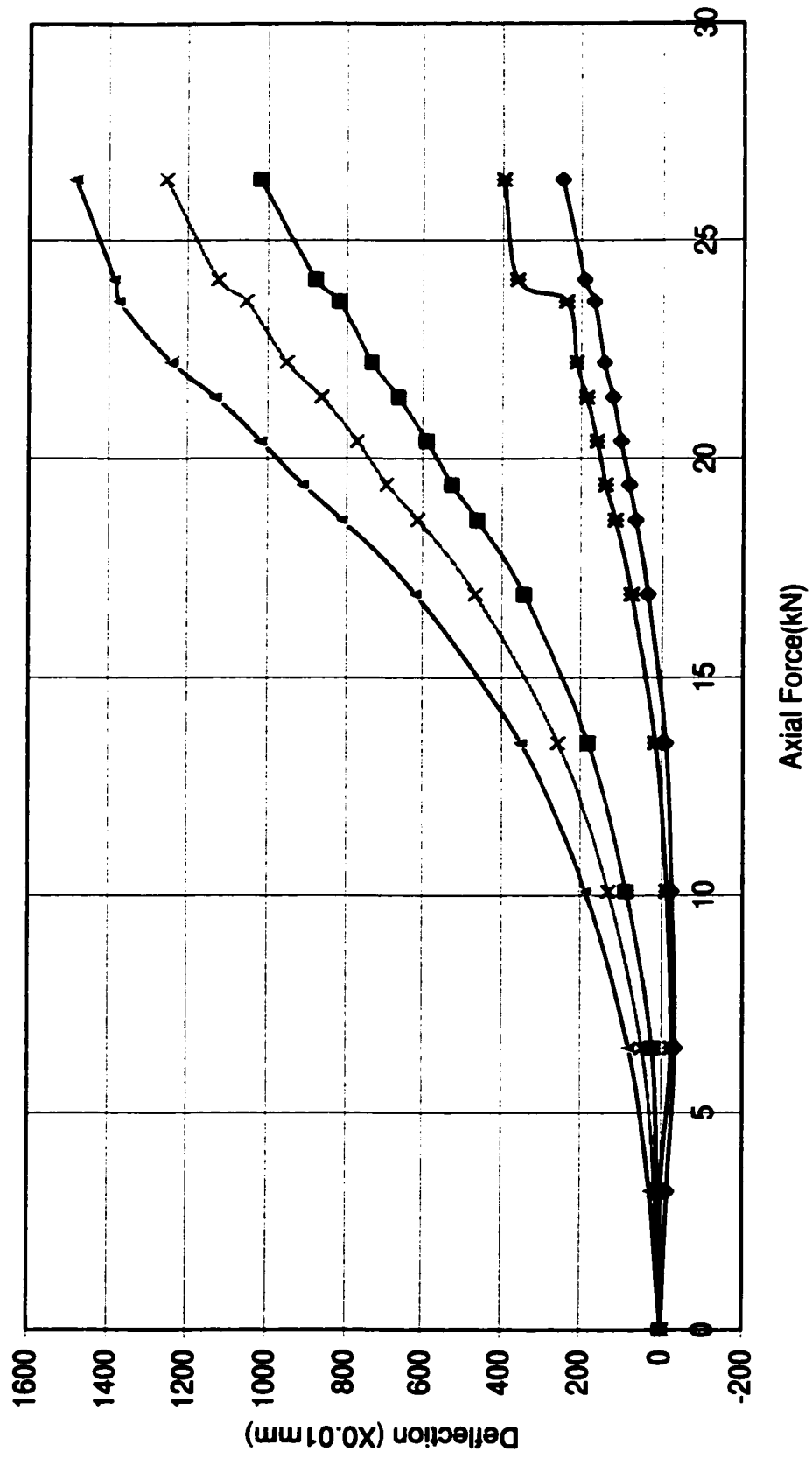


Axial Force (kN)

—◆— No. 1 —■— No. 2 —+— No. 3 —x— No. 4 —*— No. 5

Deflection of Diagonal

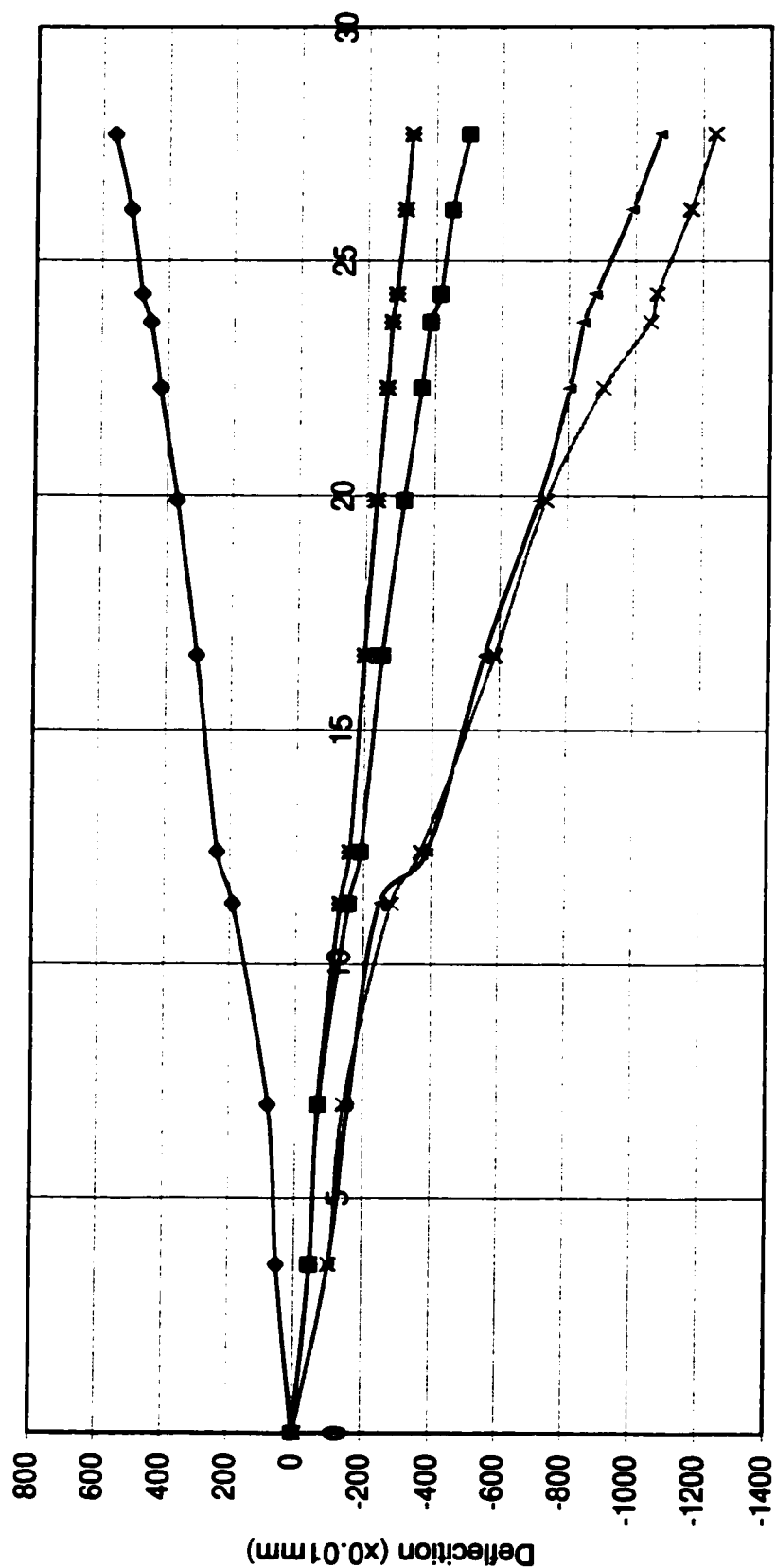
Test No. 7 S3A



—◆— No. 1 —■— No. 2 —▲— No. 3 —×— No. 4 —#— No. 5

Deflection of Diagonal

Test No. 10 S5B

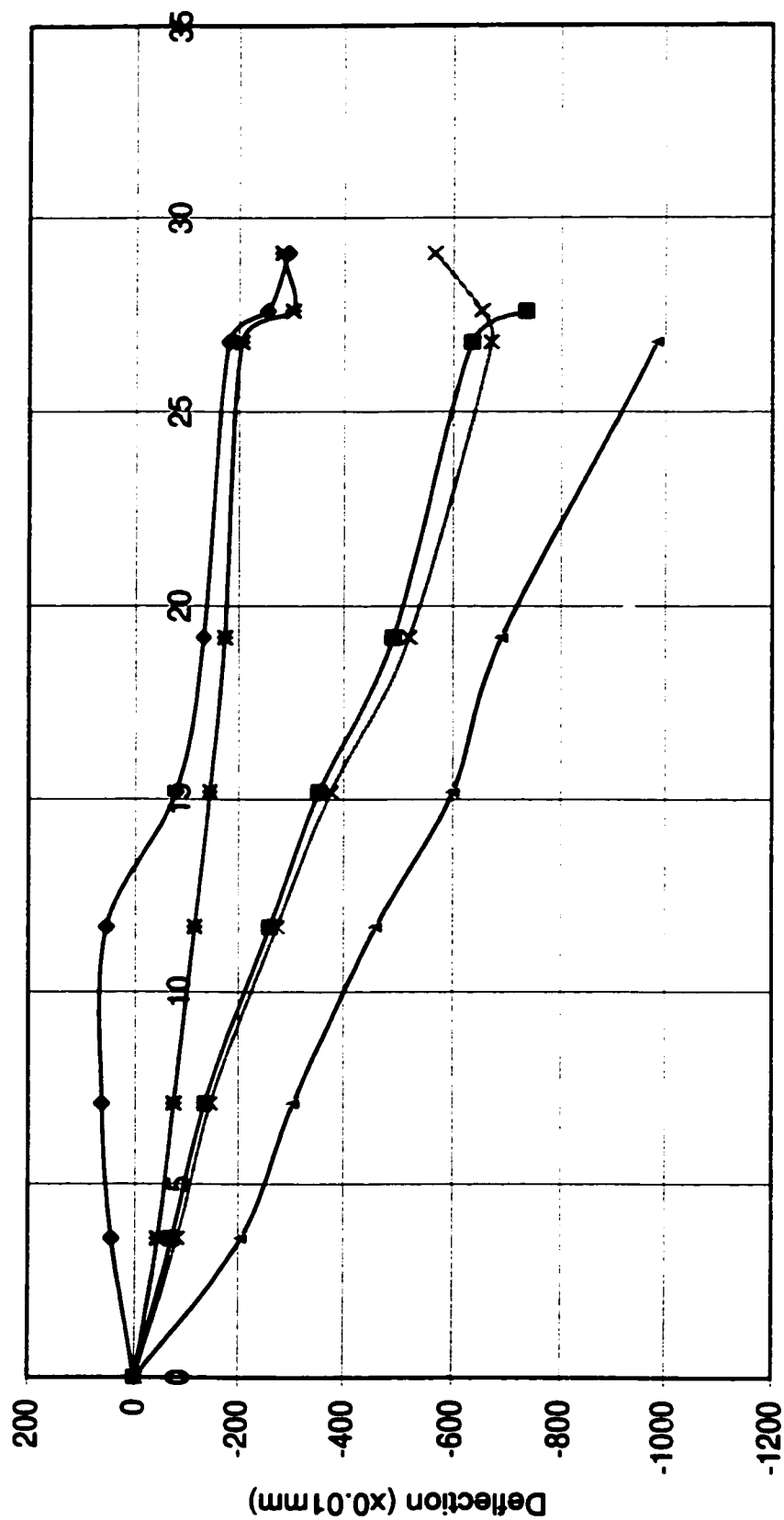


Axial force (kN)

—◆— No. 1 —■— No. 2 —+— No. 3 —x— No. 4 —*— No. 5

Deflection of Diagonal

Test No. 12 S5C

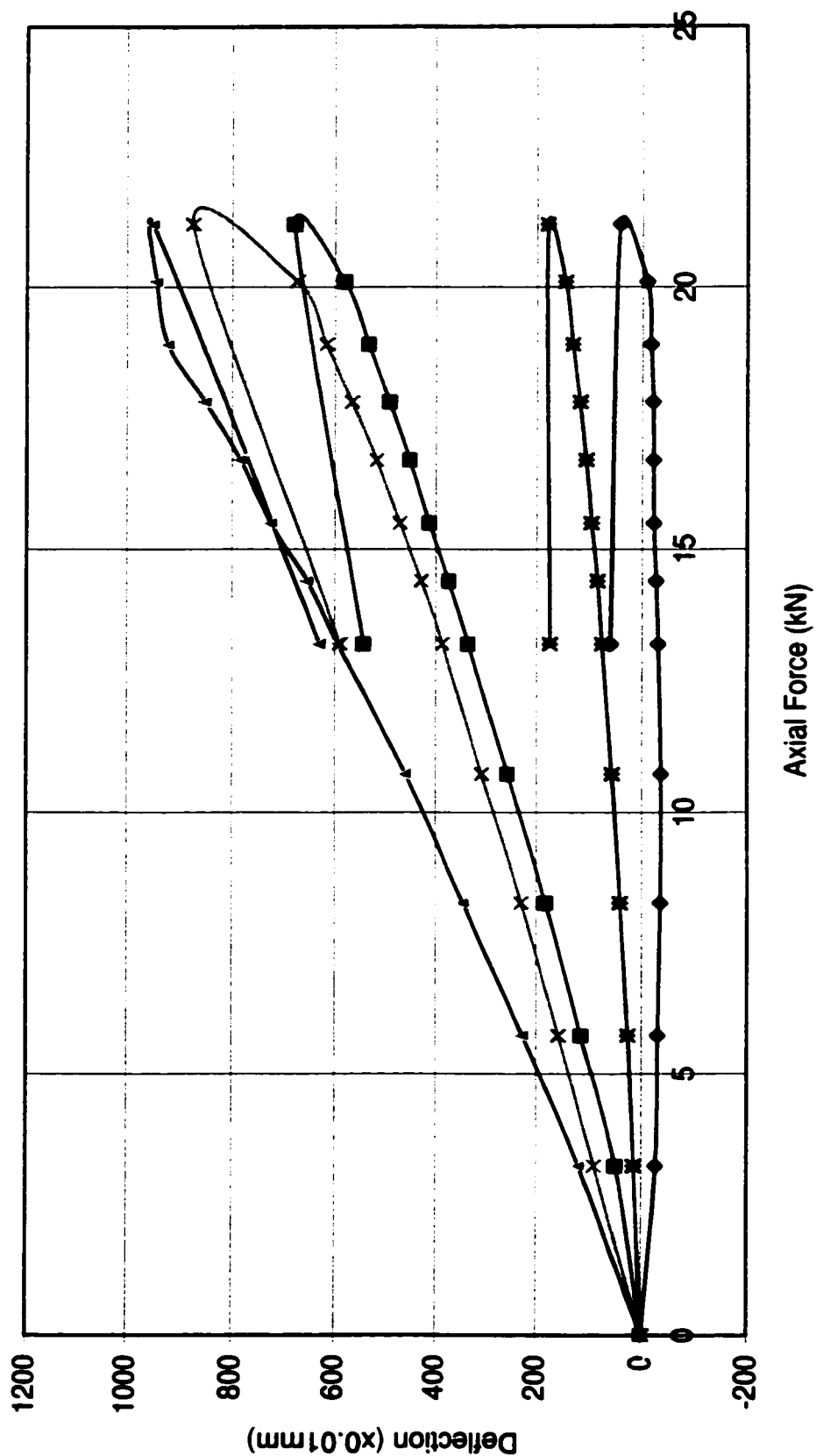


Axial force (kN)

—◆— No. 1 —■— No. 2 —▲— No. 3 —x— No. 4 —*— No. 5

Deflection of Diagonal

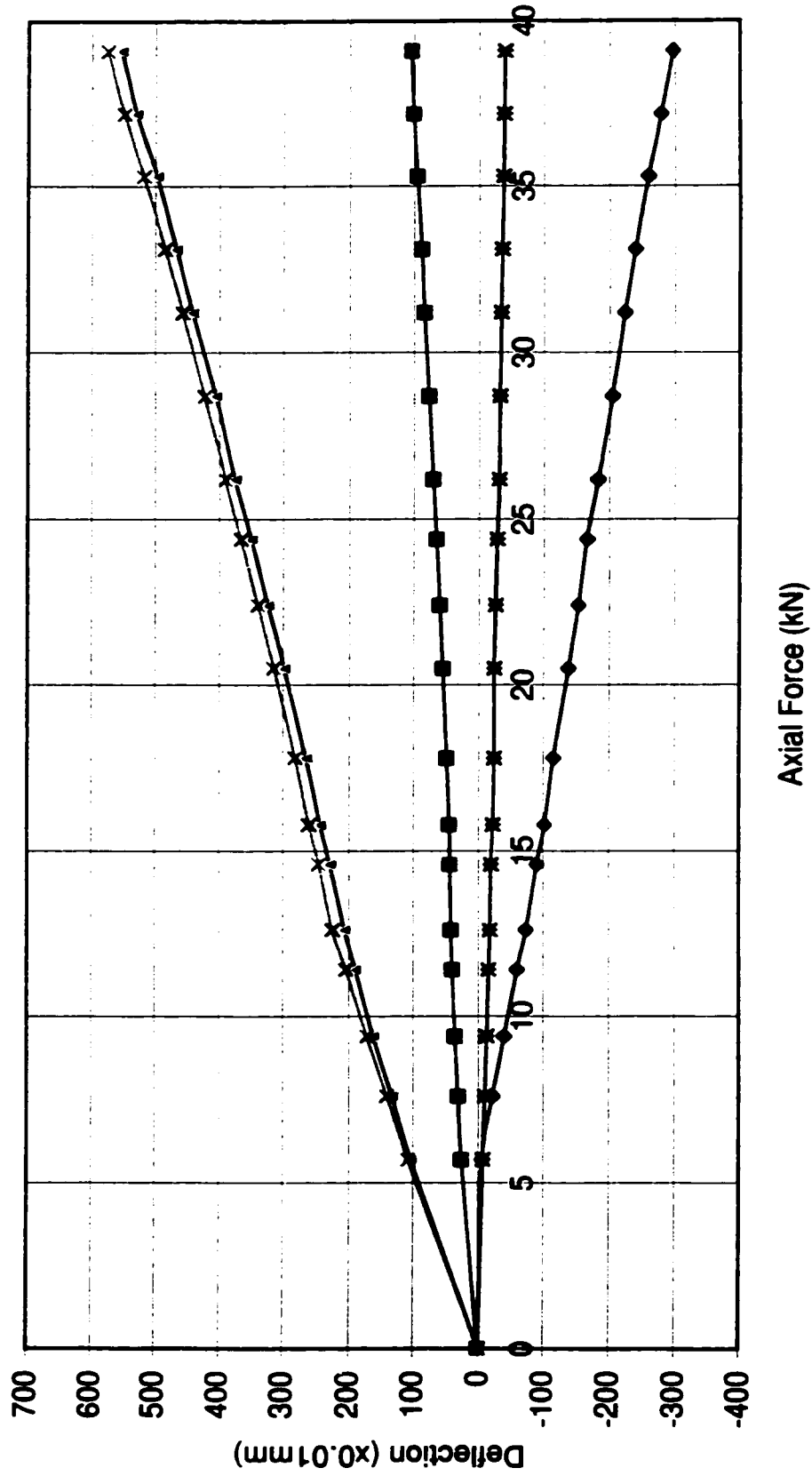
Test No. 13 S6B



—◆— No. 1 —■— No. 2 —+— No. 3 —x— No. 4 —*— No. 5

Deflection of Diagonal

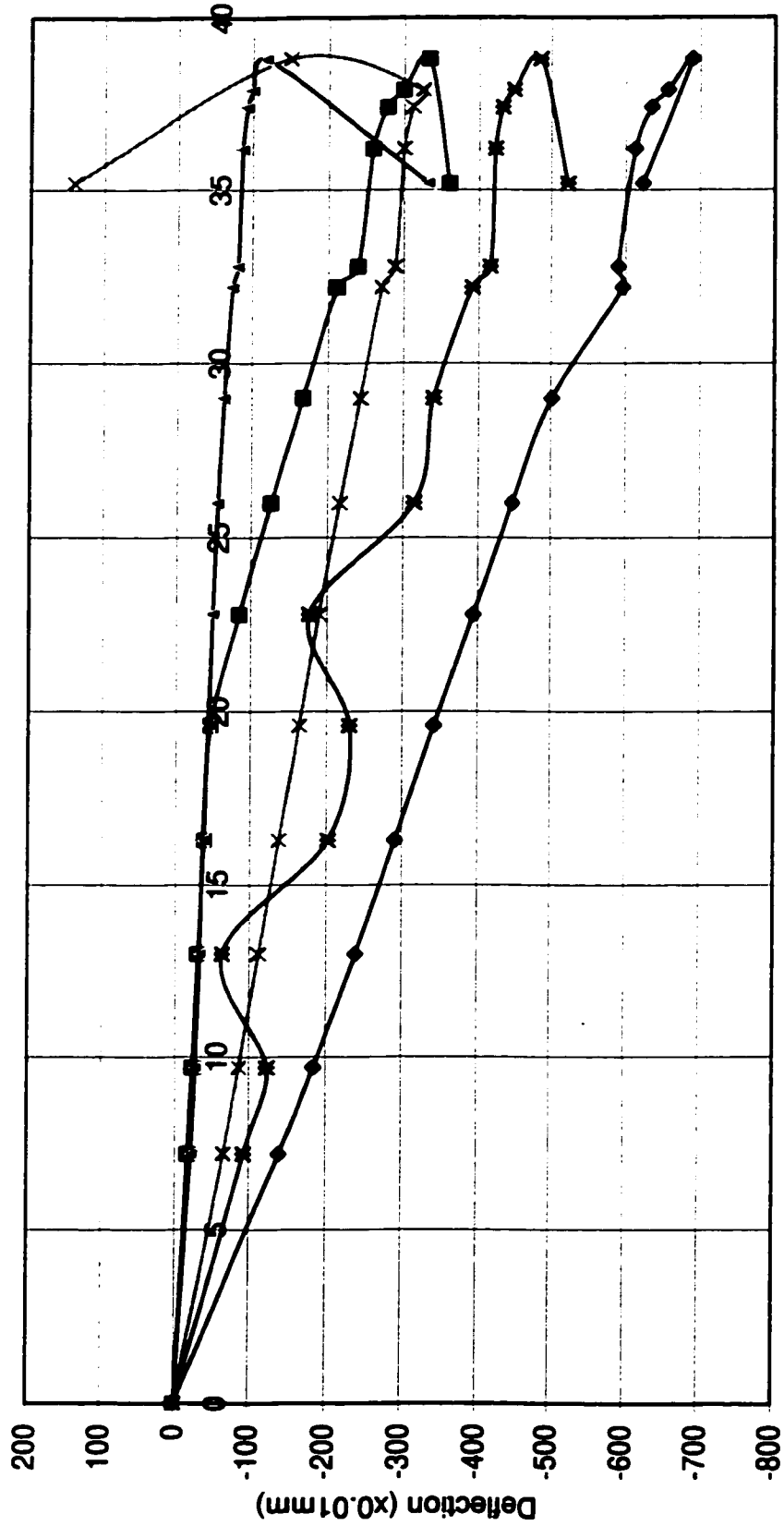
Test No. 17 P7B



—◆— No. 1 —■— No. 2 —▲— No. 3 —◆— No. 4 —●— No. 5

Deflection of Diagonal

Test No. 18 P7A

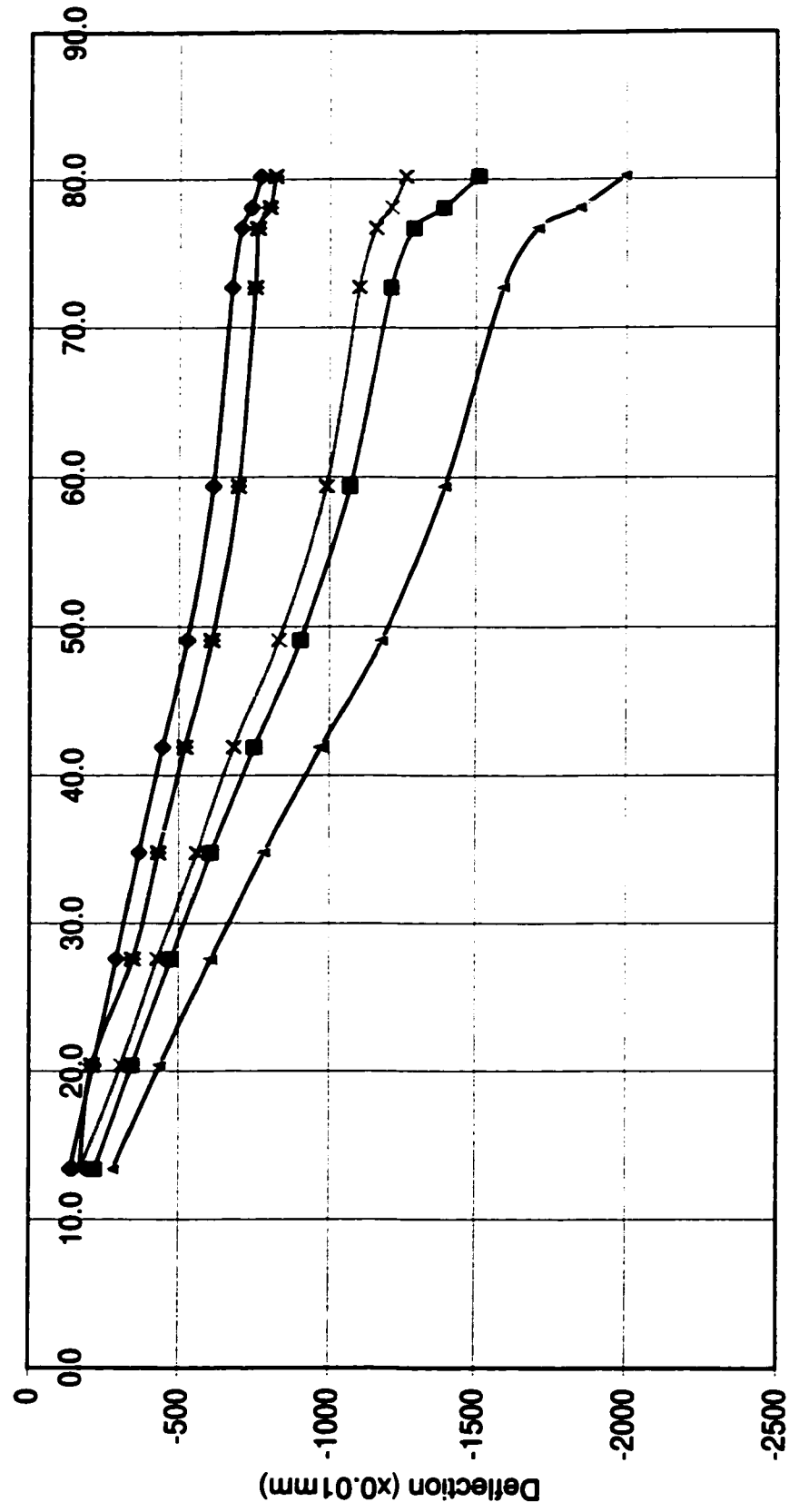


Axial Force (kN)

—●— No. 1 —■— No. 2 —+— No. 3 —x— No. 4 —*— No. 5

Deflection of Diagonal

Test No. 19 P8B

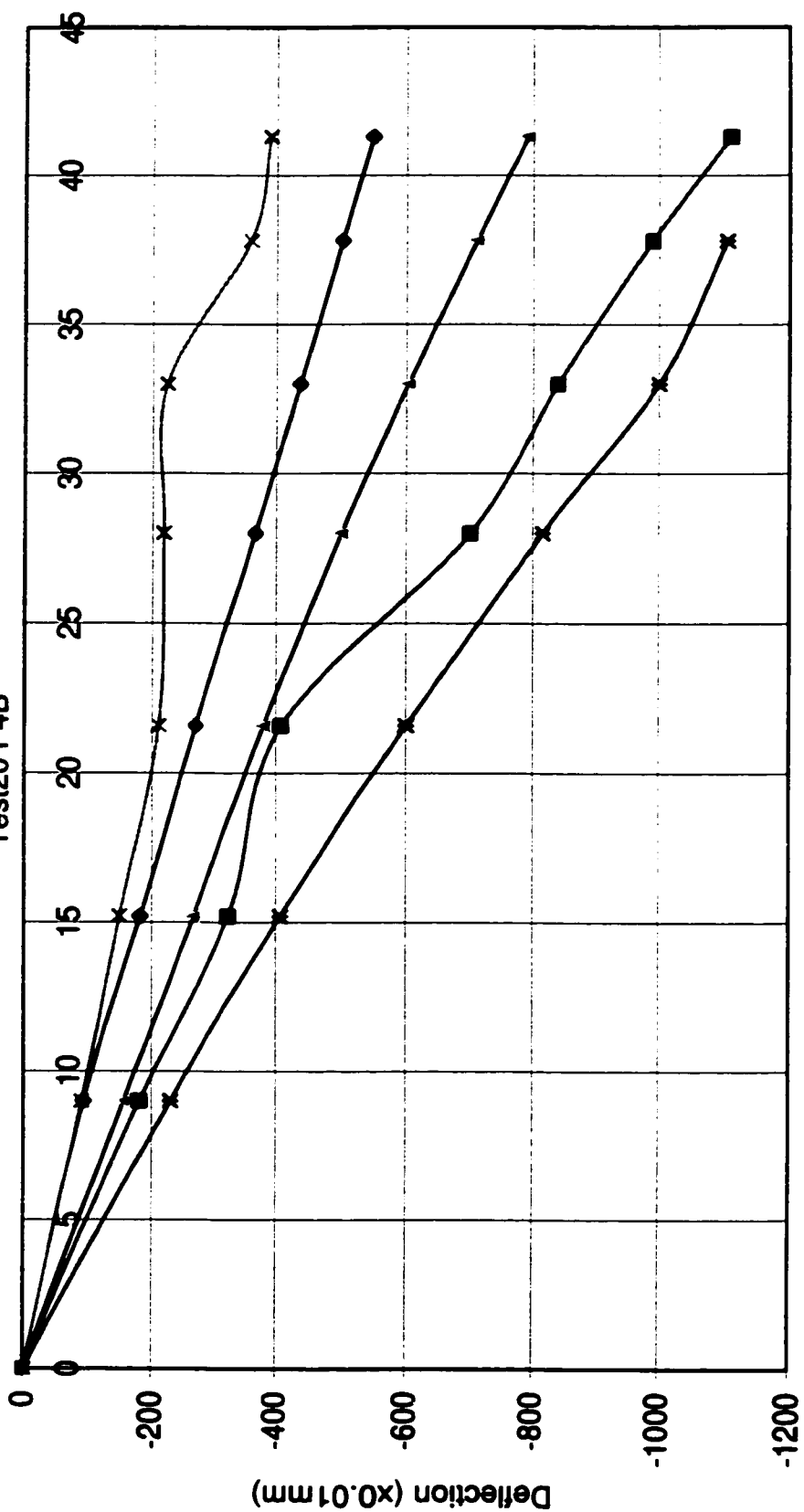


Axial Force (kN)

—◆— No. 1 —■— No. 2 —▲— No. 3 —x— No. 4 —*— No. 5

Deflection of Diagonal

Test20 P4B

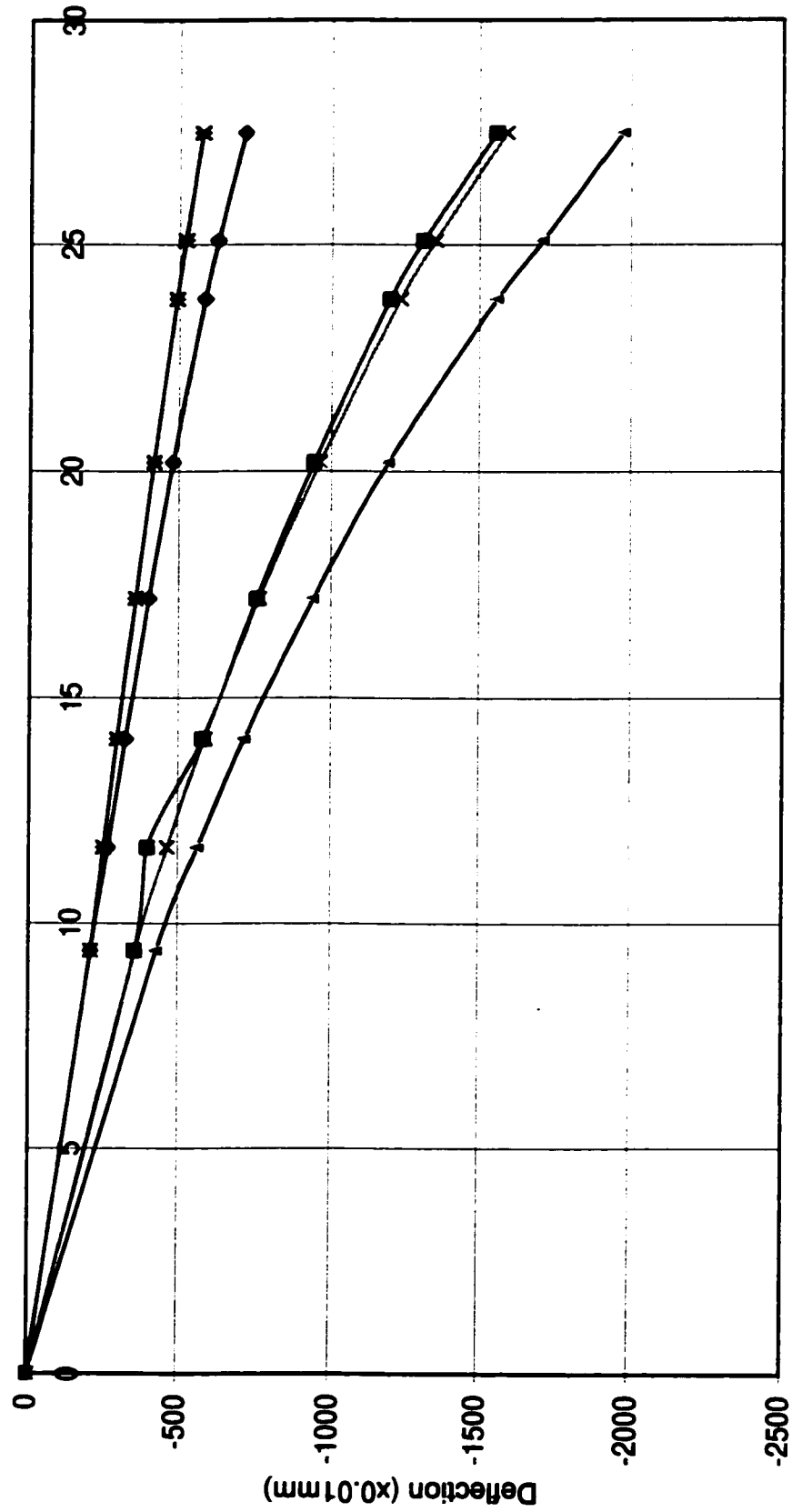


Axial Force (kN)

—◆— No. 1 —■— No. 2 —+— No. 3 —x— No. 4 —*— No. 5

Deflection of Diagonal

Test No. 21 P2A

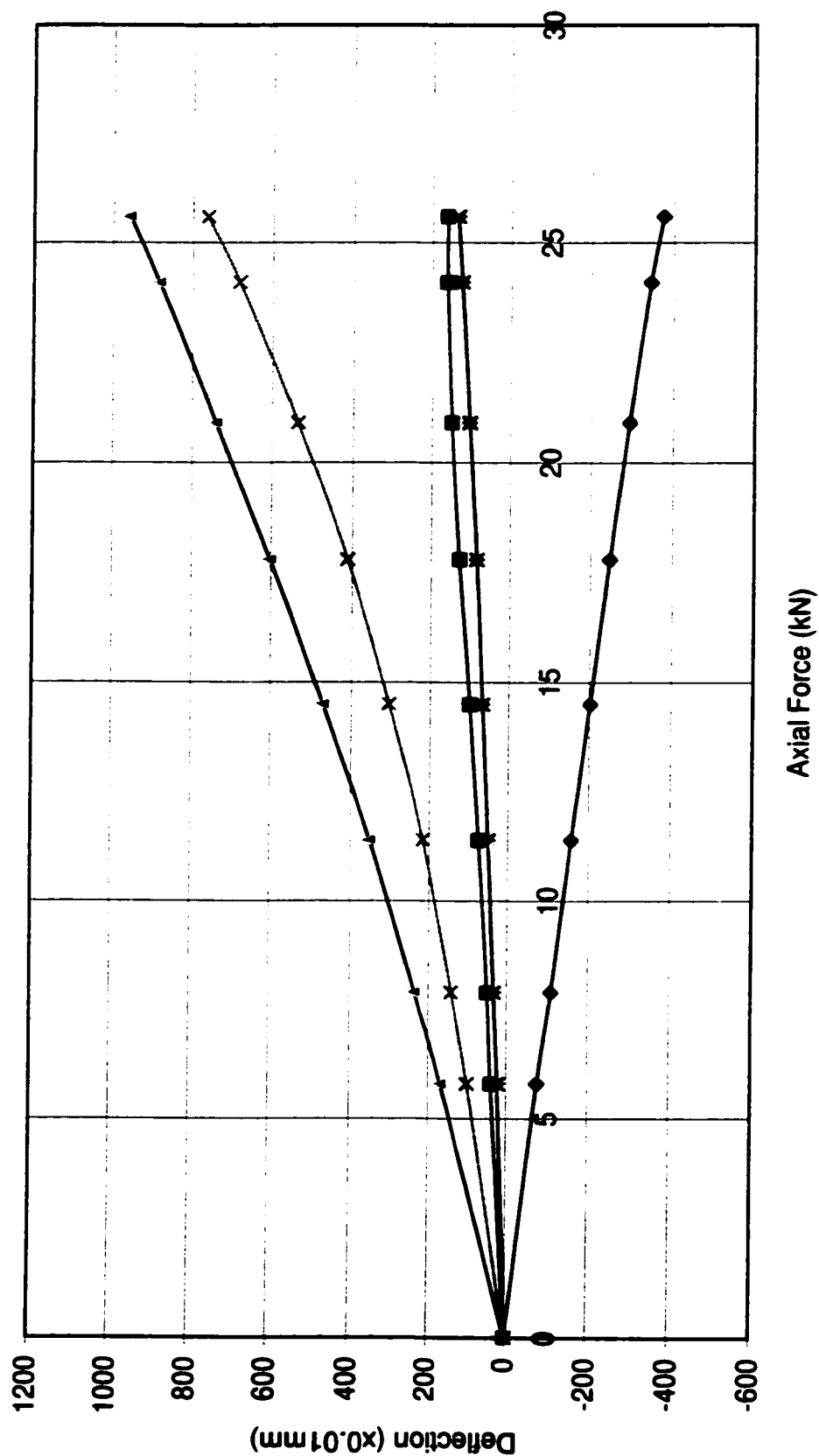


Axial Force (kN)

—x— No. 1 —x— No. 2 —x— No. 3 —x— No. 4 —x— No. 5

Deflection of Diagonal

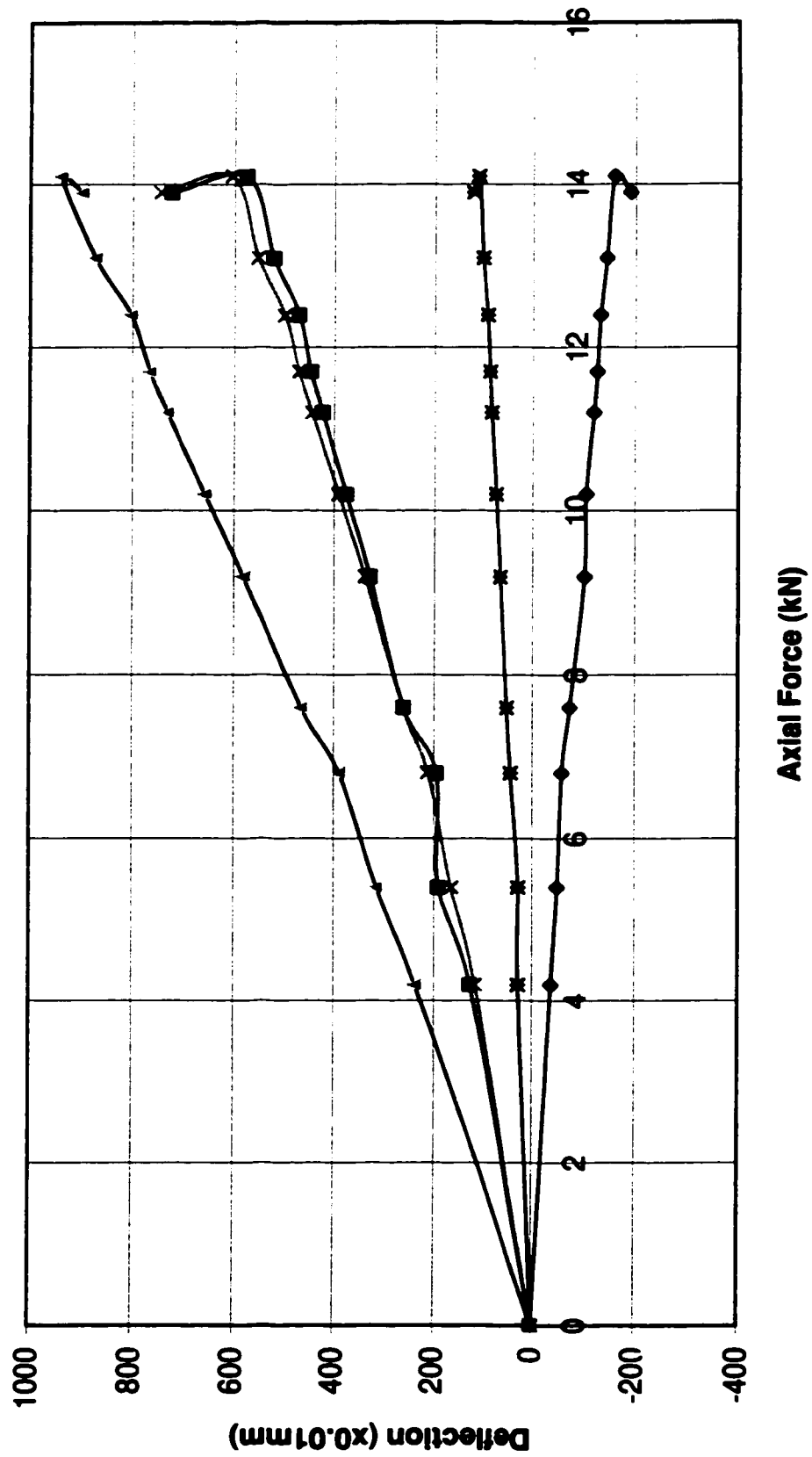
Test No. 22 P1A



—◆— No. 1 —■— No. 2 —▲— No. 3 —×— No. 4 —*— No. 5

Deflection of Diagonal

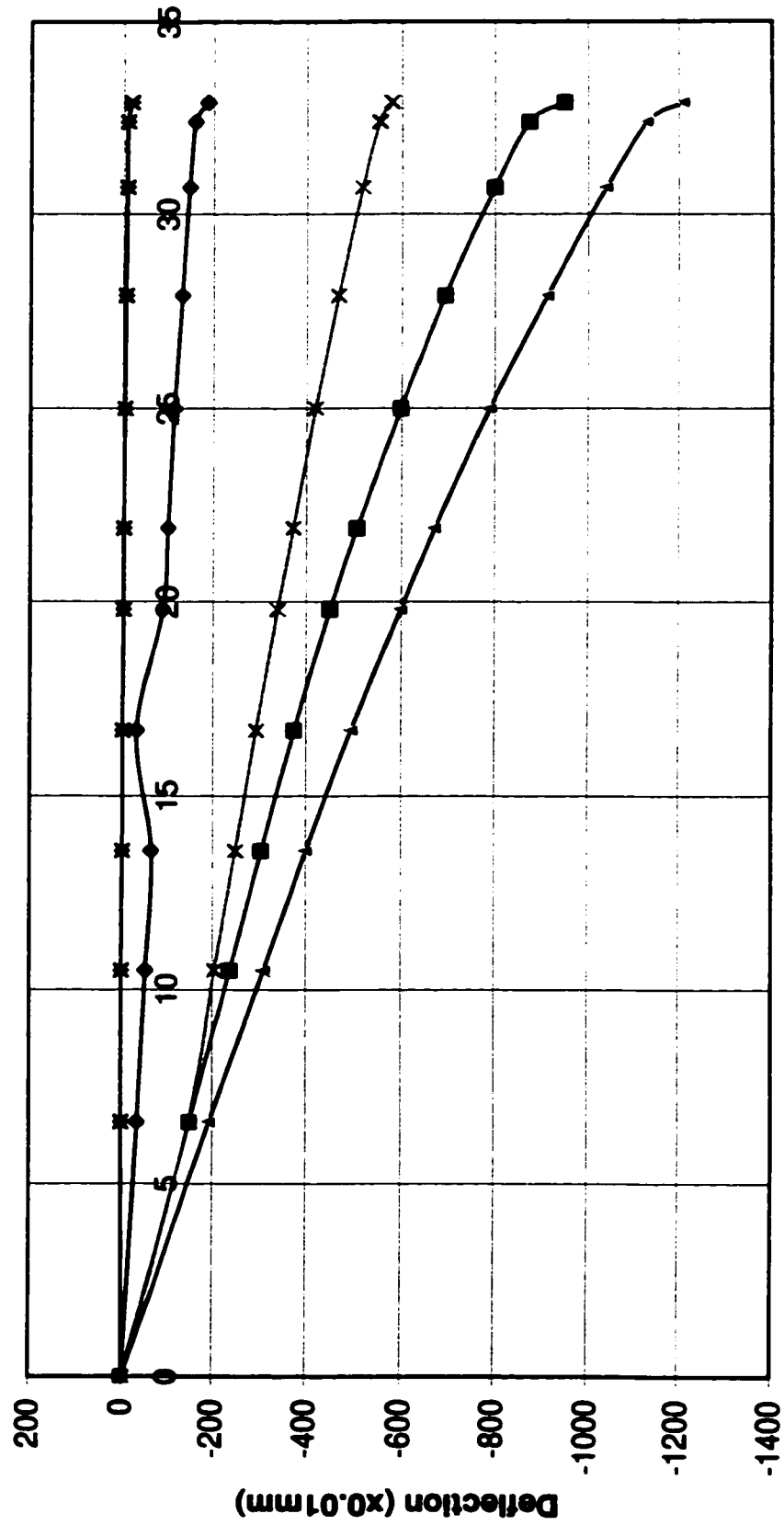
Test No. 23 S2C



—◆— No. 1 —■— No. 2 —▲— No. 3 —x— No. 4 —*— No. 5

Deflection of Diagonal

Test No. 24 S6C

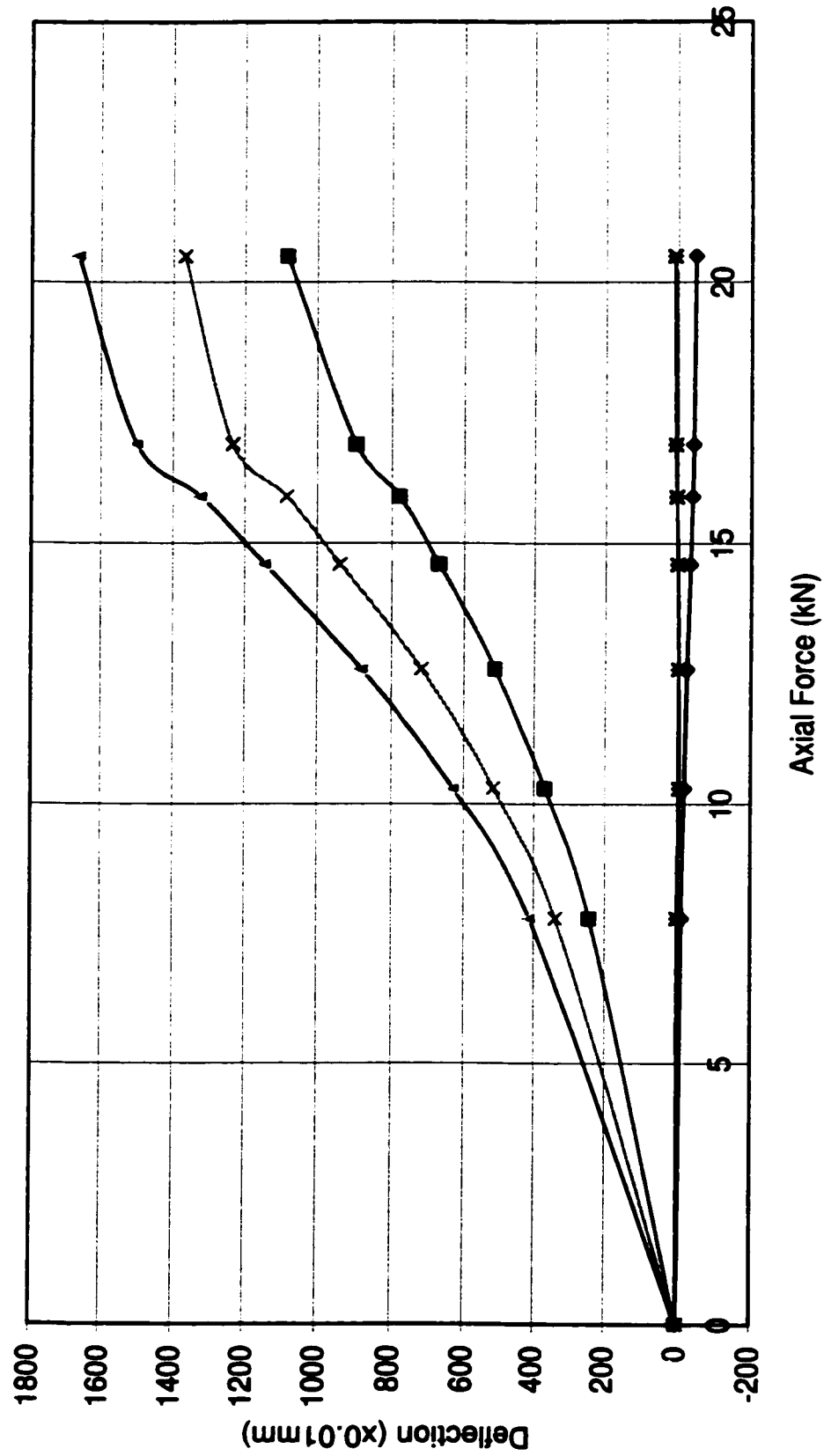


Axial Force (kN)

—◆— No. 1 —■— No. 2 —+— No. 3 —x— No. 4 —*— No. 5

Deflection of Diagonal

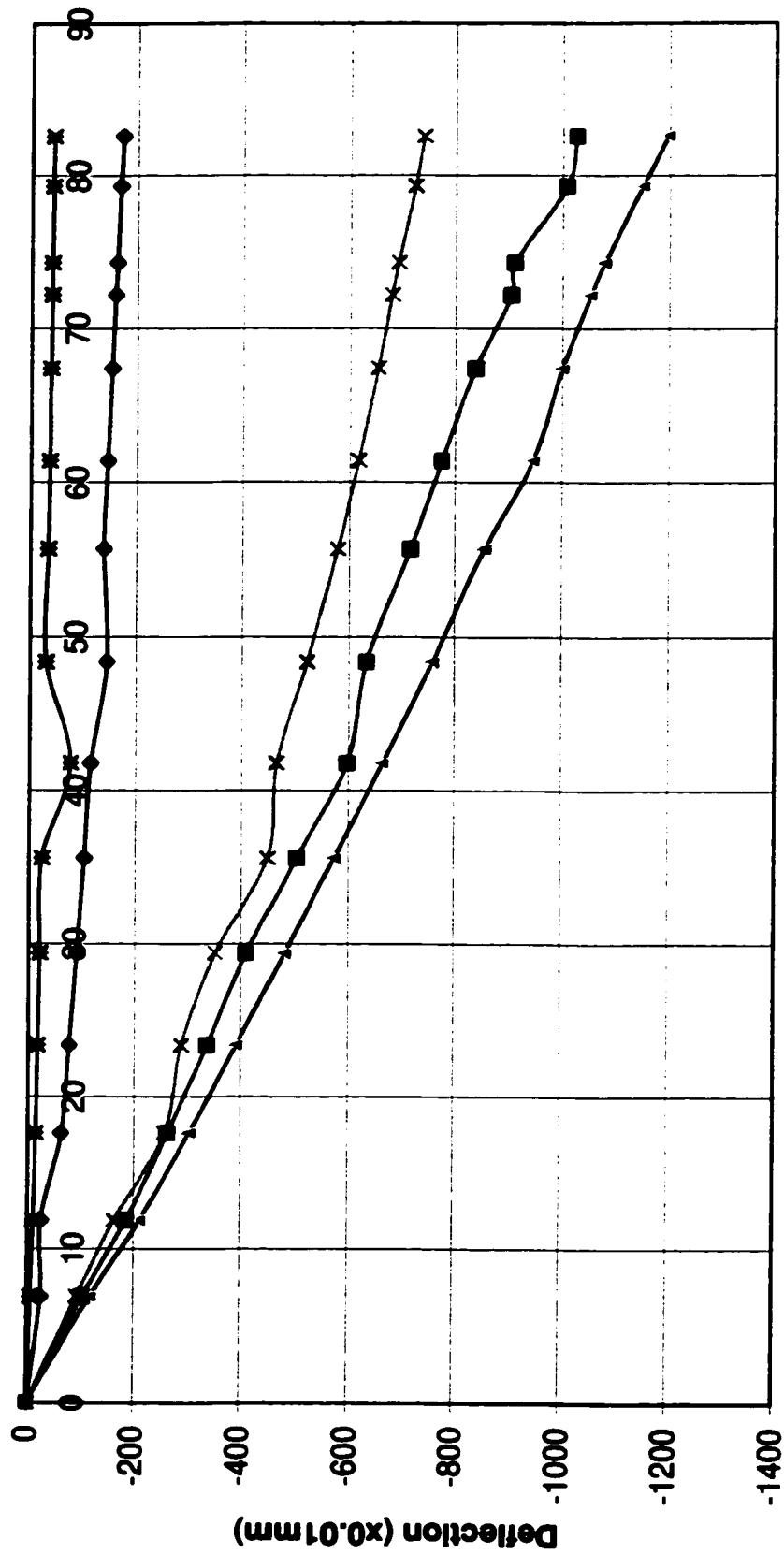
Test No. 25 S3B



—◆— No. 1 —■— NO. 2 —+— NO. 3 —x— No. 4 —#— No. 5

Deflection of Diagonal

Test 26 P5A

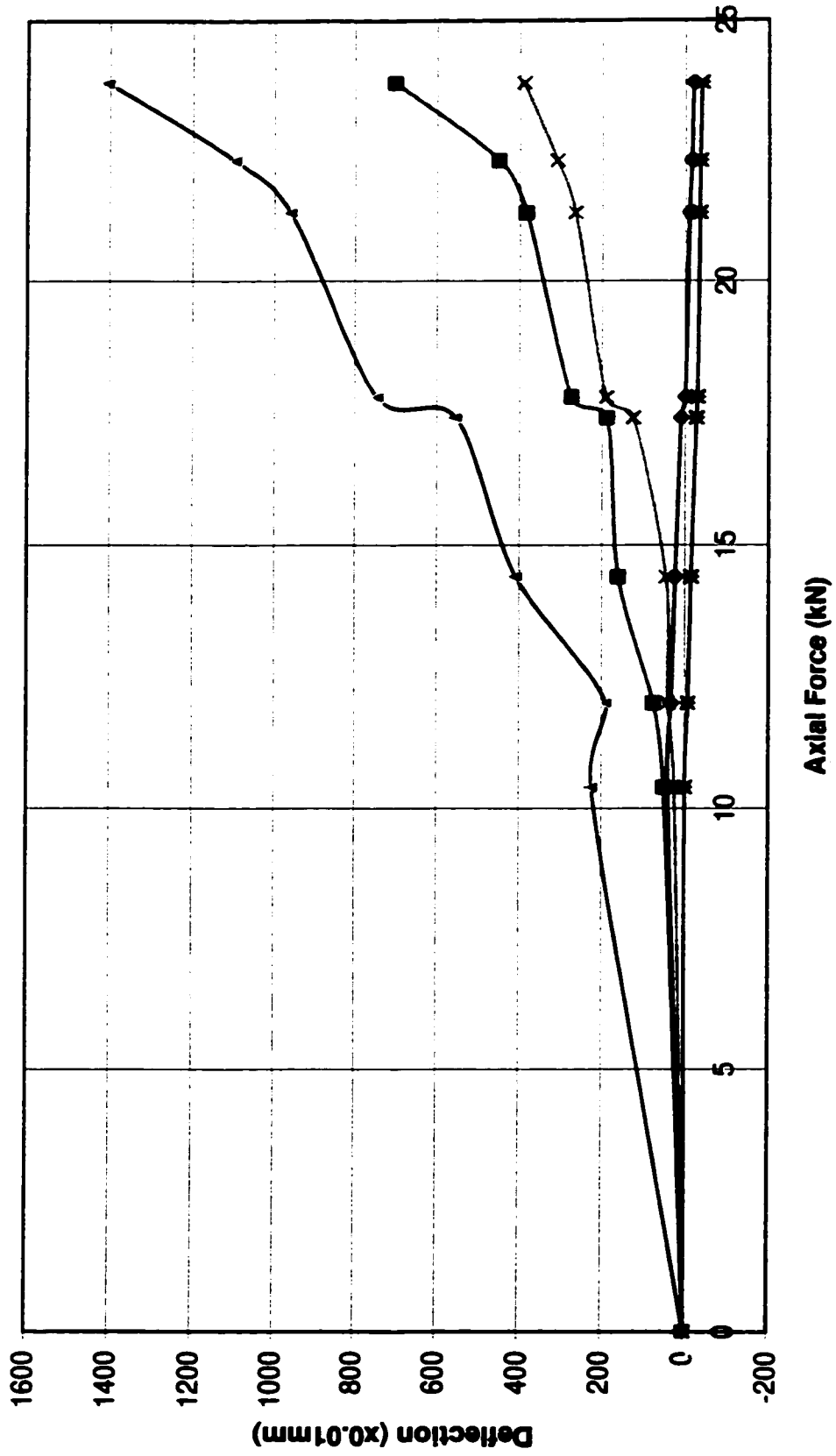


Axial Force (kN)

—◆— No. 1 —■— No. 2 —×— No. 3 —*— No. 4 —▲— No. 5

Deflection Diagonal

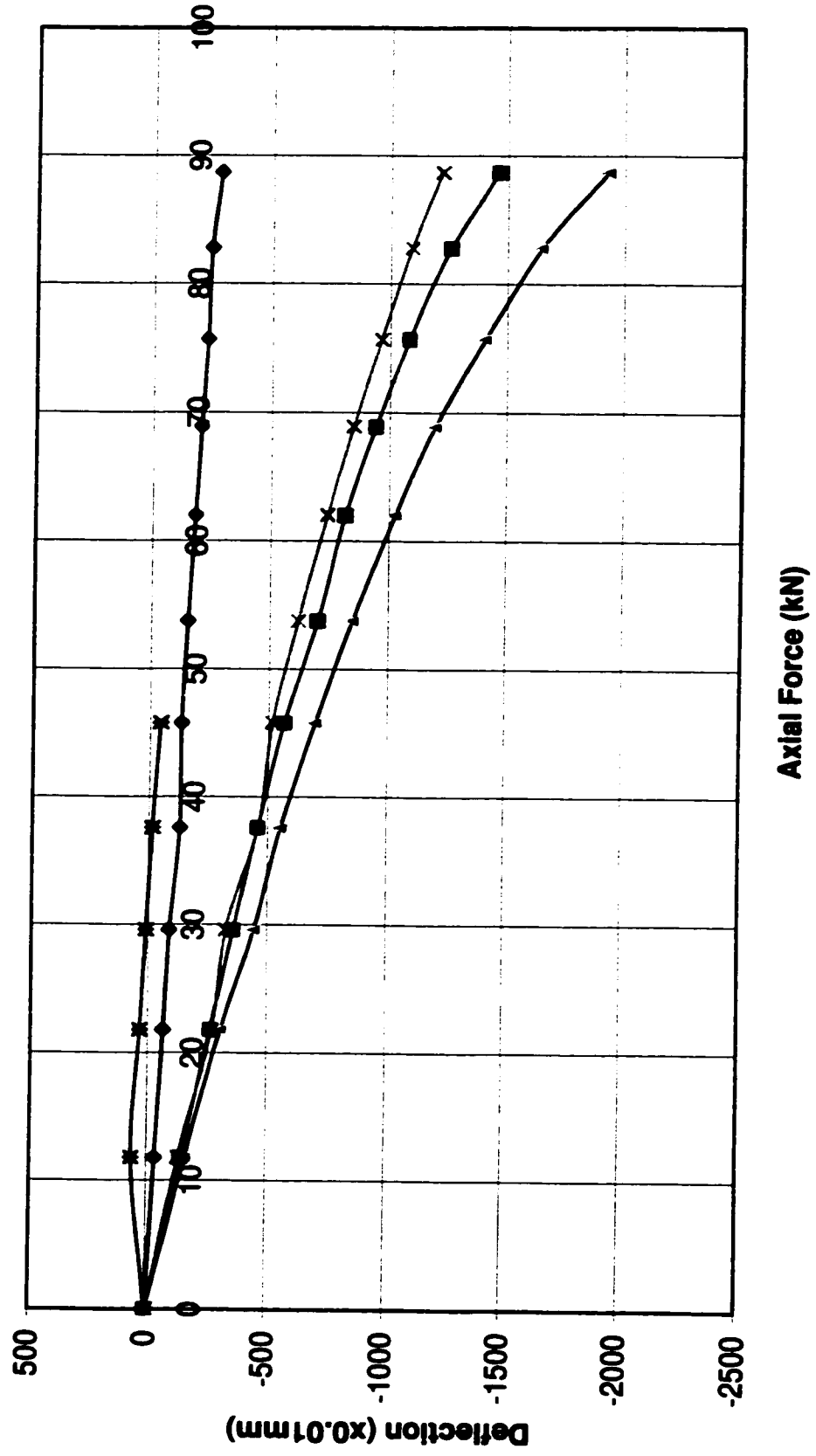
Test No. 27 P2B



—◆— No. 1 —■— No. 2 —▲— No. 3 —◆— No. 4 —✕— No. 5

Deflection of Diagonal

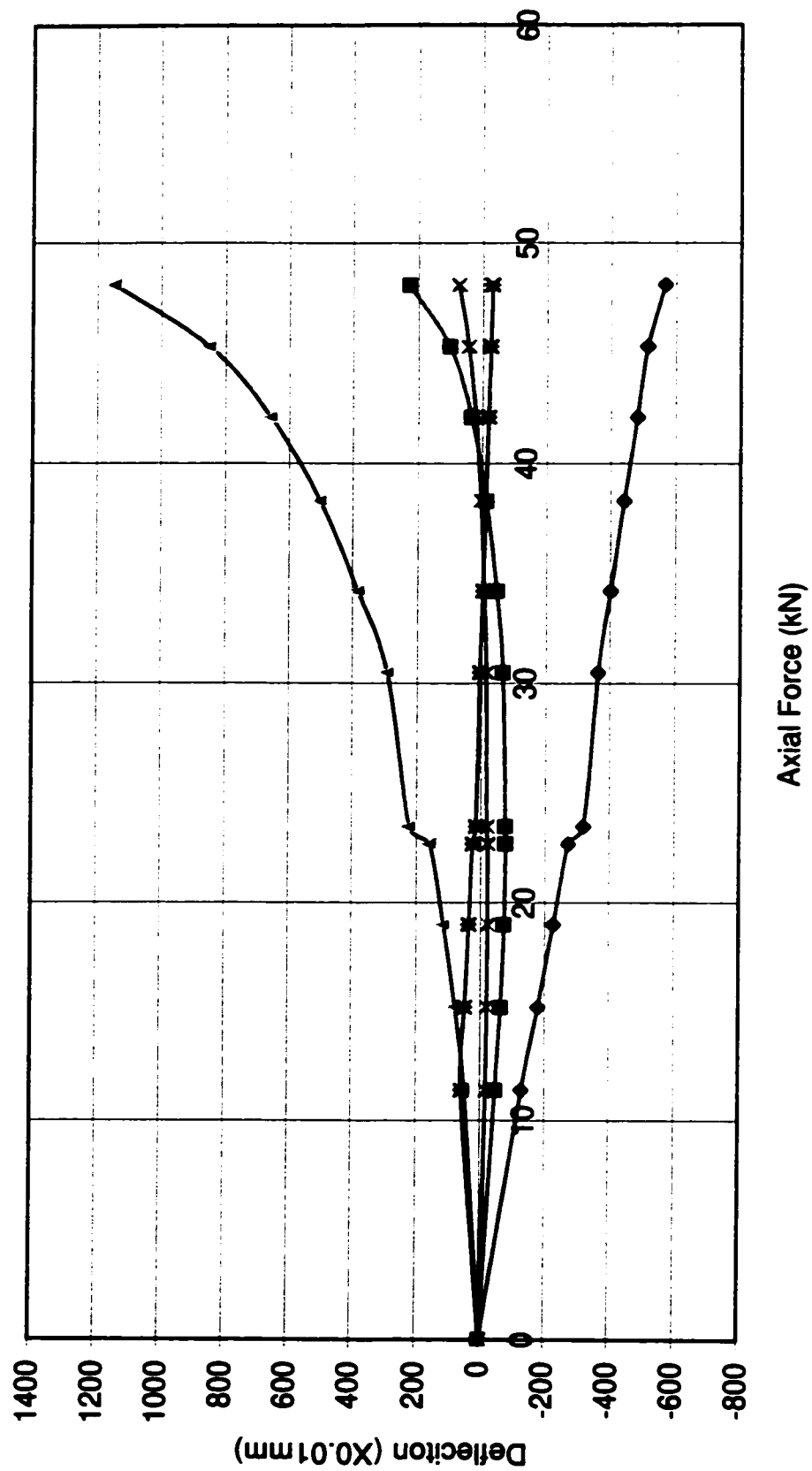
Test 28 P6A



—◆— No. 1 —■— No. 2 —▲— No. 3 —x— No. 4 —●— No. 5

Deflection of Diagonal

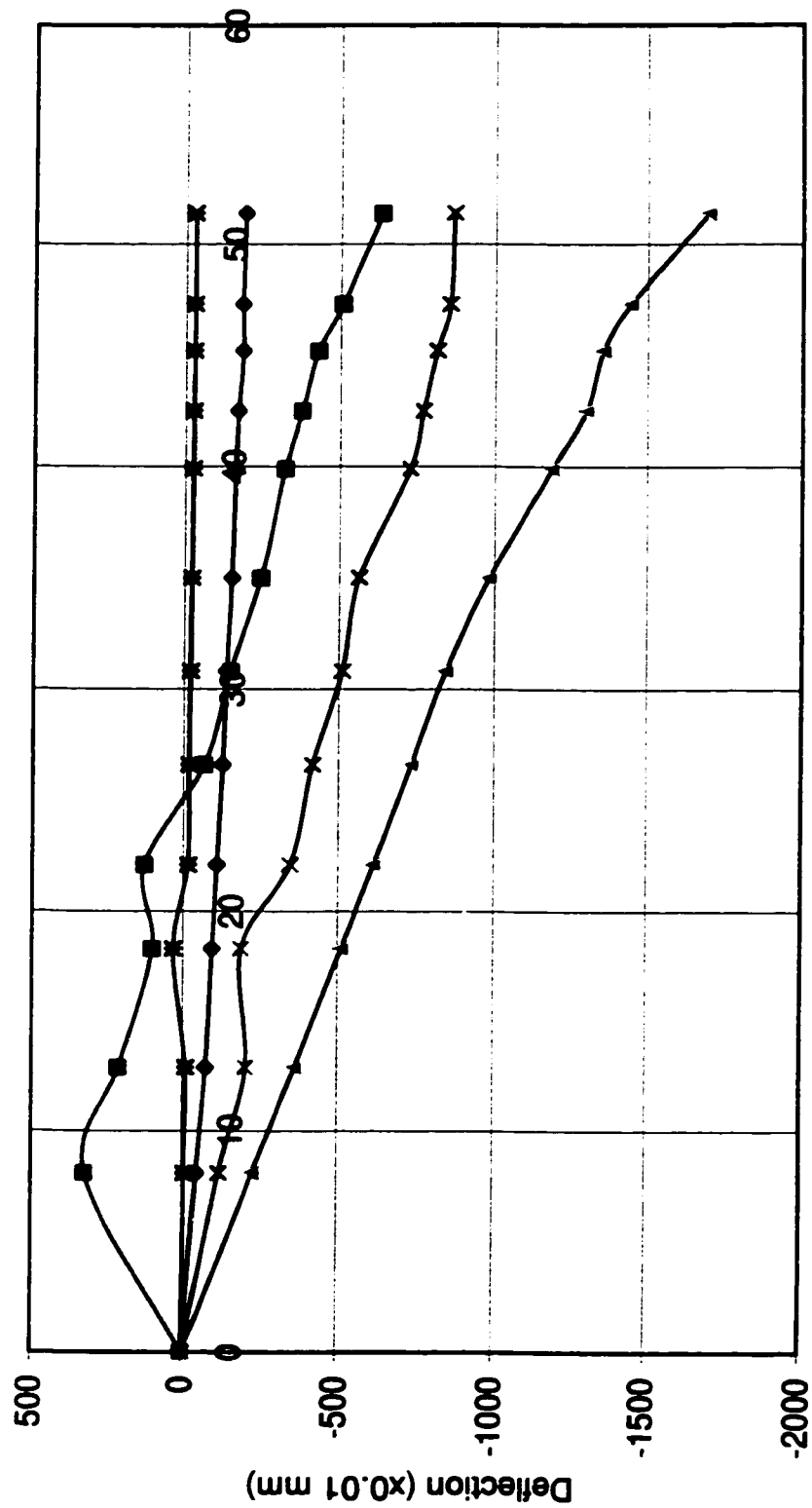
Test No. 29 P4A



—◆— No. 1 —■— No. 2 —▲— No. 3 —x— No. 4 —*— No. 5

Deflection of Diagonal

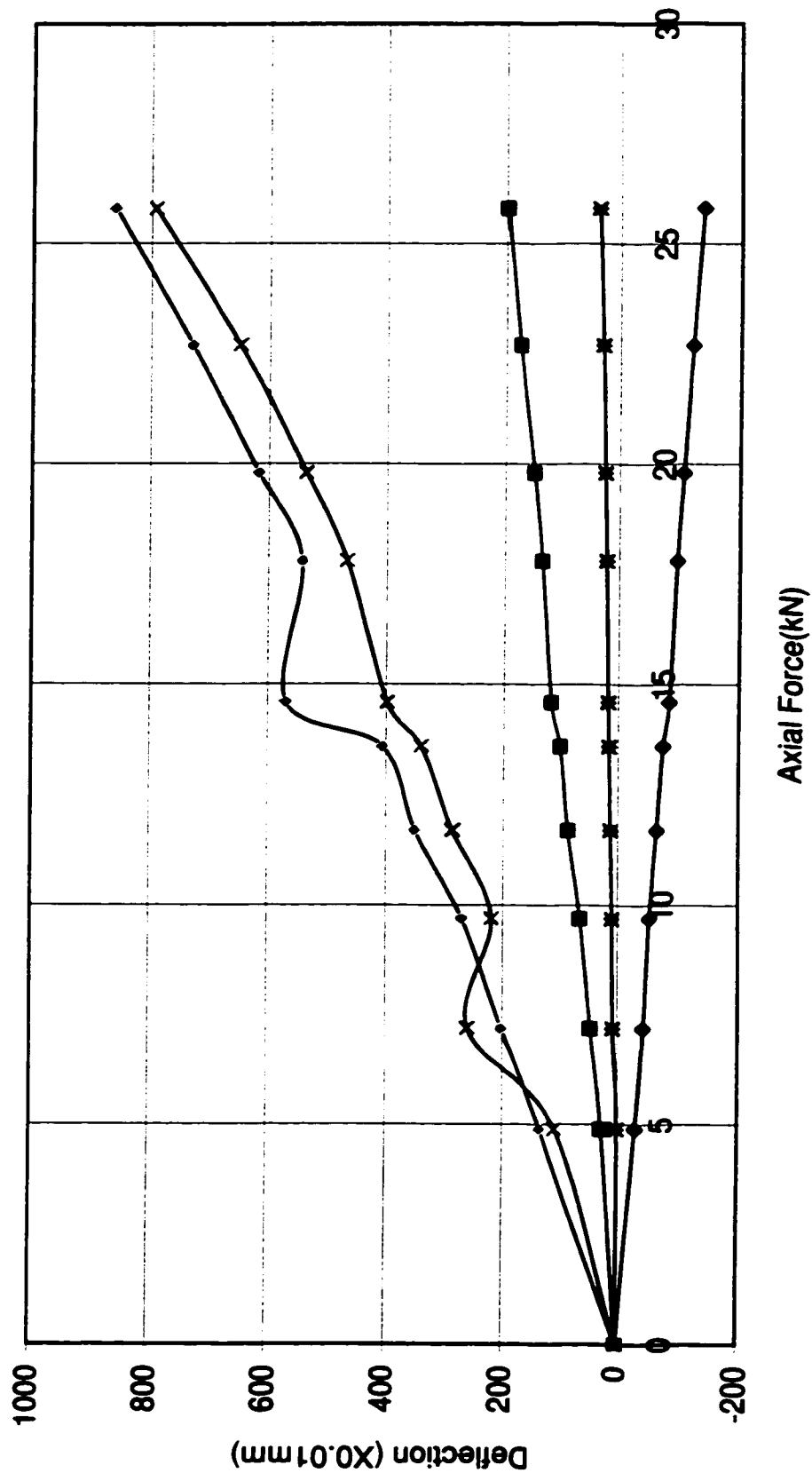
Test 30 P3A



—◆— No. 1 —■— No. 2 —+— No. 3 —x— No. 4 —*— No. 5

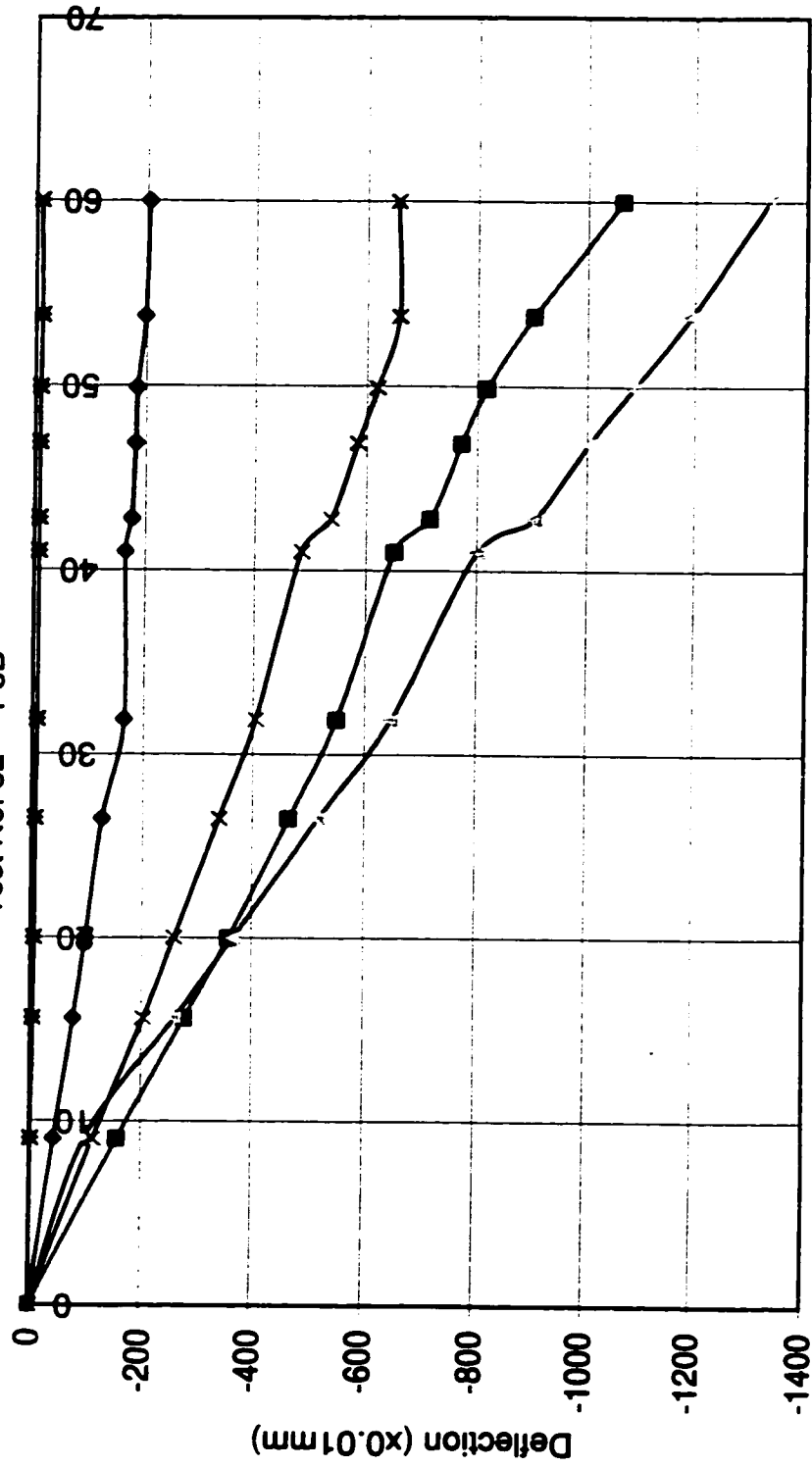
Deflection of Diagonal

Test No. 31 P1B



Deflection of Diagonal

Test No. 32 P3B

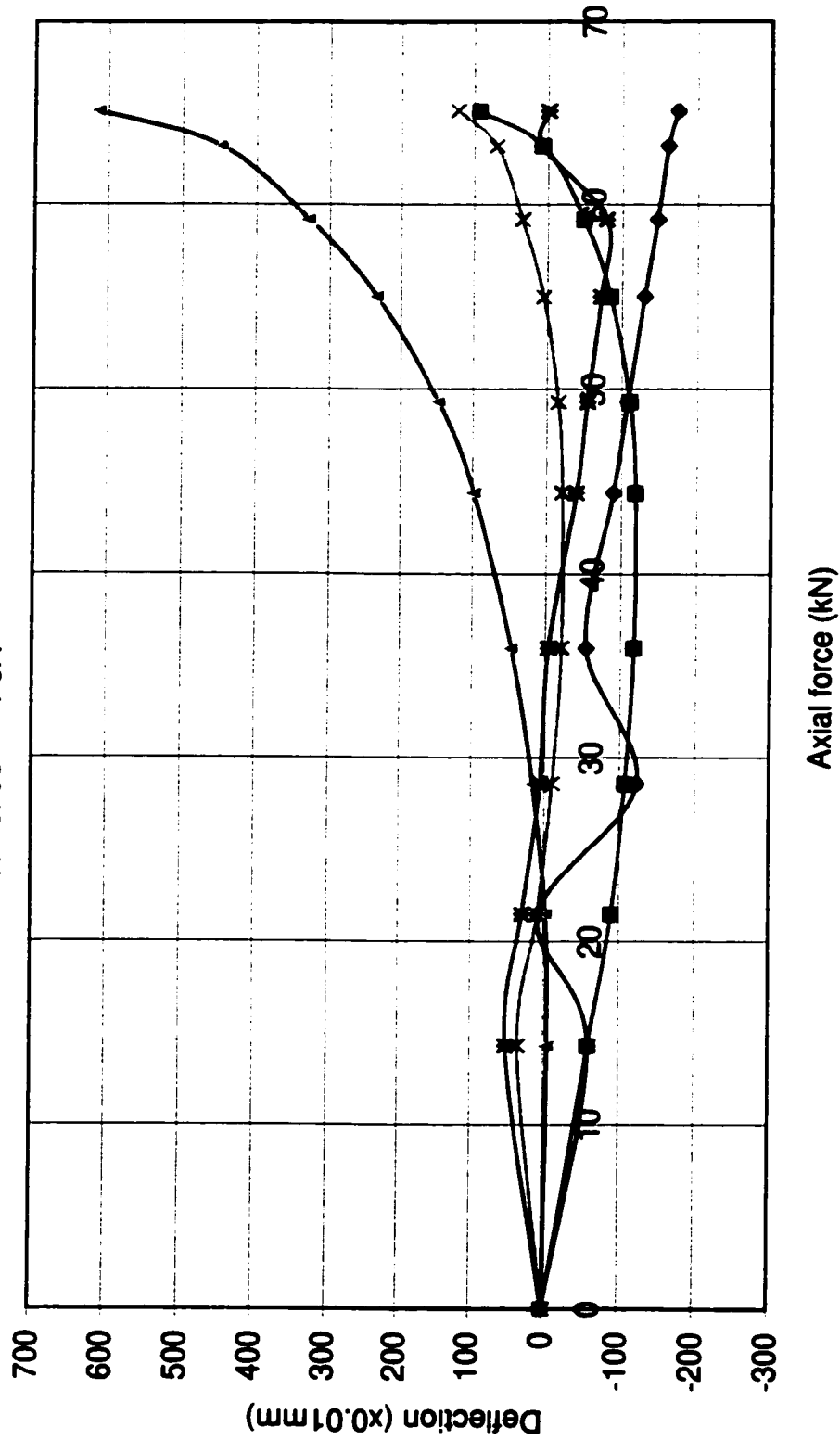


Axial Force in Diagonal (kN)

—◆— No. 1 —■— No. 2 —— No. 3 —x— No. 4 —#— No. 5

Deflection of Diagonal

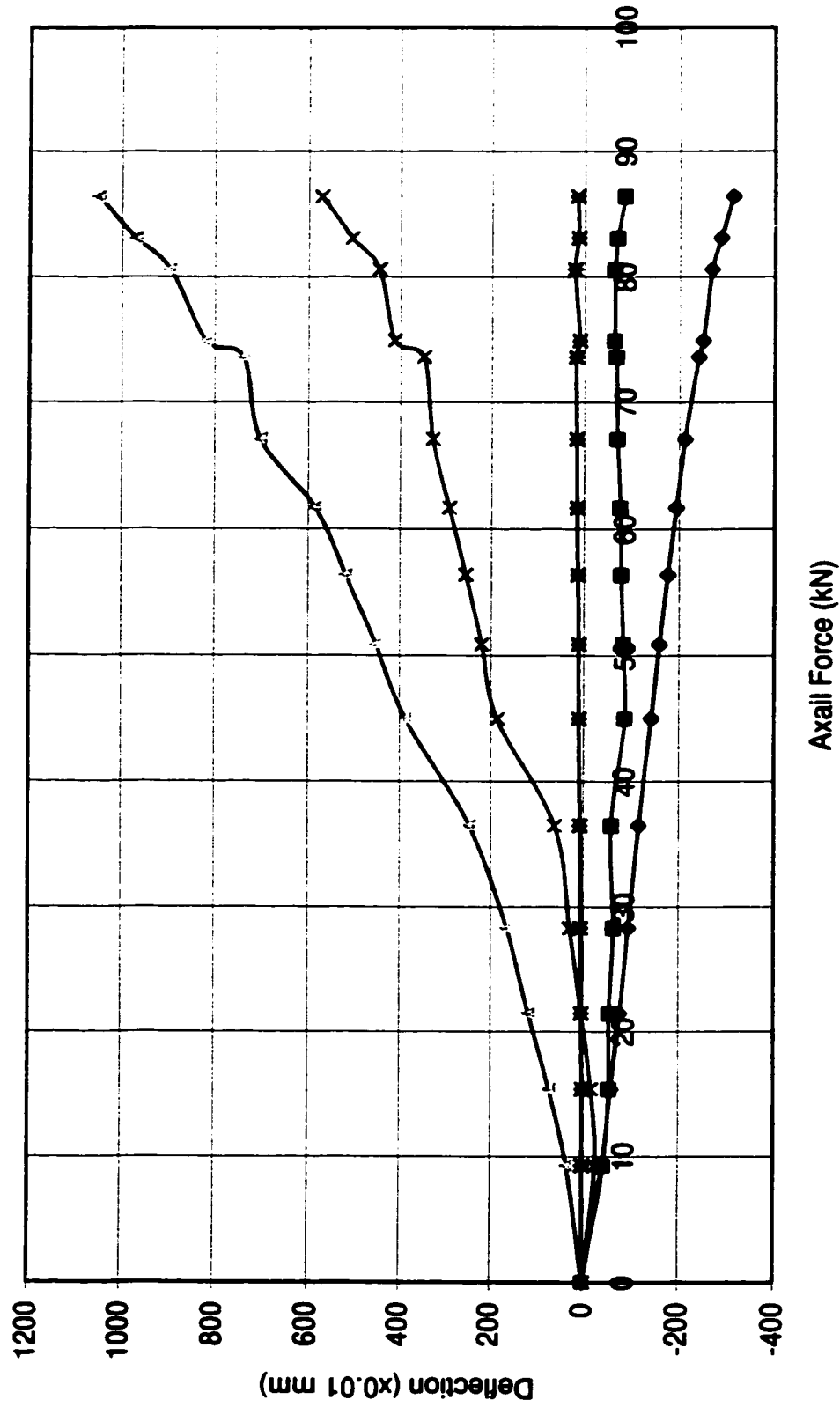
Test No. 33 P8A



—◆— No. 1 —■— No. 2 —▲— No. 3 —✕— No. 4 —◆— No. 5

Deflection of Diagonal

Test No. 34 P5B



—◆— No. 1 —■— No. 2 —+— No. 3 —x— No. 4 —#— No. 5

VITA AUCTORIS

The author was born in Fujian, People's Republic of China on December 7, 1968. He has a B. Eng. degree (1986-1990), and an M. Sc. degree(1990-1993) in Engineering Mechanics from Southwest Jiaotong University, China. He had worked for five years (1993-1998) as a Civil Engineer at Fuzhou Railway Survey Designing Institute.

He came to Canada in 1999 and is currently registered as an M.A. Sc. student in the Civil Engineering Program, Faculty of Engineering at the University of Windsor.